IMPROVEMENTS ON TANDEM MASS SPECTROMETRIC TECHNIQUES FOR THE ANALYSIS OF GLYCOSAMINOGLYCANS

by

ISAAC AGYEKUM

(Under the Direction of I. Jonathan Amster)

ABSTRACT

Structural elucidation of sulfated glycosaminoglycans necessitates the assignments of both sulfo modified sites and the C-5 hexuronic acid stereochemistry. Tandem mass spectrometry efforts targeted at resolving fine structures of GAGs have been hampered by the labile sulfate groups which undergo decomposition during ionization and ion activation and the insensitivity of mass spectrometry in assigning stereoisomers. This work presents improvements on tandem mass spectrometry methods using Fourier transform ion cyclotron resonance mass spectrometry and multivariate statistical analysis methods to resolve some of these challenges. Electron detachment dissociation (EDD) and collisionally induced dissociation (CID) have been used to sequence sulfated glycosaminoglycans including heparin and heparan sulfate and fucosylated chondroitin sulfate. Structural details aimed at assigning sites of sulfo modifications while reducing SO_3 loss in highly sulfated heparin and heparan sulfate oligosaccharide including Arixtra is presented. Also addressed in of this work is the assignment of the hexuronic acid stereochemistry using a EDD-PCA and a diagnostic ratio formula derived from an EDD-

PCA experiment. The C-5 uronic acid stereochemistry of thirty-HS tetrasaccharides have been assigned.

INDEX WORDS: Glycosaminoglycans (GAGs), Fourier transform ion cyclotron resonance (FT ICR), Electron detachment dissociation (EDD), Collision induced dissociation (CID), Principal component analysis (PCA) and Fucosylated chondroitin sulfate (FCS)

IMPROVEMENT ON TANDEM MASS SPECTROMETRIC TECHNIQUES FOR THE ANALYSIS OF GLYCOSAMINOGLYCANS

by

ISAAC AGYEKUM

B.S., University of Cape Coast, 2007

M.S., East Tennessee State University, 2011

A Dissertation Submitted to the Graduate Faculty of The University of Georgia in Partial Fulfillment of the Requirements for the Degree

DOCTOR OF PHILOSOPHY

ATHENS, GEORGIA

2017

IMPROVEMENTS ON TANDEM MASS SPECTROMETRIC TECHNIQUES FOR THE ANALYSIS OF GLYCOSAMINOGLYCANS

by

ISAAC AGYEKUM

Major Professor: I. Jonathan Amster

Committee: Ron Orlando

Joshua Sharp

Electronic Version Approved:

Suzanne Barbour

Dean of the Graduate School

The University of Georgia

August 2017

DEDICATION

To my parents Mr. and Mrs. Agyekum, my siblings Frank Agyekum and Comfort Agyekum, Pastor Samuel Obese and Joanita Emmanuella Maison

ACKNOWLEDGEMENTS

I would like to acknowledge my advisor Prof. I. Jonathan Amster for his encouragement, patience and support during my academic stay at the University of Georgia. I also want to express my sincere gratitude to my advisory committee members Prof. Ron Orlando and Prof. Joshua Sharp for their valuable contributions and comments in shaping this dissertation. Finally, this work would not have been possible without the generous support from our collaborators at the CCRC especially Prof. Geert-Jan Boons and Dr. Chengli Zong, Rensselaer Polytechnic Institute Prof. Robert Linhardt, and Prof. Chen Shiguo at Zhejiang University. Finally, to the Agyekum family, it has been a journey with the Lord. John Muchena, Lawrencia Kwarteng, Brad Acrey, Prince Osei-Sarfo and the entire family at Bread of life international ministries I am grateful for all your support.

TABLE OF CONTENTS

Page

APPENDICES

LIST OF TABLES

Page

LIST OF FIGURES

Page

CHAPTER 1

INTRODUCTION AND LITERATURE REVIEW

Proteoglycans (PGs) or mucoprotiens are highly glycosylated proteins found in all connective tissues and cell surface membranes where they are known to influence critical physiological and pathological processes [1, 2]. Their basic structure comprises a core protein with covalently attached highly anionic polysaccharides called glycosaminoglycans (GAGs) [3]. Structurally, GAGs are unbranched, polydisperse polysaccharides consisting of a repeating disaccharide unit of an amino sugar and a uronic acid.[4, 5] Depending on their disaccharide repeats, GAGs can be categorized into four major classes: heparin (Hp) and heparan sulfate (HS), chondroitin (CS) and dermatan sulfate (DS), keratan sulfate (KS), and hyaluronic acid or hyaluronan (HA) [5].

Heparin and heparan sulfate GAGs are the most structurally complex among the family of GAGs. Heparin/HS are composed of disaccharide repeating units of *N*-acetylglucosamine (GlcNAc) and glucuronic acid (GlcA) [5, 6]. The glucosamine unit may be sulfated at the 3-*O,* 6-*O* or the N-positions whereas sulfation at the 2-*O* uronic acid residue may occur upon epimerization of glucuronic acid to iduronic acid (IdoA) [6-10]. Even though heparin and HS have the same disaccharide building blocks, there exist some structural differences: heparin has higher amount of *N*- and *O*-sulfo groups compared to HS with the major disaccharide unit in heparin being IdoA2S-GlcNS6S. Epimerization of the GlcA content to IdoA is estimated to be about 80% in heparin and 20-50% in HS [7, 11, 12]. The striking difference

between these structurally related compounds is the sulfo content per disaccharide unit; heparin averages about 1.8-2.6 sulfo groups per disaccharide and 0.6-1.8 for HS [7, 13]. The structural features of heparin and HS are known to influence a myriad of biological functions including cell-cell signalling, inflammatory processes, morphogenesis, cancer metastasis and wound healing [12]. The anticoagulant efficiency of heparin upon interacting with antithrombin is also a well-documented phenomenon [14, 15]. This interaction is mostly attributed to its pentasaccharide binding motif (GlcNAc/NS(6S)-GlcA-GlcNS(3S,6S)-IdoA(2S)-GlcNS(6S) in the polymer [16, 17].

Chondroitin sulfate (CS) GAGs are composed of alternating disaccharide building blocks of *N*-actylgalactosamine (GalNAc) and glucuronic acid linked through an alternating α, ß (1, 4) and, ß (1, 3) glycosidic bonds.[5] Sulfation on the GlcNAc unit may occur at the 4-*O* and 6-*O* positions and the C-2 hydroxyl group of the uronic acid residue [4, 5]. There are many types of CS however, three main classifications are found in higher animals namely CS A, CS B also known as dermatan sulfate (DS) and CS C. CS A and CS B are predominantly sulfated at the 4-*O* position of GalNAc while CS C has mostly 6-*O* sulfated GalNAc. Dermatan sulfate differs from CS A, in that glucuronic acid moiety is replaced by its C-5 epimer, iduronic acid. CS/DS are known to influence several biological activities, which are strongly correlated to the degree and position of sulfation and their hexuronic acid stereochemistry [4, 5, 18].

The basic disaccharide sequence of Keratan sulfate (KS) consist of *N*-actylgalactosamine, and galactose (3Galβ1-4GlcNAcβ1) which may be sulfated at

the C-6 positions of both residues [19]. There are three distinct forms of KS found in nature: KSI are mostly found in the cornea and *N*-linked to asparagine in the core protein, KSII located in the cartilage are highly sulfated and O-linked to the protein via serine or threonine, KSIII (Man-*O*-linked KS) also described as proteoglycans from the brain are linked to a core protein via mannose residue (KS-Man-*O*-Ser) [19,20]. Some documented biological function of KS includes inhibiting proliferation of cancerous cells, metastatic transformations, involved in tissue hydration and regulation the assembly of collagen fibril [19, 20].

Hyaluronic acid (HA) is the only member of the GAG family that is not modified by sulfation or epimerization, and is not attached to a core protein [21]. It is composed of polymerized disaccharide repeating units of GlcAβ(1,3)GlcNAcβ(1,4) exiting as free chains with molecular weight ranges between 100-20000kDa [21]. HA forms an integral part of the skin, synovial fluid and cartilage and involved in skin repair, wound healing, control tissue hydration, tumour development, cell migration etc [21-23].

The last decade has seen a surge in the interest to structurally link GAGs to their biological activities. This has propelled advances in sensitive analytical methods for their analysis. NMR analysis has been at the forefront of glycosaminoglycan analysis but existing limitations such as sample purity and milligram amounts needed for analysis may not be available [24, 25]. Mass spectrometry is an excellent option for GAG analysis offering high sensitivity, low sample consumption and fast analysis times. The versatility to parallel most mass spectrometers to several separation platforms (liquid/gas) phase has positively

impacted structural studies of GAGs. This review focuses on current advancements in mass spectrometry analysis of GAGs from the view of sample preparation to automated interpretation of GAG MS and MS/MS data.

Isolation and purification of GAGs for mass spectrometry analysis

Animal tissues remain a major source of the production of glycosaminoglycans [26]. An established protocol for the extraction of PGs involves the treatment of homogenised defatted tissues with strong denaturing or chaotropic agents like guanidine hydrochloride (GdnHCl) containing detergent and or protease inhibitors [27]. This step is followed by the removal of GdnHCl and other salts in the extraction buffer prior to the recovery of the PGs. The release of the GAG component from the core protein is then achieved using β-elimination under reducing conditions at room temperature producing a xylitol residue at the reducing end of the GAG [28]. The resulting GAG oligomers present in the mixture after tissue extraction can be isolated using ultracentrifugation, gel-chromatography, anion-exchanged chromatography (AEC), and reverse phase (RP) chromatography [1, 29]. The extracted GAG chains are often too large and highly heterogeneous hence may require further treatment to obtain well defined fragments suited for mass spectrometry analysis [30].

Isolated GAG chains can be purified and characterised using site specific lyases. Well characterised substrate specific lyases are routinely employed to depolymerize GAGs into their basic disaccharide building blocks or partial depolymerisation into oligosaccharides [1]. The polysaccharide lyases cleave specific glycosidic bonds creating GAG fragments with delta 4, 5-unsaturated

uronosyl non-reducing end residues [13, 30, 31]. Comprehensive protocols on specific enzymatic depolymerisation of the various types of GAGs have been documented [25, 32]. Another means of depolymerisation GAGs is by use of nitrous acid. Nitrous acid depolymerisation of GAGs at lower pH (-2) is used to cleaved N-sulfated hexosamine bonds [13, 33, 34]. Fragments of heparin and HS GAGs, resulting from nitrous acid depolymerisation often vary in molecular weights depending on the N-sulfated glucosamine residues [13]. Cleavage of free hexosamine bonds can also be achieved at pH 4 upon deacetylation of the GlcNAc residues with hydrazine to GlcN [13]. The end products of these reactions have their reducing ends modified with 2,5-anhydromannose which can be reduced to anhydromannitol [35]. Notably, the C-5 uronic acid configuration of the resulting depolymerized fragments are retained [36]. These depolymerisation procedures play integral roles in obtaining less complicated samples for structural analysis of GAGs.

MS analysis of glycosaminoglycans

The principal aim of mass spectrometry analysis of GAGs is to obtain molecular weight, from which we can infer the oligomer length, degree of sulfation and other substituents that may be present [37]. The ability to acquire molecular weight information hinges on the ability to make ions. The initial application of fast atom bombardment (FAB) for the analysis of GAGs was characterized by fragmentation of the sulfate groups [30, 33]. Recent advances in mass spectrometry analysis have led to the development of soft ionization techniques amenable to GAG

studies. The two main ionization methods currently employed for GAG analysis are matrix-assisted laser desorption ionization (MALDI) and electrospray ionization (ESI) [38]. These ionization methods impart very little energy to the analyte thereby reducing thermal fragmentation of the sulfate groups [38].

Matrix-assisted laser desorption ionization (MALDI): Early reports on MALDI MS analysis of highly sulfated GAGs produced weak signals accompanied with the decomposition of the sulfate groups [39, 40]. The tendency of GAGs to form complexes with basic peptides has been exploited to produce molecular ions without SO_3 loss during MALDI analysis, thus allowing for intact molecular weight measurements [40-42]. While this method provides a great improvement in analyte sensitivity and greatly supresses sulfate decomposition [10], it is limited by lack of synthetic peptides [10, 43]. MALDI-MS analysis of uncomplexed polysulfated oligosaccharides using ionic liquid matrices (ILMs), 1-methylimidadazolium-α-cyano-4-hydroxycinnamate (ImCHCA) and butylammonium-2,5-dihydroxybenzoate, have recently been reported by Larimore et al., however, this technique could not resolve the issue of sulfate decomposition [44]. Using the same ILMs, the same group investigated the effects of alkali metal counterions on supressing SO_3 losses during a UV-MALDI-MS experiment [45]. Their results showed no SO_3 loss for both sodium and cesium salts of CSA in the positive ion MALDI-MS spectra. In another report, the use of 1,1,3,3-tetramethylguanidinium (TMG) salt of α-cyano-4-hydroxycinnamate acid (G_2-CHCA) as ionic liquid matrices to suppress loss of SO_3 in the MALDI spectra was proposed [41]. In this report, G_2-CHCA showed excellent tolerance to the presence of buffer salts

facilitating the detection of intact CS and DS oligosaccharides. MALDI-MS analysis of heparin and HS oligosaccharides using new ILMs. 2-(4-hydroxyphenylazo) benzoic acid (HABA) with TMG and spermine has shown great prospects in suppressing the dissociation of sulfate groups and improving signal to noise ratios [47]. Work done by Tissot et al.[42] using ImCHCA matrix has also shown the capability of obtaining intact molecular weight information on highly sulfated GAGs oligosaccharides, with as many as 13 sulfates. MALDI-MS analysis of isolated single components of polysulfated DS oligosaccharides varying in oligomer length (di- to decasaccharides) as well as a mixture of depolymerized CS and DS have been reported using pyrenemethylguanidine [43]. The ILM pyrenemethylguanidine used by these researchers did not only serve as a derivatizing agent but greatly enhanced the ionization efficiency.

Electrospray ionization (ESI): Conventional electrospray ionization (ESI) and nano-ESI remain the most exploited ionization methods for GAG analysis due to its high sensitivity [30, 33, 44]. With well optimized source conditions, highly sulfated GAG oligomers can be analyzed with very minimal dissociation of the labile sulfate groups [8]. Arixtra, which is an octasulfated pentasaccharide is an ideal test compound for optimization of the ion source conditions [8]. The high sulfate density per disaccharide unit of Arixtra can reveal the susceptibility of the sulfate groups to harsh ionization conditions. The modification of the spray solvent with metal cations such as Ca^{2+} and Na^{+} can also suppress the decomposition of the labile sulfate groups [44-46]. The presence of these ions, though useful, may negatively impact the sensitivity and may also complicate the

mass spectrum. Supercharging agents aimed at efficient deprotonation of the acidic protons in GAGs can greatly also suppress SO_3 loss [47]. Due to the acidic nature of GAGs, most ESI-MS analyses are done in the negative mode.[32] Additionally, the experimental setup of ESI makes it well suited for on-line liquid-phase separation techniques such as liquid chromatography (LC) and capillary electrophoresis (CE) [37]. These hyphenated MS platforms offer excellent capabilities for compositional profiling of GAG oligomers [30, 48].

Analysis and compositional profiling of GAG disaccharides using mass spectrometry

Extracted GAGs subjected to complete enzymatic depolymerization often exist as complex mixtures thereby benefiting from various online separation techniques prior to MS analysis [30]. This allows for detailed disaccharide compositional analysis of unknown GAG samples providing information about their relative and absolute amounts with the aid of commercially available disaccharide standards. The first step in carrying out compositional analysis of GAGs involves exhaustive enzymatic digestion to release the disaccharide components. The product of a complete lyase digestion of heparin/HS GAGs contains twelve delta unsaturated disaccharides while that of CS/DS proteoglycans produces eight delta unsaturated disaccharides. The resulting disaccharide mixture can be analyzed by ESI-MS or ESI-MS^n depending on the complexity of the mixture. MS quantification of unique molecular ions can be easily accessed, relative to the abundance of an internal standard [49]. Complimentary tandem mass spectrometry analysis on resulting isomeric disaccharides can provide unique diagnostic ions whose relative

abundances can be used in a system of equations to estimate their relative amounts [49, 50]. A successful application of this method by Zaia et al.[49] for the analysis of eight CS disaccharides has been implemented in the analysis of HS disaccharide mixtures including those extracted from bovine and porcine tissues [49]. Subsequent application of this method for profiling twelve heparin and HS disaccharides including free amine containing disaccharides have been reported [51]. Even though this method offers some advantages such as short analysis times and low sample consumptions, it is difficult to use diagnostic ions to quantify individual isomers when they are present in low intensities. Another factor that may also affect accurate quantitation is the effects of metal cations which may have an adverse effect on sensitivity and complicate the mass spectra. Hyphenated MS methods have been developed to resolve some of these challenges.

Liquid Chromatography (LC)-MS for GAG disaccharide analysis

LC-MS has been extensively used for the analysis of GAGs. Comprehensive review on LC application for GAG analysis beyond the scope of this review have been publish by Zaia et al. [30]. We hereby briefly discus various LC-MS techniques applied for GAG disaccharide analysis.

Reverse-phased ion pair (RPIP) LC-MS: RPIP- LC is known for its compatibility with MS detection [52]. For MS analysis, volatile lipophilic ion-pairing reagents are added to the mobile phase to facilitate ion retention and aid evaporation during electrospray.[48] The right choice of ion-paring regent and its concentration is essential for successful RPIP- LC-MS analysis [37, 53]. The ideal ion-pairing reagent concentration should be sufficient enough to resolve and provide retention

of the component of interest; however, it should be low enough to avoid suppressing the MS signal [37, 53]. Selected ion-pairing reagents that have shown great prospect for RPIP -HPLC-MS for GAG analysis include dibutylamine, [53] tributylamine,[54] propylanmine, [55, 56] and pentylamine [56]. The application of RPIP-HPLC-MS for disaccharide profiling was recently reported by Zhang et al using tributylamine as the ion-pairing reagent [57]. In their report, eight heparin and HS disaccharides were separated using reverse-phase ion-pairing micro flow high performance liquid chromatography RPIP-HPLC and the extracted ion chromatogram revealed the anomeric α, ß forms of these three disaccharides (6S, 2S and 2S6S) nicely resolved. RPIP- LC-MS analysis of CS/DS disaccharides using n-hexyl amine as the ion-pairing agent have also been reported [32]. Most recently, RPIP- LC-MS analysis of 2-aminoacridone (AMAC) labeled disaccharides of HA, CS and DS released by enzymatic digestion have been reported [58]. This work also revealed the applicability of the method to evaluate the CS disaccharide content in human plasma. Notwithstanding these great reports on the use of RPIP- LC-MS, it can be limited by its sensitivity to mobile phase components, long analysis time and the contamination of the ion source by ion-pairing reagents [59].

Ultraperformance liquid chromatography (UPLC)-MS: UPLC analyte separations are carried out on columns packed with 1.7-µm particles at high pressures (about 15000psi) [48]. This technology benefits from recent advances in liquid chromatography performance in the area of resolution, peak capacity and short analysis time [59, 60]. Rapid RPIP-UPLC-MS profiling of heparin and HS disaccharides from various bovine and porcine tissues have been reported.[61, 62]

Elution times recorded for the heparin and HS disaccharides were less than 5mins. The ability to resolve fine structural details like the α and ß anomers of heparin and HS disaccharides (ΔUA-GlcNAc6S and ΔUA2S-GlcNAc) have also been reported in compositional analysis experiment using RPIP-UPLC-MS.[57] The use of hexylamine (15mM) as the optimal ion paring agent for the analysis of eight CS disaccharides in a RPIP-UPLC-MS in both positive and negative ESI conditions have been reported by Solakyildirim et al. [63]. Surprisingly, the results under positive ESI conditions were better.

Hydrophilic interaction chromatography (HILIC)-MS: HILIC separation is a normal phase chromatography technique that employs a polar stationary phase to retain polar analytes [64]. Reports have shown that amine and amide stationary phases can enhance GAG separation on HILIC columns [30, 65]. For a successful HILIC-MS analysis, solvent modifiers and MS compatible ammonium salts are required. Some of the advantages of this technique include improved ESI-MS sensitivity, highly symmetrical analyte peak shapes, less cumbersome sample preparation and fast analysis times. Some recent reports on the application of HILIC-MS for disaccharide analysis include work done by Gill et al. [36]. This work showed the application of HILIC-MS for structural analysis of HS, CS and DS disaccharide products obtained via enzymatic and nitrous acid depolymerisation. A most recent report by Ouyang et al.[29] using an Xamide column showed the utility of HILIC-LC-MS for compositional analysis of heparin and LMWH GAGs. Their report also showed the separation of both the α and ß forms of the N-acetylated disaccharides. The best separation of these subtle

features was achieved at 40 °C. HILIC coupled with high resolution Fourier transform mass spectrometry (FTMS) has recently been used for the analysis of low molecular weight heparin (LMWH) [66]. In this report 40 oligosaccharide fragments of LMWHs were quantified including unsaturated disaccharides [66].

Size-exclusion liquid chromatography (SEC)-LC-MS: SEC-LC is different from other adsorptive mode chromatography techniques in that, it is independent of selective adsorption or desorption of molecules, but rather molecules are sieved based on their size as they go through the resin [67, 68]. SEC-LC provides the platform to do online desalting enabling a reduction in the formation of metal adduct that can complicate the MS spectra [49]. Recent reports have shown SEC-MS as a very useful tool for quantitative profiling of GAG disaccharides in mammalian tissues [69-71]. These analysis have shown the compatibility of SEC to ESI as tissue surface molecules that may interfere with the ionization of disaccharide analytes are removed [72]. A recent comparison of direct nano-ESI and SEC-LC-MS quantification of GAGs released from tissues surfaces revealed the latter produces more reproducible results even though the SEC-LC-MS analysis was slow [72]. A more rapid analysis could be achieved using ultraperformance size exclusion chromatography mass spectrometry (UPSEC-MS).

Graphitized carbon (GC)-LC-MS: GCC-LC is a widely used analytical tool for oligosaccharide purification and desalting. The chemical and physical properties of porous graphitized carbon (PGC) are well suited for GAG analysis [30]. It is robust over a wide pH range and well known for its ability to resolve isomers [73]. PGC columns do not require any form of derivatization therefore analysis time are greatly

reduced as well as cost. PGC-LCMS under negative ESI conditions have been used to resolve enzymatically derived disaccharides including heparin and HS, CS, KS and HA [74-76]. LC-MS quantification of GAG disaccharide obtained via deaminative depolymerization remains a grey area. However, PGC-LCMS analysis of HONO generated HS disaccharides was recently reported by Gill et al.[77] This work did not only demonstrate the ability to quantify HS disaccharides using PGC-LCMS, but also information pertaining to sulfate position, differentiation of the C-5 uronic acid stereochemistry as well as positional sulfation isomers could be obtained.

Capillary electrophoresis (CE)-MS

The analytical significance of CE-MS as a tool for compositional and structural analysis of GAGs has been emphasized by several reviews [78-81]. This separation method distinguishes analytes based on differences in their electrophoretic mobilities [82]. CE is known for its high sensitivity, versatility and separation efficiency. The acidic nature of GAGs makes them excellent candidates for CE-MS analysis. The pioneering work by Duteil et al. demonstrated the potential of CE-MS in both negative and positive ionization modes for compositional analysis of heparin disaccharides and oligosaccharides [83]. Subsequently, a pressure assisted CE ion trap MS method was developed for the analysis of eight heparin derived disaccharides [84]. In this report, co-eluting disaccharides were identified and quantified using MS/MS. However, several CE-MS/MS acquisitions had to be made to facilitate the identification of positional isomers. Recently a new CE-MS interface has been employed by Sun et al. for the analysis of heparin

oligosaccharides and LMWH [85]. To determine the linearity and sensitivity of this CE-MS method, various concentrations of heparin disaccharides were considered. This method offered several advantages including low injection volumes (20nL) and higher sensitivity about 1000-fold higher than ultraviolet detection.

Tandem mass spectrometry of GAGs

Tandem mass spectrometry analysis of GAGs affords specific information such as mono-saccharide composition, linkages, sulfate positions and sites of acetylation [86, 87]. These structural assignments are made possible through the production and assignment of glycosidic and cross-ring product ions. The elemental composition within a monosaccharide unit can be obtained using the glycosidic product ions. It is also possible to assign sulfate positions for GAGs with predictable monosaccharide unit for example the Gal and GlcNAc residues of KS can only be sulfated at the 6-*O* position therefore no cross-ring products are required for their assignment. However for sulfated GAG oligomers such as CS, DS, HS and Heparin with possible variability in the sulfo positions on their many sugar residues may require a combination of cross-ring(s) and glyosidic product ions for their assignment [8]. The assignments of product ions arising from an MS/MS analysis of GAGs is made using the Domon and Costello nomenclature [88]. Fig. 1. 1 illustrates the structural assignment of a Heparin/HS tetrasaccharide using the Domon and Costello nomenclature.

A routine MS/MS experiment involves the activation of a selected precursor ion from the first stage MS. The two broad categories of MS/MS activation techniques employed for GAG analysis are categorized as threshold and electron-assisted method [32].

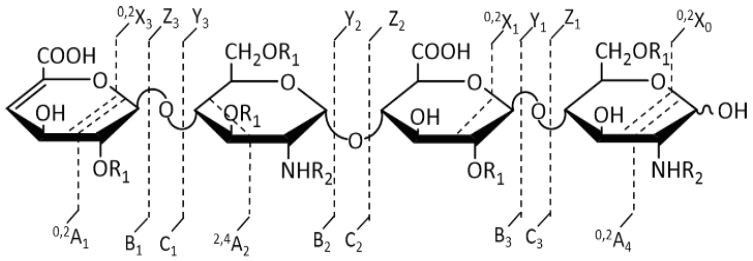

Figure 1.1: Domon and Costello nomenclature annotation of a Heparin/HS tetrasaccharide: Glycosidic cleavages containing the non-reducing end (NRE) are denoted with B or C and those with the reducing end as "Y" and "Z". Cross-ring cleavages are assigned as "A" if they contain the NRE and "X" if they contain the RE. R_1= H, SO_3H and R_2= H, SO_3H, Ac

Threshold ion activation: The two main threshold activation methods employed for MS/MS GAG analysis are collision-induced dissociation (CID) and infrared multiphoton dissociation (IRMPD). With CID, the selected molecular ion is translationally excited, then undergoes frequent collisions with neutral molecules which then induces fragmentation of the molecular ion [89]. Whereas in a typical IRMPD experiment, product ions are obtained by activating the trapped molecular ion with low-power continuous-wave CO_2 laser [90]. The threshold activation of GAGs is often associated with cleavage of the weakest bond especially the sulfate half-ester bond. Various methods geared at avoiding the decomposition of these sulfate groups include modification of the ESI spray solvent, chemical derivatization by permethylation or acetylation [45, 91, 92].

Electron assisted activation: Electron induced fragmentation can be achieved through the transfer of electrons either to or from a multiply charged selected precursor ion [38]. This method of activating molecular ions is fast gaining grounds in the field of mass spectrometry due to their ability to produce backbone fragments essential for structural analysis. The most utilized electron based activation methods for GAG analysis include electron induces dissociation (EID)[93], electron dissociation detachment (EDD)[93-96] and negative electron transfer dissociation (NETD)[97]. The proposed mechanism for the formation of product ions via these activation methods is illustrated in Fig 1.2.

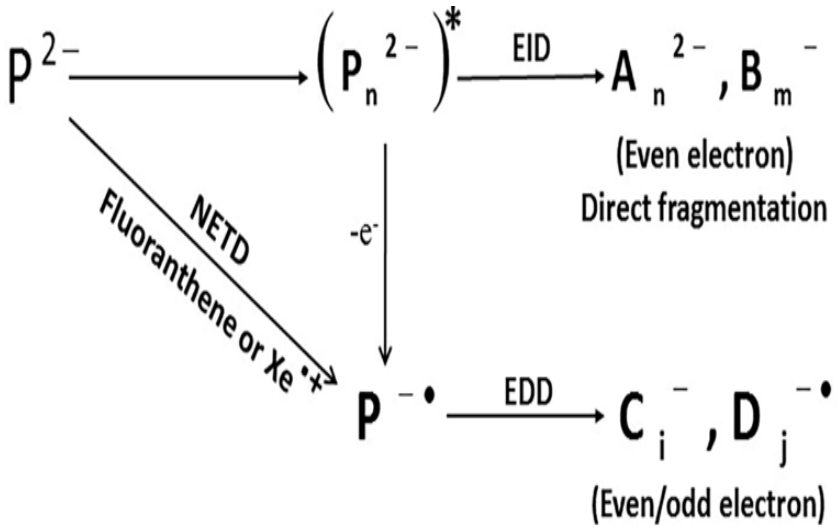

Figure 1. 2 Proposed mechanism for product ion formation via electron-assisted activation of multiply charged precursor ions. Adapted from reference 95.

Two ion activation channels can be accessed upon irradiating selected precursor (P) with low energy (15-20eV) electrons to create an excited state intermediate (P*) [98]. Fragmentation of the intermediate product may occur due to electronic excitation (EID) producing even electron ions or an electron can be detached in the cause of irradiation to create a radical ion. The radical site created on the ion can initiate fragmentation to produce even and odd product ions (EDD) [95]. For NETD, a radical ion is created upon reacting the selected multiply charged precursor ion with a radical cation (either fluoranthene or $Xe^{\cdot+}$) [99]. A radical site is created through the transfer of an electron from the precursor ion to the radical cation. The product ions formed are similar to those of EDD.

MS/MS analysis of sulfated GAGs: Tandem mass spectrometry sequencing of GAGs [100] are routinely achieved through a bottom up approach relying on fully or partially depolymerized oligosaccharides [38]. The micro heterogeneity of GAGs remains a significant challenge. Recent improvements in mass spectrometry methodologies have offered access to critical information pertaining to the assignment of sulfo positions and the C-5 uronic acid stereochemistry. For example, CID activation of CS oligosaccharides has been shown to produce distinct fragment ions whose abundance could be correlated to the pattern of sulfation and C-5 hexuronic acid stereochemistry [101]. CID activation of heparin and HS present a far greater challenge, especially heparin, because of the high sulfate density per disaccharide unit, with their MS/MS spectra often dominated by SO_3 loss fragments. Efficient deprotonation of a majority of the ionisable protons (at least all the sulfate groups) can reduce the occurrence of SO_3 loss fragments [45]. Yet, for a highly

sulfated heparin, for example Arixtra, efficient deprotonation of all the sulfate groups is difficult to achieve due to charge-charge repulsion. Early attempts at sequencing heparin/heparin-like oligomers through CID activation of Ca^{2+} adducted ions proved useful in reducing SO_3 loss fragments [45]. However, their MS/MS spectra produced very few product ions, and were inadequate for structural elucidation. Recent work by Muchena et al.[91, 102] on CID activation of Na^+ adducted heparin/HS GAGs provided highly informative MS/MS spectra. Subsequent CID analysis of Na adducted CS/DS precursor ions revealed diagnostic cross-ring product ions that could differentiate CS from DS (dp4-dp10) [103].

EDD is the most useful electron based activation method for GAG analysis in terms of producing structurally informative fragmentation. EDD provides both cross-ring and glyosidic product ions for structural analysis of GAGs [93, 95, 97, 104-106]. Early work by Wolff et al.[93, 96] also showed the capability of obtaining stereospecific EDD ions (B_3', B_3'-CO_2 and $^{0,2}A_3$) for assigning the C-5 uronic acid stereochemistry moderately sulfated HS tetrasaccharides. EDD MS/MS spectra are often densely populated with peaks, therefore statistical evaluation of the data can be very useful. One of the most useful statistical tools for evaluating EDD data is principal component analysis (PCA) [94, 105, 107]. PCA is a multivariate statistical method that reduces the dimensionality of a large data set into few variables that are capable of finding trends for a large proportion of the data.[108] ESI/FAIMS-EDD experiments projected on PCA plots have been used to differentiate synthetic HS tetrasaccharide epimers.

Even though most GAG analysis targets short oligomers, the ultimate goal for most GAGs MS/MS techniques is to handle the analysis of intact GAGs. The first top-down CID MS/MS analysis on an intact proteoglycan, bikunin, was achieved using high resolution FTICR and FT-orbitrap tandem mass spectrometry [109]. Another very important area in GAG MS/MS approaches is the ability to achieve structural details on individual components in a complex mixture. Gas phase separation techniques coupled with MS/MS have been employed for the analysis of GAG mixtures [110, 111]. While ion mobility mass spectrometry based techniques presents several advantages, a lot remains to be done in terms of their applicability to complex mixtures. A recent method involving sequential derivatization of GAG oligomers prior to LC-MS^n analysis has been developed by Huang et al [112]. In this method, GAG oligosaccharides are first permethylated to protect the free carboxyl and hydroxyl groups. This step is followed by desulfation of the oligomers. The resulting hydroxyl groups are acetylated and the derivatized oligomers are separated on a C18 column prior to MS^n analysis [112]. The application of this method for the analysis of CS hexasaccharides isomers yielded results capable of assigning the structural details of the individual isomers. With the aid of glyosidic product ions, they were able to differentiate the 4-*O* and the 6-*O* GalNAc residues of CS [112]. In subsequent work, derivatized synthetic HS-like oligosaccharides including Arixtra-like heptamer were sequenced using this LC-MS/MS approach [113]. The most recent application of this method afforded the analysis of isomeric and epimeric HS tetrasaccharides. In this report, a series of derivatized synthetic HS tetrasaccharides differing in sulfation and C-5 uronic acid stereochemistry were

analysed using LC-MS/MS.[114]. In the same report, HS oligosaccharide mixtures derived from natural sources were also sequenced.

Automated analysis of GAG MS/MS data

With the current advances in tandem spectrometry analysis of GAGs and the amount of data generated, automation of GAG MS/MS data is increasingly becoming a necessity. The amount of MS/MS data generated for a structural analysis of a GAG may vary depending on the complexity of the structure in terms of sulfation, acetylation, the length of the oligomer and the type of MS/MS technique employed. For example, GAG MS/MS data generated via electron assisted methods like EID, EDD and NETD, are often dense and highly informative compared to CID or IRMPD, thus may require more analysis time. Furthermore, MS/MS spectra complexity may also arise from ions resulting from either sulfate losses or various degrees of cationized fragments ions from the precursor ion. These arising concerns demands computational methods to help facilitate fast and accurate analysis of GAG MS/MS data.

Presently, there are very few accessible platforms for automated interpretation of GAG MS/MS data. A spreadsheet-based heparin sequencing tool HOST was developed in 2005 by Saad et al [115]. This software predicts oligosaccharide sequences by generating and computing the mass(s) of intact and fragment heparin oligomers and matching them against the acquired ESI-MS and ESI-MS/MS data. In another attempt by Spencer et al.[116], a software aimed at predicting the structure and domain organisation of HS oligosaccharide was developed. With their computational models, the average chain of HS

oligosaccharides could be predicted. GlycoWorkbench is one of the easily accessible tools for analysis and interpretation of GAG MS and MS/MS data [117, 118]. The software facilitates faster peak annotations and offers quick structural assembly of GAGs using symbolic graphical annotations [117-119]. Another promising tool called HS-SEQ for sequencing HS GAGs have been developed by Hu et al. [120]. HS-SEQ has been tested on NETD MS/MS data generated from pure HS standards differing in sulfation patterns. The software was able to predict the right structure for these oligomers from a large pool of possible candidates. The large number of analytes present in GAG mixtures and the size of LC-MS/MS data generated could frustrate efforts at obtaining sequence information on individual components [119]. GAG-ID has recently been developed to automate the interpretation of LC-MS/MS data collected on a mixture of twenty-one synthetic HS tetrasaccharides [121]. With the aid of a scoring system based on classification of peaks based on intensity, GAG-ID was able to assign the structures of individual HS tetrasaccharides from a single LC-MS/MS experiment.[114].

The biological significance of GAGs continues to drive the need for high throughput analytical methods to help facilitate structure-function relationship studies. This review highlights the impact of mass spectrometry based methods for the analysis of GAGs in recent years. Current improvement on soft ionization techniques such as MALDI and ESI allows for intact molecular weight measurement with very minimal insource fragmentation of the facile bonds. Structural information pertaining to specific monosaccharide modifications are now possible via a variety of MS/MS based applications (CID, IRMPD, EDD, EID and NETD).

Tandem mass spectrometry techniques including the modification of the ESI spray solvent followed by the activation of sodium cationized precursor ions for the micro-sequencing of GAGs is discussed in Chapters 2-7.

The experimental procedure including sample preparation, ionization and ion activation parameters are discussed in **Chapter 2.** Data processing including multivariate analysis of tandem mass spectrometry highly sulfated GAG oligomers is also presented in this chapter.

C**hapter 3** presents the effect of sodium cationization on EDD fragments of heparin and heparan sulfate oligosaccharides. Two hexasaccharides produced enzymatically and chemically were used for this study. The MS and MS/MS techniques for this experiment is covered in this chapter. The results in this chapter highlights the benefits of sodium adduction in maximizing the amount of useful ions without SO_3 loss.

Chapter 4 investigates the efficiency of providing complete structural information from a single stage MS/MS experiment for the pharmaceutical drug Arixtra. This chapter briefly describes the importance of achieving fully ionize state of highly sulfated GAGs via Na/H exchange. The results for this work is compared to a recently reported work on Arixtra using collisionally induced dissociation of fully deprotonated sodiated molecular ions.

Chapter 5, describes an electron detachment dissociation experiment aimed at assigning the C-5 hexuronic acid stereochemistry of 2-O sulfo heparan sulfate tetrasaccharides. EDD-PCA results presented in this chapter reveals diagnostic ions capable of assigning the C-5 hexuronic acid stereochemistry.

C**hapter 6** presents the efficacy of the diagnostic ions identified in chapter 5 to assign the C-5 hexuronic acid stereochemistry in a broad range of heparan sulfate tetrasaccharides varying in degree of sulfation and disaccharide repeat. In all, 33 synthetically-prepared heparan sulfate tetrasaccharide standards were used for this work. A diagnostic ratio formula is derived from ions selected from the EDD-PCA results**.**

Chapter 7 presents the first tandem mass spectrometry data for fucosylated sulfate oligosaccharides (FCS) from dp3-dp15. Collisionally induced dissociation (CID) experiments have been used to characterize these anomalous CS samples. We have confidently assigned the elemental compositions of these unusual glycosaminoglycans isolated from sea cucumber using accurate mass measurements. Highly informative MS/MS of the isomeric FCS oligomers (FCS-Pg-3,4-*O*S) and (FCS-Ib-2,4-*O*S) isolated from *pearsonothuria graeffei* (FCS-Pg) and *Isostichopus badionotus* (FCS-Ib) were sufficient to assign sites of sulfation and to differentiate the two structural isomers.

References

1. Ly, M., Laremore, T.N., Linhardt, R.J.: Proteoglycomics: recent progress and future challenges. Omics: a journal of integrative biology. **14**, 389-399 (2010)
2. Hardingham, T., Fosang, A.: Proteoglycans: many forms and many functions. The FASEB Journal. **6**, 861-870 (1992)
3. Schaefer, L., Schaefer, R.M.: Proteoglycans: from structural compounds to signaling molecules. Cell and tissue research. **339**, 237-246 (2010)
4. Raman, R., Sasisekharan, V., Sasisekharan, R.: Structural insights into biological roles of protein-glycosaminoglycan interactions. Chemistry & biology. **12**, 267-277 (2005)
5. Esko, J.D., Kimata, K., Lindahl, U.: Proteoglycans and sulfated glycosaminoglycans. (2009)
6. Esko, J.D., Lindahl, U.: Molecular diversity of heparan sulfate. Journal of Clinical Investigation. **108**, 169 (2001)
7. Xu, D., Esko, J.D.: Demystifying heparan sulfate-protein interactions. Annual review of biochemistry. **83**, 129-157 (2014)
8. Staples, G.O., Zaia, J.: Analysis of glycosaminoglycans using mass spectrometry. Current proteomics. **8**, 325 (2011)
9. Gallagher, J.T., Lyon, M.: Heparan Sulfate. Proteoglycans: Structure, Biology And Molecular Interactions. 27 (2000)
10. Venkataraman, G., Shriver, Z., Raman, R., Sasisekharan, R.: Sequencing complex polysaccharides. Science. **286**, 537-542 (1999)

11. HÖÖ, M., Lindahl, U., Iverius, P.-H.: Distribution of sulphate and iduronic acid residues in heparin and heparan sulphate. Biochemical Journal. **137**, 33-43 (1974)

12. Shriver, Z., Capila, I., Venkataraman, G., Sasisekharan, R.: Heparin and heparan sulfate: analyzing structure and microheterogeneity. Springer, (2012)

13. Sampaio, L.O., Tersariol, I.L., Lopes, C.C., Bouças, R.I., Nascimento, F.D., Rocha, H.A., Nader, H.B.: Heparins and heparans sulfates. Structure, distribution and protein interactions. Insights into carbohydrate structure and biological function. Kerala: Transworld Research Network. 51-61 (2006)

14. Teien, A.N., Abildgaard, U., Höök, M.: The anticoagulant effect of heparan sulfate and dermatan sulfate. Thrombosis research. **8**, 859-867 (1976)

15. Sasisekharan, R., Raman, R., Prabhakar, V.: Glycomics approach to structure-function relationships of glycosaminoglycans. Annu. Rev. Biomed. Eng. **8**, 181-231 (2006)

16. Rek, A., Krenn, E., Kungl, A.: Therapeutically targeting protein–glycan interactions. British journal of pharmacology. **157**, 686-694 (2009)

17. Wijnhoven, T.J., Van De Westerlo, E.M., Smits, N.C., Lensen, J.F., Rops, A.L., Van Der Vlag, J., Berden, J.H., Van Den Heuvel, L.P., van Kuppevelt, T.H.: Characterization of anticoagulant heparinoids by immunoprofiling. Glycoconjugate journal. **25**, 177-185 (2008)

18. Watanabe, H., Yamada, Y., Kimata, K.: Roles of aggrecan, a large chondroitin sulfate proteoglycan, in cartilage structure and function. Journal of biochemistry. **124**, 687-693 (1998)

19. Funderburgh, J.L.: MINI REVIEW Keratan sulfate: structure, biosynthesis, and function. Glycobiology. **10**, 951-958 (2000)

20. Funderburgh, J.L.: Keratan sulfate biosynthesis. IUBMB life. **54**, 187-194 (2002)

21. Necas, J., Bartosikova, L., Brauner, P., Kolar, J.: Hyaluronic acid (hyaluronan): a review. Veterinarni medicina. **53**, 397-411 (2008)

22. Meyer, K.: The biological significance of hyaluronic acid and hyaluronidase. Physiological reviews. **27**, 335-359 (1947)

23. Weigel, P.H., Fuller, G.M., LeBoeuf, R.D.: A model for the role of hyaluronic acid and fibrin in the early events during the inflammatory response and wound healing. Journal of theoretical biology. **119**, 219-234 (1986)

24. Joseph, P.R.B., Poluri, K.M., Sepuru, K.M., Rajarathnam, K.: Characterizing protein–glycosaminoglycan interactions using solution NMR spectroscopy. Glycosaminoglycans: Chemistry and Biology. 325-333 (2015)

25. Yarema, K.J. CRC Press, (2005)

26. Toida, T., Vlahov, I.R., Smith, A.E., Hileman, R.E., Linhardt, R.J.: C-2 epimerization of N-acetylglucosamine in an oligosaccharide derived from heparan sulfate. Journal of carbohydrate chemistry. **15**, 351-360 (1996)

27. Esko, J.D.: Special considerations for proteoglycans and glycosaminoglycans and their purification. Current protocols in molecular biology. 17.12. 11-17.12. 19 (2001)

28. Conrad, H.E.: β- Elimination for Release of O- Linked Glycosaminoglycans from Proteoglycans. Current Protocols in Molecular Biology. 17.15. 11-17.15. 13 (2001)

29. Ouyang, Y., Wu, C., Sun, X., Liu, J., Linhardt, R.J., Zhang, Z.: Development of hydrophilic interaction chromatography with quadruple time- of- flight mass spectrometry for heparin and low molecular weight heparin disaccharide analysis. Rapid Communications in Mass Spectrometry. **30**, 277-284 (2016)

30. Zaia, J.: On- line separations combined with MS for analysis of glycosaminoglycans. Mass spectrometry reviews. **28**, 254-272 (2009)

31. Linhardt, R.J.: Analysis of glycosaminoglycans with polysaccharide lyases. Current protocols in molecular biology. 17.13 B. 11-17.13 B. 16 (2001)

32. Laremore, T.N., Leach, F.E., Solakyildirim, K., Amster, I.J., Linhardt, R.J.: Chapter Three-Glycosaminoglycan Characterization by Electrospray Ionization Mass Spectrometry Including Fourier Transform Mass Spectrometry. Methods in enzymology. **478**, 79-108 (2010)

33. Zaia, J.: Mass spectrometric ionization of carbohydrates. Encyclopedia of mass spectrometry. **6**, (2007)

34. Shively, J.E., Conrad, H.E.: Formation of anhydrosugars in the chemical depolymerization of heparin. Biochemistry. **15**, 3932-3942 (1976)

35. Garg, H.G., Linhardt, R.J., Hales, C.A. Elsevier, (2011)

36. Gill, V.L., Aich, U., Rao, S., Pohl, C., Zaia, J.: Disaccharide analysis of glycosaminoglycans using hydrophilic interaction chromatography and mass spectrometry. Analytical chemistry. **85**, 1138-1145 (2013)

37. Chi, L., Amster, J., Linhardt, R.J.: Mass spectrometry for the analysis of highly charged sulfated carbohydrates. Current Analytical Chemistry. **1**, 223-240 (2005)

38. Kailemia, M.J., Ruhaak, L.R., Lebrilla, C.B., Amster, I.J.: Oligosaccharide analysis by mass spectrometry: a review of recent developments. Analytical chemistry. **86**, 196-212 (2013)

39. Juhasz, P., Biemann, K.: Mass spectrometric molecular-weight determination of highly acidic compounds of biological significance via their complexes with basic polypeptides. Proceedings of the National Academy of Sciences. **91**, 4333-4337 (1994)

40. Juhasz, P., Biemann, K.: Utility of non-covalent complexes in the matrix-assisted laser desorption ionization mass spectrometry of heparin-derived oligosaccharides. Carbohydrate research. **270**, 131-147 (1995)

41. Laremore, T.N., Zhang, F., Linhardt, R.J.: Ionic liquid matrix for direct UV-MALDI-TOF-MS analysis of dermatan sulfate and chondroitin sulfate oligosaccharides. Analytical chemistry. **79**, 1604-1610 (2007)

42. Tissot, B., Gasiunas, N., Powell, A.K., Ahmed, Y., Zhi, Z.-l., Haslam, S.M., Morris, H.R., Turnbull, J.E., Gallagher, J.T., Dell, A.: Towards GAG

glycomics: analysis of highly sulfated heparins by MALDI-TOF mass spectrometry. Glycobiology. **17**, 972-982 (2007)

43. Ohara, K., Jacquinet, J.-C., Jouanneau, D., Helbert, W., Smietana, M., Vasseur, J.-J.: Matrix-assisted laser desorption/ionization mass spectrometric analysis of polysulfated-derived oligosaccharides using pyrenemethylguanidine. Journal of the American Society for Mass Spectrometry. **20**, 131-137 (2009)
44. Zaia, J.: Principles of mass spectrometry of glycosaminoglycans. J Biomacromol Mass Spectrom. **1**, 3-36 (2005)
45. Zaia, J., Costello, C.E.: Tandem mass spectrometry of sulfated heparin-like glycosaminoglycan oligosaccharides. Analytical chemistry. **75**, 2445-2455 (2003)
46. Wolff, J.J., Laremore, T.N., Busch, A.M., Linhardt, R.J., Amster, I.J.: Influence of charge state and sodium cationization on the electron detachment dissociation and infrared multiphoton dissociation of glycosaminoglycan oligosaccharides. Journal of the American Society for Mass Spectrometry. **19**, 790-798 (2008)
47. Zaia, J.: Glycosaminoglycan glycomics using mass spectrometry. Molecular & Cellular Proteomics. **12**, 885-892 (2013)
48. Yang, B., Solakyildirim, K., Chang, Y., Linhardt, R.J.: Hyphenated techniques for the analysis of heparin and heparan sulfate. Analytical and bioanalytical chemistry. **399**, 541-557 (2011)

49. Zaia, J., Costello, C.E.: Compositional analysis of glycosaminoglycans by electrospray mass spectrometry. Analytical chemistry. **73**, 233-239 (2001)

50. Saad, O.M., Leary, J.A.: Compositional analysis and quantification of heparin and heparan sulfate by electrospray ionization ion trap mass spectrometry. Analytical chemistry. **75**, 2985-2995 (2003)

51. Behr, J.R., Matsumoto, Y., White, F.M., Sasisekharan, R.: Quantification of isomers from a mixture of twelve heparin and heparan sulfate disaccharides using tandem mass spectrometry. Rapid communications in mass spectrometry. **19**, 2553-2562 (2005)

52. Jones, C.J., Beni, S., Limtiaco, J.F., Langeslay, D.J., Larive, C.K.: Heparin characterization: challenges and solutions. Annual Review of Analytical Chemistry. **4**, 439-465 (2011)

53. Kuberan, B., Lech, M., Zhang, L., Wu, Z.L., Beeler, D.L., Rosenberg, R.D.: Analysis of heparan sulfate oligosaccharides with ion pair-reverse phase capillary high performance liquid chromatography-microelectrospray ionization time-of-flight mass spectrometry. Journal of the American Chemical Society. **124**, 8707-8718 (2002)

54. Thanawiroon, C., Rice, K.G., Toida, T., Linhardt, R.J.: Liquid chromatography/mass spectrometry sequencing approach for highly sulfated heparin-derived oligosaccharides. Journal of Biological Chemistry. **279**, 2608-2615 (2004)

55. Henriksen, J., Roepstorff, P., Ringborg, L.H.: Ion-pairing reversed-phased chromatography/mass spectrometry of heparin. Carbohydrate research. **341**, 382-387 (2006)

56. Li, D., Chi, L., Jin, L., Xu, X., Du, X., Ji, S., Chi, L.: Mapping of low molecular weight heparins using reversed phase ion pair liquid chromatography–mass spectrometry. Carbohydrate polymers. **99**, 339-344 (2014)

57. Zhang, Z., Xie, J., Liu, H., Liu, J., Linhardt, R.J.: Quantification of heparan sulfate disaccharides using ion-pairing reversed-phase microflow high-performance liquid chromatography with electrospray ionization trap mass spectrometry. Analytical chemistry. **81**, 4349-4355 (2009)

58. Volpi, N.: High-performance liquid chromatography and on-line mass spectrometry detection for the analysis of chondroitin sulfates/hyaluronan disaccharides derivatized with 2-aminoacridone. Analytical biochemistry. **397**, 12-23 (2010)

59. Yang, B., Chang, Y., Weyers, A.M., Sterner, E., Linhardt, R.J.: Disaccharide analysis of glycosaminoglycan mixtures by ultra-high-performance liquid chromatography–mass spectrometry. Journal of Chromatography A. **1225**, 91-98 (2012)

60. MacNair, J.E., Lewis, K.C., Jorgenson, J.W.: Ultrahigh-pressure reversed-phase liquid chromatography in packed capillary columns. Analytical chemistry. **69**, 983-989 (1997)

61. Korir, A.K., Limtiaco, J.F., Gutierrez, S.M., Larive, C.K.: Ultraperformance ion-pair liquid chromatography coupled to electrospray time-of-flight mass spectrometry for compositional profiling and quantification of heparin and heparan sulfate. Analytical chemistry. **80**, 1297-1306 (2008)

62. Yang, B., Weyers, A., Baik, J.Y., Sterner, E., Sharfstein, S., Mousa, S.A., Zhang, F., Dordick, J.S., Linhardt, R.J.: Ultra-performance ion-pairing liquid chromatography with on-line electrospray ion trap mass spectrometry for heparin disaccharide analysis. Analytical biochemistry. **415**, 59-66 (2011)

63. Solakyildirim, K., Zhang, Z., Linhardt, R.J.: Ultraperformance liquid chromatography with electrospray ionization ion trap mass spectrometry for chondroitin disaccharide analysis. Analytical biochemistry. **397**, 24-28 (2010)

64. Jandera, P.: Stationary and mobile phases in hydrophilic interaction chromatography: a review. Analytica Chimica Acta. **692**, 1-25 (2011)

65. Staples, G.O., Bowman, M.J., Costello, C.E., Hitchcock, A.M., Lau, J.M., Leymarie, N., Miller, C., Naimy, H., Shi, X., Zaia, J.: A chip- based amide-HILIC LC/MS platform for glycosaminoglycan glycomics profiling. Proteomics. **9**, 686-695 (2009)

66. Li, G., Steppich, J., Wang, Z., Sun, Y., Xue, C., Linhardt, R.J., Li, L.: Bottom-Up Low Molecular Weight Heparin Analysis Using Liquid Chromatography-Fourier Transform Mass Spectrometry for Extensive Characterization. Analytical chemistry. **86**, 6626-6632 (2014)

67. Kostanski, L.K., Keller, D.M., Hamielec, A.E.: Size-exclusion chromatography—a review of calibration methodologies. Journal of biochemical and biophysical methods. **58**, 159-186 (2004)

68. Hong, P., Koza, S., Bouvier, E.S.: A review size-exclusion chromatography for the analysis of protein biotherapeutics and their aggregates. Journal of liquid chromatography & related technologies. **35**, 2923-2950 (2012)

69. Staples, G.O., Shi, X., Zaia, J.: Glycomics analysis of mammalian heparan sulfates modified by the human extracellular sulfatase HSulf2. PLoS One. **6**, e16689 (2011)

70. Staples, G.O., Shi, X., Zaia, J.: Extended N-sulfated domains reside at the nonreducing end of heparan sulfate chains. Journal of Biological Chemistry. **285**, 18336-18343 (2010)

71. Shi, X., Zaia, J.: Organ-specific heparan sulfate structural phenotypes. Journal of Biological Chemistry. **284**, 11806-11814 (2009)

72. Shao, C., Shi, X., Phillips, J.J., Zaia, J.: Mass spectral profiling of glycosaminoglycans from histological tissue surfaces. Analytical chemistry. **85**, 10984-10991 (2013)

73. Chaplin, M., Kennedy, J., Charlwood, J., Birrell, H., Tolson, D., Camilleri, P., Guille, G., Rudd, P., Wing, D., Prime, S.: POROUS GRAPHITIC CARBON: LIQUID CHROMATOGRAPHY. chemistry. **240**, 226 (2000)

74. Wei, W., Niñonuevo, M.R., Sharma, A., Danan-Leon, L.M., Leary, J.A.: A comprehensive compositional analysis of heparin/heparan sulfate-derived

disaccharides from human serum. Analytical chemistry. **83**, 3703-3708 (2011)

75. Barroso, B., Didraga, M., Bischoff, R.: Analysis of proteoglycans derived sulphated disaccharides by liquid chromatography/mass spectrometry. Journal of Chromatography A. **1080**, 43-48 (2005)

76. Estrella, R.P., Whitelock, J.M., Packer, N.H., Karlsson, N.G.: Graphitized carbon LC-MS characterization of the chondroitin sulfate oligosaccharides of aggrecan. Analytical chemistry. **79**, 3597-3606 (2007)

77. Gill, V.L., Wang, Q., Shi, X., Zaia, J.: Mass spectrometric method for determining the uronic acid epimerization in heparan sulfate disaccharides generated using nitrous acid. Analytical chemistry. **84**, 7539-7546 (2012)

78. Zamfir, A.D.: Applications of capillary electrophoresis- electrospray ionization mass spectrometry in glycosaminoglycan analysis. Electrophoresis. (2015)

79. Amon, S., Zamfir, A.D., Rizzi, A.: Glycosylation analysis of glycoproteins and proteoglycans using capillary electrophoresis- mass spectrometry strategies. Electrophoresis. **29**, 2485-2507 (2008)

80. Sisu, E., Flangea, C., Serb, A., Zamfir, A.D.: Modern developments in mass spectrometry of chondroitin and dermatan sulfate glycosaminoglycans. Amino Acids. **41**, 235-256 (2011)

81. Volpi, N., Maccari, F., Linhardt, R.J.: Capillary electrophoresis of complex natural polysaccharides. Electrophoresis. **29**, 3095-3106 (2008)

82. ZARE, R.N.: Capillary electrophoresis. Science. **242**, 224-228 (1988)

83. Duteil, S., Gareil, P., Girault, S., Mallet, A., Feve, C., Siret, L.: Identification of heparin oligosaccharides by direct coupling of capillary electrophoresis/Ionspray- Mass spectrometry. Rapid communications in mass spectrometry. **13**, 1889-1898 (1999)

84. Ruiz-Calero, V., Moyano, E., Puignou, L., Galceran, M.: Pressure-assisted capillary electrophoresis–electrospray ion trap mass spectrometry for the analysis of heparin depolymerised disaccharides. Journal of Chromatography A. **914**, 277-291 (2001)

85. Sun, X., Lin, L., Liu, X., Zhang, F., Chi, L., Xia, Q., Linhardt, R.J.: Capillary Electrophoresis-Mass Spectrometry for the Analysis of Heparin Oligosaccharides and Low Molecular Weight Heparin. Analytical chemistry. (2015)

86. Zaia, J.: Mass spectrometry of oligosaccharides. Mass spectrometry reviews. **23**, 161-227 (2004)

87. Li, L., Ly, M., Linhardt, R.J.: Proteoglycan sequence. Molecular bioSystems. **8**, 1613-1625 (2012)

88. Domon, B., Costello, C.E.: A systematic nomenclature for carbohydrate fragmentations in FAB-MS/MS spectra of glycoconjugates. Glycoconjugate journal. **5**, 397-409 (1988)

89. Li, B., An, H.J., Hedrick, J.L., Lebrilla, C.B.: Collision-induced dissociation tandem mass spectrometry for structural elucidation of glycans. Glycomics: Methods and Protocols. 133-145 (2009)

90. Sleno, L., Volmer, D.A.: Ion activation methods for tandem mass spectrometry. Journal of mass spectrometry. **39**, 1091-1112 (2004)

91. Kailemia, M.J., Li, L., Xu, Y., Liu, J., Linhardt, R.J., Amster, I.J.: Structurally informative tandem mass spectrometry of highly sulfated natural and chemoenzymatically synthesized heparin and heparan sulfate glycosaminoglycans. Molecular & Cellular Proteomics. **12**, 979-990 (2013)

92. Shi, X., Huang, Y., Mao, Y., Naimy, H., Zaia, J.: Tandem mass spectrometry of heparan sulfate negative ions: sulfate loss patterns and chemical modification methods for improvement of product ion profiles. Journal of the American Society for Mass Spectrometry. **23**, 1498-1511 (2012)

93. Wolff, J.J., Laremore, T.N., Aslam, H., Linhardt, R.J., Amster, I.J.: Electron-induced dissociation of glycosaminoglycan tetrasaccharides. Journal of the American Society for Mass Spectrometry. **19**, 1449-1458 (2008)

94. Leach III, F.E., Ly, M., Laremore, T.N., Wolff, J.J., Perlow, J., Linhardt, R.J., Amster, I.J.: Hexuronic acid stereochemistry determination in chondroitin sulfate glycosaminoglycan oligosaccharides by electron detachment dissociation. Journal of the American Society for Mass Spectrometry. **23**, 1488-1497 (2012)

95. Wolff, J.J., Amster, I.J., Chi, L., Linhardt, R.J.: Electron detachment dissociation of glycosaminoglycan tetrasaccharides. Journal of the American Society for Mass Spectrometry. **18**, 234-244 (2007)

96. Wolff, J.J., Chi, L., Linhardt, R.J., Amster, I.J.: Distinguishing glucuronic from iduronic acid in glycosaminoglycan tetrasaccharides by using electron detachment dissociation. Analytical chemistry. **79**, 2015-2022 (2007)

97. Wolff, J.J., Leach III, F.E., Laremore, T.N., Kaplan, D.A., Easterling, M.L., Linhardt, R.J., Amster, I.J.: Negative electron transfer dissociation of glycosaminoglycans. Analytical chemistry. **82**, 3460-3466 (2010)

98. Leach, F.E., Arungundram, S., Al-Mafraji, K., Venot, A., Boons, G.-J., Amster, I.J.: Electron detachment dissociation of synthetic heparan sulfate glycosaminoglycan tetrasaccharides varying in degree of sulfation and hexuronic acid stereochemistry. International journal of mass spectrometry. **330**, 152-159 (2012)

99. Huzarska, M., Ugalde, I., Kaplan, D.A., Hartmer, R., Easterling, M.L., Polfer, N.C.: Negative electron transfer dissociation of deprotonated phosphopeptide anions: choice of radical cation reagent and competition between electron and proton transfer. Analytical chemistry. **82**, 2873-2878 (2010)

100. Coon, J.J., Shabanowitz, J., Hunt, D.F., Syka, J.E.: Electron transfer dissociation of peptide anions. Journal of the American Society for Mass Spectrometry. **16**, 880-882 (2005)

101. Zaia, J., Li, X.-Q., Chan, S.-Y., Costello, C.E.: Tandem mass spectrometric strategies for determination of sulfation positions and uronic acid epimerization in chondroitin sulfate oligosaccharides. Journal of the American Society for Mass Spectrometry. **14**, 1270-1281 (2003)

102. Kailemia, M.J., Li, L., Ly, M., Linhardt, R.J., Amster, I.J.: Complete mass spectral characterization of a synthetic ultralow-molecular-weight heparin using collision-induced dissociation. Analytical chemistry. **84**, 5475-5478 (2012)

103. Kailemia, M.J., Patel, A.B., Johnson, D.T., Li, L., Linhardt, R.J., Amster, I.J.: Differentiating Chondroitin Sulfate Glycosaminoglycans using CID; Uronic Acid Cross-Ring Diagnostic Fragments in a Single Stage of MS/MS. European journal of mass spectrometry (Chichester, England). **21**, 275 (2015)

104. Huang, Y., Yu, X., Mao, Y., Costello, C.E., Zaia, J., Lin, C.: De novo sequencing of heparan sulfate oligosaccharides by electron-activated dissociation. Analytical chemistry. **85**, 11979-11986 (2013)

105. Agyekum, I., Patel, A.B., Zong, C., Boons, G.-J., Amster, I.J.: Assignment of hexuronic acid stereochemistry in synthetic heparan sulfate tetrasaccharides with 2-O-sulfo uronic acids using electron detachment dissociation. International journal of mass spectrometry. **390**, 163-169 (2015)

106. Agyekum, I., Zong, C., Boons, G.-J., Amster, I.J.: Single Stage Tandem Mass Spectrometry Assignment of the C-5 Uronic Acid Stereochemistry in Heparan Sulfate Tetrasaccharides using Electron Detachment Dissociation. Journal of The American Society for Mass Spectrometry. 1-10 (2017)

107. Oh, H.B., Leach III, F.E., Arungundram, S., Al-Mafraji, K., Venot, A., Boons, G.-J., Amster, I.J.: Multivariate analysis of electron detachment dissociation and infrared multiphoton dissociation mass spectra of heparan

sulfate tetrasaccharides differing only in hexuronic acid stereochemistry. Journal of the American Society for Mass Spectrometry. **22**, 582-590 (2011)

108. Ringnér, M.: What is principal component analysis? Nature biotechnology. **26**, 303-304 (2008)

109. Ly, M., Leach III, F.E., Laremore, T.N., Toida, T., Amster, I.J., Linhardt, R.J.: The proteoglycan bikunin has a defined sequence. Nature chemical biology. **7**, 827-833 (2011)

110. Kailemia, M.J., Park, M., Kaplan, D.A., Venot, A., Boons, G.-J., Li, L., Linhardt, R.J., Amster, I.J.: High-field asymmetric-waveform ion mobility spectrometry and electron detachment dissociation of isobaric mixtures of glycosaminoglycans. Journal of The American Society for Mass Spectrometry. **25**, 258-268 (2014)

111. Seo, Y., Andaya, A., Leary, J.A.: Preparation, separation, and conformational analysis of differentially sulfated heparin octasaccharide isomers using ion mobility mass spectrometry. Analytical chemistry. **84**, 2416-2423 (2012)

112. Huang, R., Pomin, V.H., Sharp, J.S.: LC-MS n analysis of isomeric chondroitin sulfate oligosaccharides using a chemical derivatization strategy. Journal of the American Society for Mass Spectrometry. **22**, 1577-1587 (2011)

113. Huang, R., Liu, J., Sharp, J.S.: An approach for separation and complete structural sequencing of heparin/heparan sulfate-like oligosaccharides. Analytical chemistry. **85**, 5787-5795 (2013)

114. Huang, R., Zong, C., Venot, A., Chiu, Y., Zhou, D., Boons, G.-J., Sharp, J.S.: The de novo Sequencing of Complex Mixtures of Heparan Sulfate Oligosaccharides. (2016)

115. Saad, O.M., Leary, J.A.: Heparin sequencing using enzymatic digestion and ESI-MS n with HOST: a heparin/HS oligosaccharide sequencing tool. Analytical chemistry. **77**, 5902-5911 (2005)

116. Spencer, J.L., Bernanke, J.A., Buczek-Thomas, J.A., Nugent, M.A.: A computational approach for deciphering the organization of glycosaminoglycans. PLoS One. **5**, e9389 (2010)

117. Tissot, B.r.r., Ceroni, A., Powell, A.K., Morris, H.R., Yates, E.A., Turnbull, J.E., Gallagher, J.T., Dell, A., Haslam, S.M.: Software tool for the structural determination of glycosaminoglycans by mass spectrometry. Analytical chemistry. **80**, 9204-9212 (2008)

118. Damerell, D., Ceroni, A., Maass, K., Ranzinger, R., Dell, A., Haslam, S.M.: The GlycanBuilder and GlycoWorkbench glycoinformatics tools: updates and new developments. (2012)

119. Ceroni, A., Maass, K., Geyer, H., Geyer, R., Dell, A., Haslam, S.M.: GlycoWorkbench: a tool for the computer-assisted annotation of mass spectra of glycans†. Journal of proteome research. **7**, 1650-1659 (2008)

120. Hu, H., Huang, Y., Mao, Y., Yu, X., Xu, Y., Liu, J., Zong, C., Boons, G.-J., Lin, C., Xia, Y.: A computational framework for heparan sulfate sequencing using high-resolution tandem mass spectra. Molecular & Cellular Proteomics. **13**, 2490-2502 (2014)

121. Chiu, Y., Huang, R., Orlando, R., Sharp, J.S.: GAG-ID: Heparan Sulfate (HS) and Heparin Glycosaminoglycan High-Throughput Identification Software. Molecular & Cellular Proteomics. **14**, 1720-1730 (2015)

122. Ceroni, A., Maass, K., Geyer, H., Geyer, R., Dell, A., Haslam, S.M.: GlycoWorkbench: a tool for the computer-assisted annotation of mass spectra of glycans†. Journal of proteome research. **7**, 1650-1659 (2008)

123. Hu, H., Huang, Y., Mao, Y., Yu, X., Xu, Y., Liu, J., Zong, C., Boons, G.-J., Lin, C., Xia, Y.: A computational framework for heparan sulfate sequencing using high-resolution tandem mass spectra. Molecular & Cellular Proteomics. **13**, 2490-2502 (2014)

124. Chiu, Y., Huang, R., Orlando, R., Sharp, J.S.: GAG-ID: Heparan Sulfate (HS) and Heparin Glycosaminoglycan High-Throughput Identification Software. Molecular & Cellular Proteomics. **14**, 1720-1730 (2015)

CHAPTER 2

EXPERIMENTAL METHODS

Heparin and heparan sulfate oligosaccharides

Heparin oligosaccharides were obtained via enzymatic depolymerization of heparan sulfate sodium salt (Celsus Laboratories, Cincinnati, OH) using recombinant heparinase 1 (EC 4.2.2.7) followed by strong-anion-exchange-HPLC and gradient PAGE. SP-Sephadex at acidic pH 3.5 was used to remove the proteins (BSA and heparinase 1) [1]. A mixture of heparin derived oligosaccharides were then fractionated through a controlled pore membrane (mol. Wt > 5000) by pressure filtration and later size fractionated by gel column chromatography [1]. The separation step afforded oligosaccharide residues of varying sizes ranging from disaccharides to tetradeccasaccharides. A detailed account of this procedure can be found in ref [1].

Synthetic Heparan Sulfate Tetrasaccharides and Hexasaccharide

Thirty-three heparan sulfate tetrasaccharide deferring in degree of sulfation, stereochemistry and disaccharide repeat including one hexasaccharide were synthesized by a modular approach and purified by silica gel column chromatography [3, 4]. The structures of the heparan sulfates oligosaccharides were further confirmed by ^{1}H and HSQC NMR spectroscopy.

Fucosylated Chondroitin sulfate oligosaccharides

Fucosylated chondroitin sulfate polysaccharides were prepared based on a previously published protocol by Zou et al. [5]. A detailed account on how the various fractions of FCS oligomers were obtained and characterized is described in reference [6, 7]. Briefly, FCS polysaccharides isolated from two sea cucumber species Isostichopus badionotus (FCS -Ib) and pearsonothuria graeffei FCS -Pg were subjected to deaminative cleavage via nitrous degradation. The resulting oligosaccharides were further purified and characterized using IR and ^{1}H NMR spectroscopy [6-8]. A comprehensive account on the isolation, purification and characterization of the FCS oligomers is also given in chapter 7.

Mass spectrometry analysis

All ESI-MS and MS/MS analysis were done on a 9.4 Bruker Apex Ultra Qh-FTICR mass spectrometer. GAG oligosaccharides were directly infused at the rate of 120µL/hr at 0.1-0.2 mg/mL concentrations in 50:50 methanol:H_2O and ionized using negative mode using metal capillary. Approximately 0.1mM of NaOH was used as a spray solvent modifier to stabilize the facile half sulfate bonds.

First stage MS were obtained to enable the assignment of the elemental composition of the GAG oligomers. Precursor ions of interest are isolated in the quadruple for MS/MS analysis. Cross-ring and glycosidic ions obtained from the MS/MS experiments are used to assign specific sites of sulfation.

Electron detachment dissociation (EDD)

For all EDD experiments, multiply charged precursor ions selected in the quadrupole with a 3Da isolation mass window are sent into the ICR cell. These ions are

then irradiated with for 1s while the cathode heater, ECD lens and cathode bias are held at 1A, ~18.5 – 19eV and -18.6 respectively. 512k-1M data points were summed over 24-34 scans, padded with zero fills and apodized using a sinebell window. The acquired mass spectra were externally calibrated to produce a mass accuracy of 5 ppm. It was followed by internal calibration using confidently assigned glycosidic product ions as internal calibrant to produce a mass accuracy of < 1 ppm. Only peaks with S/N > 10 are considered due to the large low intensity of EDD product ions. Accurate mass measurement of glycosidic cleavage and cross-ring product ions enabled the assignment of structure with the aid of Glycoworkbench [9, 10]. These ions are reported using the Domon and Costello nomenclature [11]

Collisional induced dissociation (CID)

CID activation of carefully selected precursor ions occurred in the collision cell using argon as the collision gas. Similar to the EDD experiment, 512k-1M data points were acquired for each spectrum and summed over 24-64 scans depending on the intensity of the parent ion and the product ions in the spectra. Both external and internal calibration were carried out as described above, with product ions assignment achieved using accurate mass measurement and Glycoworkbench [9, 10]. Again, we have assigned product ions using the Domon and Costello nomenclature [11].

Principal component analysis (PCA) and Diagnostic Ratio (DR) Analysis

Principal component analysis (PCA) on quintuplicate EDD spectra acquired on the same day was performed using PLS Toolbox (Eigenvector Research, Inc.,

Wenatchee, WA). The abundances of 20 most intense product ions are normalized in reference to the total ion current (TIC) of each EDD spectrum. The normalized product ions are then pre-processed by mean centering the data and cross-validating prior to the PCA analysis. The two most informative plots generated for the data are the loadings and the scores plots. The scores plot depicts the differences in the samples sets being analyzed while the loading plots reveals the specific ions responsible for the differences.

Carefully selected diagnostic ions obtained from the EDA-PCA loadings plot can reveal subtle information in assigning stereochemistry. This ions from our experiments has been expressed as a ratio that can be used to predict the stereochemistry of heparan sulfate tetrasaccharides.

References

1. Pervin, A., Gallo, C., Jandik, K.A., Han, X.-J., Linhardt, R.J.: Preparation and structural characterization of large heparin-derived oligosaccharides. Glycobiology. **5**, 83-95 (1995)
2. Liu, R., Xu, Y., Chen, M., Weïwer, M., Zhou, X., Bridges, A.S., DeAngelis, P.L., Zhang, Q., Linhardt, R.J., Liu, J.: Chemoenzymatic design of heparan sulfate oligosaccharides. Journal of Biological Chemistry. **285**, 34240-34249 (2010)
3. Arungundram, S., Al-Mafraji, K., Asong, J., Leach III, F.E., Amster, I.J., Venot, A., Turnbull, J.E., Boons, G.-J.: Modular synthesis of heparan sulfate oligosaccharides for structure− activity relationship studies. Journal of the American Chemical Society. **131**, 17394-17405 (2009)
4. Zong, C., Venot, A., Dhamale, O., Boons, G.-J.: Fluorous supported modular synthesis of heparan sulfate oligosaccharides. Organic letters. **15**, 342-345 (2013)
5. Zou, Z.-R., Yi, Y.-H., Wu, H.-M., Wu, J.-H., Liaw, C.-C., Lee, K.-H.: Intercedensides A− C, three new cytotoxic triterpene glycosides from the sea cucumber Mensamaria intercedens Lampert. Journal of natural products. **66**, 1055-1060 (2003)
6. Chen, S., Li, G., Wu, N., Guo, X., Liao, N., Ye, X., Liu, D., Xue, C., Chai, W.: Sulfation pattern of the fucose branch is important for the anticoagulant and antithrombotic activities of fucosylated chondroitin sulfates. Biochimica et Biophysica Acta (BBA)-General Subjects. **1830**, 3054-3066 (2013)

7. Wu, N., Ye, X., Guo, X., Liao, N., Yin, X., Hu, Y., Sun, Y., Liu, D., Chen, S.: Depolymerization of fucosylated chondroitin sulfate from sea cucumber, Pearsonothuria graeffei, via 60 Co irradiation. Carbohydrate polymers. **93**, 604-614 (2013)

8. Chen, S., Xue, C., Tang, Q., Yu, G., Chai, W.: Comparison of structures and anticoagulant activities of fucosylated chondroitin sulfates from different sea cucumbers. Carbohydrate Polymers. **83**, 688-696 (2011)

9. Ceroni, A., Maass, K., Geyer, H., Geyer, R., Dell, A., Haslam, S.M.: GlycoWorkbench: a tool for the computer-assisted annotation of mass spectra of glycans†. Journal of proteome research. **7**, 1650-1659 (2008)

10. Damerell, D., Ceroni, A., Maass, K., Ranzinger, R., Dell, A., Haslam, S.M.: Annotation of glycomics MS and MS/MS spectra using the GlycoWorkbench software tool. Glycoinformatics. 3-15 (2015)

11. Domon, B., Costello, C.E.: A systematic nomenclature for carbohydrate fragmentations in FAB-MS/MS spectra of glycoconjugates. Glycoconjugate journal. **5**, 397-409 (1988)

CHAPTER 3

Effect of Sodium Cationization on Electron Detachment Dissociation of Heparin and Heparan Sulfate Oligomers

To be submitted as:

Agyekum, I; Zong, C.; Boons, G.-J.; Amster, I. J., "Effect of Sodium Cationization on Electron Detachment Dissociation of Heparin and Heparan Sulfate Oligomers", *J. Am. Soc. Mass Spectrom.*,

Abstract

Heparin (Hp) and heparan (HS) oligosaccharides are important biomolecules that have been implicated in very important biological processes including cell growth and division, cell-cell signaling, angiogenesis, and are known bind other proteins. In order to fully exploit the properties of these structurally complex polysaccharides, it is very important to link these biological activities with their fine structure. However, structural characterization of Hp/HS using tandem mass spectrometry has been accompanied with unwanted loss of its labile sulfate groups. SO_3 decomposition observed during ion activation has been attributed to the high sulfate density making Hp/HS arguably the most challenging and information dense among the family of glycosaminoglycans (GAGs). Recent studies have shown that, SO_3 loss can be reduced via Na/H^+ exchange providing a platform for obtaining detailed structural information using electron detachment dissociation (EDD) and collisionally induced dissociation (CID). Here we exploit the effects of Na^+/H^+ exchange on Hp/HS oligomers using electron detachment dissociation (EDD). Our result show an increase in the amount of structurally relevant product ions without SO_3 loss with increasing ionized state via Na/H exchange.

Introduction

Heparin and heparan sulfate oligosaccharides are structurally related glycosaminoglycans (GAGs) with repeating disaccharide units of uronic acid-(1→4)-D-glucosamine [1]. Variable sulfation patterns may occur at the N, 6-*O*, 2-*O* and positions rarely 3-*O* in heparin including variations in the C-5 hexuronic acid stereochemistry (glucuronic acid or iduronic acid) accounts for its structural complexity [1-3]. The structural features of these bio-molecule influences its interactions with a variety of proteins and also implicated in important very biological activities such as growth factor signaling, tumour metastasis, adhesion blood coagulation, viral invasion of cells [1, 4]. The biological significance of heparin and heparan sulfate oligomers continue to influence research into their structure function relationships.

Several analytical techniques such as 1D and 2D NMR [5, 6] have been used to characterize GAGs, however this powerful analytical tool can be limited my sample purity and amount (milligram quantities) [7]. Mass spectrometry as an alternative offers high sensitivity and can be couple to several separation platforms [8, 9]. The anionic nature of GAGs especially heparin and heparan sulfates is well suited for ESI MS in the negative mode nevertheless, the labile sulfate groups are susceptible to decomposition in the source or during ion activation [10]. To retain these labile sulfate groups during MS and MS/MS analysis of GAGs, few analytical MS based methodologies have been proposed. These include efficient deprotonation of the sulfate groups using super-charging agents such as sulfolane [11, 12], chemical derivitization [13, 14] and the use of metal cations [15, 16]. The latter has been used to successfully characterize the pharmaceutical drug Arixtra by modifying the spray solvent with 1mM NaOH using CID.

This approach has recently been used to sequence a wide array of enzymatically and chemoenzymatically derived heparin and heparan sulfate GAGs with minimal SO_3 loss [16]. As a compliment to CID, electronic activation techniques such as negative electron transfer dissociation (NETD) [10, 13, 17], electron induce dissociation (EID) [18] and electron detachment dissociation (EDD) [7, 19-23] have been shown to produce structurally informative MS/MS for sequencing GAGs. Work done by Wolff et al. [19] demonstrated the efficacy of reducing SO_3 via Na/H exchange by EDD activation of sodiated molecular ions of dp8 dermatan sulfate (DS) oligomer. In their reports, increasing the ionized state such at more carboxylate groups are deprotonated could lead to a reduction in the number of product ions observed. This work extends their studies to heparin and heparan sulfate GAGs which have a higher charge density compared to DS oligomers

Experimental Methods

Heparin hexasaccharide preparation.

Heparin sodium salts (6g), extracted from porcine intestinal mucosa (Celsus Laboratories, Cincinnati, OH) were partially depolymerized using recombinant heparinase 1 (E.C. 4.2.2.7). The resulting heparin oligosaccharide mixture is then fractionated into low (<5000) and high (>5000) molecular weights through high pressure filtration. The fraction containing the low molecular weight heparin mixture is further fractionated using low pressure gel permeation chromatography into well-defined mixtures of disaccharides to tetradodecasaccharides. The purity of the oligomers was ascertained by gradient polyacrylamide gel, analytical SAX-HPLC, HPLC, CE and 1D and 2D NMR spectroscopy [24]. A step-by-step account of the heparin oligosaccharide

preparation can be found in Ref [4]. The heparin hexasaccharide used for this study was acquired from the pool of low molecular weight mixture.

Synthetic Heparan sulfate hexasaccharide.

The heparan sulfate hexasaccharide was synthetized using the modular approach. A comprehensive description on the preparation of the heparan sulfate heptasaccharide using this method is captured in Ref [25]. FT- MS accurate mass measurements and ^{1}H NMR were used to confirm the structure of the compound.

Mass Spectrometry Analysis

Electron detachment dissociation experiments were performed on a 9.4T Bruker Apex Ultra QeFTMS (Billerica, MA). This FT-ICR platform is fitted with an indirectly heated hollow dispenser cathode (HeatWave, Watsonville, CA) for generating electrons. 0.1 mg/ml sample solutions in 50:50 methanol/H_2O modified with 0.1mM NaOH were infused at a rate of 120 □L/h and ionized using electrospray using a metal capillary in the negative mode (Agilent Technologies, Santa Clara, CA, #G2427A). To obtain the free -5 charged state molecular ion [M-5H]5-, the sample was sprayed in 50:50 methanol/H_2O with 0.1% Formic acid. ESI-MS of both hexasaccharide produced multiply charged precursor ions with their corresponding sodium adducts. Multiply charged precursor ions were isolated in the external quadrupole and accumulated for 1-4s before injection into the FT-MS cell for the EDD experiment. 2 isolation cell fills were applied per scan, while the precursor ion selection was further refined by in-cell isolation using a coherent excitation frequency (CHEF) event. The mass isolated precursor ions were then irradiated with 19eV electrons for 1s. This was achieved with the following instrumental conditions; the extraction lens was held at -18.5 ± 0.5V while the cathode bias was set to 19 with the

cathode heater at 1.5A. At least 36 acquisitions were signal averaged per spectrum. 512 K points were acquired for each EDD spectrum, padded with one zero fill, and apodized using a sine bell window. The data reported in this work was first internally calibrated using confidently assigned glycosidic bond cleavage product ions as internal calibrants, resulting in a mass accuracy of <1 ppm. We report only peaks with S/N> 10 due to the large number of low intensity products formed by EDD. Glycosidic and cross-ring product ions were assigned using accurate mass measurement and GlycoWorkbench [26, 27]. These product ions are reported using the annotation proposed by Domon and Costello [28]. A m/z list for the highest ionized state for both ionized state is included in Appendix A.

Results and discussions

ESI MS of Heparin and Heparan Sulfate Oligosaccharides

The ESI MS of both hexasaccharides HEX1 (Δ*U2S-GlcNS6S-IdoA2S-GlcNS6S-GlcA-GlcNS6S*) and *GlcA-GlcNS6S-IdoA-GlcNS6S-GlcA-GlcNS6S-*$(CH_2)_5NH_2$ in 1mM NaOH is shown on Figures 3.1 a and b. The impact of the dilute amount of NaOH produced higher charged molecular ions with the sodiated states, ensuring efficient deprotonation of the ionizable protons. The highest charge observed for Hex 1 was -5 with sodiated states (0-5Na) while that Hex 2 was -6 with sodiated states (0-3Na). Even through these hexasaccharides differ in structure and degree of sulfation, the highest ionized state observed for the highest charge ensure all but 1 of their ionizable protons deprotonated. Only ions in these high charged regions were selected for the EDD experiment

(a)

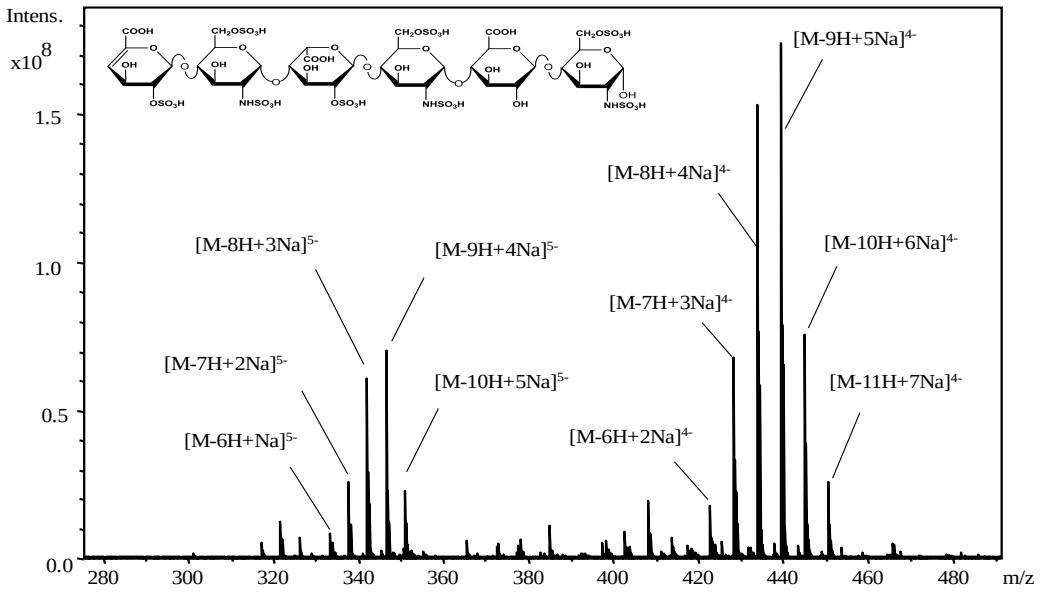

(b)

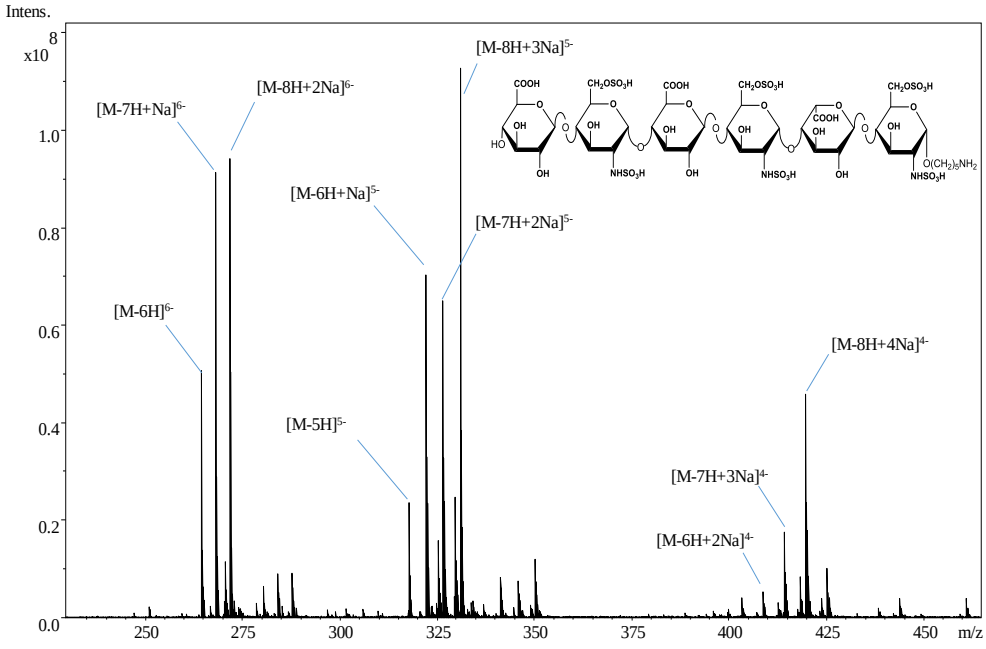

Figure 3.1. (a) ESI-MS of Δ*U2S-GlcNS6S-IdoA2S-GlcNS6S-GlcA-GlcNS6S* (b) ESI-MS of *GlcA-GlcNS6S-IdoA-GlcNS6S-GlcA-GlcNS6S-*$(CH_2)_5NH_2$

Results and discussion

EDD of Δ*U2S-GlcNS6S-IdoA2S-GlcNS6S-GlcA-GlcNS6S*

The total number of ionizable protons for the enzymatic derived heparin hexasaccharide Δ*U2S-GlcNS6S-IdoA2S-GlcNS6S-GlcA-GlcNS6S* is 11 comprising 8 sulfate groups and 3 carboxyl groups. The minus five-charged state precursor ions molecular ions for this compound were selected with increasing other of ionized state. The MS/MS spectrum for the $[M-5H]^{5-}$ produced intense SO_3 loss fragment from the parent ion with very few structurally relevant ions. The calculated amount of useful ions relative to the total amount of glycosidic and cross-ring product ions was 4% (Figure 3.2).

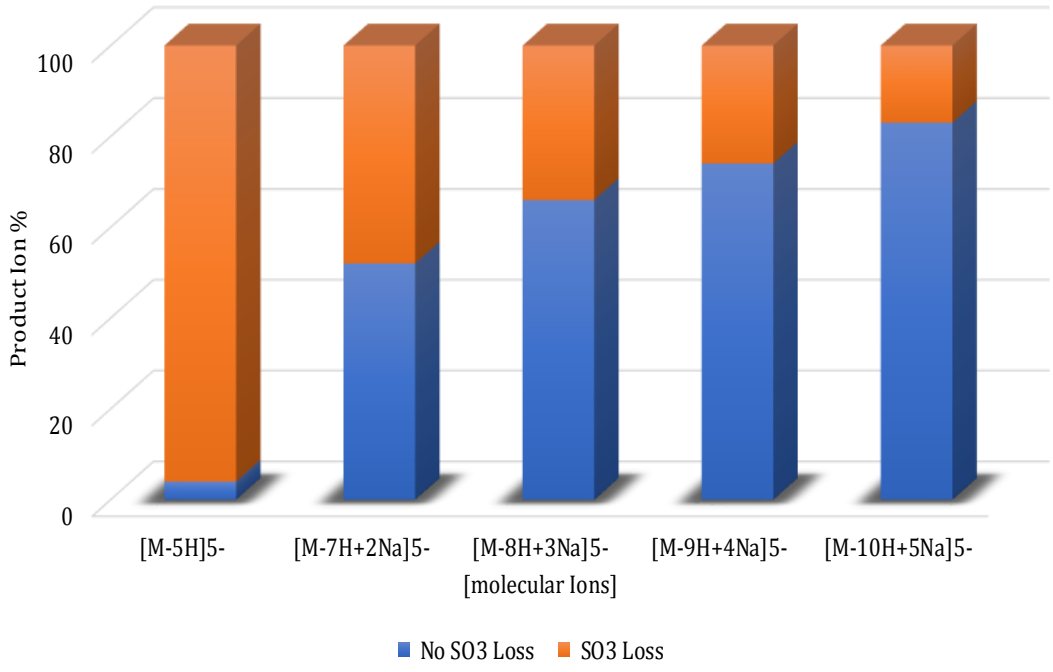

Figure 3. 2 This bar graph shows the effects of increasing the ionized state of the five-charged molecular ion via Na/H exchange for Δ*U2S-GlcNS6S-IdoA2S-GlcNS6S-GlcA-GlcNS6S*.

The next molecular ion analyzed was $[M-7H+2Na]^{5-}$. We observe an increase in product ion coverage for this molecular ion as shown in the annotated EDD spectra in Appendix A. The calculated amount of useful ions without SO_3 loss increased ten-fold (47%) compared to the$[M-5H]^{5-}$ molecular ion. The remaining precursor ions showed consistent increase in the amount of useful ions with increasing degree of sodiation as shown on Figure 3. 2.

The most structurally informative EDD spectra was obtained for $[M-8H+3Na]^{5-}$ molecular ion with 8 out of the 11 ionizable protons deprotonated. The highest ionized state $[M-8H+3Na]^{5-}$ with 10 out of the 11 ionizable protons deprotonated had 83% of its most useful ions without SO_3. Even though this precursor ions produced fewer ions, the EDD spectra shown on Figure 3 produced sufficient structurally relevant product ions capable of locating sites of sulfation, especially those located on the second and forth glucosamine residue from the non-reducing end (NRE) including that of the reducing end. The accurate mass of the $^{0,2}A_6$ and $^{0,2}X_0$ we used to assign the N-sulfo group while the mass difference between $^{0,2}A_6$ and $^{2,4}A_6$ was used to locate the 6-O sulfo group. Accurate mass or mass differences of glycosidic bond cleavages were used to establish the presence or absence of a sulfate group on the uronic acid residues.

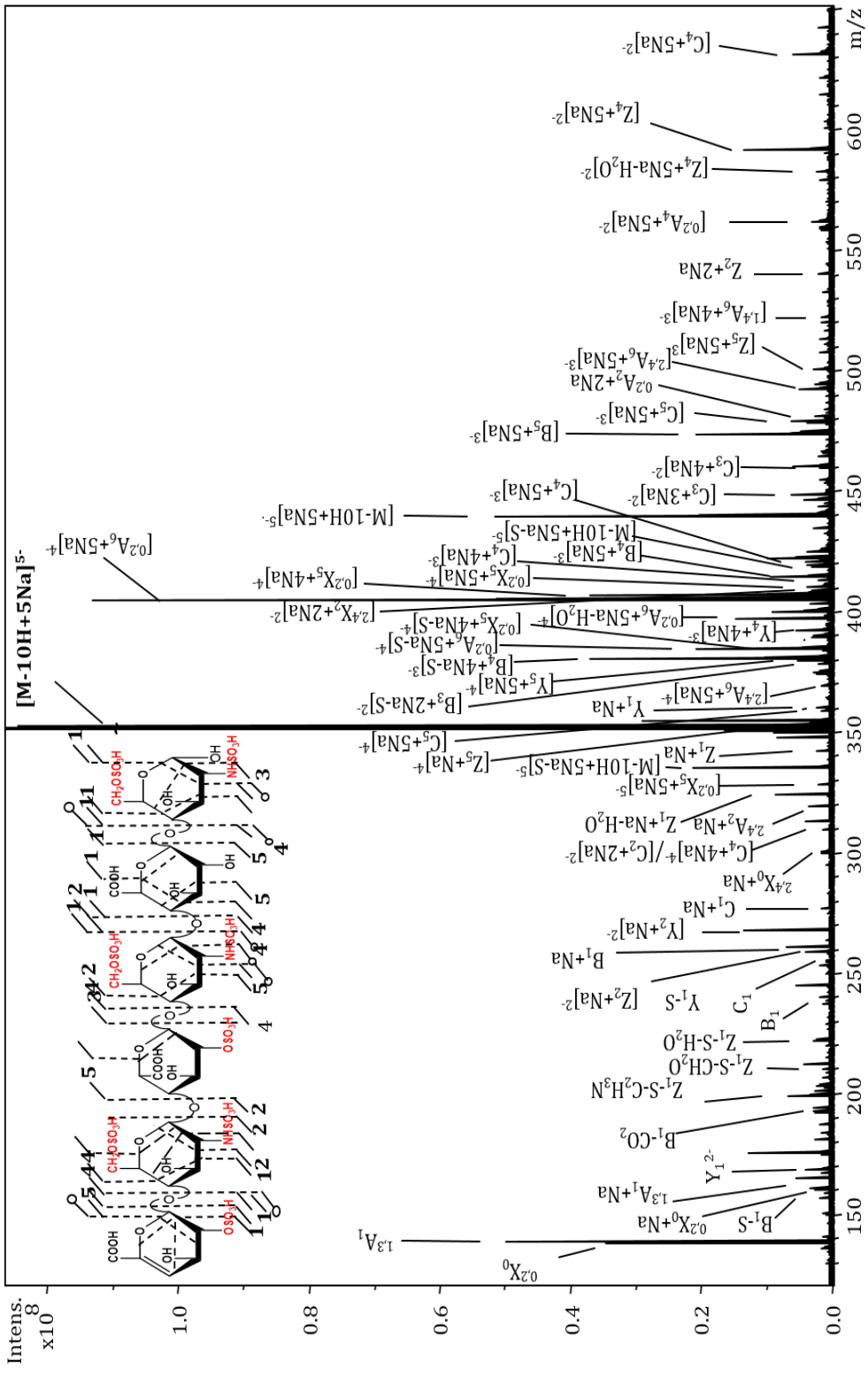

Figure 3. 3 Annotated EDD mass spectra and structure of the $[M-10H+5Na]^{5-}$ molecular ion for Δ*U2S-GlcNS6S-IdoA2S-GlcNS6S-GlcA-GlcNS6S*

EDD of *GlcA-GlcNS6S-IdoA-GlcNS6S-GlcA-GlcNS6S-$(CH_2)_5NH_2$*

The synthetically produced heparan sulfate hexasaccharide has 10 ionizable protons (6 sulfo groups and 3 carboxyl groups). The highest charge observed for this compound allows for fewer Na adducts to achieve full deprotonation. Extensive EDD fragmentation of these molecular ions $[M-6H]^{6-}$, $[M-7H+Na]^{6-}$ and $[M-8H+2Na]^{6-}$ produced abundant glycosidic and cross-ring product ions capable of assigning the sulfate positions on all the glucosamine units except the one at the reducing end. The N, and 6-*O* sulfo positions have been assigned using a combination of cross-ring ($^{2,4}An$ and $^{0,2}A_n$ where n = 2, 4) and glycosidic ions (B_2 and B_4). We do note the importance of multiple sodiated state of these product ions, as they serve as confirmatory ions for sulfate modification assignments. The amount of useful ions without SO_3 loss were computed and the results are shown on Figure 3.4. Compared to the results of enzymatically the derived hexasaccharide with a sulfate density of 2.7 per disaccharide, the synthetically produced hexasaccharide (showed sulfate density of 2.0 per disaccharide) showed a similar trend of decrease in SO_3 with increasing degree of ionized state via Na/H exchange. However, the change in SO_3 loss of structurally relevant product ions was minimal due to the low sulfate density per disaccharide. The percent amount of useful ions recorded without SO_3 loss for the molecular $[M-6H]^{6-}$, $[M-7H+Na]^{6-}$ and $[M-8H+2Na]^{6-}$ was 76%, 80% and 82% respectively. Figure 3.5 Shows the annotated structure and EDD spectra for the three six-charged molecular ions for *GlcA-GlcNS6S-IdoA-GlcNS6S-GlcA-GlcNS6S-$(CH_2)_5NH_2$*.

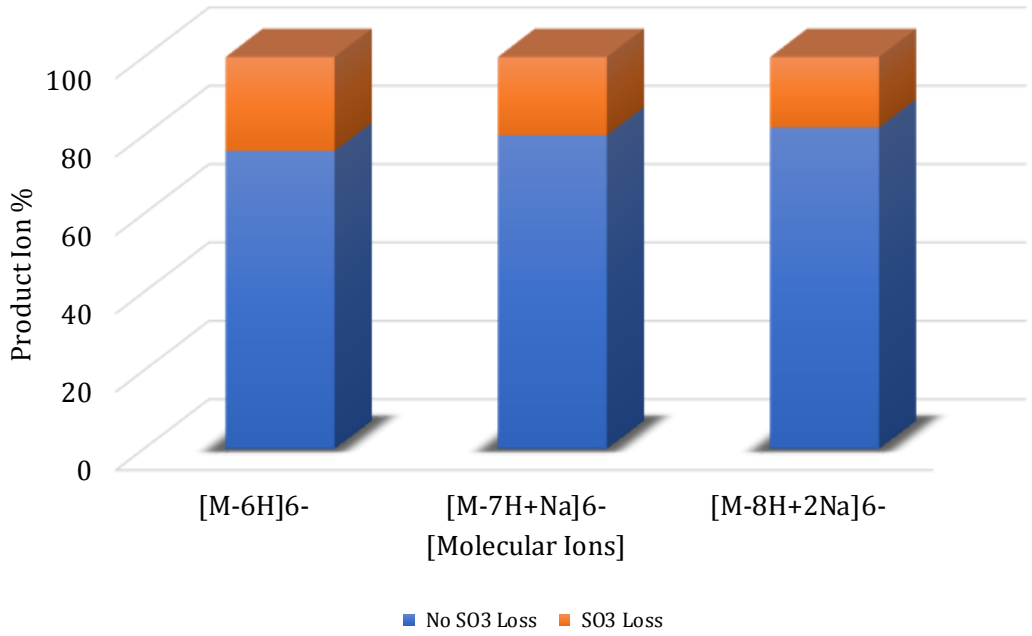

Figure 3.4. This bar graph shows the effects of increasing the ionized state of the 6 charged molecular ion via Na/H exchange for *GlcA-GlcNS6S-IdoA-GlcNS6S-GlcA-GlcNS6S-*$(CH_2)_5NH_2$.

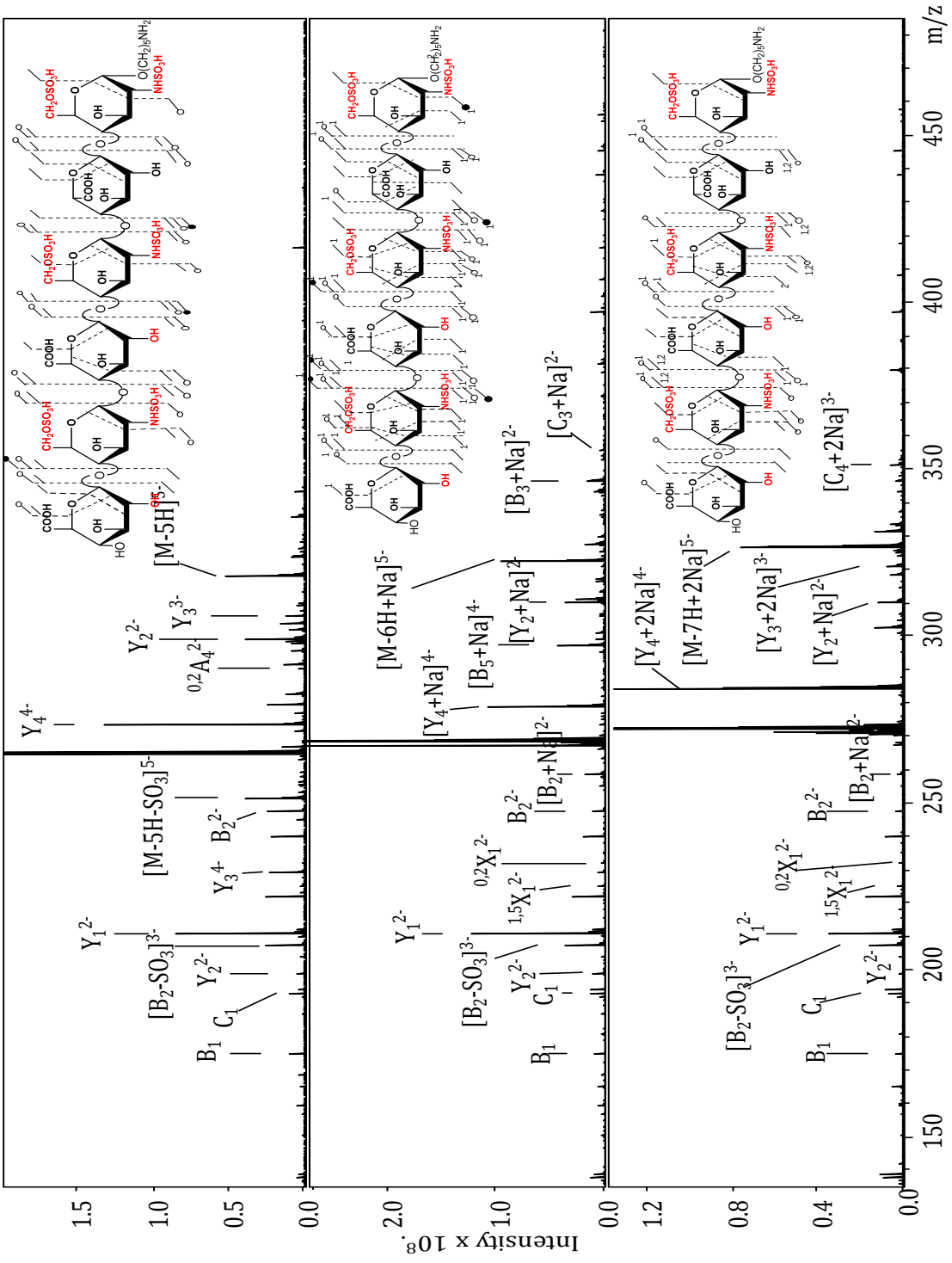

Figure 3.5. Annotated EDD structure and spectra and of 6 charged state molecular ions of *GlcA-GlcNS6S-IdoA-GlcNS6S-GlcA-GlcNS6S-(CH₂)₅NH₂*. A selected number intense structurally relevant ions are shown on the spectra.

Conclusions

In this work, we have shown EDD as a powerful analytical tool for assigning sites of sulfate modifications. The effect of sodiation for carefully selected precursor ions led to an increase in the amount of structurally relevant product ions for the two compounds analyzed. For the enzymatically derived hexasaccharide Δ*U2S-GlcNS6S-IdoA2S-GlcNS6S-GlcA-GlcNS6S,* there was a twenty-fold (4%→83) increase in the amount of useful ions without SO_3 loss while that for the chemically synthesized hexasaccharide *GlcA-GlcNS6S-IdoA-GlcNS6S-GlcA-GlcNS6S-*$(CH_2)_5NH_2$ was very little (76%→82%) comparing the highest ionized state via Na/H for the molecular ions studied to their molecular ions without sodium adduction. Product ions observed where present in multiple cationized state which proved to confirm the existence of low intensity cross-ring products without their isotopes. EDD of both hexasaccharides produced structurally informative MS/MS spectra even at ionized states greater than the number of sulfate groups present.

References

1. Rabenstein, D.L.: Heparin and heparan sulfate: structure and function. Natural product reports. **19**, 312-331 (2002)
2. Bernfield, M., Götte, M., Park, P.W., Reizes, O., Fitzgerald, M.L., Lincecum, J., Zako, M.: Functions of cell surface heparan sulfate proteoglycans. Annual review of biochemistry. **68**, 729-777 (1999)
3. Esko, J.D., Lindahl, U.: Molecular diversity of heparan sulfate. The Journal of clinical investigation. **108**, 169-173 (2001)
4. Weiss, R.J., Esko, J., Tor, Y.: Targeting Heparin–and Heparan Sulfate–Protein Interactions. Organic & Biomolecular Chemistry. (2017)
5. Horne, A., Gettins, P.: 1H-Nmr spectral assignments for two series of heparin-derived oligosaccharides. Carbohydrate research. **225**, 43-57 (1992)
6. Zong, C., Venot, A., Dhamale, O., Boons, G.-J.: Fluorous supported modular synthesis of heparan sulfate oligosaccharides. Organic letters. **15**, 342-345 (2013)
7. Wolff, J.J., Chi, L., Linhardt, R.J., Amster, I.J.: Distinguishing glucuronic from iduronic acid in glycosaminoglycan tetrasaccharides by using electron detachment dissociation. Analytical chemistry. **79**, 2015-2022 (2007)
8. Zaia, J.: Mass spectrometry of oligosaccharides. Mass spectrometry reviews. **23**, 161-227 (2004)
9. Kailemia, M.J., Ruhaak, L.R., Lebrilla, C.B., Amster, I.J.: Oligosaccharide analysis by mass spectrometry: a review of recent developments. Analytical chemistry. **86**, 196-212 (2013)

10. Leach, F.E., Riley, N.M., Westphall, M.S., Coon, J.J., Amster, I.J.: Negative Electron Transfer Dissociation Sequencing of Increasingly Sulfated Glycosaminoglycan Oligosaccharides on an Orbitrap Mass Spectrometer. Journal of The American Society for Mass Spectrometry. 1-11 (2017)
11. Zaia, J.: Glycosaminoglycan glycomics using mass spectrometry. Molecular & Cellular Proteomics. **12**, 885-892 (2013)
12. Shi, X., Huang, Y., Mao, Y., Naimy, H., Zaia, J.: Tandem mass spectrometry of heparan sulfate negative ions: sulfate loss patterns and chemical modification methods for improvement of product ion profiles. Journal of the American Society for Mass Spectrometry. **23**, 1498-1511 (2012)
13. Huang, R., Liu, J., Sharp, J.S.: An approach for separation and complete structural sequencing of heparin/heparan sulfate-like oligosaccharides. Analytical chemistry. **85**, 5787-5795 (2013)
14. Huang, R., Pomin, V.H., Sharp, J.S.: LC-MSn analysis of isomeric chondroitin sulfate oligosaccharides using a chemical derivatization strategy. Journal of the American Society for Mass Spectrometry. **22**, 1577 (2011)
15. Kailemia, M.J., Li, L., Ly, M., Linhardt, R.J., Amster, I.J.: Complete mass spectral characterization of a synthetic ultralow-molecular-weight heparin using collision-induced dissociation. Analytical chemistry. **84**, 5475-5478 (2012)
16. Kailemia, M.J., Li, L., Xu, Y., Liu, J., Linhardt, R.J., Amster, I.J.: Structurally Informative Tandem Mass Spectrometry of Highly Sulfated

Natural and Chemoenzymatically Synthesized Heparin and Heparan Sulfate Glycosaminoglycans*□ S. Molecular & Cellular Proteomics. **12**, 979 (2013)

17. Wolff, J.J., Leach III, F.E., Laremore, T.N., Kaplan, D.A., Easterling, M.L., Linhardt, R.J., Amster, I.J.: Negative electron transfer dissociation of glycosaminoglycans. Analytical chemistry. **82**, 3460-3466 (2010)
18. Wolff, J.J., Laremore, T.N., Aslam, H., Linhardt, R.J., Amster, I.J.: Electron-induced dissociation of glycosaminoglycan tetrasaccharides. Journal of the American Society for Mass Spectrometry. **19**, 1449-1458 (2008)
19. Leach, F.E., Ly, M., Laremore, T.N., Wolff, J.J., Perlow, J., Linhardt, R.J., Amster, I.J.: Hexuronic acid stereochemistry determination in chondroitin sulfate glycosaminoglycan oligosaccharides by electron detachment dissociation. Journal of the American Society for Mass Spectrometry. **23**, 1488-1497 (2012)
20. Wolff, J.J., Laremore, T.N., Busch, A.M., Linhardt, R.J., Amster, I.J.: Influence of charge state and sodium cationization on the electron detachment dissociation and infrared multiphoton dissociation of glycosaminoglycan oligosaccharides. Journal of the American Society for Mass Spectrometry. **19**, 790-798 (2008)
21. Wolff, J.J., Laremore, T.N., Busch, A.M., Linhardt, R.J., Amster, I.J.: Electron detachment dissociation of dermatan sulfate oligosaccharides. Journal of the American Society for Mass Spectrometry. **19**, 294-304 (2008)
22. Agyekum, I., Patel, A.B., Zong, C., Boons, G.-J., Amster, I.J.: Assignment of hexuronic acid stereochemistry in synthetic heparan sulfate

tetrasaccharides with 2-O-sulfo uronic acids using electron detachment dissociation. International journal of mass spectrometry. **390**, 163-169 (2015)

23. Agyekum, I., Zong, C., Boons, G.-J., Amster, I.J.: Single Stage Tandem Mass Spectrometry Assignment of the C-5 Uronic Acid Stereochemistry in Heparan Sulfate Tetrasaccharides using Electron Detachment Dissociation. Journal of The American Society for Mass Spectrometry. 1-10 (2017)
24. Pervin, A., Gallo, C., Jandik, K.A., Han, X.-J., Linhardt, R.J.: Preparation and structural characterization of large heparin-derived oligosaccharides. Glycobiology. **5**, 83-95 (1995)
25. Arungundram, S., Al-Mafraji, K., Asong, J., Leach III, F.E., Amster, I.J., Venot, A., Turnbull, J.E., Boons, G.-J.: Modular synthesis of heparan sulfate oligosaccharides for structure− activity relationship studies. Journal of the American Chemical Society. **131**, 17394-17405 (2009)
26. Ceroni, A., Maass, K., Geyer, H., Geyer, R., Dell, A., Haslam, S.M.: GlycoWorkbench: a tool for the computer-assisted annotation of mass spectra of glycans†. Journal of proteome research. **7**, 1650-1659 (2008)
27. Damerell, D., Ceroni, A., Maass, K., Ranzinger, R., Dell, A., Haslam, S.M.: Annotation of glycomics MS and MS/MS spectra using the GlycoWorkbench software tool. Glycoinformatics. 3-15 (2015)
28. Domon, B., Costello, C.E.: A systematic nomenclature for carbohydrate fragmentations in FAB-MS/MS spectra of glycoconjugates. Glycoconjugate journal. **5**, 397-409 (1988)

CHAPTER 4

Single Stage MS/MS Analysis of Sodium Cationized Ions of Ultralow Molecular Weight Heparin Using Electron Detachment Dissociation

To be submitted as:

Agyekum, I; Amster, I. J., "Single Stage MS/MS Analysis of Sodium Cationized Ions of Ultralow Molecular Weight Heparin Using Electron Detachment Dissociation", *J. Am. Soc. Mass Spectrom.*,

Abstract

Heparin oligosaccharides are known as the most acidic biomolecule in nature. This structurally complex molecule is well known for its anticoagulant activity. Heparin has been implicated in very important biological processes including cell growth and division, cell-cell signaling, angiogenesis, and are known bind other proteins. In order to fully exploit the biological properties of Hp, it is very important to link these biological activities with their fine structure. However, structural characterization of Hp using tandem mass spectrometry has been accompanied with unwanted loss of its labile sulfate groups. Recent studies have shown that, SO_3 loss can be reduced via Na/H^+ exchange providing a platform for obtaining detailed structural information using collision induced dissociation (CID). Here we extend the efficiency of fragmenting sodiated precursor ions using electron detachment dissociation to characterize Ultra-low molecular weight heparin (Arixtra) from a single stage MS/MS. MS/MS of the fully deprotonated molecular ion $[M-10H+5Na]^{5-}$ obtained via Na/H exchange is provided.

Introduction

Heparin and heparan sulfate glycosaminoglycans (GAGs) are sulfated unbranched polysaccharides composed of a repeating disaccharide unit of hexuronic acid (1,4) linked to D-glucosamine [1]. The uronic acid residue within each disaccharide unit may exist as either α-L-iduronic acid (IdoA) or β-D-glucuronic acid (GlcA) and can be sulfonated at the 2-O position. The glucosamine unit on the other hand may undergo sulfation at the N, 6-O or 3-O positions [1-4]. This class of carbohydrates are very complex and their structural complexity is attributed to the variable sulfation and epimerized states resulting from their non-template biosynthesis [5]. The biosynthesis of heparin occurs in the endoplasmic reticulum and the Golgi apparatus of the mast cells of connective tissues while HS GAGs are expressed by mammalian cells and mostly located on cell surfaces and in the extracellular matrices [4, 6]. Heparin and HS are known to influence several physiological and pathophysiological processes including tumorigenesis, angiogenesis, growth control, cell adhesion, inflammation, hemostasis, neural development and regeneration [4, 7, 8]. Heparin is a widely used clinical drug mainly for its anti-coagulant activity which occurs through its interaction with the antithrombin III [9, 10]. The structure of the heparin pentasaccharide binding motif responsible for its interaction with AT-III is shown in Figure 1. To enable a better understanding of the biological roles of Heparin and HS GAGs, micro-sequencing of these compounds remains paramount.

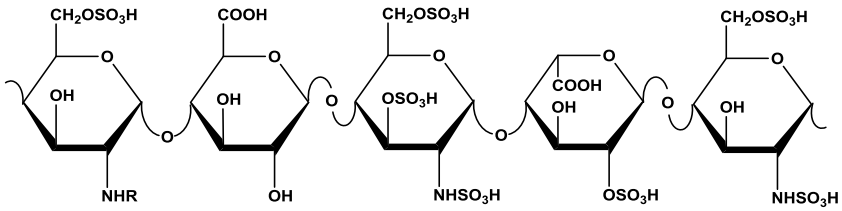

Figure 4.1. Structure of AT III pentasaccharide heparin binding motif. R= Ac/SO_3H

Mass spectrometry, for the past decade, continues to impact the field of glycomics. With current advances in ionization techniques such as MALDI and ESI, molecular weight information of intact GAGs is now possible with minimal or no decomposition of the facile sulfate half ester bonds [11]. The molecular weight obtained can reveal the length and elemental composition of the oligomer. Specific location of monosaccharide modifications mostly the sulfate groups and site of acetylation can be achieved using tandem mass spectrometry. Sulfate losses, especially at the ion activation stage of MS/MS experiment are a common occurrence. This phenomenon is more pronounced in heparin oligomers as they contain a high degree of sulfate groups per disaccharide unit. Initial attempts at addressing this challenge was reported by Zaia et al. [12] where they witnessed a reduction in sulfate loss product ions upon CAD fragmentation of Ca adducted precursor ions of heparin-like oligomers. However, the MS/MS information was not enough for structural sequencing of the oligomers. Recently, CID activation of Na adducted precursor ions have also been shown to reduce sulfate losses and provide structurally informative fragment [13, 14]. Alternatively, super charging agents such as sulfolane can be employed to obtain higher ionized states [15]. This approach works well with moderately sulfated oligomers however for highly sulfated Heparin GAGs, it is not efficient due to charge-charge repulsion. Chemical derivatization of GAG oligomers prior to CID MS/MS analysis present an alternative approach in dealing with SO3 loss [16-18].

Electron assisted fragmentation of GAGs is one of the well utilized platforms for structural analysis. Ion activation methods such as electron detachment dissociation (EDD) [19-24], electron induced dissociation (EID) [25] and negative electron transfer dissociation (NETD) [24, 26] have been shown to provide sufficient cross-ring and

glycosidic ions for structural analysis of GAGs. The ability to obtain stereospecific ions ($^{0,2}A_3$, B_3', and B_3'-CO_2) for moderately sulfated HS tetrasaccharides using EDD have been reported [22]. The effect of sodium cationization on EDD fragments of dermatan sulfate oligosaccharides have been reported by Wolff et al.[20] . This report also showed the ability to reduce sulfate decomposition via metal cation exchange. To test the efficiency of most ionization and ion activation methods, Arixtra has been the gold standard. Recent work by Muchena el. [14] revealed the usefulness to produce obtained highly informative product ions for arixtra with minimal sulfate decomposition. However, the structural assignment of Arixtra was made using MS/MS information obtained from CID activation of multiple precursor ions. This work extends efficiency of reducing sulfate decomposition via Na/H and the extensive fragmentation of product ions using EDD to provide full structural details of Arixtra from a single acquired spectrum. We also present a means of reducing the MS spectra complexity associated with Arixtra resulting from their propensity to form metal adducts.

Experimental

All chemicals and solvents used for this work were of HPLC-grade and purchased from Sigma-Aldrich. Arixtra was acquired from the hospital formulary and desalted on a BioGel P2 column BioRad (Hercules, CA, USA). Arixtra was introduced at a concentration 0.1 mg/ml in 50:50 methanol/H_2O with the degree of sodiation controlled by adding 1mM NaOH. The sample solutions were infused at a rate of 120 µL/hr and ionized with ESI in the negative mode. For the EDD experiments, precursor ions were isolated in the external quadrupole and accumulated for 2s before injection into the FTMS cell. The selection of the precursor ion was refined by using in-cell isolation. Electron irradiation for 1s was

achieved by setting the cathode bias at -19V and extraction lens -18.5±0.5V. 24 acquisitions were signaled averaged per mass spectrum. External calibration of mass spectra was performed to ensure a mass accuracy of 5 ppm. This was followed by internal calibration of the EDD spectrum using confidently assigned glycosidic bond cleavage products ions as internal calibrants. Product ion assignments were made using accurate mass measurement and Glycoworkbench [27, 28]. All MS/MS fragment ions have been reported using the Domon and Costello nomenclature [29].

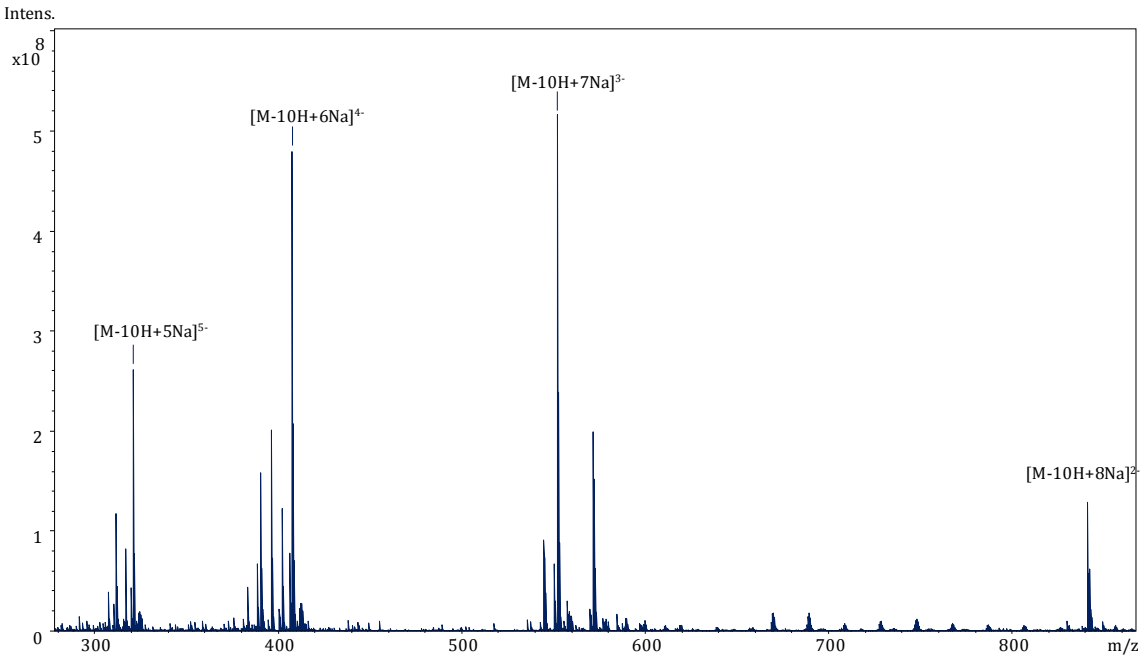

Figure 4.2. ESI MS of Arixtra showing the annotations for the fully deprotonated molecular ions.

Results and Discussions

MS of Ultra-low molecular weight heparin (Arixtra)

The mass spectra of Ultra-low molecular weight heparin (Arixtra) are often complicated as molecular ions usually exist in several mass channels of Na^+ and K^+ adducts

because of their polyanionic nature. We show in Figure 1 an MS of Arixtra in 50:50 methanol/H_2O. The modification of the spray solvent with 1mM NaOH suppresses the potassium ions allowing for clean isolation of preferred precursor ions. As much as this technique has some advantages, the spreading of a particular ion over several ionized state via Na/H can suppress the ions signal. The most stable precursor ions that is $[M-10H+8Na]^{2-}$, $[M-10H+7Na]^{3-}$, $[M-10H+6Na]^{4-}$, and $[M-10H+5Na]^{5-}$ occurring at m/z 840.39.62, 552.6010, 408.7035 and 322.3649 respectively are shown on Figure 3. With this technique, it is possible to reduce the intensity of unwanted precursor ions that may be caught in the isolation window since un-intentional fragmentation of these ions can also complicate the MS/MS spectrum.

EDD MS/MS of Ultra-low molecular weight heparin (Arixtra)

Figure 4. 3 shows extensive EDD fragmentation of the most intense precursor ions $[M-10H+5Na]^{5-}$. With all ten ionizable protons deprotonated, we observe minimal SO3 loss from the structurally relevant product ions. Assignment of all the sites of sulfation is made possible with a combination of both cross-ring and glycosidic product ions. We make definitive assignment of the sulfate group on the non-reducing end sugar with cross-ring product ions $^{3,5}A_1$, $^{0,3}A_1$ and $^{0,3}A_1$+Na. The accurate mass of each of these cross-ring products confirms the presence of the 6-*O* sulfate group on the glucosamine residue. The same sulfate group could be confirmed with the $^{0,3}X_4$+5Na ion. The position of N sulfo group is further confirmed by accurate mass by obtaining the mass difference between the B_1/C_1 and $^{0,2}A_1$ product ions. These multiple product ions obtained on a single sugar residue further increases the confidence of each sulfo group assignment. The assignment of the three sulfo groups (3-*O*, 6-*O* and N) on the third glucosamine unit can be made by taking

the mass difference between the B_2/C_2 and B3/C3 or Z_2/Y_2 and Z_3/Y_3. Again, having the full compliments of these ions further confirms these sulfo group assignments. The di-sulfated glucosamine unit (6-O and N-) at the reducing end underwent several fragmentations. Specifically, we assign the 6-O sulfate by taking the mass difference between the $^{3,5}A_5$ and B_4/C_4 ions. The accurate mass of the 0,2X0 ions unambiguously locates the N-sulfo group.

Sulfation on the uronic acid residue can only be at the 2-O position, therefore a combination of glycosidic ions for example B_3/C_3 and B_4/C_4 or Z_1/Y_1 and Z_2/Y_2 are enough for its location. However, we can confirm the uronic acid towards the reducing end is 2-O sulfated using the $^{0,2}X_1$ and Z_1/Y_1. Furthermore, the presence of 6-O and N-sulfo groups on the NRE and RE can also be achieved by taking the mass difference between the $^{2,4}X_4$+5Na and $^{1,5}X_4$+4Na/$^{1,5}X_4$+5Na. We however prefer the latter approach in assigning the individual sulfate groups on the NRE glucosamine since $^{2,4}X_4$+5Na and $^{1,5}X_4$+4Na/$^{1,5}X_4$+5Na are isobaric with $^{2,4}A_5$+4Na/$^{2,4}A_5$+5Na and $^{1,5}A_4$+5Na respectively. It is worth noting that EDD fragmentation of the $[M-10H+5Na]^{5-}$ produced a full complement of all glycosidic cleavages necessary for obtaining the constituent of monosaccharide residues [23]. The quality of MS/MS data especially those produced could significantly fast tract currently attempts at automating spectra analysis. Structure annotations for all isobaric cross-ring are illustrated with the same color shown on Figure 3.

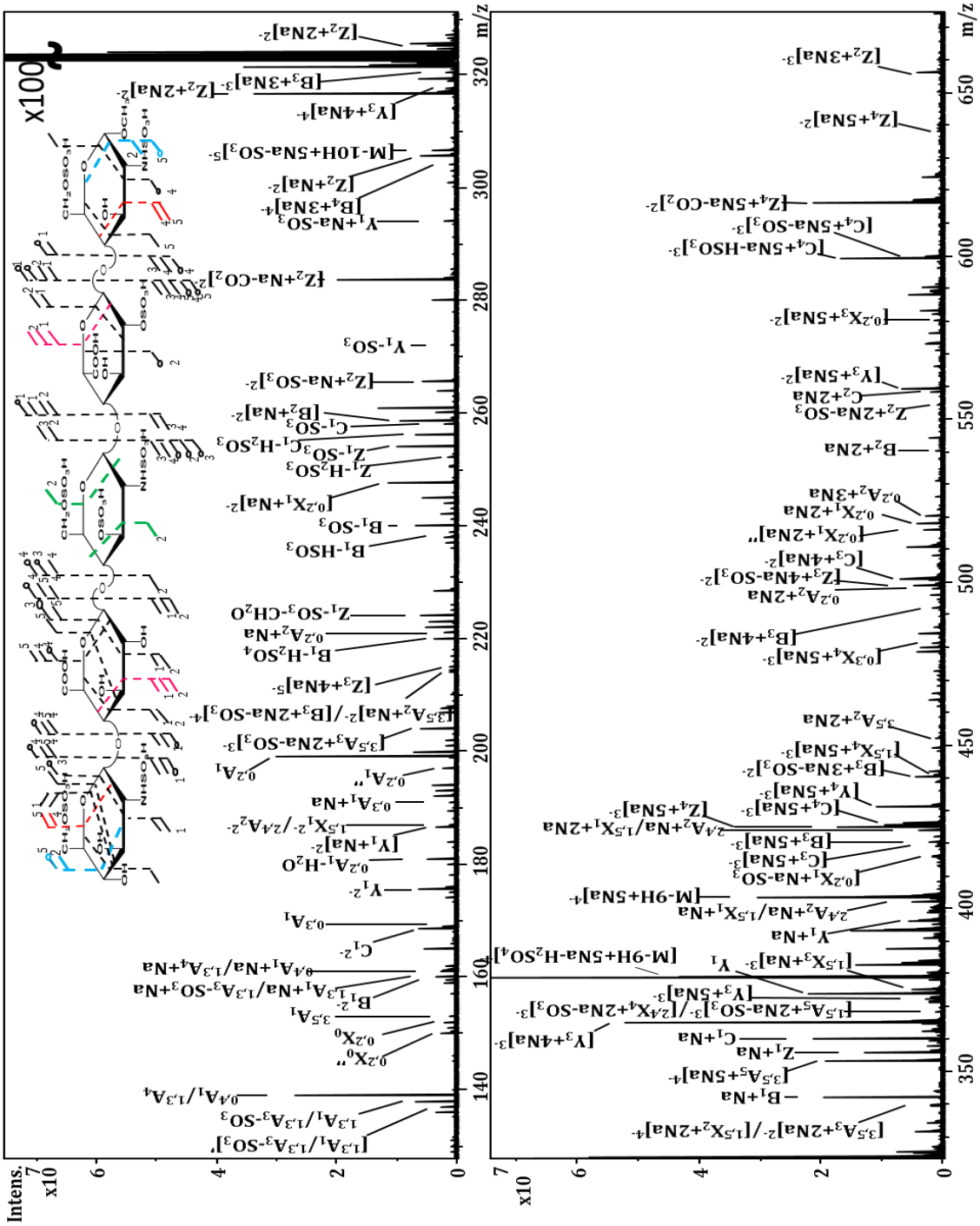

Figure 4.3. EDD structure and spectra annotations for the $[M-10H+5Na]^{5-}$ molecular ion for Arixtra

EDD Hexuronic acid stereochemistry of Arixtra

Electron based radical site initiated fragmentation of HS tetrasaccharide has been shown to produce stereospecific ions that can be associated with the C-5 hexuronic acid stereochemistry [22]. This is seen in the extensive fragmentation of the two uronic acid residues present in arixtra especially the GlcA residue. A careful study of the fragmentation pattern of the $[M-10H+5Na]^{5-}$ reveal cross-rings product ions that can be associated with the C-5 hexuronic acid stereochemistry. The 2,4A2 ion observed on the GlcA residue is absent on the IdoA2S residue. Even though this cross-ring fragment is isobaric with 1,5X1, the latter assignment ($^{2,4}A_2$) has been confirmed through an H/D exchanged experiment from previous studies [14]. The diagnostic ion $^{2,4}An$ has recently been shown to distinguish the uronic acid stereochemistry in a variety of chondroitin and dermatan sulfate oligomers (dp4-dp10) [30]. The results were achieved by CID fragmentation of carefully selected precursor ions. A careful comparison of this EDD report to the referenced CID of $[M-10H+5Na]^{5-}$ precursor ion Arixtra further revealed other cross-rings product ions unique to the GlcA residue [14]. These ions include $^{0,2}A_2$ and $^{0,3}X_3$. The reproducibility of this diagnostic ions could be exploited in determining alternating uronic acid configurations in heparin and heparan sulfate oligosaccharides. The m/z list for the five-charged fully deprotonated ion is included in Appendix B

Conclusions

In this report, we have shown the ability to reduce the spectra complexity by suppressing the presence of K^+ adducts with the addition of 1mM NaOH the spray solvent. Molecular ions observed for Arixtra were $[M-10H+7Na]^{3+}$, $[M-10H+6Na]^{4+}$ and $[M-10H+5Na]^{5+}$. EDD fragmentation of a single molecular ion $[M-10H+5Na]^{5+}$ have been shown to provide structurally informative cross-ring product ions and the full compliments

of glycosidic bond cleavages capable of assigning the sites of sulfation and the C-5 hexuronic acid stereochemistry of Arixtra. Multiple confirmation of sites of sulfation using several cross-rings product ions from the EDD spectrum was achieved. With current interest in automating the analysis of GAGs, the ability to obtain highly informative MS/MS spectra from single stage experiment will significantly maximize accuracy of up and coming software products in producing the right information.

References

1. Jones, C.J., Beni, S., Limtiaco, J.F., Langeslay, D.J., Larive, C.K.: Heparin characterization: challenges and solutions. Annual Review of Analytical Chemistry. 4, 439-465 (2011)
2. Xu, D., Esko, J.D.: Demystifying heparan sulfate-protein interactions. Annual review of biochemistry. 83, 129-157 (2014)
3. Chi, L., Amster, J., Linhardt, R.J.: Mass spectrometry for the analysis of highly charged sulfated carbohydrates. Current Analytical Chemistry. 1, 223-240 (2005)
4. Sasisekharan, R., Venkataraman, G.: Heparin and heparan sulfate: biosynthesis, structure and function. Current opinion in chemical biology. 4, 626-631 (2000)
5. Esko, J.D., Kimata, K., Lindahl, U.: Proteoglycans and sulfated glycosaminoglycans. (2009)
6. Gallagher, J.T., Walker, A.: Molecular distinctions between heparan sulphate and heparin. Analysis of sulphation patterns indicates that heparan sulphate and heparin are separate families of N-sulphated polysaccharides. Biochemical Journal. 230, 665-674 (1985)
7. Rosenberg, R.D., Shworak, N., Liu, J., Schwartz, J., Zhang, L.: Heparan sulfate proteoglycans of the cardiovascular system. Specific structures emerge but how is synthesis regulated? The Journal of clinical investigation. 99, 2062 (1997)
8. Shriver, Z., Liu, D., Sasisekharan, R.: Emerging views of heparan sulfate glycosaminoglycan structure/activity relationships modulating dynamic biological functions. Trends in cardiovascular medicine. 12, 71-77 (2002)

9. Meneghetti, M.C., Hughes, A.J., Rudd, T.R., Nader, H.B., Powell, A.K., Yates, E.A., et al.: Heparan sulfate and heparin interactions with proteins. Journal of The Royal Society Interface. 12, 20150589 (2015)

10. Nugent, M.A.: Heparin sequencing brings structure to the function of complex oligosaccharides. Proceedings of the National Academy of Sciences. 97, 10301-10303 (2000)

11. Zaia, J.: Principles of mass spectrometry of glycosaminoglycans. J Biomacromol Mass Spectrom. 1, 3-36 (2005)

12. Zaia, J., Costello, C.E.: Tandem mass spectrometry of sulfated heparin-like glycosaminoglycan oligosaccharides. Analytical chemistry. 75, 2445-2455 (2003)

13. Kailemia, M.J., Li, L., Xu, Y., Liu, J., Linhardt, R.J., Amster, I.J.: Structurally informative tandem mass spectrometry of highly sulfated natural and chemoenzymatically synthesized heparin and heparan sulfate glycosaminoglycans. Molecular & Cellular Proteomics. 12, 979-990 (2013)

14. Kailemia, M.J., Li, L., Ly, M., Linhardt, R.J., Amster, I.J.: Complete mass spectral characterization of a synthetic ultralow-molecular-weight heparin using collision-induced dissociation. Analytical chemistry. 84, 5475-5478 (2012)

15. Huang, Y., Shi, X., Yu, X., Leymarie, N., Staples, G.O., Yin, H., et al.: Improved liquid chromatography-MS/MS of heparan sulfate oligosaccharides via chip-based pulsed makeup flow. Analytical chemistry. 83, 8222-8229 (2011)

16. Huang, R., Zong, C., Venot, A., Chiu, Y., Zhou, D., Boons, G.-J., et al.: The de novo Sequencing of Complex Mixtures of Heparan Sulfate Oligosaccharides. (2016)

17. Huang, R., Liu, J., Sharp, J.S.: An approach for separation and complete structural sequencing of heparin/heparan sulfate-like oligosaccharides. Analytical chemistry. 85, 5787-5795 (2013)
18. Huang, R., Pomin, V.H., Sharp, J.S.: LC-MS n analysis of isomeric chondroitin sulfate oligosaccharides using a chemical derivatization strategy. Journal of the American Society for Mass Spectrometry. 22, 1577-1587 (2011)
19. Leach III, F.E., Ly, M., Laremore, T.N., Wolff, J.J., Perlow, J., Linhardt, R.J., et al.: Hexuronic acid stereochemistry determination in chondroitin sulfate glycosaminoglycan oligosaccharides by electron detachment dissociation. Journal of the American Society for Mass Spectrometry. 23, 1488-1497 (2012)
20. Wolff, J.J., Laremore, T.N., Busch, A.M., Linhardt, R.J., Amster, I.J.: Influence of charge state and sodium cationization on the electron detachment dissociation and infrared multiphoton dissociation of glycosaminoglycan oligosaccharides. Journal of the American Society for Mass Spectrometry. 19, 790-798 (2008)
21. Wolff, J.J., Amster, I.J., Chi, L., Linhardt, R.J.: Electron detachment dissociation of glycosaminoglycan tetrasaccharides. Journal of the American Society for Mass Spectrometry. 18, 234-244 (2007)
22. Wolff, J.J., Chi, L., Linhardt, R.J., Amster, I.J.: Distinguishing glucuronic from iduronic acid in glycosaminoglycan tetrasaccharides by using electron detachment dissociation. Analytical chemistry. 79, 2015-2022 (2007)
23. Agyekum, I., Patel, A.B., Zong, C., Boons, G.-J., Amster, I.J.: Assignment of hexuronic acid stereochemistry in synthetic heparan sulfate tetrasaccharides with

2-O-sulfo uronic acids using electron detachment dissociation. International Journal of Mass Spectrometry. 390, 163-169 (2015)

24. Huang, Y., Yu, X., Mao, Y., Costello, C.E., Zaia, J., Lin, C.: De novo sequencing of heparan sulfate oligosaccharides by electron-activated dissociation. Analytical chemistry. 85, 11979-11986 (2013)

25. Wolff, J.J., Laremore, T.N., Aslam, H., Linhardt, R.J., Amster, I.J.: Electron-induced dissociation of glycosaminoglycan tetrasaccharides. Journal of the American Society for Mass Spectrometry. 19, 1449-1458 (2008)

26. Wolff, J.J., Leach III, F.E., Laremore, T.N., Kaplan, D.A., Easterling, M.L., Linhardt, R.J., et al.: Negative electron transfer dissociation of glycosaminoglycans. Analytical chemistry. 82, 3460-3466 (2010)

27. Damerell, D., Ceroni, A., Maass, K., Ranzinger, R., Dell, A., Haslam, S.M.: The GlycanBuilder and GlycoWorkbench glycoinformatics tools: updates and new developments. (2012)

28. Ceroni, A., Maass, K., Geyer, H., Geyer, R., Dell, A., Haslam, S.M.: GlycoWorkbench: a tool for the computer-assisted annotation of mass spectra of glycans†. Journal of proteome research. 7, 1650-1659 (2008)

29. Domon, B., Costello, C.E.: A systematic nomenclature for carbohydrate fragmentations in FAB-MS/MS spectra of glycoconjugates. Glycoconjugate journal. 5, 397-409 (1988)

30. Kailemia, M.J., Patel, A.B., Johnson, D.T., Li, L., Linhardt, R.J., Amster, I.J.: Differentiating Chondroitin Sulfate Glycosaminoglycans using CID; Uronic Acid

Cross-Ring Diagnostic Fragments in a Single Stage of MS/MS. European journal of mass spectrometry (Chichester, England). 21, 275 (2015)

CHAPTER 5

Assignment of Hexuronic Acid Stereochemistry in Synthetic Heparan Sulfate Tetrasaccharides with 2-*O*-Sulfo Uronic Acids Using Electron Detachment Dissociation

Published as:

Agyekum, I.; Patel, A. B.; Zong, C.; Boons, G.-J.; Amster, I. J. "Assignment Of Hexuronic Acid Stereochemistry In Synthetic Heparan Sulfate Tetrasaccharides With 2-*O*-Sulfo Uronic Acids Using Electron Detachment Dissociation", *Int. J. Mass Spectrom.* **2015**, *390*, 163-169.

Abstract

The present work focuses on the assignment of uronic acid stereochemistry in heparan sulfate (HS) oligomers. The structural elucidation of HS glycosaminoglycans is the subject of considerable importance due to the biological and biomedical significance of this class of carbohydrates. They are highly heterogeneous due to their non-template biosynthesis. Advances in tandem mass spectrometry activation methods, particularly electron detachment dissociation (EDD), has led to the development of methods to assign sites of sulfo modification in glycosaminoglycan oligomers, but there are few reports of the assignment of uronic acid stereochemistry, necessary to distinguish glucuronic acid (GlcA) from iduronic acid (IdoA). Whereas preceding studies focused on uronic acid epimers with no sulfo modification, the current work extends the assignment of the hexuronic acid stereochemistry to 2-*O*-sulfo uronic acid epimeric tetrasaccharides. The presence of a 2-*O*-sulfo group on the central uronic acid was found to greatly influence the formation of B_3, C_2, Z_2, and Y_1 ions in glucuronic acid and Y_2 and $^{1,5}X_2$ for iduronic acid. The intensity of these peaks can be combined to yield a diagnostic ratios (DR), which can be used to confidently assign the uronic acid stereochemistry.

Introduction

Heparan sulfate (HS) glycosaminoglycans (GAGs) are a unique class of proteoglycans present on the surface of mammalian cells and in the extracellular matrix [1, 2]. These compounds are known to bind to a variety of proteins, and are implicated in several biological activities including angiogenesis, embryonic development, inflammation, and microbial infections [3, 4]. Structurally, they are synthesized as alternating disaccharide units of uronic acid [D-glucuronic acid (GlcA) or L-iduronic acid (IdoA)] linked to a glucosamine in the Golgi apparatus [5]. Selective sulfo modification of the disaccharide may occur at the *N*, 3-*O* and 6-*O* positions of the glucosamine while 2-*O*-sulfo modification can be observed on the acidic sugar [1, 4, 6]. The enzyme, 2-*O*-sulfotransferase, responsible for the transfer of the sulfo group to the 2-*O* position of a uronic acid, preferentially modifies IdoA, but can also modify GlcA to a limited extent, forming IdoA2S and GlcA2S [4]. These structural modifications of the HS chain are known to contribute to its various biological functions [1]. A well-documented example is the role of IdoA2S in binding several proteins including antithrombin, the fibroblast growth factors [7], and hepatocyte growth factors [8]. Even though the function of its epimeric isomer, GlcA2S, has yet to be elucidated, substantial amounts have been found in the human cerebral cortex [9], implicating an important role for this less commonly observed modification. Robust analytical methods for obtaining all structural details of GAG oligomers, including uronic acid stereochemistry, are required to aid researchers in their quest to gain a deeper understanding of the biological role GAGs.

Tandem mass spectrometry is well known as a tool for the analysis of biomolecules, offering high sensitivity, throughput, and accuracy [10]. However, MS/MS analysis of HS

oligosaccharides is challenging due to their heterogeneity in oligomer length, degree and sites of sulfo modifications, and hexuronic acid C-5 stereochemistry. The labile nature of a sulfate half-ester hinders structural characterization, especially during ion activation, due to the facile decomposition of the sulfo group. To address these challenges, researchers have focused their efforts on the development and refinement of ion activation methods to minimize sulfo decomposition while maximizing the fragmentation that provides useful structural information.

Chemical derivatization methods such as permethylation and acetylation followed by MS/MS have been successfully employed to locate sites of sulfation in HS oligomers [11]. Another approach to reducing sulfo decomposition is via metal cation exchange, which has been used with positive ionization to facilitate fragmentation by electron capture dissociation [12-14]. An alternative method involves efficient deprotonation of the acidic groups using supercharging agents like sulfolane [15]. This approach works well with less sulfated GAGs, but is limited in its applicability to highly sulfated GAG oligomers due to charge repulsion. Recent work showed that by adding sodium hydroxide to the spray solution, one can ionize sulfo groups in highly sulfated GAGs, while reducing the overall charge of the precursor ion. With this approach, one can obtain very rich and structurally informative MS/MS spectra [16, 17].

Electron based activation methods such electron detachment dissociation (EDD) [16-21], electron induced dissociation (EID) [18-20], and negative electron transfer dissociation (NETD) [22, 23] have been particularly useful for the tandem mass spectrometry analysis of GAGs. Compared to threshold activation methods like collision induced dissociation (CID) and infrared multi-photon dissociation (IRMPD), EDD

produces more structurally relevant ions with less SO_3 loss [19]. Prior studies have shown the capability of EDD for sequencing dp4-dp10 chondroitin sulfate (CS) oligomers, and assigning the hexuronic acid stereochemistry of HS tetrasaccharides [18, 20]. With the aid of sodium cation pairing of ionizable acidic protons, EDD has been established as an excellent tool for characterizing highly sulfated heparin tetrasaccharides [24]. Recent EDD applications to the highly sulfated pentasaccharide, Arixtra, showed remarkable product ion coverage for assigning sites of modifications [25]. The density of peaks in EDD mass spectra has driven the application of multivariate statistical methods like principal component analysis (PCA) to maximize the amount of information retrieved in a data set. PCA was used to differentiate the EDD spectra of four diastereoisomeric HS tetrasaccharides with very similar spectral features [26], and also used for the analysis of mixtures of epimer pairs that were resolved by field asymmetric ion mobility spectrometry (FAIMs) [27].

Most of the previous efforts to develop tandem mass spectrometry methods for analyzing GAG oligomers have focused on assigning sites of sulfo modification. However, a few examples of the assignment of C-5 stereochemistry in the uronic acids of glycosaminoglycans using tandem mass spectrometry can be found in the literature. Zaia and coworkers have been able to assign the global ratio of chondroitin sulfate (CS) versus dermatan sulfate (DS) in mammalian extracellular matrix by using collision induced dissociation [28, 29]. The ability to distinguish the C-5 stereochemistry in uronic acid residues of 4-*O*-sulfo chondroitin sulfate epimers, based on diagnostic ion intensities in EDD mass spectra has been reported by Leach *et al* [18]. The results showed doubly deprotonated $^{0,2}X$ and Y_3 were indicative of CS-A containing GlcA, in agreement with the

prior CID results for CS oligomers examined by Zaia and co-workers (*vide infra*). Wolff and Amster have reported diagnostic ions that can be used for assigning IdoA versus GlcA in unsulfated and monosulfated heparan sulfate (HS) tetramers by using EDD [20].

Despite these promising results, there is still a need for a more general approach to identifying uronic acid C-5 stereochemistry in GAG oligomers, particularly in HS and heparin (Hp) oligomers, where 2-*O*-sulfo modification of the uronic acid can occur. In prior work using EDD to examine HS tetramers, stereospecific product ions B_3'-CO_2 and $^{0,2}A_3$ indicated the presence of glucuronic acid in enzymatically produced HS tetrasaccharides [20]. For IdoA residues, the relative intensities of C_3'' is higher compared to C_3. Later work on more highly sulfated HS tetrasaccharides found that these same ions were not as useful for assigning uronic acid stereochemistry [26]. This has motivated us to examine in more detail the capability of EDD mass spectrometry to assign uronic acid stereochemistry in HS GAGs.

In the present work, we study the significance of 2-*O*-sulfo modification of the uronic acid residue on product ion formation during EDD activation. Synthetically produced epimeric 2-*O*-sulfo modified HS tetrasaccharides, with varying degrees of sulfation (0.5-2.5 sulfates per disaccharide subunit) serve as standards to examine differences in the EDD mass spectra. Principal component analysis identifies statistically significant peaks that are diagnostic of the C-5 stereochemistry in a uronic acid. With these data, we can assign the stereochemistry of the reducing end uronic acid in a tetrasaccharide with a single stage of tandem mass spectrometry, based on diagnostic ratios of selected product ions.

Experimental method

Sample Preparation

Epimeric heparan sulfate tetrasaccharides; I-A[GlcA-GlcNAc-IdoA2S-GlcNAc-$(CH_2)_5NH_2$], I-B [GlcA-GlcNAc-GlcA2S-GlcNAc-$(CH_2)_5NH_2$], II-A [GlcA-GlcNAc-IdoA2S-GlcNAc6S-$(CH_2)_5NH_2$], II-B [GlcA-GlcNAc-GlcA2S-GlcNAc6S-$(CH_2)_5NH_2$], III-A [GlcA-GlcNS-IdoA2S-GlcNS-$(CH_2)_5NH_2$], III-B [GlcA-GlcNS-GlcA2S-GlcNS-$(CH_2)_5NH_2$, IV-A [GlcA-GlcNS-IdoA2S-GlcNS6S-$(CH_2)_5NH_2$], IV-B [GlcA-GlcNS-GlcA2S-GlcNS6S- $(CH_2)_5NH_2$], V-A [GlcA-GlcNS6S-Ido2SA-GlcNS6S- $(CH_2)_5NH_2$], and VI-A [IdoA-GlcNS6S-Ido2SA-GlcNS6S- $(CH_2)_5NH_2$] ,were synthesized by the modular approach [30]. FT-ICR MS accurate mass measurements and ^1H NMR were used to confirm all structures.

Mass Spectrometry Analysis

All tandem mass spectrometry experiments were performed on a 9.4T Bruker Apex Ultra QeFTMS (Billerica, MA) fitted with an indirectly heated hollow cathode (HeatWave, Watsonville, CA) to generate electrons for EDD. 0.1 mg/ml sample solutions in 50:50 methanol/H_2O were infused at a rate of 120 □L/h and ionized by electrospray using a metal capillary (Agilent Technologies, Santa Clara, CA, #G2427A) [19].

For the EDD experiments, precursor ions were isolated in the external quadrupole and accumulated for 1 to 3s before injection into the FT-MS cell. Two isolation cell fills were applied per scan, and the selection of the precursor ion was further refined by using in-cell isolation with a coherent excitation frequency (CHEF) event. Selected precursor ions were then irradiated with electrons for 1s. For electron irradiation, the cathode bias was set to 19 and extraction lens set to -18.5 ± 0.5V with the cathode heater set to 1.5A. 36 acquisitions

were signal averaged per spectrum. 512 K points were acquired for each spectrum, padded with one zero fill, and apodized using a sine bell window. Internal calibration was also performed using confidently assigned glycosidic bond cleavage products as internal calibrants, providing mass accuracy of <1 ppm. Due to the large number of low intensity products formed by EDD, only peaks with S/N> 10 are reported. Product ions were assigned using accurate mass measurement and GlycoWorkbench. All products are reported using the annotation proposed by Wolff and Amster, derived from the Domon and Costello nomenclature [31].

Principal Component Analysis

Principal component analysis (PCA) was performed using PLS Toolbox (Eigenvector Research, Inc., Wenatchee, WA), as reported earlier [26]. The abundances of 30 assigned product ions were normalized with respect to the total ion current in each EDD spectrum. An input matrix with each row containing the mass spectrum of a single tetrasaccharide epimer and each column the normalized abundance of an assigned fragment ion (variables) is constructed. For each sample quintuplicate EDD spectra were acquired in the same day. Each data set was mean-centered and cross-validated prior to PCA analysis. Principal component scores plot shows the relationship between the samples, whereas the loading plot reveals the variables that contribute to the sample differences. All referenced figures and the supplemental material in chapter 5 is included in Appendix C.

Results and discussions

The compounds selected for this study provide the means to examine differences between HS tetramers that differ only in C-5 stereochemistry of the uronic acid closest to the reducing end of the oligomer. The uronic acid at the nonreducing end is of little consequence, as this residue is often converted to a □-uronic acid during the enzymatic processing of proteoglycans to produce oligomers of a size that can be sequenced by tandem mass spectrometry. Such enzymatic processing eliminates stereochemical differences between IdoA and GlcA in the nonreducing end sugar. In the following discussion, references to the uronic acid are to the residue closest to the reducing end. Several EDD mass spectra were recorded for each compound, so that statistical significant differences between compounds could be differentiated from variations that occur spectrum-to-spectrum for the same compound. Previous studies of differences in the EDD mass spectra of epimeric GAGs focused on uronic acids lacking 2-*O*-sulfo, and have little or no sulfo modifications elsewhere in the oligomer chain. Here, all the samples have 2-*O*-sulfo modifications in the uronic acid closest to the reducing end. Furthermore, we examine HS tetramers with up to five sulfo modifications, to find product ions that are diagnostic of the uronic acid stereochemistry, yet insensitive to the degree of sulfation.

EDD and PCA results for mono-sulfated HS tetrasaccharides epimers I-A and I-B

EDD mass spectra and annotated structures for $[M-2H]^{2-}$ precursor ions for I-A (contains IdoA2S) and I-B (contains GlcA2S) are shown in Fig. 5. 1. Abundant cross-ring cleavages occur on the hexuronic acid near the reducing end, consistent with the prior observations that electron detachment is favored on a carboxyl group, particularly if it is ionized [19, 20]. Glycosidic cleavage products, B_3 and C_2, locate a sulfo modification on

the uronic acid; definitive assignment of the 2-*O*-sulfo modification in compound I-B can be made with the $^{0,2}A_3$ ion, which is absent in I-A. This ion has been shown to indicate the presence of GlcA in previous EDD studies [20]. B_3' and B_3'-CO_2, indicative of GlcA in prior studies of oligomers lacking 2-*O*-sulfo modification, were not observed in I-B. We attribute this difference to the presence of 2-*O*-sulfo, which introduces extra charge on the uronic acid residue. We find instead the products [B_3-HSO_3], [B_3-H_2SO_3] and [B_3-H_2SO_3-CO_2] in the EDD spectrum of I-B. To better identify diagnostic ions that distinguish the epimer pair, the data was subjected to PCA, and the scores and loadings plots are shown in Fig. 5. 2. 99.78% of the differences between the EDD spectra of the epimers are found in a single principal component. Ions contributing to the clear distinction of these isomers are B_3, Y_1, Z_2, and Z_3, which correlate with GlcA2S, while Y_2, Y_3, and $^{1,5}X_2$ correlate with IdoA2S.

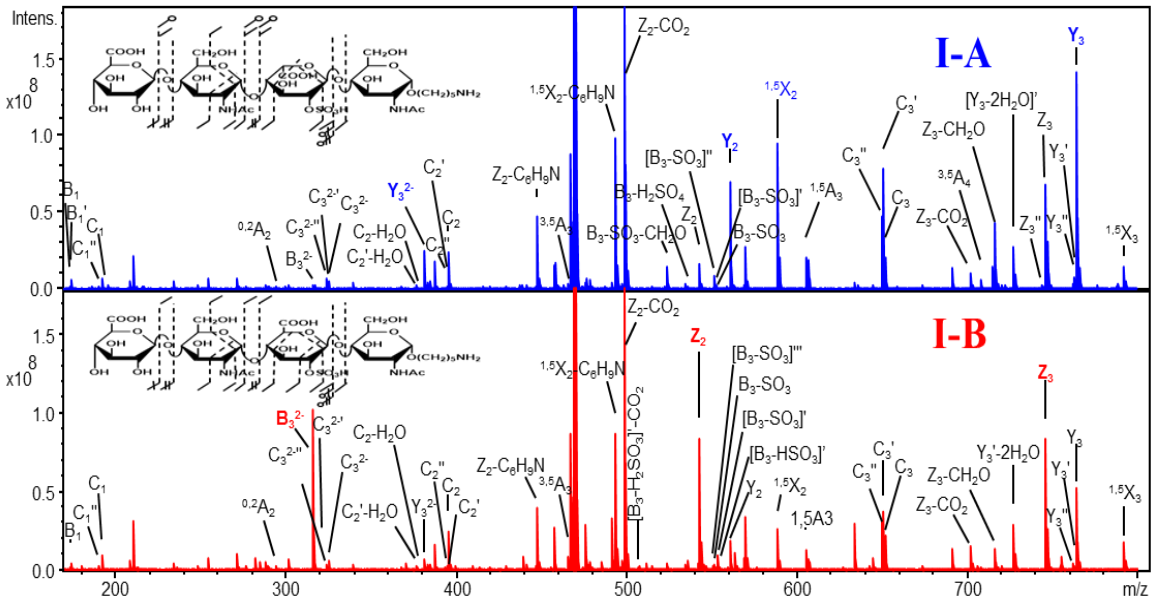

Figure 5. 1. EDD spectra and annotated structures for $[M-2H]^{2-}$ precursor ion for I-A and I-B.

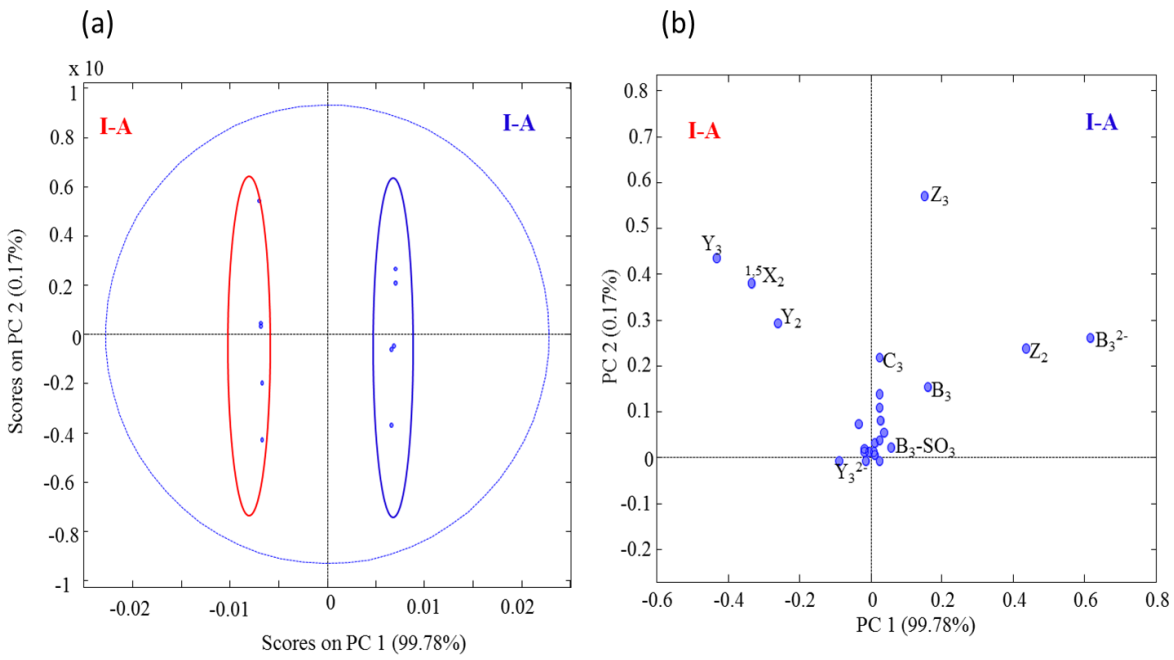

Figure 5. 2. PCA projection of EDD results for I-A and I-B. Score Plot (a) PC1 and PC2 (b) loadings plot showing PC1 and PC

EDD and PCA results for di-sulfated HS tetrasaccharides epimers II-A and II-B

The introduction of a 6-*O*-sulfo modification on the reducing end amino sugar distinguishes epimer pair II-A and II-B from the first set of standards. The EDD mass spectra and annotated structure of the $[M-3H]^{3-}$ precursor ion for both for epimers are shown in Fig.5. 3. The EDD data unambiguously determine the locations of the two sulfo modifications. The mass difference between $^{0,2}X_1$ and B_3 assigns 2-*O*-sulfo on the central uronic acid, while $^{3,5}A_4$ and Z_1 locates the 6-*O*-sulfo on the reducing terminus amino sugar. PCA of the EDD mass spectra for II-A and II-B established a high variance of 99.9% in a single principal component. Fig. 5. 4 shows the scores and loadings plot for IIA and IIB. From the loadings plot, B_3^{2-}, Y_1, C_2 and Z_3, are observed to be diagnostic for II-B (containing GlcA2S) and Y_3^{2-}, $^{1,5}X_2^{2-}$, $[Y_3\text{-}SO_3]^{2-}$ and $Z_2\text{-}SO_3$ for II-A (containing IdoA2S).

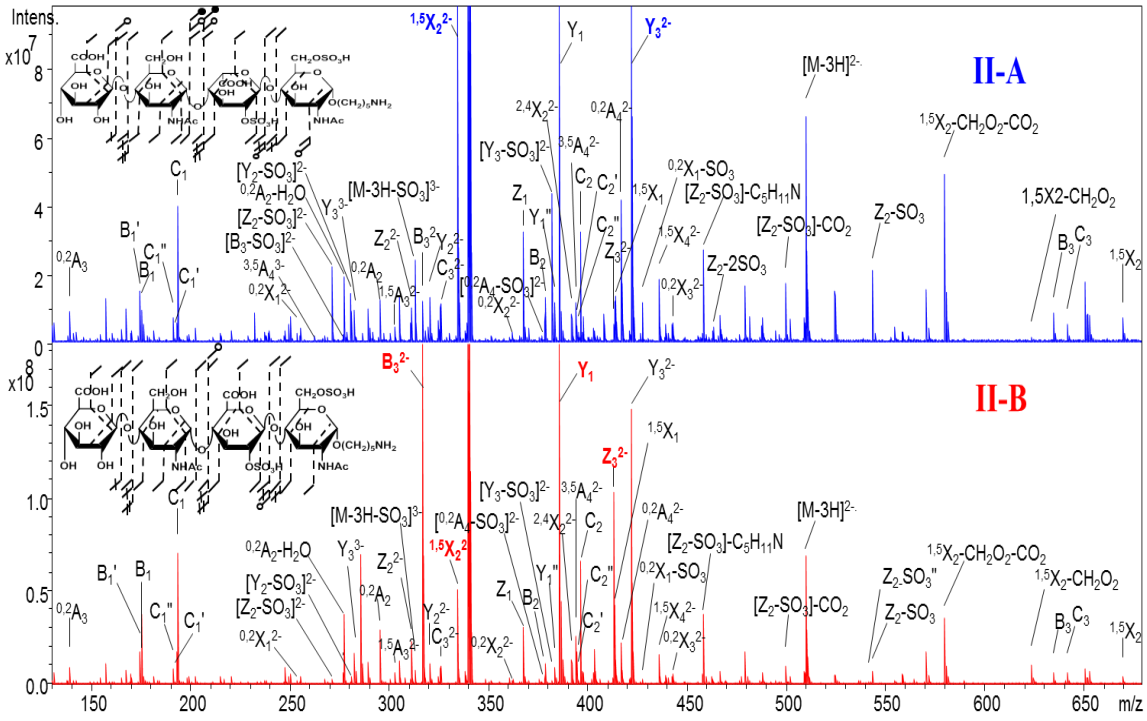

Figure 5. 3. EDD spectra with structural annotations of $[M-2H]^{2-}$ precursor ion for II-A and II-B.

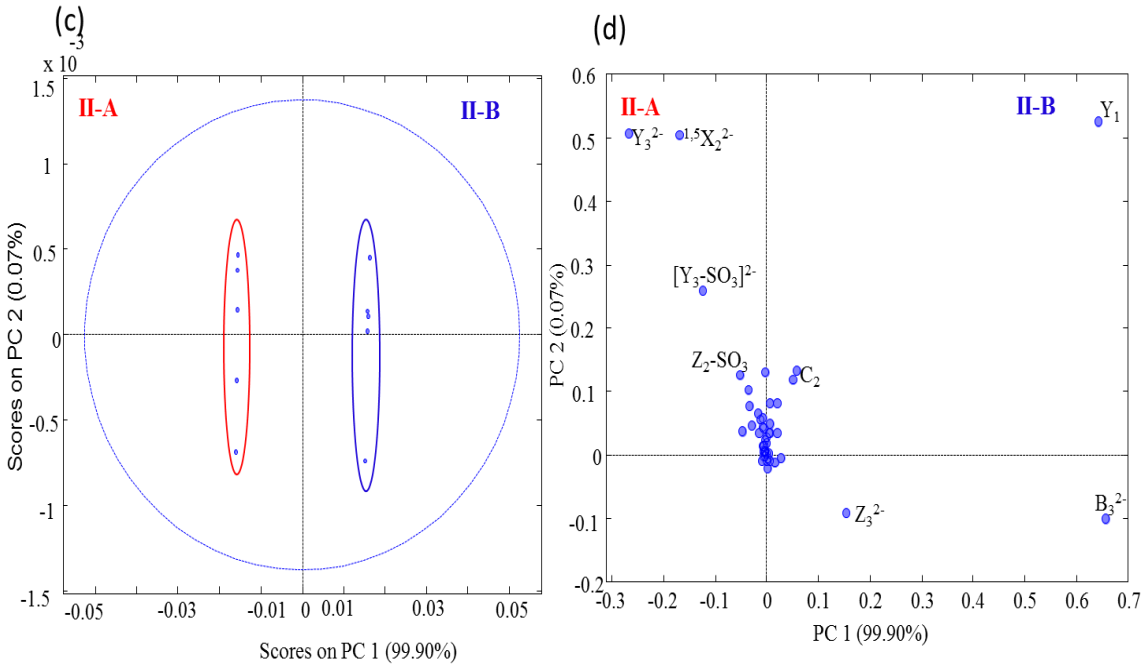

Figure 5. 4. PCA scores plot (c) and loadings plot (d) for II-A and II-B

EDD and PCA results for tri-sulfated HS tetrasaccharides epimers III-A and III-B

Product ion assignments for the EDD mass spectra of epimers with three sulfo modifications are shown in Fig. 5. 5. The sulfo modifications are distributed on the three reducing end saccharides. Prior work has shown that all sulfo groups must be ionized for such high sulfated HS oligomers to fragment by pathways other than SO_3 loss [16]. The $[M-4H+Na]^{3-}$ precursor ion for III-A and III-B was thus selected for EDD fragmentation. Supplementary information, fig. S1, shows the tandem mass spectrum for III-A and III-B. Complete glycosidic product ions with cross ring product ions observed for these epimers were enough to locate all the sites of sulfation. EDD-PCA scores and loadings plot shown in Fig. 5. 6. show that 99.9% of variance between the epimers occurs in one principal component. The loadings plot shows very high positive loading values for complementary ions $[B_3+Na]^{2-}$ and Y_1 for III-B and negative loadings value for $[Y_2+Na]^{2-}$,Y_2^{2-}, $[Y_3+Na]^{2-}$ and $^{1,5}X_2$+Na for III-A.

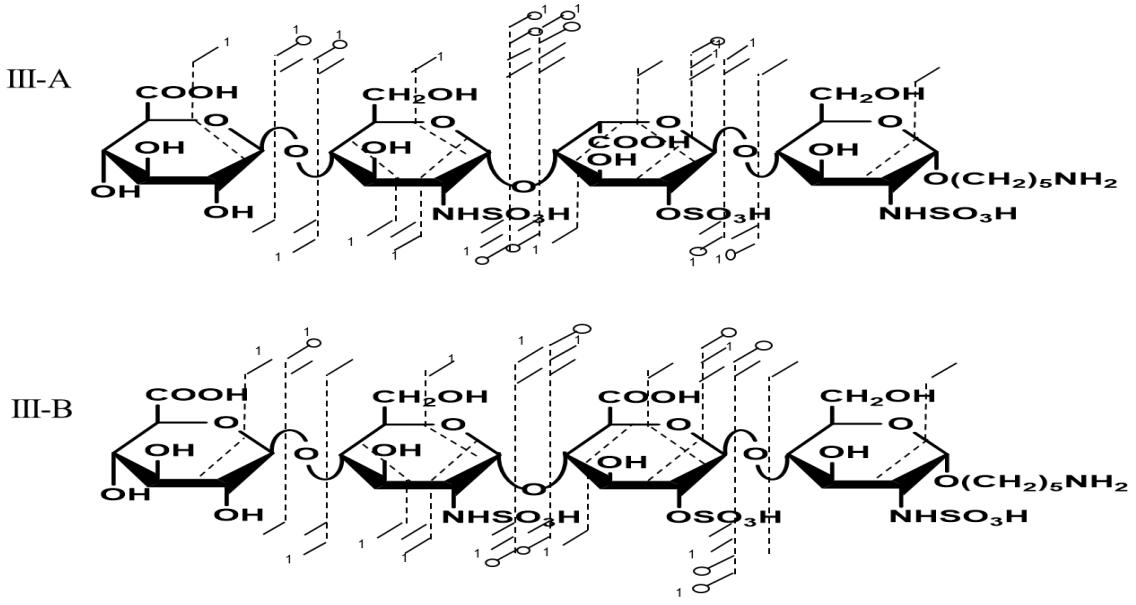

Figure 5. 5. Annotated structure for EDD fragmentation of $[M-4H+Na]^{3-}$ for III-A and III-B

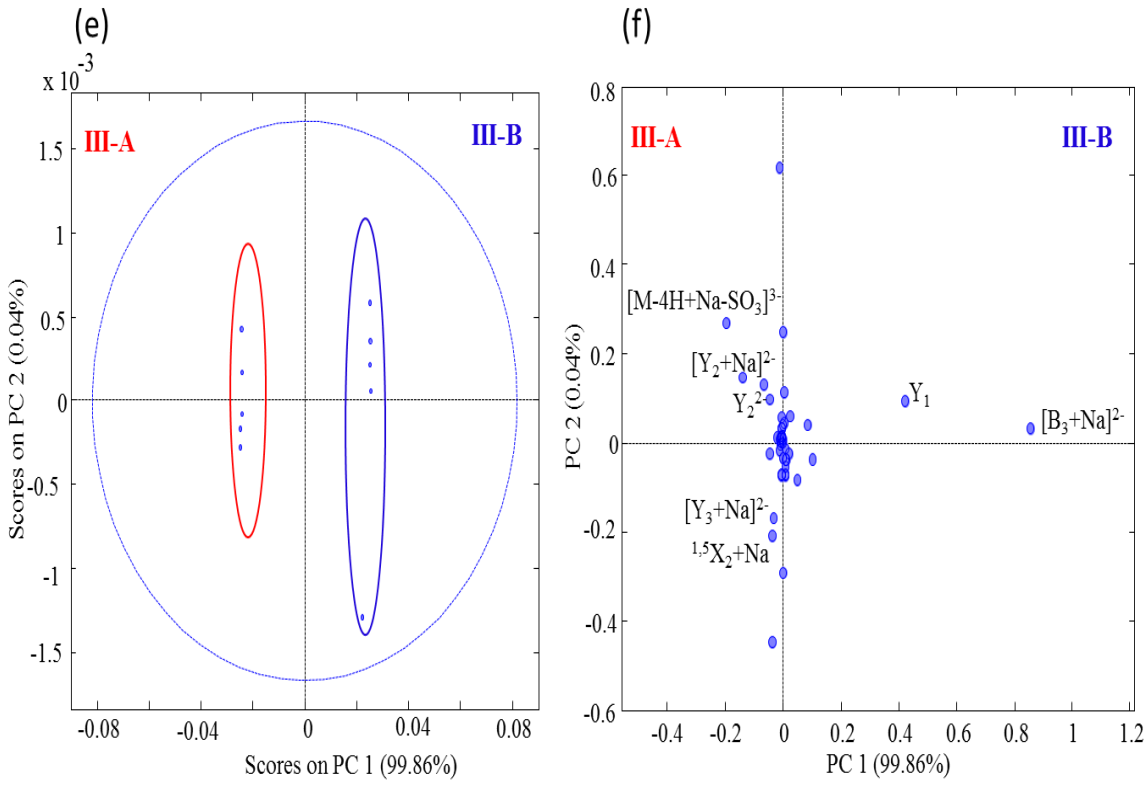

Figure 5. 6. PCA scores plot (e) and loadings plot (f) for III-A and III-B

EDD and PCA results for tetra-sulfated HS tetrasaccharides epimers IV-A and IV-B

Sulfo modification at the 6-*O* position on the reducing end amino-sugar of IV-A and IV-B distinguish these compounds from the tri-sulfated HS tetrasaccharides described above. This modification increases the number of sulfates per disaccharides from 1.5 to 2, making it even more prone to SO_3 loss. To prevent excessive sulfo decomposition from occurring, the $[M-5H+Na]^{4-}$ precursor ion was selected for the EDD experiment. EDD product ions spanning the range m/z 120-600 as shown in the Supplemental Information, Fig. S2, were sufficient to locate all four sites of sulfo modification. Fig. 5. 7 shows the structural annotations for IV-A and IV-B. PCA projection of the EDD results shown in Fig. 8 revealed these two epimeric

tetrasaccharides could be differentiated with a single principal component (99.1% of the variance is in PC1). High positive loadings values again for $[B_3+Na]^{2-}$ and Y_1 were observed for IV-B and $[Y_2+Na]^{3-}$ showed negative loading values for II-A.

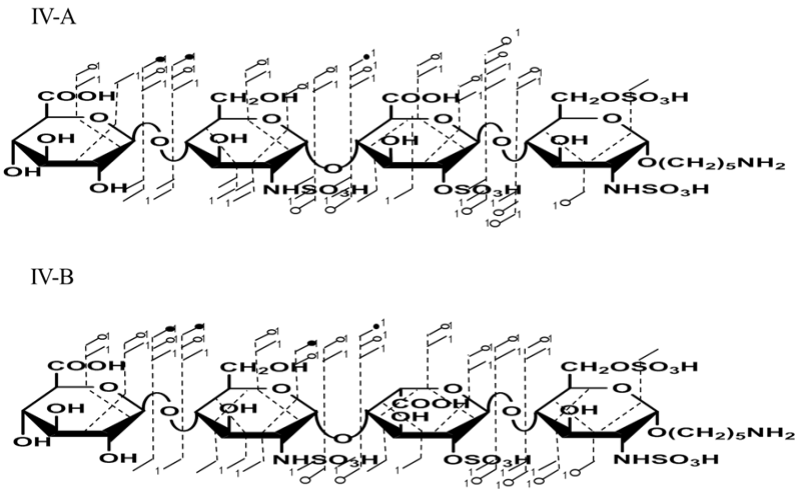

Figure 5. 7. Annotated structure for EDD fragmentation of $[M-5H+Na]^{4-}$ for IV-A and IV-B

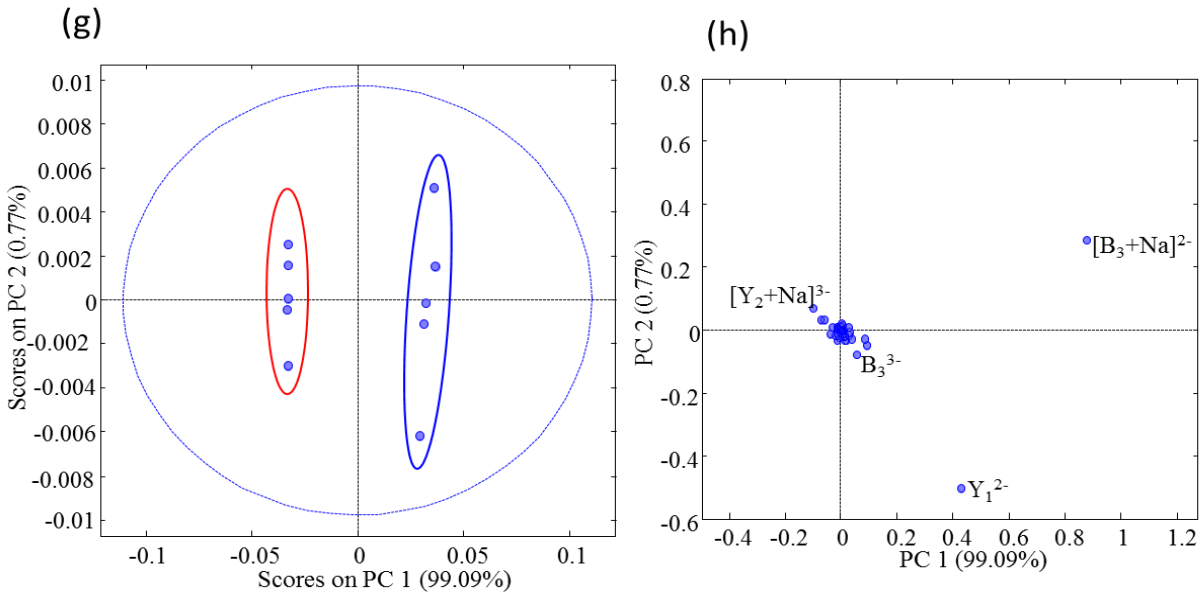

Figure 5. 8. PCA scores plot (g) and loadings plot (h) for IV-A and IV-B

Careful analysis of EDD-PCA results for all eight synthetic 2-*O*-sulfo tetrasaccharides revealed a pattern of glycosidic and cross-ring product ions that correlate with hexuronic acid stereochemistry in their EDD spectra, specifically, the glycosidic cleavages surrounding the uronic residue, B_3, Y_1, Z_2, and C_2 were observed to be diagnostic for GlcA2S. The more remote glycosidic cleavage, Y_2, as well as the cross ring fragment in the adjacent amino sugar, $^{1,5}X_2$, are found to be diagnostic for IdoA2S.

Diagnostic ratio (DR) analysis of 2-O-sulfo HS tetrasaccharides

A tandem mass spectrometric method for assigning uronic acid stereochemistry in HS oligomers, and that is applicable to compounds with a wide variation in sulfo modification, has not previously been reported. Contrary to initial tandem mass spectrometric assignments of uronic acid stereochemistry in chondroitin sulfate oligosaccharides [28] which has a defined sulfation pattern, HS oligosaccharides presents a more complex challenge due to the variability in sulfation pattern and hexuronic acid stereochemistry. Earlier attempt using EDD to assign the hexuronic acid stereochemistry in HS tetrasaccharides yielded promising results. However, the sulfate density was very low (0-0.25 sulfates per disaccharide) for the compounds that were tested, and 2-*O*-sulfo was not present [19]. To provide a more robust analysis for assigning the hexuronic acid stereochemistry in a single mass spectrum using EDD, we have considered 4 epimers pairs with varying degree of sulfation (0.25-2.0). From the PCA loadings plots, we observe strong positive loading values for Glc2AS diagnostic ions and negative loadings values for IdoA2S. The strong variations between these epimer pairs from the EDD PCA loadings plots suggest the possibility of combining diagnostic ions could to assign the stereochemistry in a mass spectrum. Combining the results from all 4 PCA plots, we have

selected diagnostic ions indicative of Glc2AS (B_3, Y_1, C_2 and Z_2) and Ido2AS (Y_2 and $^{1,5}X_2$). The ratio of these summed peaks could predict the hexuronic acid stereochemistry for all the 2-*O*-sulfated HS tetrasaccharides examined. Equation 1 below compares the intensity ratios of Glc2AS ions to Ido2AS.

$$DR = \frac{\sum I(GlcA2S)}{\sum I(IdoA2S)} = \frac{\sum I(B_3, Y_1, C_2, Z_2)}{\sum I(Y_2, {}^{1,5}X2)} \qquad (1)$$

In equation 1, *DR* is the diagnostic ratio calculated from the abundance of the designated fragment ions in the EDD spectra. *I(GlcA2S), I(IdoA2S)* are the intensities for all diagnostic ions, including those accompanied by sulfo decomposition, for the fragment ions that are diagnostic of Glc2AS and Ido2AS. DR results for the four epimer pairs are found to segregate in to low ratios (≤1.6) for IdoA2S containing tetrasaccharides, and high ratios (9 or higher) for tetrasaccharides with GlcA2S, as shown in Table 1, with up to four sulfo modifications. The large gap between the DR values of the GlcA2S and the IdoA2S tetrasaccharides allows the confident assignment of stereochemistry for the uronic acid residue closest to the reducing end. This was tested on even more highly sulfo modified oligomers, two penta-sulfo modified tetramers that contain IdoA2S, GlcA-GlcNS6S-IdoA2S-GlcNS6S-$(CH_2)_5NH_2$ (DR = 13) and IdoA-GlcNS6S-IdoA2S-GlcNS6S-$(CH_2)_5NH_2$ (DR=0.6), shown Table 1. EDD spectra for the pentasulfated tetrasaccharides are shown in Supplementary data, Fig. S3 and Fig. S4. Also included in the supplementary material are mass (m/z) - intensity table for the ions used for the DR calculations. These data suggest that the DR calculation from assigned peaks in EDD mass spectra of HS tetramers can be used to accurately and confidently assign uronic acid C-5 stereochemistry.

IdoA2S	DR	GlcA2S	DR
GlcA-GlcNAc-IdoA2S-GlcNAc-$(CH_2)_5NH_2$	0.5	GlcA-GlcNAc-GlcA2S-GlcNAc-$(CH_2)_5NH_2$	12.5
GlcA-GlcNAc-IdoA2S-GlcNAc6S-$(CH_2)_5NH_2$	1.0	GlcA-GlcNAc-GlcA2S-GlcNAc6S-$(CH_2)_5NH_2$	13.5
GlcA-GlcNS-IdoA2S-GlcNS-$(CH_2)_5NH_2$	1.6	GlcA-GlcNS-GlcA2S-GlcNS-$(CH_2)_5NH_2$	21.6
GlcA-GlcNS-IdoA2S-GlcNS6S-$(CH_2)_5NH_2$	1.2	GlcA-GlcNS-GlcA2S-GlcNS6S-$(CH_2)_5NH_2$	9.3
GlcA-GlcNS6S-IdoA2S-GlcNS6S-$(CH_2)_5NH_2$	1.3		
IdoA-GlcNS6S-IdoA2S-GlcNS6S-$(CH_2)_5NH_2$	0.6		

Table 5. 1, shows DR results for 10 synthetic 2-*O*-sulfo HS tetrasaccharides

Conclusions

EDD fragmentation is known to provide useful data for the assignment of sulfo locations in HS oligomers, but the assignment of uronic acid stereochemistry has remained an open issue. This work demonstrates for the first time the assignment of C-5 stereochemistry in 2-*O*-sulfated uronic acid epimers using EDD data. The relative abundance of glycosidic products B_3, Y_1, Z_2 and C_2 as projected onto the PCA loadings plots are found to be diagnostic of GlcA2S while Y_2, Y_3 and $^{1,5}X_2$ are diagnostic of IdoA2S near the reducing end of HS or Hp tetramers. By summing the intensities of the GlcA2S diagnostic

fragments, and dividing by the sum of the IdoA2S diagnostic fragments, a ratio is obtained that allows one to assign the hexuronic acid stereochemistry for a number of HS/Hp tetramers with a broad range of sulfo modifications. Since there are several structural variations of HS oligomers, future work will test the value of the diagnostic ratio (DR) for a full range of HS tetrasaccharides. We also plan to test this approach on hexasaccharides and longer oligomers, to see if it extends to the assignment of more than one uronic acid residue in an oligomer.

Acknowledgments

The authors acknowledge generous financial support from the National Institutes of Health, grant P41 GM103390.

References

1. Chi, L., Amster, J., Linhardt, R.J.: Mass spectrometry for the analysis of highly charged sulfated carbohydrates. Current Analytical Chemistry. **1**, 223-240 (2005)
2. Rabenstein, D.L.: Heparin and heparan sulfate: structure and function. Natural product reports. **19**, 312-331 (2002)
3. Desai, U.R., Wang, H., Ampofo, S.A., Linhardt, R.J.: Oligosaccharide composition of heparin and low-molecular-weight heparins by capillary electrophoresis. Anal. Biochem. **213**, 120-127 (1993)
4. Liu, C., Sheng, J., Krahn, J.M., Perera, L., Xu, Y., Hsieh, P.-H., Dou, W., Liu, J., Pedersen, L.C.: Molecular mechanism of substrate specificity for heparan sulfate 2-O-sulfotransferase. J. Biol. Chem. **289**, 13407-13418 (2014)
5. Warda, M., Toida, T., Zhang, F., Sun, P., Munoz, E., Xie, J., Linhardt, R.J.: Isolation and characterization of heparan sulfate from various murine tissues. Glycoconjugate J. **23**, 555-563 (2006)
6. Ai, X., Do, A.-T., Lozynska, O., Kusche-Gullberg, M., Lindahl, U., Emerson, C.P.: QSulf1 remodels the 6-O sulfation states of cell surface heparan sulfate proteoglycans to promote Wnt signaling. J. Cell Biol. **162**, 341-351 (2003)
7. Pellegrini, L.: Role of heparan sulfate in fibroblast growth factor signalling: a structural view. Curr. Opin. Struct. Biol. **11**, 629-634 (2001)
8. Fuster, M.M., Wang, L.: Endothelial heparan sulfate in angiogenesis. Progress in Molecular Biology and Translational Science. **93**, 179-212 (2010)

9. Lindahl, B., Eriksson, L., Lindahl, U.: Structure of heparan sulphate from human brain, with special regard to Alzheimer's disease. Biochem. J. **306**, 177-184 (1995)

10. Zaia, J., Costello, C.E.: Tandem mass spectrometry of sulfated heparin-like glycosaminoglycan oligosaccharides. Analytical chemistry. **75**, 2445-2455 (2003)

11. Huang, R., Pomin, V.H., Sharp, J.S.: LC-MSn analysis of isomeric chondroitin sulfate oligosaccharides using a chemical derivatization strategy. Journal of the American Society for Mass Spectrometry. **22**, 1577 (2011)

12. Zhou, W., Hakansson, K.: Electron Capture Dissociation of Divalent Metal-adducted Sulfated N-Glycans Released from Bovine Thyroid Stimulating Hormone. J. Am. Soc. Mass Spectrom. **24**, 1798-1806 (2013)

13. Zaia, J.: Mass spectrometry of oligosaccharides. Mass spectrometry reviews. **23**, 161-227 (2004)

14. Liu, H.C., Hakansson, K.: Electron capture dissociation of divalent metal-adducted sulfated oligosaccharides. Int. J. Mass spectrom. **305**, 170-177 (2011)

15. Shi, X., Huang, Y., Mao, Y., Naimy, H., Zaia, J.: Tandem mass spectrometry of heparan sulfate negative ions: sulfate loss patterns and chemical modification methods for improvement of product ion profiles. J. Am. Soc. Mass Spectrom. **23**, 1498-1511 (2012)

16. Kailemia, M.J., Li, L., Ly, M., Linhardt, R.J., Amster, I.J.: Complete mass spectral characterization of a synthetic ultralow-molecular-weight heparin

using collision-induced dissociation. Analytical chemistry. **84**, 5475-5478 (2012)

17. Kailemia, M.J., Li, L., Xu, Y., Liu, J., Linhardt, R.J., Amster, I.J.: Structurally informative tandem mass spectrometry of highly sulfated natural and chemoenzymatically synthesized heparin and heparan sulfate glycosaminoglycans. Mol. Cell. Proteomics. **12**, 979-990 (2013)
18. Leach III, F.E., Ly, M., Laremore, T.N., Wolff, J.J., Perlow, J., Linhardt, R.J., Amster, I.J.: Hexuronic acid stereochemistry determination in chondroitin sulfate glycosaminoglycan oligosaccharides by electron detachment dissociation. J. Am. Soc. Mass Spectrom. **23**, 1488-1497 (2012)
19. Wolff, J.J., Amster, I.J., Chi, L., Linhardt, R.J.: Electron detachment dissociation of glycosaminoglycan tetrasaccharides. J. Am. Soc. Mass Spectrom. **18**, 234-244 (2007)
20. Wolff, J.J., Chi, L., Linhardt, R.J., Amster, I.J.: Distinguishing glucuronic from iduronic acid in glycosaminoglycan tetrasaccharides by using electron detachment dissociation. Anal. Chem. **79**, 2015-2022 (2007)
21. Wolff, J.J., Laremore, T.N., Busch, A.M., Linhardt, R.J., Amster, I.J.: Electron detachment dissociation of dermatan sulfate oligosaccharides. Journal of the American Society for Mass Spectrometry. **19**, 294-304 (2008)
22. Leach III, F.E., Wolff, J.J., Xiao, Z., Ly, M., Laremore, T.N., Arungundram, S., Al-Mafraji, K., Venot, A., Boons, G.-J., Linhardt, R.J.: Negative electron transfer dissociation Fourier transform mass spectrometry of glycosaminoglycan carbohydrates. Eur. J. Mass Spectrom. **17**, 167 (2011)

23. Wolff, J.J., Leach III, F.E., Laremore, T.N., Kaplan, D.A., Easterling, M.L., Linhardt, R.J., Amster, I.J.: Negative electron transfer dissociation of glycosaminoglycans. Anal. Chem. **82**, 3460-3466 (2010)

24. Leach, F.E., Xiao, Z., Laremore, T.N., Linhardt, R.J., Amster, I.J.: Electron detachment dissociation and infrared multiphoton dissociation of heparin tetrasaccharides. Int. J. Mass spectrom. **308**, 253-259 (2011)

25. Huang, Y., Yu, X., Mao, Y., Costello, C.E., Zaia, J., Lin, C.: De Novo Sequencing of Heparan Sulfate Oligosaccharides by Electron-Activated Dissociation. Anal. Chem. **85**, 11979-11986 (2013)

26. Oh, H.B., Leach III, F.E., Arungundram, S., Al-Mafraji, K., Venot, A., Boons, G.-J., Amster, I.J.: Multivariate analysis of electron detachment dissociation and infrared multiphoton dissociation mass spectra of heparan sulfate tetrasaccharides differing only in hexuronic acid stereochemistry. J. Am. Soc. Mass Spectrom. **22**, 582-590 (2011)

27. Kailemia, M.J., Park, M., Kaplan, D.A., Venot, A., Boons, G.-J., Li, L., Linhardt, R.J., Amster, I.J.: High-field asymmetric-waveform ion mobility spectrometry and electron detachment dissociation of isobaric mixtures of glycosaminoglycans. J. Am. Soc. Mass Spectrom. **25**, 258-268 (2014)

28. Zaia, J., Li, X.-Q., Chan, S.-Y., Costello, C.E.: Tandem mass spectrometric strategies for determination of sulfation positions and uronic acid epimerization in chondroitin sulfate oligosaccharides. Journal of the American Society for Mass Spectrometry. **14**, 1270-1281 (2003)

29. Miller, M.J.C., Costello, C.E., Malmstrom, A., Zaia, J.: A tandem mass spectrometric approach to determination of chondroitin/dermatan sulfate oligosaccharide glycoforms. Glycobiology. **16**, 502-513 (2006)

30. Arungundram, S., Al-Mafraji, K., Asong, J., Leach, F.E., Amster, I.J., Venot, A., Turnbull, J.E., Boons, G.J.: Modular Synthesis of Heparan Sulfate Oligosaccharides for Structure-Activity Relationship Studies. J. Am. Chem. Soc. **131**, 17394-17405 (2009)

31. Domon, B., Costello, C.E.: A systematic nomenclature for carbohydrate fragmentations in FAB-MS/MS spectra of glycoconjugates. Glycoconjugate journal. **5**, 397-409 (1988)

CHAPTER 6

Single Stage Tandem Mass Spectrometry Assignment of the C-5 Uronic Acid Stereochemistry in Heparan Sulfate Tetrasaccharides Using Electron Detachment Dissociation

Accepted for publication as:

Agyekum, I; Zong, C.; Boons, G.-J.; Amster, I. J., "Single Stage MS/MS Analysis of the C-5 Uronic Acid Stereochemistry In Heparan Sulfate Tetrasaccharides Using Electron Detachment Dissociation", *J. Am. Soc. Mass Spectrom.*, in press.

Abstract

The analysis of heparan sulfate (HS) glycosaminoglycans presents many challenges, due to the high degree of structural heterogeneity arising from their nontemplate biosynthesis. Complete structural elucidation of glycosaminoglycans necessitates the unambiguous assignments of sulfo modifications and the C-5 uronic acid stereochemistry. Efforts to develop tandem mass spectrometric-based methods for the structural analysis of glycosaminoglycans have focused on the assignment of sulfo positions. The present work focuses on the assignment of the C-5 stereochemistry of the uronic acid that lies closest to the reducing end. Prior work with electron based tandem mass spectrometry methods, specifically electron detachment dissociation (EDD), have shown great promise in providing stereo-specific product ions, such as the B3 ´ –CO2, which has been found to distinguish glucuronic acid (GlcA) from iduronic acid (IdoA) in some HS tetrasaccharides. The previously observed diagnostic ions are generally not observed with 2-O-sulfo uronic acids or for more highly sulfated heparan sulfate tetrasaccharides. A recent study using electron detachment dissociation and principal component analysis revealed a series of ions that correlate with GlcA versus IdoA for a set of 2-O-sulfo HS tetrasaccharide standards. The present work comprehensively investigates the efficacy of these ions for assigning the C-5 stereochemistry of the reducing end uronic acid in 33 HS tetrasaccharides. A diagnostic ratio can be computed from the sum of the ions that correlate to GlcA to those that correlate to IdoA.

Keywords: Glycosaminoglycans, Heparan sulfate, Uronic acids, Stereochemistry, FTICR, Electron detachment dissociation

Introduction

A large portion of the extracellular matrix and basement membranes are comprised of proteoglycans, composed of proteins covalently attached to the class of carbohydrates called glycosaminoglycans (GAGs) [1–3]. GAGs are linear negatively charged biopolymers, the basic building blocks of which consist of a repeating disaccharide sequence of an amino sugar and a uronic acid or galactose [4, 5]. They are categorized as either keratan sulfate (KS), chondroitin sulfate (CS), dermatan sulfate (DS), hyaluronan (HA), or heparan sulfate (HS) depending on their disaccharide repeating unit [1–6]. Among these classes of GAGs, HS is the most structurally complex [6, 7]. They are initially synthesized in the Golgi apparatus as alternating disaccharide units of D-glucuronic acid and N-acetylated glucosamine [6, 8]. C5-epimerization of glucuronic acid (GlcA) to iduronic acid (IdoA) occurs during the biosynthesis of HS followed by a series of sulfo modifications [7, 8]. Sulfo modifications may occur at the 2-O position of the uronic acid, and the N-, 3-O, and 6-O positions of the glucosamine unit [8]. These structural modifications often do not go to completion, producing HS chains with varying sequences of sulfation, acetylation, and IdoA/GlcA content [6, 9]. Despite these varying structural modifications, specific structural motifs on HS chains have been reported to bind target proteins with high specificity. These categories of proteins, called heparan sulfate binding proteins (HSBPs), include chemokines, cytokines, blood coagulation factors, such as serine proteases, cell adhesion proteins, growth factors, and morphogenetic factors [7, 10, 11]. Documented physiologic processes influenced by HS interactions with proteins include growth and development, cancer, inflammation, viral infectivity, and blood coagulation [12–15]. The numerous biological functions of this bio-molecule continue to inspire

research into structure–function relationships of HS oligomers. However, this research has been hampered by their enormous microheterogeneity and limited availability requiring very sensitive and robust analytical methods for their analysis.

Advanced analytical methods like nuclear magnetic resonance (NMR) spectroscopy have been used to determine sulfo modifications and the C-5 stereochemistry of the uronic acid in GAGs [16, 17]. However, the quantity and purity of GAGs extracted from natural sources are often not suitable for NMR analysis [18]. These drawbacks make mass spectrometry an excellent alternative for GAG analysis. Negative electrospray ionization mass spectrometry offers an excellent platform for GAG analysis, offering high sensitivity, throughput, and accuracy [19, 20]. However, tandem mass spectrometry of GAGs, especially heparan sulfate, is often challenging due to variations in oligomer length, hexuronic acid stereochemistry, and sulfation heterogeneity [6, 21]. ESI-MS is able to determine the length, degree of sulfation of GAGs, and other features affecting the elemental composition. To determine sites of sulfation, N-acetylation, and hexuronic acid stereochemistry, more advanced methods are required. Recent advances in tandem mass spectrometric applications to GAGs using collision-induced dissociation (CID) [22, 23], infrared multiphoton dissociation (IRMPD) [24], electron induced dissociation (EID) [2, 5], electron detachment dissociation(EDD) [26–28], and negative electron transfer dissociation (NETD) [29] have addressed some of the challenges encountered during their structural analysis. Inherent sulfo decomposition of the labile sulfate half ester group present in GAGs hinders structural characterization. This phenomenon occurs mostly during the ionization and ion activation stages of the experiment. Chemical derivatization [30], deprotonation of the acidic groups [23, 31, 32], and metal cation exchange [22, 23]

have been reported to effectively reduce sulfo decomposition depending on the degree of sulfation. Recent CID MS/MS reports on Arixtra and highly sulfated heparan sulfate GAGs showed that one can obtain very rich and structurally informative product ion coverage by adding dilute NaOH to the spray solution [33, 34]. Electron-based activation methods, especially EDD, have shown great potential in providing highly informative cross-ring products as well as the corresponding glycosidic cleavages, which are essential for localization of sulfo positions [25–27]. Although mass spectrometry methodologies continue to gain ground in assigning sites of sulfo modifications, a remaining challenge has been the inability to discriminate diastereomers that differ by the chirality of the uronic acid C-5 center. Zaia and coworkers were the first to address this challenge. Using collision induced dissociation, they were able to differentiate chondroitin sulfate (CS) from dermatan sulfate (DS) in mammalian extracellular matrix, and quantitatively assign the amount of the diastereomers present in mixtures [35]. The ability to assign the C-5 stereochemistry in uronic acid residues of 4-O-sulfo chondroitin sulfate epimers with varying oligomer lengths (dp4-dp10) based on diagnostic cross-ring ions $^{2,4}A_n$ and $^{0,2}X_n$ in CID mass spectra has also been reported by Kailemia et al. [36]. Compared with heparan sulfates, chondroitin sulfates have a well-defined sulfation pattern; hence, the former requires a more sensitive activation method for stereochemistry assignments. EDD results for HS tetrasaccharides reported by Wolff et al. showed the possibility of obtaining a stereospecific ion B_3'-CO_2 for assigning the C-5 stereochemistry for moderately sulfated tetramers (0–0.25 sulfates per disaccharide) [18]. Gas-phase separation of epimeric mixtures of HS tetrasaccharides using field asymmetric ion mobility spectrometry (FAIMS) followed by EDD fragmentation confirmed the presence of the B_3'-CO_2 ion for

the GlcA containing epimer [37]. Recent EDD reports, however, showed that the presence of a sulfo group at the 2-O position of the uronic acid hinders production of the $B_3´$- CO_2 ion in GlcA-containing epimers [38]. More recent work on the assignment of the C-5 stereochemistry for 2-O-sulfated HS tetramers (0.5–2.5 sulfates per disaccharide) revealed the possibility of assigning the C-5 stereochemistry of HS tetrasaccharides using a ratio combination of selected ions obtain from EDD-PCA experiments [38]. Such analyses are useful when epimeric compounds are available. The scarcity of naturally occurring epimeric HS samples has motivated the development of a technique that assigns the stereochemistry of these tetramers without reference to their isomers. Here we present for the first time a more general approach in assigning the C-5 hexuronic stereochemistry for 33 HS tetrasaccharide standards from a single stage EDD tandem mass spectrum. Experimental Sample Preparation Thirty-three heparan sulfate tetrasaccharides standards were synthesized using a modular approach [39]. All the compounds examined had their compositions confirmed using FTICR MS accurate mass measurement and had their structures confirmed by 1 H NMR, HSQC, and COSY. Supplementary Figures 1–4 show the chemical structures of all 33 compounds. Mass Spectrometry Analysis EDD experiments were performed on a 9.4T Bruker Apex Ultra QeFTMS (Billerica, MA, USA) with a hollow cathode (Heat Wave, Watsonville, CA, USA), which serves as the I. Agyekum et al.: Assigning Uronic Acid in HS by EDD source of electrons for EDD; 0.1 mg/mL of each standard were injected at a rate of 120 μL/h in 50:50 methanol:H2O and ionized by a metal electrospray capillary (#G2427A; Agilent Technologies, Santa Clara, CA, USA). Where necessary, 0.1 mM NaOH was added to the spray solvent to enhance the intensity of preferred sodium adducted precursor ions for analysis. All the HS

tetrasaccharides were analyzed in the negative ion mode. Each EDD experiment was repeated three times with almost similar results for each HS standard examined. For the EDD experiment, multiply charged precursor ions were isolated in the external quadruple and accumulated for 1– 4 s before injection into the FT-ICR cell. Precursor ion selections were refined using in-cell isolation with a coherent excitation frequency (CHEF) event. These ions were then irradiated with 19 eV electrons for 1 s. The extraction lens was set to – 18.5 ± 0.5 V with the cathode heater at 1.5 A. Twenty-four acquisitions were signal averaged per spectrum; 512 K points were acquired for each spectrum, padded with one zero fill, and apodized using a sine bell window. Internal calibration was achieved using confidently assigned glycosidic product ions as internal calibrants, providing mass accuracy of 10 due to the large number of low intensity product ions formed by EDD. All cross-ring and glycosidic product ions generated from the EDD experiment were assigned using accurate mass measurement and GlycoWorkbench [40]. These ions are reported using the Domon and Costello nomenclature [41].

Results and Discussion

Determination of Sulfo Positions Electron detachment dissociation has been shown to provide excellent product ion coverage for the structural analysis of glycosaminoglycans. Figure 1 shows abundant glycosidic and cross-ring product ions for the epimeric di-sulfated HS standards epimers, labeled (2b, 2f, 2d, and 2g). EDD fragmentation of the $[M – 3H]^{3-}$ precursor ion produced almost identical fragmentation for these compounds as one would expect for these epimers (Figure 6. 1). These compounds differ only in the C-5 hexuronic acid stereochemistry and have both their glucosamine unit

sulfated at the 6-O position. We are able to unambiguously assign the sites of sulfation on these epimers with a combination of cross-ring and glycosidic product ions. The mass difference between product ions C_1 and $^{3,5}A_2$, and C_3. and $^{3,5}A_4$, confidently identifies the two 6-O sulfo groups on the second and fourth glucosamine units towards the reducing end for HS standards 2b, 2d, and 2g (Figure 1). A similar assignment of the 6-O sulfo group on the second glucosamine unit from the non-reducing end can be made using the C_1 and $^{3,5}A_2$ for compound 2f; however, the sulfate group on the reducing end sugar is assigned using the mass difference between cross-ring ions product ions $^{2,4}A_4$ and $^{0,2}A_4$.

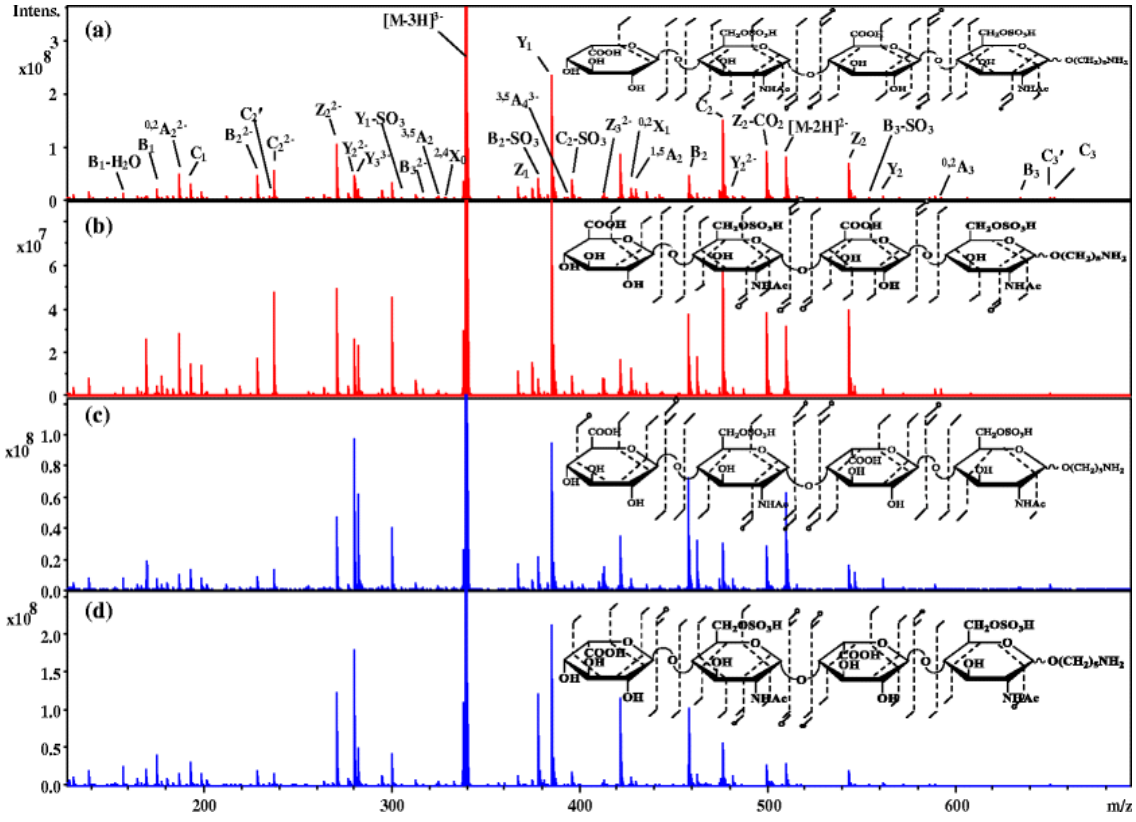

Figure 6. 1 EDD mass spectra with structural annotations for four epimeric synthetic di-sulfated HS tetrasaccharides: **(a)** 2b-(IdoA-GlcNAc6S-GlcA-GlcNAc6S-$(CH_2)_5NH_2$), **(b)** 2f-(GlcA-GlcNAc6S-GlcA-GlcNAc6S- $(CH_2)_5NH_2$), **(c)** 2d-(GlcA-GlcNAc6S-IdoA-GlcNAc6S-$(CH_2)_5NH_2$), and **(d)** 2g-(IdoA-GlcNAc6S-IdoA-GlcNAc6S-$(CH_2)_5NH_2$).

We also show in Figure 2, efficient EDD fragmentation for tri-sulfated epimers 3b-(IdoA-GlcNS6S-GlcA-GlcNS-$(CH_2)_5NH_2$ and 3h- (GlcA-GlcNS6S-IdoA-GlcNS-$(CH_2)_5NH_2$) for the $[M - 4H + Na]^{3-}$ precursor ion. The N- and 6-O sulfo groups on the second residue near the non-reducing ends can be assigned using the mass difference between $^{0,2}A_2$ and B_2, and $^{2,4}A_2$ and $^{0,2}A_2$ product ions, respectively. The N-sulfo group on the reducing end glucosamine is assigned using cross-ring product ion $^{0,2}X_0$. We have included a comprehensive mass list (m/z and intensity) showing similar fragmentation efficiency for triplicate EDD experiment for all the 33 standards in the accompanying supplemental material.

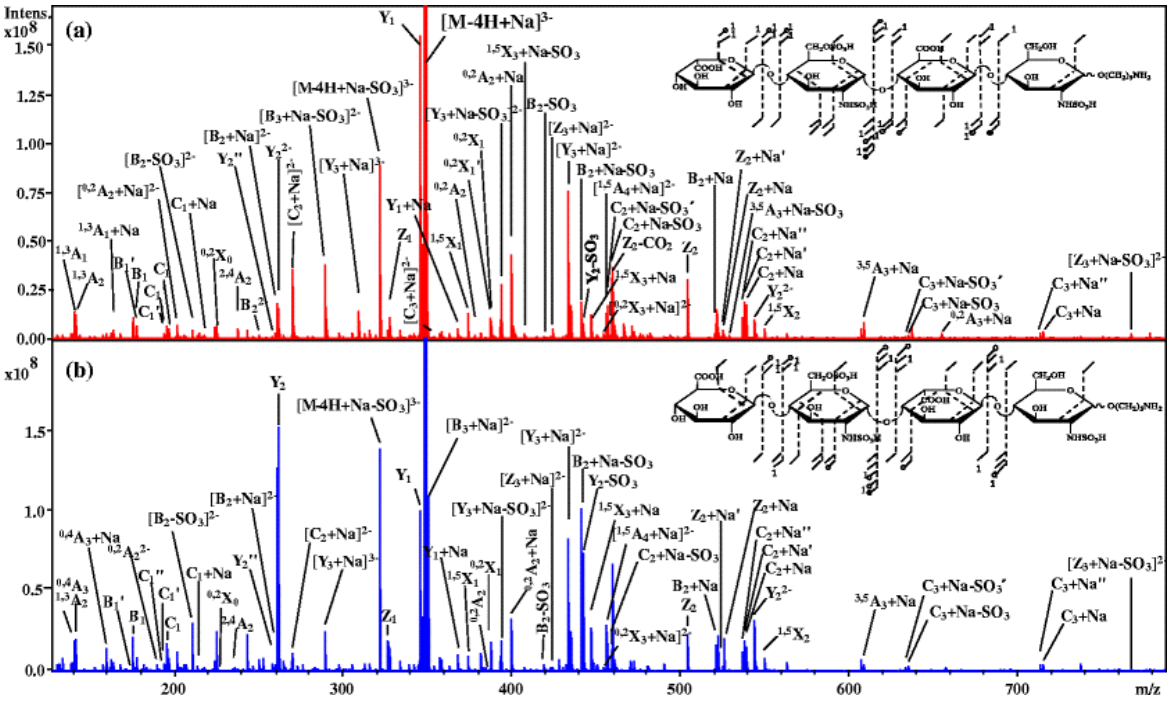

Figure 6. 2 EDD mass spectra and annotated structures for the tri-sulfated HS tetrasaccharides: **(a)** 3b-(IdoA-GlcNS6S-GlcA-GlcNS-$(CH_2)_5NH_2$, and **(b)** 3h-(GlcA-GlcNS6S-IdoA-GlcNS-$(CH_2)_5NH_2$) for the $[M - 4H + Na]^{3-}$ precursor ion

Assignment of the Reducing End Hexuronic Acid Stereochemistry Electrospray ionization mass spectra for all HS standards considered for this work produced abundant multiply

charged ions for the EDD experiment. Figure 3 shows the general structure for the synthetic heparan sulfate tetrasaccharides epimers with an aminopentyl linker on the anomeric carbon.

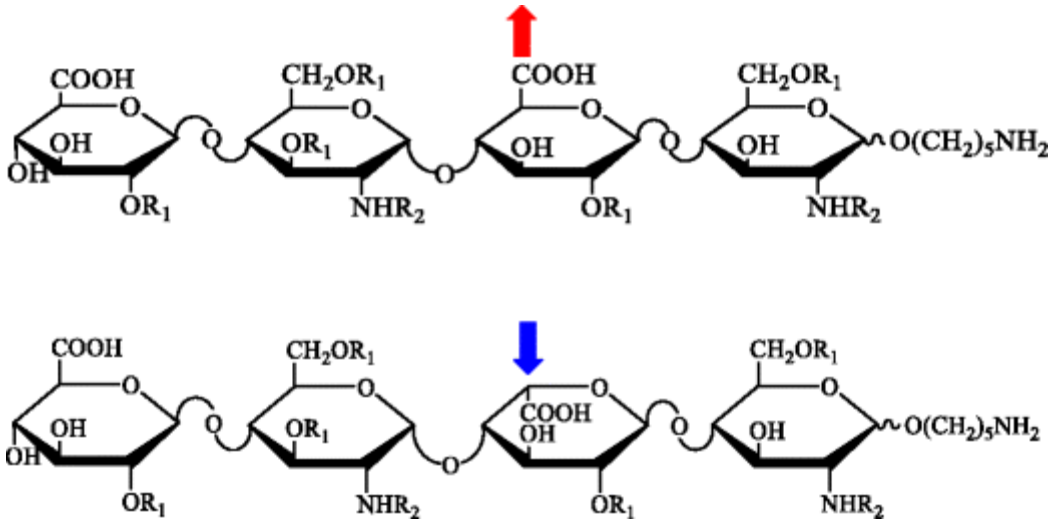

Figure 6. 3 General structure for the synthetic heparan sulfate tetrasaccharide epimers with an anomeric aminopentyl linker, where R_1 = H, SO_3H and R_2 = H, SO_3H, Ac

This modification provides a mass shift for the resulting reducing end fragments ions that enable confident assignment of product ions that would otherwise exhibit identical masses for reducing end and non-reducing end products. In this figure, arrows highlight the C-5 carbon of the uronic acid residue that is the focus of this investigation, namely the acidic sugar closest to the reducing end. ESI-MS of the mono-sulfated synthetic heparan sulfate standards yield abundant doubly charged ions molecular ions, $[M - 2H]^{2-}$. With this charge state, two of the three acidic protons are removed during ionization. Close examination of the EDD spectra for the GlcA-containing standards 1a and 1b, Figure 6. 4a, reveals results consistent with previous EDD reports on modestly sulfated HS tetrasaccharides [35, 40]. Diagnostic ion B_3'-CO_2 indicative of glucuronic acid in less sulfated HS GAGs (0–0.25 sulfates per disaccharide) reported for naturally extracted and synthetically produced HS

tetrasaccharides [18, 21] are observed for only samples 1a (IdoA2S-GlcNAc-GlcAGlcNAc-$(CH_2)_5NH_2$) and 1b (IdoA-GlcNAc6S-GlcAGlcNAc-$(CH_2)_5NH_2$), Figure 4a, occurring at m/z 589.0972. An expanded mass spectra region for the stereospecific ion B_3'- CO_2 is shown in Figure 6. 4a. An intense B_3' ion relative to its original B3 ion is a feature also reported for being diagnostic for GlcA-containing HS [18]. These ions for standards 1a and 1b stand in stark contrast to standards 1d (GlcA-GlcNAc-IdoAGlcNAc6S-$(CH_2)_5NH_2$) and 1f (IdoA-GlcNAc-IdoA- GlcNAc6S-$(CH_2)_5NH_2$), with the B_3' ion with a lower intensity relative to its B3 ion (Figure 4b). The absence of the B3′ ion for standard 1c (GlcA-GlcNAc-IdoA2S-GlcNAc-$(CH_2)_5NH_2$) and 1e (GlcA-GlcNAc-GlcA2S-GlcNAc-$(CH_2)_5NH_2$) further confirmed the influence of the 2-O sulfation on the uronic acid in the formation of the B_3'-CO_2 for 1e as reported earlier [38].

The non-specificity of this previously reported ion over a wide range of sulfo modifications has been the main motivation for this work. Principal component analysis of EDD results from our most recent work revealed several ions that could be used to differentiate GlcA2S from IdoA2S. These ions included, B_3, Y_1, C_2, and Z_2 fragments, found to be diagnostic for GlcA2S, whereas Y_2 and $^{1,5}X_2$ were diagnostic for IdoA2S. We combine these ions into a diagnostic ratio formula below (Equation 2) capable of assigning the C-5 stereochemistry of HS tetrasaccharide standards.

$$DR = \log\left(1/3\left(\left(\sum (GlcA) / \sum (IdoA)\right)\right)\right) = \log\left(1/3\left(\left(\sum (B_3, Y_1, C_2, Z_2) / \sum (Y_2, {}^{1,5}X_2)\right)\right)\right) \quad (2)$$

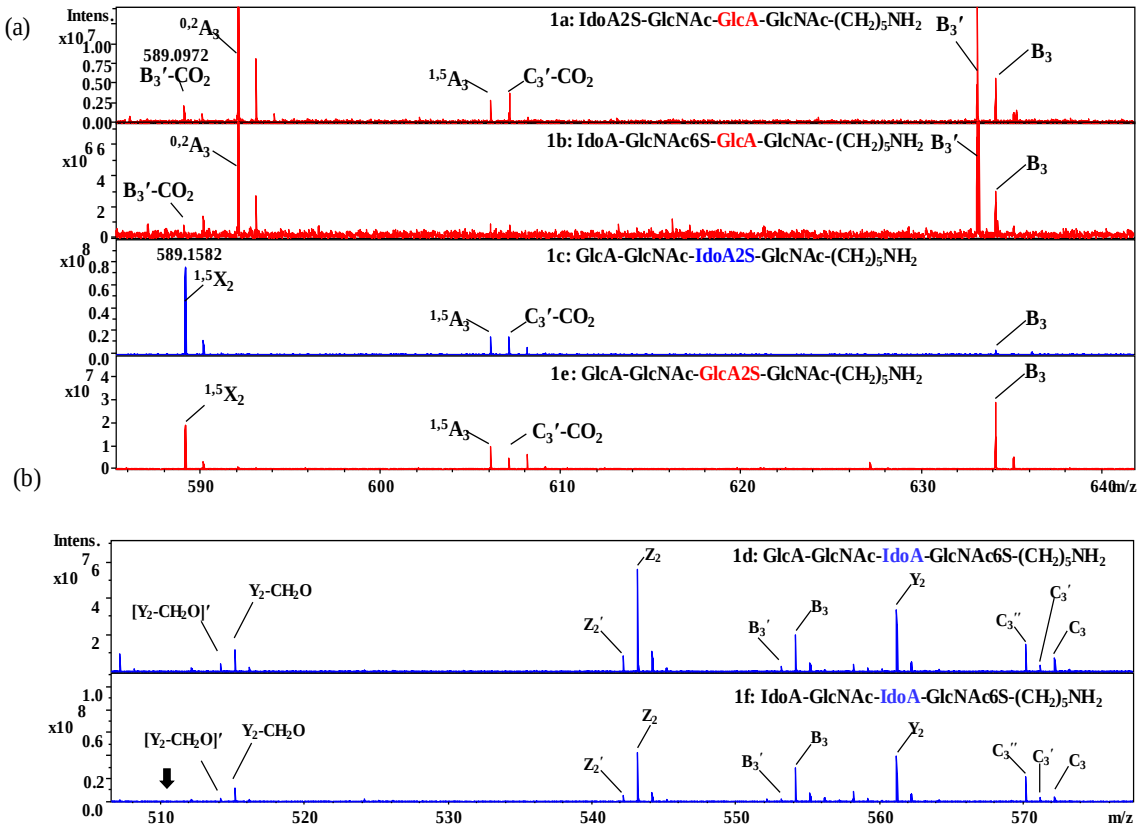

Figure 6. 4 Expanded EDD spectra for the $[M - 2H]^{2-}$ precursor ion for the mono-sulfated HS standards showing the region for the stereospecific ion B_3'-CO_2**(a)** for compounds 1a, 1b, 1c, and 1e *m/z* 570–640, and **(b)** compounds 1d and 1f *m/z* 509–580.

Equation 2 computes the ratio of the sum of intensities of ions that are statistically validated as diagnostic for the presence of GlcA to the sum of intensities of ions diagnostic of IdoA. The factor of one-third applied to each sum was determined empirically to produce a positive value for the diagnostic ratio (DR) when GlcA is present at the second residue from the reducing end, and negative values when IdoA is present in the same position. The DR values computed for all the standards include fragments with sulfo losses from the

selected ions. The discussion below examines the results for a comprehensive set of HS standards with 1 to 4 sulfo modifications.

Diagnostic Ratio Results for Mono-Sulfated HS Standards

Diagnostic ratio (DR) results for all six HS standards for the mono-sulfated tetrasaccharides labeled 1a to 1f are shown in Figure 6. 5. For a common precursor ion selection [M – 2H]2-, at m/z 469.6327 and subsequent electron irradiation, we are able to confidently resolve the C-5 hexuronic acid stereochemistry for the residue closest to the reducing end, for singly sulfated standards. All the GlcA-containing standards showed positive diagnostic ratio results, whereas those for IdoA where negative. The lowest DR results obtained for these set of HS tetramers GlcA was 0.61 ± 0.07 (GlcA-GlcNAc-GlcA2S-GlcNAc-$(CH_2)_5NH_2$) and the highest for mono-sulfated standards containing IdoA was –0.38 ± 0.09 (IdoA-GlcNAc-IdoAGlcNAc6S-$(CH_2)_5NH_2$). Epimeric pair 1c (GlcA-GlcNAcIdoA2S-GlcNAc-$(CH_2)_5NH_2$) and 1e (GlcA-GlcNAcGlcA2S-GlcNAc-$(CH_2)_5NH_2$) with 2-O sulfo modification on the central uronic unit are clearly differentiated, as shown in Figure 6. 5. We also note the non-reducing end stereochemistry has a negligible impact on the DR results for the mono-sulfated set of compounds. This is evident comparing the diagnostic ratio results, which were –0.44 ± 0.03 for standards 1d (GlcAGlcNAc-IdoA-GlcNAc6S-$(CH_2)_5NH_2$) and –0.38 ± 0.09 for 1f (IdoA-GlcNAc-IdoA-GlcNAc6S-$(CH_2)_5NH_2$).

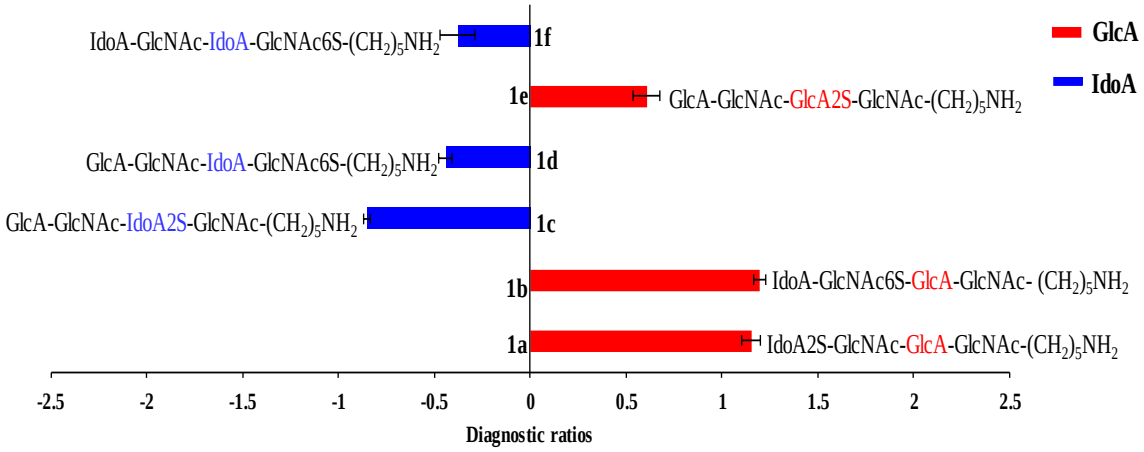

Figure 6. 5 EDD diagnostic ratio results for the mono-sulfated HS tetrasaccharides standards (1a–1f), for the $[M - 2H]^{2-}$ precursor ion.

Diagnostic Ratio Results for Di-Sulfated HS Standards

ESI-MS of the di-sulfated HS standards produced abundant [M – 3H]3- ions at m/z 339.4050 and 325.4015 depending on the disaccharide repeating sequence. These tetrasaccharides have four ionizable protons, two on the sulfo groups and two on the carboxyl groups. Figure 6. 6 shows the diagnostic ratio results obtained for all the eight HS standards examined upon EDD fragmentation of the [M – 3H]3- precursor ion. Again, we show the standards containing GlcA residues towards the reducing end have positive diagnostic ratio values relative to those containing IdoA residues. The broad selection of standards allowed for the applicability of diagnostic ratio formula to discriminate epimers. Standards 2b (IdoA-GlcNAc6S-GlcAGlcNAc6S-$(CH_2)_5NH_2$) and 2d (GlcA-GlcNAc6S-IdoAGlcNAc6S-$(CH_2)_5NH_2$) differing in the C-5 stereochemistry for the non-reducing end and central uronic acid residues were unambiguously resolved with diagnostic ratio values 0.64 ± 0.01 and –0.22 ± 0.01, respectively. The diagnostic ratio results for the remaining epimer pairs, [2c (GlcA-GlcNAc-IdoA2SGlcNAc6S-$(CH_2)_5NH_2$): –0.33 ± 0.05, and 2e

(GlcA-GlcNAc-GlcA2S-GlcNAc6S-$(CH_2)_5NH_2$: 0.83 ± 0.11] and [2f (GlcAGlcNAc6S – GlcA-GlcNAc6S-$(CH_2)_5NH_2$ 0.60 ± 0.06 and, 2g (IdoA-GlcNAc6S-IdoA-GlcNAc6S-$(CH_2)_5NH_2$: –0.11 ± 0.03] further established the usefulness of the formula to discriminate epimers. The overall contribution of the non-reducing end uronic acid stereochemistry is again observed to have very minimal impact on the diagnostic ratio values as we compare standards 2b and 2f (Figure 6. 6). Standard 2h IdoA-GlcNAcIdoA2S-GlcNS-$(CH_2)_5NH_2$, which has a different disaccharide repeating sequence compared with the seven di-sulfated standards produced results consistent with the IdoA-containing tetramers. The lowest diagnostic ratio value recorded for the GlcA-containing standards was 0.11 ± 0.04 for 2a (GlcA2SGlcNAc6S-GlcA-GlcNAc-$(CH_2)_5NH_2$) and the highest for with IdoA was –0.11 ± 0.03 recorded for 2g (IdoAGlcNAc6S-IdoA-GlcNAc6S-$(CH_2)_5NH_2$).

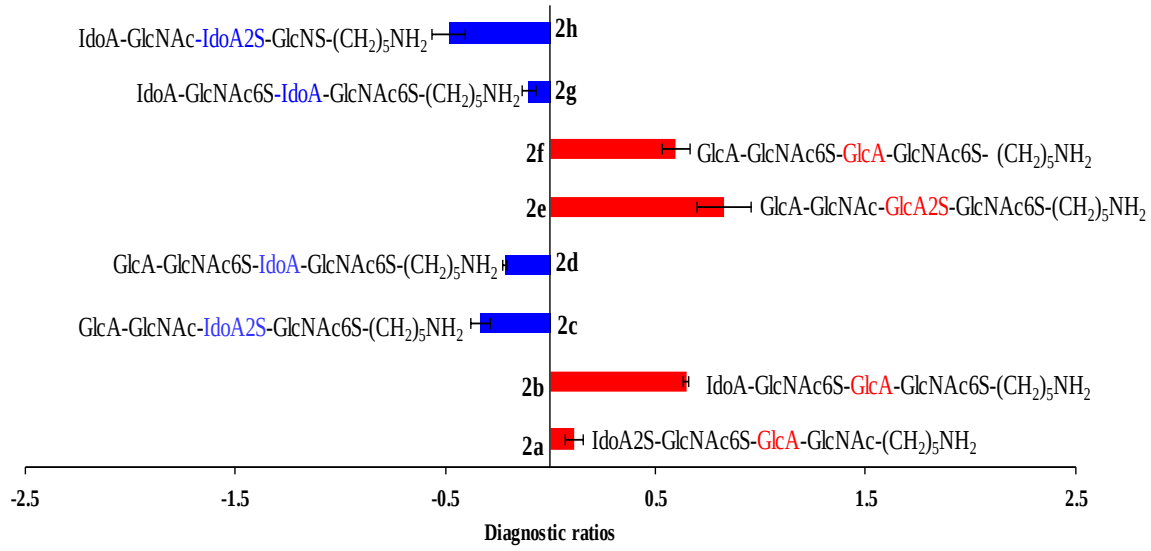

Figure 6. 6 EDD diagnostic ratio results for the di-sulfated HS tetrasaccharides standards (2a–2h) for the $[M - 3H]^{3-}$ precursor ion.

Diagnostic Ratio Results for Tri-Sulfated HS Standards

Previous EDD and CID reports have shown that the presence of sodium counter ions can provide a means to control stereochemical dependent fragmentation [21, 36]. We found that to be very useful for the tri- and tetra-sulfated HS standards. For the tri-sulfated HS standards, the $[M - 4H + Na]^{3-}$ precursor ion at m/z 345.3775 was selected for the EDD experiment. This ionized state allows for all the sulfo groups and a carboxylic group to be ionized. Figure 6. 7 shows diagnostic ratio results for 10 HS tetrasaccharides standards. The C-5 stereochemistry of the central uronic acid is clearly resolved using the respective diagnostic ratios for the isomers. The lowest diagnostic ratio recorded for the GlcA-containing isomers was 0.05 ± 0.01 for standard 3a (IdoA2S-GlcNS-GlcA-GlcNS-$(CH_2)_5NH_2$, and the closest to zero for those with IdoA was –0.12 ± 0.01, recorded for sample 3i (IdoA-GlcNS-IdoA-GlcNS6S-$(CH_2)_5NH_2$). The ability to resolve epimers for the tri-sulfated HS standards using the diagnostic ratio formula is tested with standards 3b (IdoA-GlcNS6S-GlcA-GlcNS-$(CH_2)_5NH_2$) and 3h (GlcA-GlcNS6S-IdoA-GlcNS-$(CH_2)_5NH_2$), and 3c (GlcAGlcNS-IdoA2S-GlcNS-$(CH_2)_5NH_2$) and 3e (GlcA-GlcNSGlcA2S-GlcNS-$(CH_2)_5NH_2$), as shown on Figure 6. 7. Even though standards 3f (GlcA-GlcNAc6S-IdoA2S-GlcNAc6S-$(CH_2)_5NH_2$, 3g(IdoA2S-GlcNAc6S-GlcA-GlcNAc6S-$(CH_2)_5NH_2$), and 3j (IdoA-GlcNAc6S-IdoA2S-GlcNAc6S-$(CH_2)_5NH_2$) have different repeating disaccharide units compared with the other seven isomers, EDD fragmentation of the $[M - 4H + Na]^{3-}$ precursor ion (m/z 373.3846) for 3f, 3g, and 3j produced diagnostic ratio results consistent for assigning their hexuronic acid stereochemistry. We observe a minor diagnostic ratio difference between standards 3f (–0.12 ± 0.01) and 3j (– 0.24 ± 0.01), which differ only at the non-reducing end uronic acid.

However, this minor difference had no impact on the assignment of the stereochemistry of the central uronic acid.

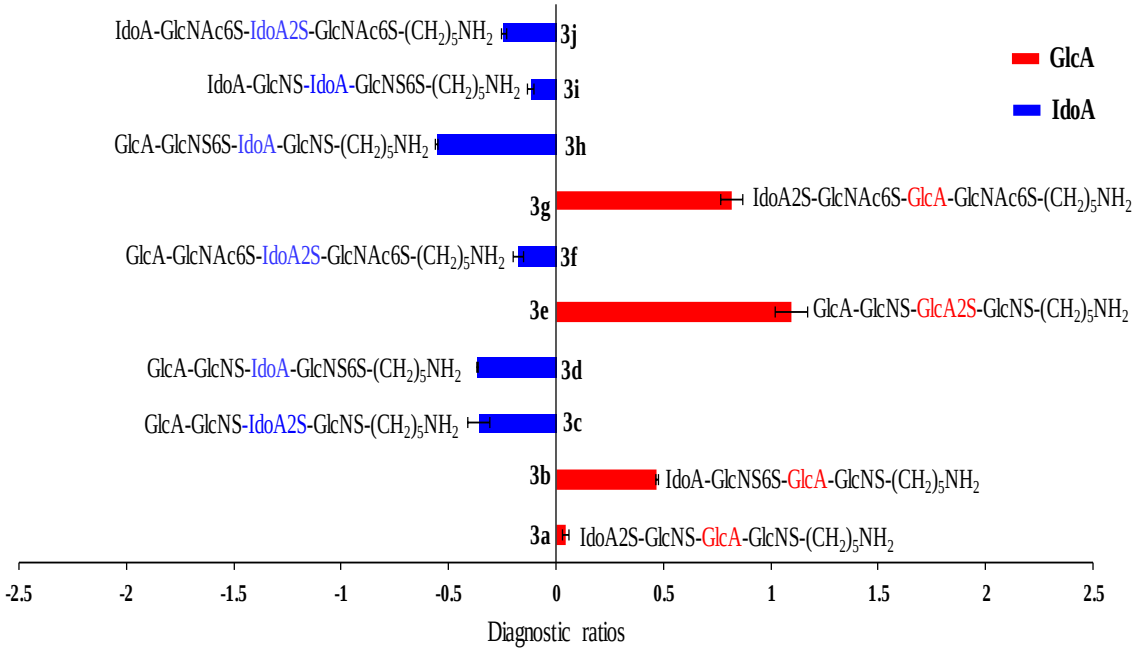

Figure 6. 7. EDD diagnostic ratio results for the tri-sulfated HS tetrasaccharides standards (3a–3j), for the $[M - 4H + Na]^{3-}$ precursor ion.

Diagnostic Ratio Results for the Tetra-Sulfated HS Standards

Highly sulfated HS GAGs are difficult to characterize due to loss of the labile sulfo groups. However, we show, in Figure 6. 8, reproducible diagnostic ratio results for these highly sulfated tetramers for the $[M - 5H + 2Na]^{3-}$ precursor for all seven isomers (standards 4a–4g) and $[M - 5H + Na]^{4-}$ for 4h and 4i. The selected precursor ion for the diagnostic ratio analysis ensured at least all sulfo groups are ionized. The diagnostic ratio values obtained for this degree of sulfation allowed for confident assignment of their respective C-5 uronic acid stereochemistry. The lowest diagnostic ratio recorded for the GlcA-containing tetra-sulfated standards was 0.066 ± 0.006 and the closest to zero for the

IdoA standards was –0.06 ± 0.01, recorded for 4a (IdoA2S-GlcNS6S-GlcA-GlcNS-$(CH_2)_5NH_2$) and 4f (IdoA-GlcNS6S-IdoA-GlcNS6S-$(CH_2)_5NH_2$), respectively. Epimeric pairs 4c (GlcA-GlcNS-IdoA2S-GlcNS6S-$(CH_2)_5NH_2$) and 4d (GlcA-GlcNSGlcA2S-GlcNS6S-$(CH_2)_5NH_2$) are clearly resolved as shown on Figure 6. 8, with diagnostic ratio values –0.40 ± 0.03 and 0.109 ± 0.007, respectively. Epimeric standards 4b (IdoA-GlcNS6SGlcA-GlcNS6S-$(CH_2)_5NH_2$) and 4f (IdoA-GlcNS6S-IdoAGlcNS6S-$(CH_2)_5NH_2$) are also differentiated unambiguously based on the diagnostic ratio values 0.35 ± 0.01 and –0.06 ± 0.01, respectively. We again compare the diagnostic ratio results for standards 4b (IdoA-GlcNS6S-GlcA-GlcNS6S-$(CH_2)_5NH_2$)) and 4e (GlcA-GlcNS6S-GlcA-GlcNS6S-$(CH_2)_5NH_2$)) differing only at the nonreducing end uronic acid. Their respective diagnostic values, 0.35 ± 0.01 and 0.36 ± 0.02, again indicated the non-reducing end uronic acid stereochemistry had little or negligible impact on the diagnostic ratio results. Standards 4c (GlcA-GlcNSIdoA2S-GlcNS6S-$(CH_2)_5NH_2$) and 4g (IdoA-GlcNSIdoA2S-GlcNS6S-$(CH_2)_5NH_2$), also differing at the non-reducing end uronic acid residue, produced almost similar diagnostic ratio values as shown in Figure 8. A mass list (mass (m/z) – intensity table) for the ions used for the DR calculations for all 33 HS standards are included in the Supplemental Material shown in Appendix D.

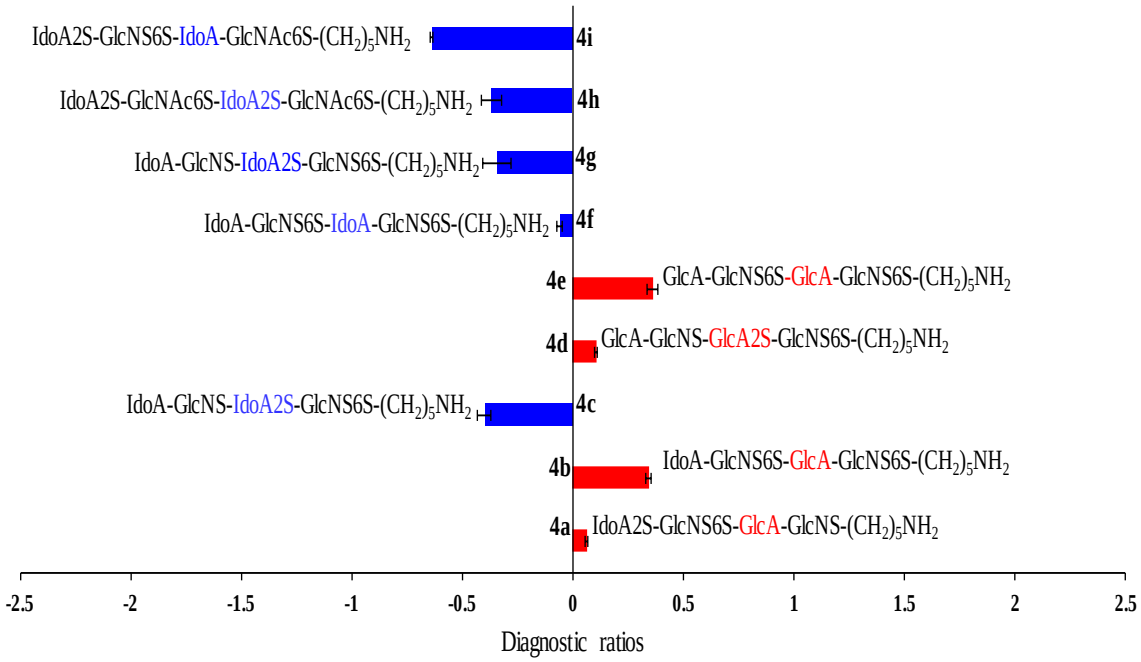

Figure 6. 8 EDD diagnostic ratio results for the tetra-sulfated HS tetrasaccharides standards 4a–4g for the $[M - 5H + 2Na]^{3-}$ precursor ion and $[M - 5H + Na]^{4-}$ for standards 4h and 4i.

Conclusions

In this study, we have demonstrated the capability to assign the C-5 hexuronic acid stereochemistry from a single stage tandem mass spectrum using EDD. The diagnostic ratio provides the means to assign the stereochemistry of the uronic acid near the reducing end for HS tetrasaccharides. For all 33 tetramers that were examined, the diagnostic ratio was positive for GlcA near the reducing end, whereas those having IdoA residues near the reducing end had negative DR values. The smallest absolute value of DR for an IdoA-containing tetrasaccharide standard was –0.06 ± 0.01, and for a GlcA was 0.05 ± 0.01. These data show that the diagnostic ratio clearly distinguishes the uronic acid stereochemistry, not by comparison to a standard, but with a number derived directly from

the data. The applicability of this approach to typical analytical problems faced by glycosaminoglycan researchers remains to be demonstrated. Generally speaking, researchers are confronted with mixtures of GAG oligomers, and these would need to be resolved before the type of analysis presented in this paper could be performed, as the diagnostic ratio only has significance for single component samples. Secondly, the diagnostic ratio presented here has been demonstrated on tetramers that are alkylated at the reducing end. This modification breaks the symmetry of the structure and allows one to easily distinguish reducing end from non-reducing end fragments. This derivatization can be performed on real world samples, but will require an extra step in the work-up procedure. Finally, this approach has been demonstrated only for assigning the stereochemistry of the uronic acid residue closest to the reducing end. Future work will focus on extending this approach to assign the C-5 hexuronic acid stereochemistry of additional residues in longer chain HS GAGs using EDD.

References

1. Sugahara, K., Kitagawa, H.: Recent advances in the study of the biosynthesis and functions of sulfated glycosaminoglycans. Curr. Opin. Struct. Biol. **10**, 518–527 (2000)
2. Bülow, H.E., Hobert, O.: The molecular diversity of glycosaminoglycans shapes animal development. Annu. Rev. Cell Dev. Biol. **22**, 375–407 (2006)
3. Linhardt, R.J., Toida, T.: Role of glycosaminoglycans in cellular communication. Acc. Chem. Res. **37**, 431–438 (2004)
4. Gandhi, N.S., Mancera, R.L.: The structure of glycosaminoglycans and their interactions with proteins. Chem. Biol. Drug Des. **72**, 455–482 (2008)
5. Esko, J.D., Kimata, K., Lindahl, U.: Proteoglycans and sulfated glycosaminoglycans. In: Essentials of Glycobiology. 2nd Edition.;A. Varki; Cold Spring Harbor Laboratory Press, pp. 229–248 Cold Spring Harbor, NY (2009)
6. Esko, J.D., Lindahl, U.: Molecular diversity of heparan sulfate. J. Clin. Investig. **108**, 169 (2001)
7. Xu, D., Esko, J.D.: Demystifying heparan sulfate-protein interactions. Annu. Rev. Biochem. **83**, 129–157 (2014)
8. Rabenstein, D.L.: Heparin and heparan sulfate: structure and function. Nat. Prod. Rep. **19**, 312–331 (2002)
9. Chi, L., Amster, J., Linhardt, R.J.: Mass spectrometry for the analysis of highly charged sulfated carbohydrates. Curr. Anal. Chem. **1**, 223–240 (2005)
10. Pellegrini, L.: Role of heparan sulfate in fibroblast growth factor signalling: a structural view. Curr. Opin. Struct. Biol. **11**, 629–634 (2001)

11. Fuster, M.M., Wang, L.: Endothelial heparan sulfate in angiogenesis. Prog. Mol. Biol. Transl. Sci. **93**, 179–212 (2010)

12. Romagnani, P., Lasagni, L., Annunziato, F., Serio, M., Romagnani, S.: CXC chemokines: the regulatory link between inflammation and angiogenesis. Trends Immunol. **25**, 201–209 (2004)

13. Liu, J., Thorp, S.C.: Cell surface heparan sulfate and its roles in assisting viral infections. Med. Res. Rev. **22**, 1–25 (2002)

14. Kleeff, J., Ishiwata, T., Kumbasar, A., Friess, H., Büchler, M.W., Lander, A.D., Korc, M.: The cell-surface heparan sulfate proteoglycan glypican-1 regulates growth factor action in pancreatic carcinoma cells and is overexpressed in human pancreatic cancer. J. Clin. Investig. **102**, 1662 (1998)

15. Sasisekharan, R., Shriver, Z., Venkataraman, G., Narayanasami, U.: Roles of heparan-sulphate glycosaminoglycans in cancer. Nat. Rev. Cancer **2**, 521–528 (2002)

16. Horne, A., Gettins, P.: 1 HN. MR spectral assignments for two series of heparin-derived oligosaccharides. Carbohydr. Res. **225**, 43–57 (1992)

17. Pomin, V.H., Sharp, J.S., Li, X., Wang, L., Prestegard, J.H.: Characterization of glycosaminoglycans by 15N NMR spectroscopy and in vivo isotopic labeling. Anal. Chem. **82**, 4078–4088 (2010)

18. Wolff, J.J., Chi, L., Linhardt, R.J., Amster, I.J.: Distinguishing glucuronic from iduronic acid in glycosaminoglycan tetrasaccharides by using electron detachment dissociation. Anal. Chem. **79**, 2015–2022 (2007)

20. Zaia, J.: Mass spectrometry of oligosaccharides. Mass Spectrom. **23**, 161–227 (2004)

21. Leach, F.E., Arungundram, S., Al-Mafraji, K., Venot, A., Boons, G.-J., Amster, I.J.: Electron detachment dissociation of synthetic heparan sulfate glycosaminoglycan tetrasaccharides varying in degree of sulfation and hexuronic acid stereochemistry. Int. J. Mass Spectrom. **330**, 152–159 (2012)

22. Zaia, J.: Mass spectrometry of oligosaccharides. Mass Spectrom. Rev. **23**, 161–227 (2004)

23. Zaia, J., Costello, C.E.: Tandem mass spectrometry of sulfated heparin-like glycosaminoglycan oligosaccharides. Anal. Chem. **75**, 2445–2455 (2003)

24. Leach, F.E., Xiao, Z., Laremore, T.N., Linhardt, R.J., Amster, I.J.: Electron detachment dissociation and infrared multiphoton dissociation of heparin tetrasaccharides. Int. J. Mass Spectrom. **308**, 253–259 (2011)

25. Wolff, J.J., Laremore, T.N., Aslam, H., Linhardt, R.J., Amster, I.J.: Electron-induced dissociation of glycosaminoglycan tetrasaccharides. J. Am. Soc. Mass Spectrom. **19**, 1449–1458 (2008)

26. Wolff, J.J., Amster, I.J., Chi, L., Linhardt, R.J.: Electron detachment dissociation of glycosaminoglycan tetrasaccharides. J. Am. Soc. Mass Spectrom. **18**, 234–244 (2007)

27. Wolff, J.J., Laremore, T.N., Busch, A.M., Linhardt, R.J., Amster, I.J.: Electron detachment dissociation of dermatan sulfate oligosaccharides. J. Am. Soc. Mass Spectrom. **19**, 294–304 (2008)

28. Huang, Y., Yu, X., Mao, Y., Costello, C.E., Zaia, J., Lin, C.: De novo sequencing of heparan sulfate oligosaccharides by electron-activated dissociation. Anal. Chem. **85**, 11979–11986 (2013)

29. Wolff, J.J., Leach III, F.E., Laremore, T.N., Kaplan, D.A., Easterling, M.L., Linhardt, R.J., Amster, I.J.: Negative electron transfer dissociation of glycosaminoglycans. Anal. Chem. **82**, 3460–3466 (2010)

30. Huang, R., Pomin, V.H., Sharp, J.S.: LC-MS^n analysis of isomeric chondroitin sulfate oligosaccharides using a chemical derivatization strategy. J. Am. Soc. Mass Spectrom. **22**, 1577–1587 (2011)

31. Zaia, J., Miller, M.J.C., Seymour, J.L., Costello, C.E.: The role of mobile protons in negative ion CID of oligosaccharides. J. Am. Soc. Mass Spectrom. **18**, 952–960 (2007)

32. Zaia, J., McClellan, J.E., Costello, C.E.: Tandem mass spectrometric determination of the 4S/6S sulfation sequence in chondroitin sulfate oligosaccharides. Anal. Chem. **73**, 6030–6039 (2001)

33. Kailemia, M.J., Li, L., Ly, M., Linhardt, R.J., Amster, I.J.: Complete mass spectral characterization of a synthetic ultralow-molecular-weight heparin using collision-induced dissociation. Anal. Chem. **84**, 5475–5478 (2012)

34. Kailemia, M.J., Li, L., Xu, Y., Liu, J., Linhardt, R.J., Amster, I.J.: Structurally informative tandem mass spectrometry of highly sulfated natural and chemoenzymatically synthesized heparin and heparan sulfate glycosaminoglycans. Mol. Cell. Proteomics **12**, 979–990 (2013)

35. Zaia, J., Li, X.-Q., Chan, S.-Y., Costello, C.E.: Tandem mass spectrometric strategies for determination of sulfation positions and uronic acid epimerization in chondroitin sulfate oligosaccharides. J. Am. Soc. Mass Spectrom. **14**, 1270–1281 (2003)

36. Kailemia, M.J., Patel, A.B., Johnson, D.T., Li, L., Linhardt, R.J., Amster, I.J.: Differentiating chondroitin sulfate glycosaminoglycans using CID; uronic acid cross-ring diagnostic fragments in a single stage of MS/MS. Eur. J. Mass Spectrom. (Chichester, England) **21**, 275 (2015)

37. Kailemia, M.J., Park, M., Kaplan, D.A., Venot, A., Boons, G.-J., Li, L., Linhardt, R.J., Amster, I.J.: High-field asymmetric-waveform ion mobility spectrometry and electron detachment dissociation of isobaric mixtures of glycosaminoglycans. J. Am. Soc. Mass Spectrom. **25**, 258–268 (2014)

38. Agyekum, I., Patel, A.B., Zong, C., Boons, G.-J., Amster, I.J.: Assignment of hexuronic acid stereochemistry in synthetic heparan sulfate tetrasaccharides with 2-O-sulfo uronic acids using electron detachment dissociation. Int. J. Mass Spectrom. **390**, 163–169 (2015)

39. Arungundram, S., Al-Mafraji, K., Asong, J., Leach III, F.E., Amster, I.J., Venot, A., Turnbull, J.E., Boons, G.-J.: Modular synthesis of heparan sulfate oligosaccharides for structure–activity relationship studies. J. Am. Chem. Soc. **131**, 17394–17405 (2009)

40. Ceroni, A., Maass, K., Geyer, H., Geyer, R., Dell, A., Haslam, S.M.: GlycoWorkbench: a tool for the computer-assisted annotation of mass spectra of glycans. J. Proteome Res. **7**, 1650–1659 (2008)

41. Domon, B., Costello, C.E.: A systematic nomenclature for carbohydrate fragmentations in FAB-MS/MS spectra of glycoconjugates. Glycoconj. J. **5**, 397–409 (1988)

CHAPTER 7

Structural Elucidation of Fucosylated Chondroitin Sulfates from Sea Cucumber Using FTICR-MS/MS

Under review as:

Agyekum, I.; Pepi, L.; Yu, Y.; Li, J.; Yan, L.; Linhardt, R. J.; Chen, S.; Amster, I. J., "Structural Elucidation Of Fucosylated Chondroitin Sulfates From Sea Cucumber Using FTICR-MS/MS", *Eur. J. Mass Spectrom.*, submitted.

Abstract

Fucosylated chondroitin sulfates (FCS) are complex polysaccharides extracted from sea cucumber. They have been extensively studied for their anticoagulant properties and have been implicated in other biological activities. While NMR spectroscopy has been used to extensively characterize FCS oligomers, we herein report the first detailed mass characterization of FCS using high resolution FTICR-MSMS. The two species of fucosylated chondroitin sulfates considered for this work include *pearsonothuria graeffei* (FCS-Pg) and *Isostichopus badionotus* (FCS-Ib). FCS oligosaccharides were prepared by *N*-deacetylation–deaminative cleavage of the two FCSs and purified on by repeated gel filtration. Accurate mass measurements obtained from ESI-FTICR-MS measurements confirmed the oligomeric nature of these two FCS oligosaccharides with each trisaccharide repeating unit averaging four sulfates per trisaccharide. CID activations of efficiently deprotonated molecular ions through Na^+/H^+ exchange proved useful in providing structurally relevant glycosidic and cross-ring product ions, capable of assigning the sulfate modifications on the FCS oligomers. Careful examination of the MS/MS of both species, deferring in the positions of sulfate groups on the fucose residue (FCS-Pg-3,4-*O*S) and (FCS-Ib-2,4-*O*S) revealed cross-ring products $^{0,2}A_{\alpha f}$ and $^{2,4}X_{\beta f}$ which were diagnostic for (FCS-Pg-3,4-*O*S) and $^{0,2}X_{\beta f}$ for (FCS-Ib-2,4-*O*S). MS and MS/MS data acquired for both species varying in oligomer length (dp3-dp15) is presented.

Keywords: FTICR-MS/MS; carbohydrates; fucosylated chondroitin sulfate; sea cucumber

Introduction

Acidic polysaccharides isolated from sea cucumber have been reported to have antithrombic, anti-tumor, and anticoagulant properties and are involved in several biological activities.[1-9] The two main acidic polysaccharides isolated from sea cucumber include fucosylated chondroitin sulfates (FCS) and fucan.[3, 10-14] FCS is a rare glycosaminoglycan (GAG) with a backbone similar to that of mammalian chondroitin sulfate, containing large numbers of sulfated α-L-fucopyranosyl (Fuc) branches.[12, 15, 16] Their basic tri-saccharide repeating unit is composed of [4-β-D-glucuronic acid (GlcA)-1→3-β-D-*N*-acetyl galactosamine (GalNAc)-1]$_n$ with the third position of the β-GlcA residue substituted with α-L-Fuc branches.[17, 18] The β-D-GlcNAc unit could be sulfated (S) at the 4-*O*, 6-*O* or both (4, 6-*O*S) whereas the 2-*O* position of its β-D-glucuronic acid unit is unsubstituted.[17] Sulfate modifications on the fucose branches could either be mono-sulfated or di-sulfated depending on the species of sea cucumber from which they are isolated.[3, 6, 8, 19, 20] Recently, the similarity in structure between FCS and glycosaminoglycans isolated from other tissues has led to investigations about its anticoagulant and antithrombic activities.[21] Reports of increased anticoagulant activities of FCS have been linked to its ability to increase the inhibition of thrombin and factor Xa by antithrombin or heparin cofactor II.[2, 6, 22, 23] These observations have been attributed to the sulfated α-L-fucopyranosyl branches.[3, 18, 24, 25] Notably, desulfation or de-fucosylation of FCS leading to loss of its anticoagulant activities have been reported.[2, 26] Other documented roles of FCS, include their ability to interact with the selectin family of cell-adhesion molecules.[7] FCS extracted from *L. grisea* shows a 4-8, fold increase in inhibiting interactions of P- and L-selectin with sialyl Lewis x (sLe^x) antigen compared to heparin. This work further highlighted the fact that, the removal of

the sulfated fucose branches on FCS obliterated its inhibitory potential *in vitro* and *in vivo*. The structure-activity relationship of FCS continues to drive the search for analytical methods that can efficiently elucidate the structural features of these compounds.

Typical of most sulfated polysaccharides, the structural analysis FCS can be challenging. This is mainly due to variations in sulfation patterns, degree of branching and oligomer length. NMR [3, 18, 27, 28] has been the choice analytical tool for obtaining structural details on FCS, however, limitations due to sample quantity and purity can be problematic.[29, 30] Recently, electrospray ionization tandem mass spectrometry analysis of sulfated polysaccharides is emerging as an alternative to NMR as it offers high sensitivity, fast analysis times and requires sub microgram amounts of sample. [29] ESI-MS is a widely recognized analytical tool for the analysis of sulfated polysaccharides as they also ionized efficiently in the negative mode.[31-34] Nevertheless, the labile sulfate groups are very susceptible to decomposition during ESI or during ion activation.[29, 35-39] Suggested protocols for reducing sulfate decomposition include chemical derivatization methods such as methylation and acetylation and coupling of the sulfate groups with metals. Recent EDD and CID reports on dermatan sulfate, heparan sulfate, and heparin by activating sodium cationized molecular ions showed a reduction in sulfate decomposition and improvements in the amount of product ions observed especially those occurring from cross-ring cleavages essential for locating sulfo modified sites.[30, 35, 40-42] Additional information pertaining to the influence of sodium cationized molecular ions on the hexuronic acid stereochemistry of chondroitin, dermatan sulfate and heparan sulfate oligomers have also been reported.[40-42] Apart from the possibility of sulfation on the fucose ring, the labile nature of the α-L-fucopyranosyl branches can pose a challenge for

MS and MS/MS analysis. To date, we have no knowledge of a reported tandem mass spectrometric analysis of FCS. We present for the first time a detailed MS/MS analysis of isolated from *Pearsonothuria graeffei* (FCS-Pg) and *Isostichopus badionotus* (FCS-Ib). These two species differ in the position of the sulfo groups; FCS-Pg is 3,4-*O*-sulfated whereas FCS-Ib is 2,4-*O*-is sulfated. Information regarding the location of sulfo groups and differentiation of these two-isomeric species are also discussed.

Methods

Sample preparation and PAGE analysis

Dried sea cumcumbers, *P. graeffei* and *I. badionotus,* were locally purchased in Qingdao, China. The FCSs were prepared as previously described.[43] Briefly, FCS-Pg and FCS-Ib were each extracted from 100 g of dried sea cucumber body wall, digested with protease, precipitated with cetyl pyridinium chloride and fractionated using ethanol precipitation.

FCS oligosaccharides were prepared by *N*-deacetylation-deaminative cleavage followed by gel filtration chromatography. The *N*-deacetylation was accomplished by a hydrazinolysis step following the method of Fukuda and coworkers.[44] Briefly, dried FCS (100 mg) and 1.50 mL hydrazine hydrate containing 1% hydrazine sulfate were added in a reaction tube. The tube was sealed and incubated at 90 ℃ for 12 h on a magnetic stirrer at 250 rpm. After the reaction, the solution was added to 6 mL of ethanol. When several drops of saturated sodium chloride were added, a white precipitate was formed. The precipitate was collected by centrifugation and dissolved in distilled water. This precipitation and dissolution procedure was repeated 4-times to remove the hydrazine and hydrazine sulfate.

The resulting solution was dialyzed against flowing tap water for 2 d and distilled water for 1 d with a 3500 Da molecular weight cut-off and subsequently lyophilized.

Deaminative cleavage followed Bienkowski's method[45] with some modification. Nitrous acid reagent was prepared by mixing 0.5 M H_2SO_4 and 5.5 M $NaNO_2$ at volume ratio of 3:5. Deacetylated FCS solution (20 mg in 1 mL ice-cold water) was added to 2 mL of pre-cooled nitrous acid reagent in a reaction tube. The reaction was performed for 10 min in an ice bath, and the excess nitrous acid was neutralized by adding 1.5 mL 0.5 M NaOH. Immediately, 150 μL of 300 mg/mL $NaBH_4$ (dissolved in 0.05 M NaOH) was added and allowed to react with the FCS oligosaccharides at 50 ℃ for 2 h. Finally, the sample was dialyzed against distilled water in 500 Da molecular weight cut-off bags and lyophilized.

The resulting oligosaccharide mixtures were fractionated by gel filtration on a Superdex 30 prep grade column (2.6 × 120 cm) eluted with 0.3 M NH_4HCO_3 at a flow rate of 0.3 mL/min, and were collected in a tube every 6 min. Every tube of sample was analyzed using a Superdex Peptide 10/300 GL column (10 mm × 300 mm) and monitored with a refractive index detector, those showing a single peak of the same retention time were collected together, and five main fractions were collected for each oligosaccharide mixture. Polyacrylamide gel electrophoresis (PAGE) on an isocratic 22% gel stained with Alcian blue[46] was used to analyze the FCS oligosaccharides that had been fractionated by gel filtration by gel filtration. The size in dp was determined and purity of each FCS oligosaccharide was estimated to be >80%.

Mass Spectrometry analysis

Collisionally induced dissociation (CID) experiments were performed on a 9.4T Bruker Apex Ultra QeFTMS (Billerica, MA). 0.1 mg/mL of each sample (dp3-dp15) from both species was injected at a rate of 120μL/h in 50:50 methanol: H_2O and ionized in the negative mode by electrospray using a heated metal capillary (Agilent Technologies, Santa Clara, CA, #G2427A). Dilute amounts of NaOH (1mM) was added to the spray solvent to stabilize the labile sulfate groups which are susceptible to decomposition. Multiply charged sodium adducted molecular ions were carefully selected using a 3Da window and activated using CID. 512K points were acquired for each spectrum, padded with one zero-fill, and apodized using a sinebell window. External calibration was performed to achieve a mass accuracy of 5-ppm. Internal calibration using confidently assigned glycosidic bond cleavage products ions was also performed to obtain mass accuracy of less than 1ppm. MS/MS product ions have been assigned using accurate mass measurements and Glycoworkbench.[47, 48] These ions have been illustrated and discussed using both the Domon-Costello[49] nomenclature and structures obtain from Glycoworkbench.

Results and discussions

ESI accurate mass measurements obtained from intact FCS oligosaccharides confirmed the basic trisaccharide sequence of both FCS species to be [4-β-D-GlcA-1→3-β-D-GalNAc-1]$_n$ with the third-position of the β-GlcA acid residues substituted with di-sulfated α-Fuc branches averaging four sulfates per tri-saccharide. The modification of the terminal GalNAc to β-3-anhydrotalitol-(4,6-*O*S) resulting from deaminative cleavage with nitrous acid is also confirmed by high-resolution accurate mass measurements. With the

addition of dilute amounts of NaOH to the spray solvent, we are able to observe higher ionized state for the intact FCSs oligomers with their corresponding cationized molecular ions. The annotated ESI-MS for these isomeric FCSs oligomers (dp3-dp15) is included in the supplemental material (Figures 1-6). The paragraphs below discuss the mass spectrometric results for both species for each degree of polymerization. All referenced supplemental Figures can be found in Appendix E.

MS/MS of FCS-Pg dp3 and FCS-Ib dp3

Negative-mode ESI-MS of both dp3 FCS-Pg and FCS-Ib produced abundant multiply charged molecular ions -4, -3 and -2 as well as their Na^+ counterions for MS/MS as shown in Supplementary Figure 1. Fully ionized molecular ions considered for the MS/MS experiment include $[M-5Na-3Na]^{2-}$, $[M-5H-2Na]^{3-}$ and $[M-5H-Na]^{4-}$ with m/z 434.9585, 282.3093 and 205.9846, respectively. Structurally informative fragment ions observed for these molecular ions have enabled the assignment of sulfo modifications especially on the differing fucose units of both isomers FCS-Pg and FCS-Ib. For FCS-Pg, the two sulfo groups 2,3-*O*S located on the fucose residue can be confidently assigned using the accurate masses of cross-ring product ions $^{2,4}X_{\beta f}$ and $^{0,2}A_{\alpha f}$. Confirmatory fragments such as $^{3,5}A_{\alpha f}$, $^{3,5}X_{\beta f,}$ $^{0,3}A_{\alpha f}$ and $^{0,3}X_{\beta f}$ can locate the presence of the 4-*O* sulfo group. The symmetric nature of these molecules resulting from the formation of the β-3-anhydrotalitol-(4,6-*O*S) residue which has the same elemental composition as the di-sulfated fucose unit could be challenging especially in the absence of cross-ring product ions. Despite this structural feature of the compound, we can confidently assign the number of sulfates on the fucose ring using the accurate mass of distinct cross-rings products $^{1,5}A_{\alpha f}$ and $^{1,4}A_{\alpha f}$. Spectra to spectra comparison of dp3 FCS-Ib and FCS-Pg reveal cross-ring

products $^{0,2}A_{\alpha f}$ and $^{2,4}X_{\beta f}$ occurring at m/z 284.9356 and 303.0093 as diagnostic for FCS-Pg and $^{0,2}X_{\beta f}$ for FCS-Ib-2,4-*O*S at m/z 331.9654 (Supplemental Figure 7). Similarly, we observe the highest number of fragmentation for dp3 FCS-Ib on the fucose ring. The accurate mass of the $^{0,3}A_1$ ion, occurring from the MS/MS of all the three selected molecular ions can locate the 4-*O*S on the fucose ring. The positions of the two sulfo groups on the fucose ring (2, 4-*O*S) increases the possibility of fragments ions ($^{0,2}A_{\alpha f}$ and $^{0,2}X_{\beta f}$) being isobaric with ($^{2,4}X_0$ and $^{2,4}A_3$) on the β-3-anhydrotalitol residue. However, the $^{0,2}A_n$ and $^{0,2}X_n$ product ions have been reported for MS/MS of 2-*O* and 4-*O* sulfated fucoidan L-fucose isomers,[50] of highly sulfated fucan from algal *Laminaria cichorioides*[51] and Ascophyllum nodosum [52].

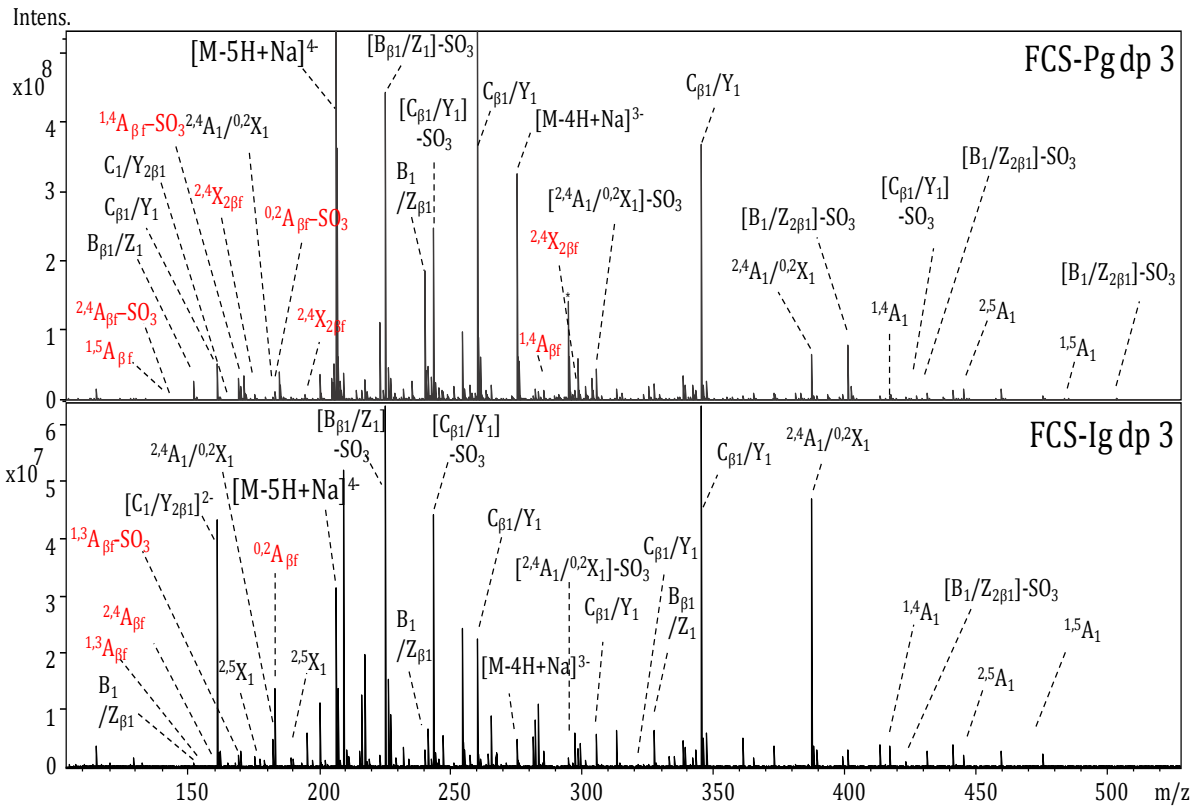

Figure 7. 1. CID MS/MS spectra comparison of FCS Pg dp3 and FCS Ib dp3 for the $[M-5H+Na]^{4-}$ molecular ion.

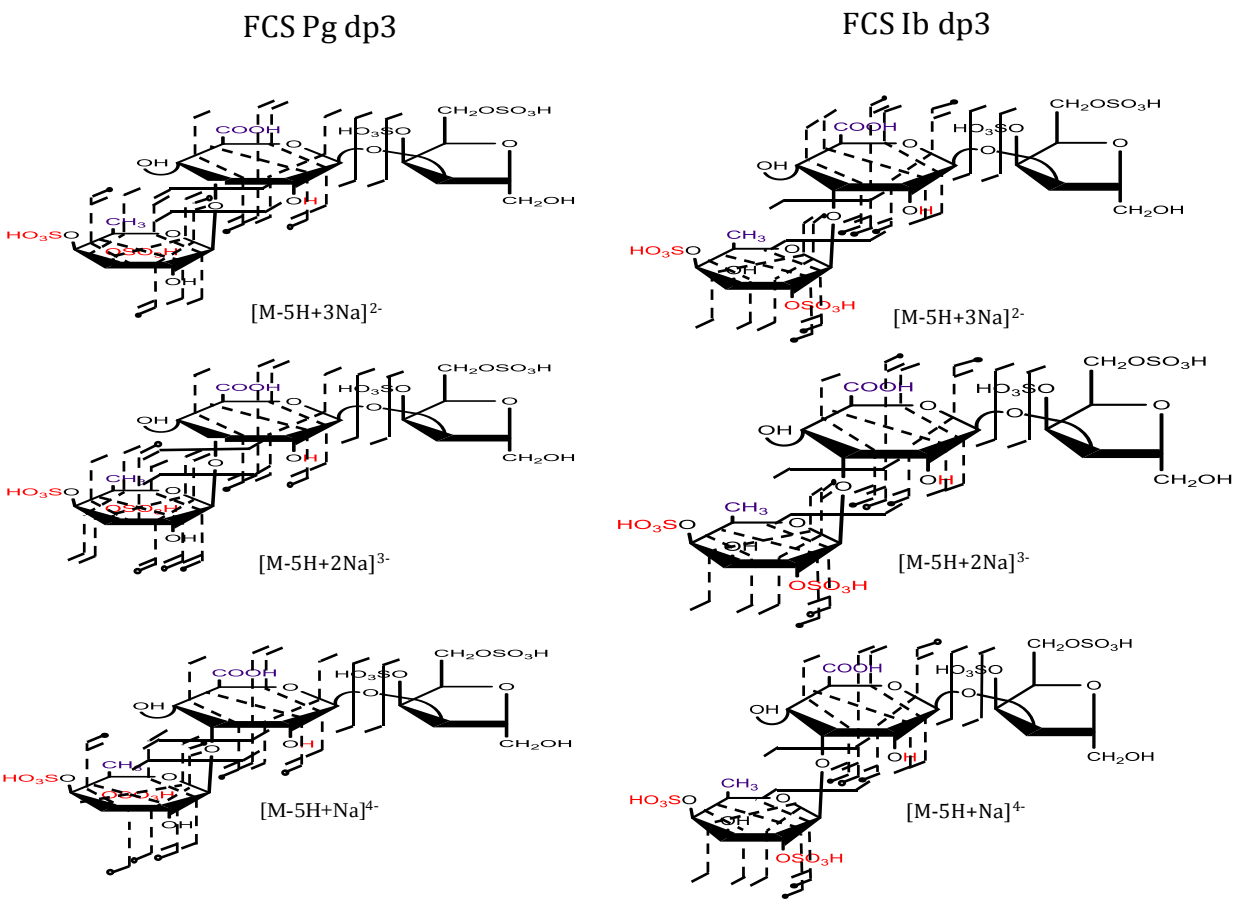

Figure 7. 2 Structural annotations for CID activation of $[M-5H+3Na]^{2-}$, $[M-5H+2Na]^{3-}$ and $[M-5H+Na]^{4-}$ molecular ions for FCS Pg dp3 and FCS Ib dp3.

The postulated mechanism supported by computational studies for the occurrence of the $^{0,2}A_n$ and $^{0,2}X_n$ product ions occurring on the L-fucose isomers by Tissot et. al. supports a McLafferty rearrangement fragmentation pathway following the cleavage of the C-1-O-5 fucose bond.[50] It is also worth noting from recent EDD[29, 53] and CID[40, 54] reports on mammalian chondroitin, dermatan sulfate and hyaluronic acid[55] oligosaccharide the rare occurrence of cross-ring fragmentation on the GalNAc residues. The above-referenced works support the $^{0,2}A_{\alpha f}$ and $[^{0,2}X_2 + 2Na]^{2-}$ ions with m/z 182.9968 and 331.9661 respectively more likely to occur on the fucose residue. Thus the 2-*O* sulfo groups on the fucose could be assigned with these ions. The position of the 4-*O* sulfo group on the fucose

ring is assigned using the accurate mass of the $^{3,5}A_{\alpha f}$ ion, with the mass $^{1,5}A_{\alpha f}$ confirming the presence of two sulfate groups on the fucose ring. The cross-ring product ions $^{0,2}A_n$, $^{0,2}X_n$, $^{0,3}X_n$, and $^{0,3}A_n$ observed on the fucose residues of both dp 3 isomers have also been reported on 2-*O*, 3-*O* and 4-*O* sulfated fucose residues of fucoidan oligosaccharides.[50-52] The annotated MS/MS spectra comparison for the $[M-5H-Na]^{4-}$ molecular ion for the two isomers is shown in Figure 7. 1. Figure 7. 2, also shows the CID MS/MS structural annotations for all the fully deprotonated molecular ions for dp3 FCS-Pg and FCS-Ib. Only structurally informative product ions are shown in the annotated structures.

MS/MS of FCS-Pg dp6 and FCS-Ib dp6

The structural composition of the dp6 FCS oligomers indicates ten ionizable protons comprising 8 sulfate groups and 2 carboxyl groups. With the aid of the ESI-MS shown in Supplementary Figure 2, we are able to confirm the elemental composition of both FCS-Ib and FCS-Pg hexasaccharides. Charged states observed for both isomers ranged from -6 to -3. The favorable intensities of the fully deprotonated ion $[M-10H+5Na]^{5-}$ for both FCS-Ib and FCS-Pg dp6 have been considered for MS/MS analysis. Additionally, the abundance of the $[M-9H+3Na]^{6-}$ observed in the MS of FCS-Pg dp6 proved to be more structurally informative. Figure 3 shows the MS/MS spectra annotations for the $[M-9H+3Na]^{6-}$ precursor ion for FCS-Pg dp6. Structural annotations showing extensive fragmentation on the fucose ring allowing for the location of the 3, 4-*O* sulfo groups is shown for the $[M-10H+5Na]^{5-}$ and $[M-9H+3Na]^{6-}$ molecular ions in Figure 4. The $^{0,2}A_{\alpha f}$ ion locating unambiguously position of positions of both sulfo groups with $^{3,5}A_{\alpha f}$, and $^{0,3}A_{\alpha f}$

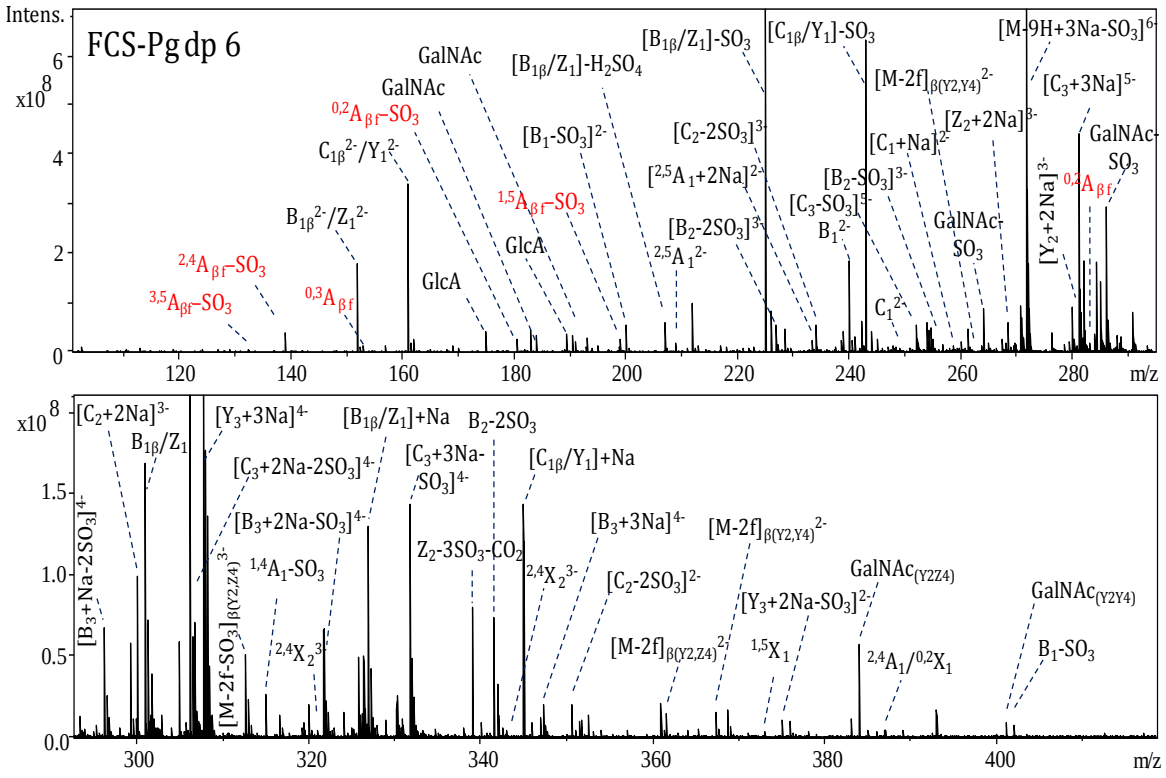

Figure 7. 3. FCS Pg dp6 CID MS/MS annotated spectra for the $[M-9H+3Na]^{6-}$ molecular ion.

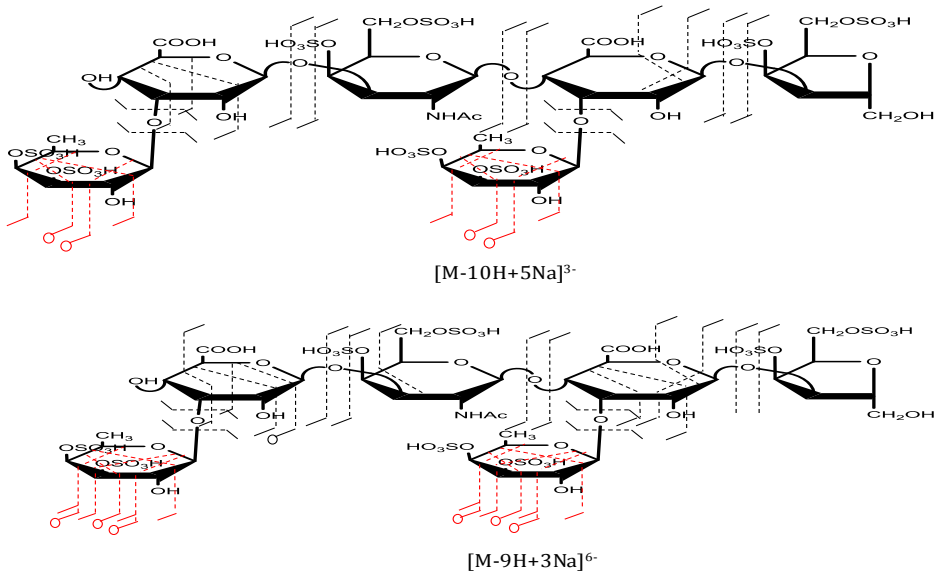

Figure 7. 4. **S**tructural annotations from observed CID fragments for FCS Pg dp6 for the $[M-10H+5Na]^{5-}$ and $[M-9H+3Na]^{6-}$ molecular ions.

confirming the presence of the 4-*O* sulfo group on the fucose. Complete glycosidic bond fragmentations are also observed including loss of a single and both fucose rings. Figure 7. 5, also shows the structural annotations and MS/MS of FCS-Ib dp6 for the [M-10H+5Na]^{5} precursor ion. The cross-ring product ions observed on the fucose ring are very similar to those of dp3 FCS-Ib.

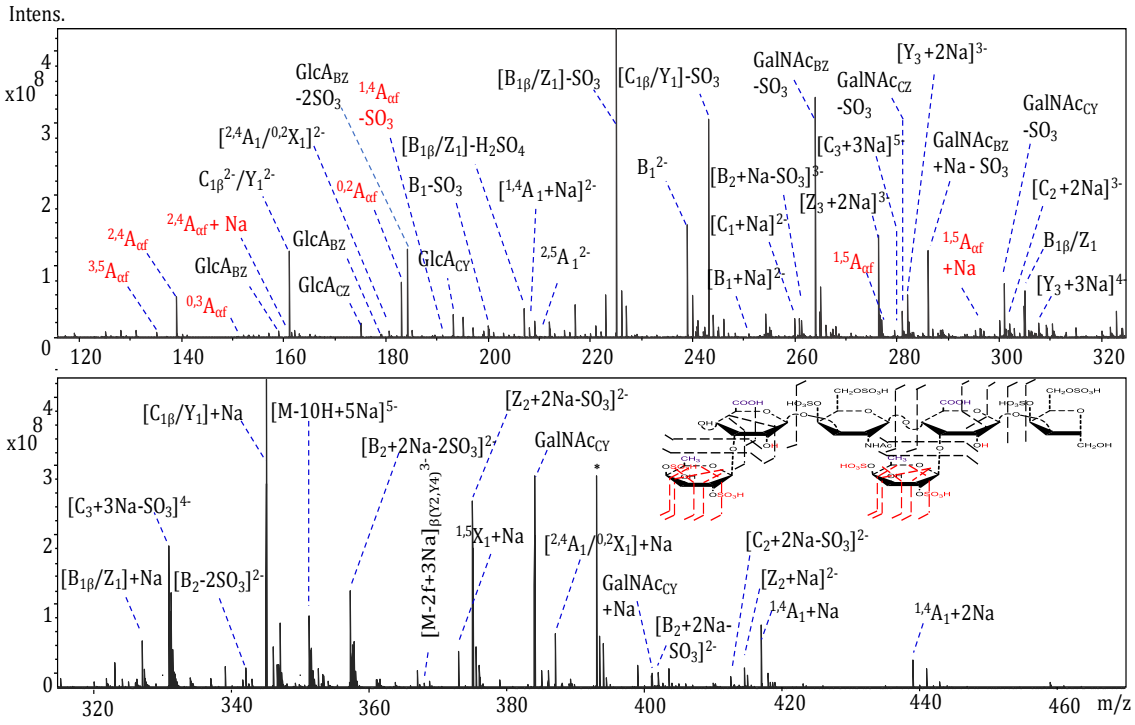

Figure 7. 5 CID MS/MS spectra annotations for the [M-10H+5Na]$^{5-}$ molecular ion for FCS Ib dp6.

We have assigned the two sulfate groups on fucose rings using similar cross-rings ions as discussed for the Ib dp3. As expected, we observe glycosidic cleavages resulting in the loss fucose residues in both dp6 isomers. Loss of the fucose residue and subsequent loss of sulfate from the fucose residue were observed to dominate the MS/MS spectrum for both isomers. This was expected due to the labile nature of the α-L-Fuc branches and the sulfate half-ester bonds. Again, most cross-ring fragmentations are observed on the Fuc ring

residues. Similar to MS/MS of mammalian chondroitin sulfate,[29, 40, 53] we observe extensive cross-ring fragmentation on the GlcA units. Fragment ions resulting from internal cleavages are also observed, yielding mostly GalNAc monosaccharide residues in MS/MS spectra of both Pg dp6 and Ib dp6. Internal cleavages resulting from the cleavage of multiple glycosidic bonds have been reported in MS/MS of both branched and linear oligosaccharides.[56-61] We are able to confirm the presence of the di-sulfated monosaccharide GalNAc residues from the observed internal cleavages as shown in Figures 3 and 5. Isobaric ions have been designated the come color on the annotated structures of the dp6 isomers as shown in Figures 4 and 5.

MS/MS of FCS-Pg dp9 and FCS-Ib dp9

The MS and MS/MS results for the nonasaccharide isomers for Pg and Ib are discussed below. Precursor ion selection for these isomers was based on the number of ionizable protons deprotonated and ion abundance. For FCS-Pg dp9, the molecular ion $[M-15H+8Na]^{7-}$ with m/z 380.6834 was subjected to CID activation. This ionized state represents a deprotonation of all the fifteen ionizable protons comprising twelve sulfate groups and three carboxyl groups. We again observe extensive cross-ring fragmentation on the fucose residues as shown in Figure 6a. Cross-ring product ions such as $^{3,5}A_{\alpha f}$ positions a sulfate group at the 4-*O* position whereas $^{1,4}A_{\alpha f}$ ion establishes a di-sulfated fucose ring. Other cross-ring product observed were accompanied with SO_3 losses. It is worth noting that we observed glycosidic product ions adjacent each sugar residue. The structural annotation for CID MS/MS activation of $[M-15H+7Na]^{8-}$ molecular ion for FCS Ib dp 9 is also shown in Figure 7. 6b. This ionized state represents a complete deprotonation of all

the 15 acidic acid groups. The MS/MS result provided sufficient product ions for the assignment of the structure.

(a)

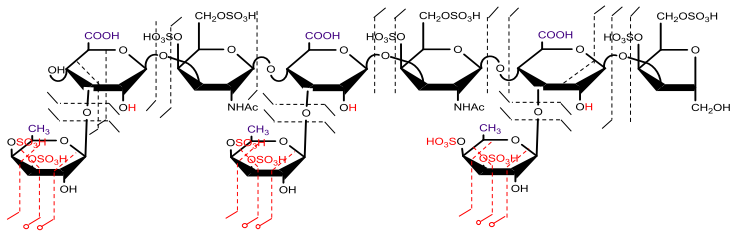

FCS Pg dp9 $[M-14H+7Na]^{7-}$

(b)

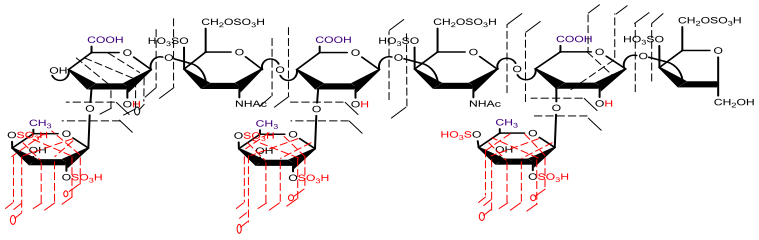

FCS Ib dp9 $[M-15H+7Na]^{8-}$

Figure 7. 6. CID structural annotations for (a) $[M-14H+7Na]^{7-}$ molecular ion for FCS Pg dp9 and (b) $[M-15H+7Na]^{8-}$ molecular ion for FCS Ib dp9.

MS/MS of FCS-Pg dp12 and FCS-Ib dp12

The elemental composition of both dp12 FCS fractions has been confirmed by accurate mass measurement from ESI-MS. Supplementary Figure 3, shows the annotated MS spectra for the ions considered to CID analysis. The accompanying sodium cationized molecular ions for example $[M-20H+10Na]^{10-}$ ensures all the ionizable protons have been deprotonated. For FCS-Pg dp12, the $[M-19H+10Na]^{9-}$ molecular ion with m/z 392.1942 was selected and subjected to CID activation. Supplementary Figure 8 shows the CID MS/MS product ion annotations while the structural annotations for FCS-Pg dp12 are shown in Figure 7. 7a. The MS/MS was mostly dominated by glycosidic bond fragments.

A similar fragmentation was observed for the CID activation of the $[M-20H+10Na]^{10-}$ for FCS-Ib dp12. The selected molecular ion has nineteen out of the twenty ionizable protons deprotonated. The annotated MS/MS structure for the observed product ions for FCS-Ib dp12 is shown in Figure 7. 7b for the $[M-20H+10Na]^{10-}$ molecular ion with m/z 355.0722. The accompanying supplemental material contains the annotated CID spectra showing a selected number of structurally informative ions (Supplementary Figure 8 (Appendix E)). With all the acidic groups deprotonated, CID activation of the molecular ion yielded abundant cross-ring and glycosidic product ions for the structural assignment. For example, the $^{1,4}A_{\alpha f}$ peak confirms the presence of the two sulfate groups on the fucose residue with the $^{2,5}A_{\alpha f}$ eliminating the presence of a 3-O on the FCS-Ib dp12 oligomer.

(a)

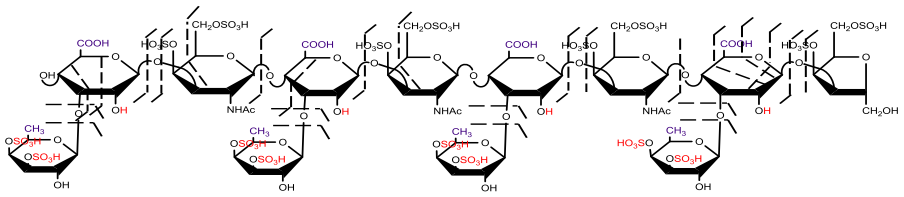

FCS Pg dp12 $[M-19H+10Na]^{9-}$

(b)

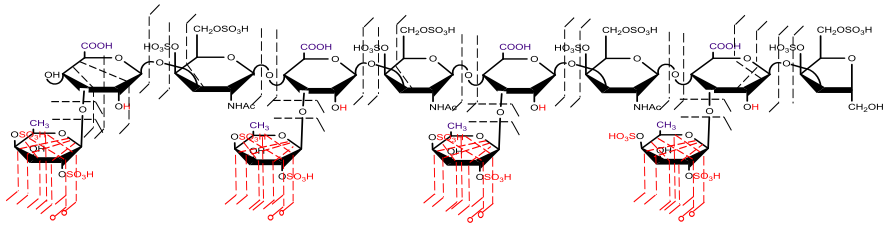

FCS Ib dp12 $[M-20H+10Na]^{10-}$

Figure 7. 7 CID MS/MS and structural annotations for (a) the $[M-19H+10Na]^{9-}$ molecular ion for FCS Pg dp12 and (b) the $[M-19H+9Na]^{10-}$ molecular ion for FCS Ib dp12.

MS/MS of FCS-Pg dp15 and FCS-Ib dp15

The polymeric structure for both FCS-Ib and FCS-Pg dp15 oligomers have been confirmed from ESI-MS accurate mass measurements. With optimized ionization conditions, we are able to observe higher ionized states for the dp15 oligomers having twenty-five ionized groups. The MS of FCS-Pg dp15 showing a charged state distribution from -8 to -5 is shown in Supplementary Figure 5. The highest deprotonated molecular ion observed for this oligomer was $[M-23H+15Na]^{8-}$. However, the $[M-22H+14Na]^{8-}$ ion with twenty-two out of the twenty-five ionizable protons deprotonated was selected for the CID experiment due to its abundance. The insert shown in Supplementary Figure 5, displays the isotopic distribution of the $[M-22H+14Na]^{8-}$ m/z 560.7070 molecular ion. The Annotated MS/MS spectrum for the FCS-Pg dp15 is shown in Supplementary Figure 10. With twenty-two out of the twenty-five ionizable protons deprotonated, we observe SO_3 loss fragments from the molecular ion upon CID activation. Figure 7. 8a shows the annotated product ion structure for the FCS Pg dp15 oligomer. We show in Supplementary Figure 6, the 9 charged state molecular ions $[M-23H+14Na]^{9-}$, $[M-24+15Na]^{9-}$ and $[M-25H+16Na]^{9-}$ for the ESI-MS of FCS-Ib dp15. The CID MS/MS spectra and structural annotations for FCS-Ib dp15 for the $[M-24+15Na]^{9-}$ m/z 500.7373 are shown in Supplementary Figure 6 and Figure 8b. Compared to the CID spectra for the FCS-Pg dp15, we observe more structurally informative cross-ring product ions on the Fuc ring for FCS-Ib dp15.

(a)

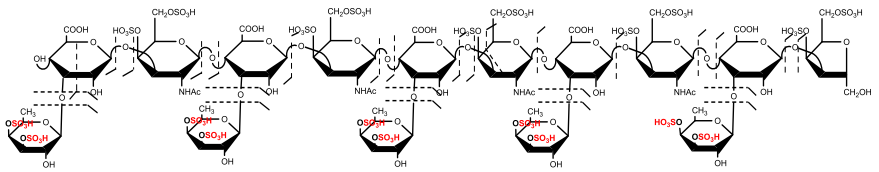

FCS Pg dp15 $[M-22H+14Na]^{8-}$

(b)

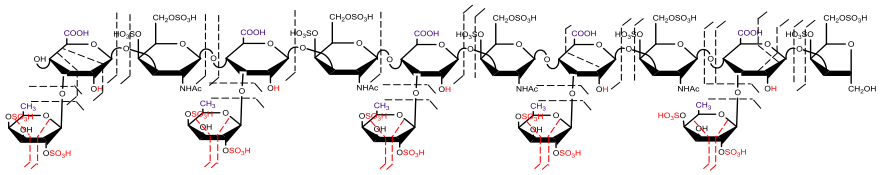

FCS Ib dp15 $[M-24H+15Na]^{9-}$

Figure 7. 8 CID MS/MS structural annotations for, (a) the $[M-22H+14Na]^{8-}$ molecular ion for FCS Pg dp15 and (b) the structural annotations for the $[M-24H+15Na]^{9-}$ molecular ion for FCS Ib dp15.

It is worth noting that the MS/MS spectra for both isomers produced abundant glycosidic product ions essential for assigning the number of sulfate per monosaccharide residue. Compared to FCS-Pg dp15, the MS/MS of FCS-Ib dp15 produced very little sulfate loss fragments mainly due to the effective deprotonation of all the acidic groups except for one (twenty-four out of twenty-five ionizable protons). supplemental list of m/z and intensity is included in Appendix E.

Conclusions

ESI-MS/MS experiments have been carried out on two isomeric FCS samples isolated from two sea cucumber species, *Isostichopus badionotus* (FCS-Ib) and *pearsonothuria graeffei* (FCS-Pg) ranging from dp3-dp15 using a 9.4T FTICR. With the aid dilute NaOH added to the spray solvents, we are able to achieve efficient deprotonation of the molecular ions of

intact FCS oligomers. Our ESI-MS results confirm the polymeric trisaccharide sequence for the FCS samples examined: [4-β-D-GlcA-1→3-β-D-GalNAc4, (4,6-*O*S)-1]$_n$ with the third position of the β-glucuronic acid residue substituted with di-sulfated (FCS-Pg (3, 4-*O*S) from FCS-Ib (2, 4-*O*S)) α-L-fucopyranosyl branches. With careful selection of efficiently deprotonated molecular ions, we have been able to produce structurally informative MS/MS spectra rich in both glycosidic and cross-ring product ions for assigning sites of sulfation. From accurate mass measurements and spectra comparison both isomers, diagnostic ions $^{2,4}X_{\beta f}$, $^{0,2}A_{\alpha f}$ and $^{0,2}X_{\beta f}$ were able to differentiate the FCS-Pg (3, 4-*O*S) from FCS-Ib (2, 4-*O*S). Future work will focus on extending this method for sequencing other species of fucosylated chondroitin sulfates.

Acknowledgements

IA and IJA gratefully acknowledge generous financial support from the National Institutes of Health, grant P41GM103390. This work was also supported by National Science Foundation of China (31301417) and by grants from the China Scholarship Council.

References

1. Fonseca, R.J., Mourão, P.A.: Fucosylated chondroitin sulfate as a new oral antithrombotic agent. Thrombosis and haemostasis. **96**, 822-829 (2006)
2. Mourão, P.A., Pereira, M.S., Pavão, M.S., Mulloy, B., Tollefsen, D.M., Mowinckel, M.-C., Abildgaard, U.: Structure and anticoagulant activity of a fucosylated chondroitin sulfate from echinoderm sulfated fucose branches on the polysaccharide account for its high anticoagulant action. J Biol Chem. **271**, 23973-23984 (1996)
3. Chen, S., Xue, C., Tang, Q., Yu, G., Chai, W.: Comparison of structures and anticoagulant activities of fucosylated chondroitin sulfates from different sea cucumbers. Carbohydrate Polymers. **83**, 688-696 (2011)
4. Mourão, P.A., Boisson-Vidal, C., Tapon-Bretaudière, J., Drouet, B., Bros, A., Fischer, A.-M.: Inactivation of thrombin by a fucosylated chondroitin sulfate from echinoderm. Thrombosis research. **102**, 167-176 (2001)
5. Pomin, V.H.: Marine medicinal glycomics. Frontiers in cellular and infection microbiology. **4**, 5 (2014)
6. Wu, M., Huang, R., Wen, D., Gao, N., He, J., Li, Z., Zhao, J.: Structure and effect of sulfated fucose branches on anticoagulant activity of the fucosylated chondroitin sulfate from sea cucumber Thelenata ananas. Carbohydrate Polymers. **87**, 862-868 (2012)
7. Borsig, L., Wang, L., Cavalcante, M.C., Cardilo-Reis, L., Ferreira, P.L., Mourão, P.A., Esko, J.D., Pavão, M.S.: Selectin blocking activity of a fucosylated chondroitin sulfate glycosaminoglycan from sea cucumber effect

on tumor metastasis and neutrophil recruitment. J Biol Chem. **282**, 14984-14991 (2007)

8. Luo, L., Wu, M., Xu, L., Lian, W., Xiang, J., Lu, F., Gao, N., Xiao, C., Wang, S., Zhao, J.: Comparison of physicochemical characteristics and anticoagulant activities of polysaccharides from three sea cucumbers. Marine drugs. **11**, 399-417 (2013)
9. Pereira, M.S., Mulloy, B., Mourão, P.A.: Structure and anticoagulant activity of sulfated fucans comparison between the regular, repetitive, and linear fucans from echinoderms with the more heterogeneous and branched polymers from brown algae. J Biol Chem. **274**, 7656-7667 (1999)
10. Kariya, Y., Watabe, S., Hashimoto, K., Yoshida, K.: Occurrence of chondroitin sulfate E in glycosaminoglycan isolated from the body wall of sea cucumber Stichopus japonicus. J Biol Chem. **265**, 5081-5085 (1990)
11. Kariya, Y., Mulloy, B., Imai, K., Tominaga, A., Kaneko, T., Asari, A., Suzuki, K., Masuda, H., Kyogashima, M., Ishii, T.: Isolation and partial characterization of fucan sulfates from the body wall of sea cucumber Stichopus japonicus and their ability to inhibit osteoclastogenesis. Carbohydrate research. **339**, 1339-1346 (2004)
12. Vieira, R.P., Mourao, P.A.: Occurrence of a unique fucose-branched chondroitin sulfate in the body wall of a sea cucumber. J Biol Chem. **263**, 18176-18183 (1988)
13. Nagase, H., Enjyoji, K.-i., Minamiguchi, K., Kitazato, K.T., Kitazato, K., Saito, H., Kato, H.: Depolymerized holothurian glycosaminoglycan with

novel anticoagulant actions: antithrombin III-and heparin cofactor II-independent inhibition of factor X activation by factor IXa-factor VIIIa complex and heparin cofactor II-dependent inhibition of thrombin. Blood. **85**, 1527-1534 (1995)

14. Hu, Y., Li, S., Li, J., Ye, X., Ding, T., Liu, D., Chen, J., Ge, Z., Chen, S.: Identification of a highly sulfated fucoidan from sea cucumber Pearsonothuria graeffei with well-repeated tetrasaccharides units. Carbohydrate polymers. **134**, 808-816 (2015)
15. Myron, P., Siddiquee, S., Al Azad, S.: Fucosylated chondroitin sulfate diversity in sea cucumbers: A review. Carbohydrate polymers. **112**, 173-178 (2014)
16. Mourão, P.A., Pereira, M.S.: Searching for alternatives to heparin: sulfated fucans from marine invertebrates. Trends in Cardiovascular Medicine. **9**, 225-232 (1999)
17. Panagos, C.G., Thomson, D.S., Moss, C., Hughes, A.D., Kelly, M.S., Liu, Y., Chai, W., Venkatasamy, R., Spina, D., Page, C.P.: Fucosylated Chondroitin Sulfates from the Body Wall of the Sea Cucumber Holothuria forskali CONFORMATION, SELECTIN BINDING, AND BIOLOGICAL ACTIVITY. J Biol Chem. **289**, 28284-28298 (2014)
18. Ustyuzhanina, N.E., Bilan, M.I., Dmitrenok, A.S., Shashkov, A.S., Nifantiev, N.E., Usov, A.I.: The structure of a fucosylated chondroitin sulfate from the sea cucumber Cucumaria frondosa. Carbohydrate Polymers. **165**, 7-12 (2017)

19. Yoshida, K.-i., Minami, Y., Nemoto, H., Numata, K., Yamanaka, E.: Structure of DHG, a depolymerized glycosaminoglycan from sea cucumber, Stichopus japonicus. Tetrahedron letters. **33**, 4959-4962 (1992)

20. Ustyuzhanina, N.E., Bilan, M.I., Dmitrenok, A.S., Shashkov, A.S., Kusaykin, M.I., Stonik, V.A., Nifantiev, N.E., Usov, A.I.: Structure and biological activity of a fucosylated chondroitin sulfate from the sea cucumber Cucumaria japonica. Glycobiology. **26**, 449-459 (2016)

21. Mourão, P.A.: Perspective on the use of sulfated polysaccharides from marine organisms as a source of new antithrombotic drugs. Marine drugs. **13**, 2770-2784 (2015)

22. Glauser, B.F., Pereira, M.S., Monteiro, R.Q., Mourão, P.A.: Serpin-independent anticoagulant activity of a fucosylated chondroitin sulfate. Thrombosis and haemostasis. **100**, 420-428 (2008)

23. Pacheco, R., Vicente, C., Zancan, P., Mourão, P.: Different antithrombotic mechanisms among glycosaminoglycans revealed with a new fucosylated chondroitin sulfate from an echinoderm. Blood coagulation & fibrinolysis. **11**, 563-573 (2000)

24. Chen, S., Li, G., Wu, N., Guo, X., Liao, N., Ye, X., Liu, D., Xue, C., Chai, W.: Sulfation pattern of the fucose branch is important for the anticoagulant and antithrombotic activities of fucosylated chondroitin sulfates. Biochimica et Biophysica Acta (BBA)-General Subjects. **1830**, 3054-3066 (2013)

25. Fonseca, R., Sucupira, I., Oliveira, S., Santos, G., Mourão, P.: Improved anticoagulant effect of fucosylated chondroitin sulfate orally administered as gastro-resistant tablets. Thrombosis and Haemostasis. (2017)

26. Mulloy, B., Mourao, P., Gray, E.: Structure/function studies of anticoagulant sulphated polysaccharides using NMR. Journal of Biotechnology. **77**, 123-135 (2000)

27. Ustyuzhanina, N.E., Bilan, M.I., Dmitrenok, A.S., Nifantiev, N.E., Usov, A.I.: Two fucosylated chondroitin sulfates from the sea cucumber Eupentacta fraudatrix. Carbohydrate Polymers. (2017)

28. Ustyuzhanina, N.E., Dmitrenok, A.S., Bilan, M.I., Shashkov, A.S., Gerbst, A.G., Usov, A.I., Nifantiev, N.E.: Variations of pH as an additional tool in the analysis of crowded NMR spectra of fucosylated chondroitin sulfates. Carbohydrate research. **423**, 82-85 (2016)

29. Wolff, J.J., Laremore, T.N., Busch, A.M., Linhardt, R.J., Amster, I.J.: Influence of charge state and sodium cationization on the electron detachment dissociation and infrared multiphoton dissociation of glycosaminoglycan oligosaccharides. J Am Soc Mass Spectr. **19**, 790-798 (2008)

30. Wolff, J.J., Laremore, T.N., Busch, A.M., Linhardt, R.J., Amster, I.J.: Electron detachment dissociation of dermatan sulfate oligosaccharides. J Am Soc Mass Spectr. **19**, 294-304 (2008)

31. Zaia, J.: Mass spectrometry and glycomics. Omics: a journal of integrative biology. **14**, 401-418 (2010)

32. Kailemia, M.J., Ruhaak, L.R., Lebrilla, C.B., Amster, I.J.: Oligosaccharide analysis by mass spectrometry: a review of recent developments. Analytical chemistry. **86**, 196-212 (2013)

33. Zaia, J.: Glycosaminoglycan glycomics using mass spectrometry. Molecular & Cellular Proteomics. **12**, 885-892 (2013)

34. Zaia, J.: Mass spectrometry of oligosaccharides. Mass spectrometry reviews. **23**, 161-227 (2004)

35. Kailemia, M.J., Li, L., Ly, M., Linhardt, R.J., Amster, I.J.: Complete mass spectral characterization of a synthetic ultralow-molecular-weight heparin using collision-induced dissociation. Analytical chemistry. **84**, 5475-5478 (2012)

36. Kailemia, M.J., Li, L., Xu, Y., Liu, J., Linhardt, R.J., Amster, I.J.: Structurally Informative Tandem Mass Spectrometry of Highly Sulfated Natural and Chemoenzymatically Synthesized Heparin and Heparan Sulfate Glycosaminoglycans*□ S. Molecular & Cellular Proteomics. **12**, 979 (2013)

37. Huang, R., Liu, J., Sharp, J.S.: An approach for separation and complete structural sequencing of heparin/heparan sulfate-like oligosaccharides. Analytical chemistry. **85**, 5787-5795 (2013)

38. Huang, R., Pomin, V.H., Sharp, J.S.: LC-MSn analysis of isomeric chondroitin sulfate oligosaccharides using a chemical derivatization strategy. J Am Soc Mass Spectr. **22**, 1577 (2011)

39. Zaia, J., Costello, C.E.: Tandem mass spectrometry of sulfated heparin-like glycosaminoglycan oligosaccharides. Analytical chemistry. **75**, 2445-2455 (2003)

40. Kailemia, M.J., Patel, A.B., Johnson, D.T., Li, L., Linhardt, R.J., Amster, I.J.: Differentiating chondroitin sulfate glycosaminoglycans using collision-induced dissociation; uronic acid cross-ring diagnostic fragments in a single stage of tandem mass spectrometry. European Journal of Mass Spectrometry. **21**, 275-285 (2015)

41. Agyekum, I., Patel, A.B., Zong, C.L., Boons, G.J., Amster, I.J.: Assignment of hexuronic acid stereochemistry in synthetic heparan sulfate tetrasaccharides with 2-O-sulfo uronic acids using electron detachment dissociation. International Journal of Mass Spectrometry. **390**, 163-169 (2015)

42. Agyekum, I., Zong, C., Boons, G.J., Amster, I.J.: Single Stage Tandem Mass Spectrometry Assignment of the C-5 Uronic Acid Stereochemistry in Heparan Sulfate Tetrasaccharides using Electron Detachment Dissociation. J Am Soc Mass Spectrom. (2017)

43. Li, S., Li, J., Zhi, Z., Wei, C., Wang, W., Ding, T., Ye, X., Hu, Y., Linhardt, R.J., Chen, S.: Macromolecular properties and hypolipidemic effects of four sulfated polysaccharides from sea cucumbers. Carbohydrate Polymers. **173**, 330-337 (2017)

44. Fukuda, M., Kondo, T., Osawa, T.: Studies on Hydrazinolysis of Glycoproteins - Core Structures of Oligosaccharides Obtained from Porcine

Thyroglobulin and Pineapple Stem Bromelain. Journal of Biochemistry. **80**, 1223-1232 (1976)

45. Bienkowski, M.J., Conrad, H.E.: Structural Characterization of the Oligosaccharides Formed by Depolymerization of Heparin with Nitrous-Acid. Journal of Biological Chemistry. **260**, 356-365 (1985)

46. Rice, K.G., Rottink, M.K., Linhardt, R.J.: Fractionation of Heparin-Derived Oligosaccharides by Gradient Polyacrylamide-Gel Electrophoresis. Biochemical Journal. **244**, 515-522 (1987)

47. Ceroni, A., Maass, K., Geyer, H., Geyer, R., Dell, A., Haslam, S.M.: GlycoWorkbench: a tool for the computer-assisted annotation of mass spectra of glycans†. Journal of proteome research. **7**, 1650-1659 (2008)

48. Damerell, D., Ceroni, A., Maass, K., Ranzinger, R., Dell, A., Haslam, S.M.: Annotation of glycomics MS and MS/MS spectra using the GlycoWorkbench software tool. Glycoinformatics. 3-15 (2015)

49. Domon, B., Costello, C.E.: A systematic nomenclature for carbohydrate fragmentations in FAB-MS/MS spectra of glycoconjugates. Glycoconjugate journal. **5**, 397-409 (1988)

50. Tissot, B., Salpin, J.-Y., Martinez, M., Gaigeot, M.-P., Daniel, R.: Differentiation of the fucoidan sulfated L-fucose isomers constituents by CE-ESIMS and molecular modeling. Carbohydrate research. **341**, 598-609 (2006)

51. Anastyuk, S.D., Shevchenko, N.M., Nazarenko, E.L., Imbs, T.I., Gorbach, V.I., Dmitrenok, P.S., Zvyagintseva, T.N.: Structural analysis of a highly

sulfated fucan from the brown alga Laminaria cichorioides by tandem MALDI and ESI mass spectrometry. Carbohydrate Research. **345**, 2206-2212 (2010)

52. Daniel, R., Chevolot, L., Carrascal, M., Tissot, B., Mourão, P.A., Abian, J.: Electrospray ionization mass spectrometry of oligosaccharides derived from fucoidan of Ascophyllum nodosum. Carbohydrate Research. **342**, 826-834 (2007)

53. Leach, F.E., Ly, M., Laremore, T.N., Wolff, J.J., Perlow, J., Linhardt, R.J., Amster, I.J.: Hexuronic acid stereochemistry determination in chondroitin sulfate glycosaminoglycan oligosaccharides by electron detachment dissociation. J Am Soc Mass Spectr. **23**, 1488-1497 (2012)

54. Zaia, J., Li, X.-Q., Chan, S.-Y., Costello, C.E.: Tandem mass spectrometric strategies for determination of sulfation positions and uronic acid epimerization in chondroitin sulfate oligosaccharides. J Am Soc Mass Spectr. **14**, 1270-1281 (2003)

55. Tao, L., Song, F., Xu, N., Li, D., Linhardt, R.J., Zhang, Z.: New insights into the action of bacterial chondroitinase AC I and hyaluronidase on hyaluronic acid. Carbohydrate Polymers. **158**, 85-92 (2017)

56. Shi, S.D.-H., Hendrickson, C.L., Marshall, A.G., Siegel, M.M., Kong, F., Carter, G.T.: Structural validation of saccharomicins by high resolution and high mass accuracy fourier transform-ion cyclotron resonance-mass spectrometry and infrared multiphoton dissociation tandem mass spectrometry. J Am Soc Mass Spectr. **10**, 1285-1290 (1999)

57. Brüll, L., Heerma, W., Thomas-Oates, J., Haverkamp, J., Kovácik, V., Kovác, P.: Loss of internal 1→ 6 substituted monosaccharide residues from underivatized and per-O-methylated trisaccharides. J Am Soc Mass Spectr. **8**, 43-49 (1997)

58. Kováčik, V., Hirsch, J., Kováč, P., Heerma, W., Thomas- Oates, J., Haverkamp, J.: Oligosaccharide characterization using collision- induced dissociation fast atom bombardment mass spectrometry: Evidence for internal monosaccharide residue loss. Journal of Mass Spectrometry. **30**, 949-958 (1995)

59. Stephens, E., Maslen, S.L., Green, L.G., Williams, D.H.: Fragmentation characteristics of neutral N-linked glycans using a MALDI-TOF/TOF tandem mass spectrometer. Analytical chemistry. **76**, 2343-2354 (2004)

60. Harvey, D.J.: Fragmentation of negative ions from carbohydrates: part 1. Use of nitrate and other anionic adducts for the production of negative ion electrospray spectra from N-linked carbohydrates. J Am Soc Mass Spectr. **16**, 622-630 (2005)

61. Zhao, C., Xie, B., Chan, S.Y., Costello, C.E., O'Connor, P.B.: Collisionally activated dissociation and electron capture dissociation provide complementary structural information for branched permethylated oligosaccharides. Journal of the American Society for Mass Spectrometry. **19**, 138-150 (2008)

CHAPTER 8

CONCLUSIONS

Improvement on current ESI tandem mass spectrometry analysis of sulfated glycosaminoglycans using electron detachment dissociation (EDD) and collisionally induced dissociation (CID) is highlighted this work. This work extends the activation of carefully selected sodium cationized molecular ions of highly sulfated GAGs including heparin, heparan sulfate and fucosylated chondroitin sulfate (FCS).

The efficiency of EDD product ion coverage in relation to the amount of useful ions produced without SO_3 loss has been shown to increase as the ionized state of the selected charged state molecular ion increased through Na/H. The efficacy of using EDD to obtain even more structurally informative spectra of fully deprotonated sodium cationized precursor ion is tested with the pharmaceutical drug Arixtra. In comparison to recently reported CID activation of fully deprotonated multiply charged molecular ions of Arixtra, EDD of a single precursor ion $[M\text{-}10H+5Na]^{3-}$ produced more structurally informative product ions. Both N and 6-*O* sulfo positions on the reducing and non-reducing end glucosamine units where confidently assigned based on accurate mass measurements of cross-ring product ions with distinct elemental composition. In contrast, the earlier CID activation of $[M\text{-}10H+6Na]^{4-}$ and $[M\text{-}10H+5Na]^{5-}$ molecular ions yielding cross-ring cleavages with the same elemental composition; ${}^{1,5}A_5 = {}^{2,4}X_4$, ${}^{2,4}A_5 = {}^{1,5}X_4$ and ${}^{2,4}X_0 = {}^{1,5}A_1$ on both glucosamine units. Since these ions were indistinguishable, it was

difficult to assign the exact positions of two sulfate groups on the reducing and non-reducing end glucosamine units using CID.

The bulk part of this work also focused on the assignment of the hexuronic acid stereochemistry of heparan sulfate tetrasaccharides. EDD-PCA results on 2-*O*-Sulfo uronic acid heparan sulfate tetrasaccharides proved useful in revealing diagnostic ions capable of assigning the C-5 hexuronic acid stereochemistry of these standards. We have combine these ions into a diagnostic ratio formula capable of assigning the C-5 hexuronic acid stereochemistry of heparan sulfate tetrasaccharides from a single EDD MS/MS experiment without comparing it to a standard. The Formula proved efficient in assigning the C-5 hexuronic acid stereochemistry 33 HS tetrasaccharide standards. Future works hope to extend this method to longer heparan sulfate oligomers with multiple or alternating C-5 hexuronic acid stereochemistry.

Lastly, MS and MS/MS sequence information for fucosylated chondroitin sulfate (FCS) a rare glycosaminoglycan is presented. To our knowledge, this work presents the first tandem mass spectrometry sequence information on FCS. ESI MS of the two species of fucosylated chondroitin pearsonothuria graeffei (FCS-Pg) and Isostichopus badionotus (FCS-Ib) showed they were repeating polymers of the trisaccharide repeats of [4-β-D-GlcA-1→3-β-D-GalNAc-1]$_n$ with the third-position of the β-glucuronic acid residues substituted with di-sulfated α-fucose branches. Each subunit averages 4 Sulfates per disaccharide making this rare class chondroitin sulfate the most sulfated chondroitin sulfate yet to be sequenced. Again, with abundant cross-ring and glycosidic cleavages, we have been able to assign the positions of the sulfate groups and differentiate these two positional isomers. FCS-Pg oligomers were sulfated at the 3, 4-*O* positions on the fucose

residues whereas FCS-Ib were sulfated at the 2, 4-*O* positions. Key diagnostic ions identified for FCS Pg were $^{0,2}A_{\alpha f}$ and $^{2,4}X_{\beta f}$ and that for FCS Ib was $^{0,2}X_{\beta f}$.

APPENDIX A

CHAPTER 3

SUPPLEMENATRY INFORMATION

EDD mass list for $[M-10H+5Na]^{5-}$

Mass to charge	Intensity	Type
157.0139	2269305	B_1-SO_3
159.9682	2829748	0,2X0+Na
168.4888	4428038	Y12-
168.9809	1712765	1,4X0
171.5113	610654	1,4X1-SO3
175.0245	1878493	C1-SO3
186.5167	662031	2,4X1-SO3
208.9759	1098290	1,5A1
236.9707	1799777	B1
240.0178	2222688	Z1-SO3
249.485	1233792	[B2+Na-SO3]2-
254.9811	1150941	C1
258.4905	1675319	[Z2+Na]2-
258.4905	1675319	[C2+Na-SO3]2-
258.4905	1675319	C1+Na
258.9525	4451621	B1+Na
259.1736	733665	[0,2X5+4Na]5-
267.4957	1.39E+07	[Y2+Na]2-
274.9837	1083178	[2,4A6+Na-SO3]5-
276.963	1876413	C1+Na

282.5022	793975	3,5A3+Na-SO3
290.9752	769091	[2,4A6+Na]5-
299.9465	1876162	2,4X0+Na
300.4544	1861424	[B2+2Na]2-
309.4603	1705589	[C2+2Na]2-
318.9737	3838630	2,4A2+Na
323.3667	1090004	[0,2A6+5Na]5-
327.9637	2438727	[0,2X5+5Na]5-
335.1741	2.18E+07	[M-10H+5Na-SO3]5-
341.9565	2584676	Z1+Na
351.1654	1.65E+09	[M-10H+5Na]5-
353.2301	2890713	[Z5+Na]4-
358.9637	1857758	[C5+5Na]4-
359.2137	1114952	[2,4X4+4Na]4-
359.9674	2729128	Y1+Na
369.4658	2034181	[2,4A6+5Na]4-
369.7171	1073245	[Z5+4Na]4-
378.9758	1316275	[0,2A6+4Na-SO3]4-
378.9948	1404376	0,2A2+Na-SO3
379.714	5657200	[Y5+5Na]4-
380.2931	3.72E+07	[B4+4Na-SO3]3-
384.471	2.10E+07	[0,2A6+5Na-SO3]4-
384.7218	8802961	[0,2X5+5Na-SO3]4-

386.7145	928909	[1,5X5+5Na]4-
387.9618	1034677	1,5X1+Na
388.4707	1009998	[B3+2Na-SO3]2-
389.9951	1662333	[Z3+2Na-SO3]2-
390.967	874883	[C4+Na]3-
399.4624	1061401	[B3+3Na-SO3]2-
404.4604	1.13E+08	[0,2A6+5Na]4-
404.7107	5.38E+07	[0,2X5+5Na]4-
406.9449	3.72E+07	[B4+4Na]3-
408.4667	3343969	[C3+3Na-SO3]2-
408.9673	1040588	[2,4X2+2Na]2-
412.9496	2532142	[C4+4Na]3-
414.2727	9790793	[B4+5Na]3-
419.2192	4081361	[M-9H+5Na-O3]4-
420.2757	4464789	[C4+5Na]3-
427.957	1030767	1,4A2+Na
432.66	857321	[Z5+3Na-SO3]3-
434.2806	2244661	[2,4A5+5Na]3-
440.9647	2517378	[Z3+3Na]2-
446.2983	4625413	[B5+5Na-SO3]3-
448.4457	6610068	[C3+3Na]2-
449.9698	1144332	[Y3+3Na]2-
459.4374	2262625	[C3+4Na]2-

465.6228	1620866	[B5+4Na]3-
472.9499	2.10E+07	[B5+5Na]3-
474.959	2005633	[1,5X3+4Na]2-
478.9534	6545010	[C5+5Na]3-
479.2882	1256287	[2,4X4+4Na]3-
480.934	2955589	0,2A2+2Na
489.302	1139213	[1,5X5+5Na-SO3]3-
492.9567	2186107	[0,2X3+5Na-SO3]2-
492.9567	2186107	[2,4A6+5Na]3-
500.6182	3098474	[Z5+5Na]3-
510.4511	1393153	[0,2A4+4Na-SO3]2-
521.9584	2002580	[1,4A6+4Na]3-
539.9725	2456760	Z2+2Na/C2+2Na-SO3
543.9616	1109317	[1,5A6+5Na-SO3]3-
561.4219	3483401	[0,2A4+5Na]2-
569.9801	1116104	[1,5X4+4Na]2-
570.9448	940268	[B4+4Na-SO3]2-
590.9413	1.39E+07	[Z4+5Na]2-
590.9413	1.39E+07	[C4+5Na-SO3]2-
601.9175	937365	B2+2Na
602.952	1389534	[1,5X4+2Na]2-
611.9469	957400	[2,4A5+5Na-SO3]2-
613.9444	2310682	[1,5X4+5Na]2-

621.9154	1381560	[B4+5Na]2-
630.9205	6383592	[C4+5Na]2-

EDD Mass list for $[M-8H+2Na]^{6-}$

Mass to charge	Intensity	Type
175.0248	4158408	B1
187.0085	792456	0,2A22-
193.0355	7793361	C1
199.031	2473728	Y33-
207.5217	1.67E+07	[B2-SO3]2-
211.034	3.72E+07	Y1
223.0762	647596	0,2X0
225.0314	3187669	1,5X12-
229.2671	1060749	Y34-
232.0392	2804537	0,2X1
235.0463	1518673	2,4A2
247.5003	4195002	B22-
256.5059	672669	C22-
257.0279	1032474	2,4A2+Na
258.4912	3656627	[B2+Na]2-
259.0724	658802	[Y2-SO3]2-
267.4966	4867152	[C2+Na]2-
271.5194	1.17E+07	[B3-SO3]4-

272.5414	889967	^{0,2}A_{GlcN}
272.6779	8.03E+07	^{2,5}A_{GlcN}
273.2753	1.97E+07	Y44-
279.373	1624551	[Y3-SO3]3-
279.7642	1785312	[Z4+2Na]4-
280.697	1006076	[Z3+Na-SO3]3-
281.0054	763157	0,2A54-
284.2663	1.49E+08	[Y4+2Na]4-
297.0042	1037309	[B5+Na]4-
297.3349	897922	[0,2A4+Na]3-
299.0502	2031879	Y22-
302.4992	1.41E+07	[3,5A2+Na]2-
302.4992	1.41E+07	[B5+2Na]4-
304.6631	3353933	[0,2A4+2Na]3-
306.0251	1309526	Y33-
306.5293	712934	[B3+Na-SO3]2-
310.0412	1.27E+07	[Y2+Na]2-
311.0229	915561	0,3X44-
317.0492	1114891	[0,2A2+Na-SO3]3-
318.3386	7172773	[B4+2Na-SO3]3-
320.6801	8801233	[Y3+2Na]2-
324.0385	768518	[1,5X2+Na]2-
324.3414	1514415	[C4+2Na-SO3]3-

325.1085	2352521	Z1-SO3
327.0145	3.02E+07	[0,2A6+Na-SO3]4-
330.0104	1256415	[1,5X3+2Na]3-
334.6828	861458	[0,2X3+Na]3-
335.5155	1423146	B32-
336.0939	1153453	B2-SO3
340.0188	1133193	[Z5+2Na-SO3]4-
343.119	3744142	Y1-SO3
344.9909	1940093	[B4+2Na]3-
346.5076	3855094	[B3+Na]2-
346.7017	981446	[Z3+2Na-SO3]3-
350.9943	6862560	[C4+2Na]3-
355.5124	1501428	[C3+Na]2-
364.0222	802823	0,2X54-
364.7018	1552491	Y43-
365.1014	1056434	Y1+Na-SO3
366.0256	1179006	[Z4+Na]3-
371.113	692623	1,5X1-SO3
373.3537	1030519	[Z4+2Na]4-
379.0119	791748	[2,5X5+2Na]4-
379.3575	6628974	[Y4+2Na]3-
385.1295	788112	0,2X1-SO3
387.5088	794023	[2,4A4+2Na]2-

388.6885	1192885	[1,5X4+2Na]2-
397.0063	6400996	0,2A2+Na
397.0203	2693029	[1,4X2+2Na]2-
416.0511	1094624	B2-SO3
438.0331	3241240	B2+Na-SO3
441.545	1189642	[Y3+Na-SO3]2-
445.0572	4946515	Y1+Na
457.4973	2361206	[0,2A4+Na]2-
487.0146	748135	[C4+2Na-SO3]2-
517.9881	823064	[B4+2Na]2-
517.9881	823064	B2+Na

APPENDIX B

SUPPLEMENTAL DATA FOR CHAPTER 2

Single Stage MS/MS Analysis of Sodium Cationized Ions of Ultra-low molecular weight Heparin Using Electron Detachment Dissociation

Isaac Agyekum,[1] Lauren Elizabeth Pepi,[1] Robert J. Linhardt,[2] I. Jonathan. Amster[1]*

[1]Department of Chemistry, University of Georgia, Athens, GA 30602

[2]Department of Chemistry and Chemical Biology, [§]Department of Chemical and Biological Engineering, [⊥]Department of Biology, [∥]Department of Biomedical Engineering, Center for Biotechnology and Interdisciplinary Studies, Rensselaer Polytechnic Institute, Troy, New York, United States

Mass list for $[M-10H+5Na]^{5-}$ precursor ion

Mass to charge	Intensity	Relative Intensity	Type	Accuracy PPM
137.9867	7208342	0.101795183	$^{1,3}A_1$	-0.348504602
137.9867	7.21E+06	0.101795183	$^{1,3}A_3$-SO_3	-0.348504602
137.9867	7208342	0.101795183	$^{1,3}A_5$	-0.348504602
138.9706	2.73E+07	0.385528026	$^{0,4}A_1$	0.485685462
138.9706	2.73E+07	0.385528026	$^{1,3}A_2$	0.485685462
138.9706	2.73E+07	0.385528026	$^{0,4}A_3$-SO_3	0.485685462
152.0023	2283744	0.032250709	$^{0,2}X_0$	0.012993224
152.9863	1389110	0.019616814	$^{3,5}A_1$	0.11478152
159.484	2119879	0.02993663	B_1	-0.36338128
159.9686	3708470	0.052370487	$^{1,3}A_1$+Na	-0.021572984
159.9686	3.71E+06	0.052370487	$^{1,3}A_3$+Na-SO_3	-0.021572984
159.9686	3.71E+06	0.052370487	$^{1,3}A_5$+Na	-0.021572984
160.9526	2912499	0.041129898	$^{0,4}A_1$+Na	0.075388655
160.9526	2912499	0.041129898	$^{1,3}A_2$+Na	0.075388655
160.9526	2912499	0.041129898	$^{0,4}A_5$+Na	0.075388655
168.4892	6356821	0.089770124	C_1	0.144754085
168.9812	2661507	0.037585424	$^{0,3}A_1$	0.190447221
175.4971	6.40E+06	0.090330776	Y_1	-0.288201344
186.4881	3.77E+06	0.05325412	Y_1+Na	-0.419648761
189.4947	1.81E+06	0.025490123	$^{2,4}A_2$	-1.019909792

189.4947	1805012	0.025490123	$^{1,5}X_1$	-1.019909792
190.9633	1.43E+06	0.020206967	$^{0,3}A_1$+Na	-0.645045409
198.9918	3.06E+07	0.432824417	$^{0,2}A_1$	-0.015739342
214.4829	1460588	0.020626217	$[B_3+2Na-SO_3]^{2-}$	0.16953566
214.4829	1460588	0.020626217	$^{3,5}A_2$+Na	0.16953566
214.9632	1.37E+06	0.019316555	$[Z_3+4Na]^{4-}$	1.523488671
220.9737	2175203	0.030717908	$^{0,2}A_1$+Na	0.187832307
240.0183	7.21E+06	0.101777107	B_1-SO_3	0.191522896
241.0259	1.03E+06	0.014599601	$[^{0,3}A_2+2Na-SO_3]^{2-}$	2.540294079
243.9898	2223766	0.031403708	$[^{2,5}A_2+2Na-SO_3]^{2-}$	-0.866706313
243.9898	2223766	0.031403708	$[^{1,4}X_3+2Na-SO_3]^{2-}$	-0.866706313
247.4718	1.16E+07	0.163636226	$^{0,2}X_1$+Na	-0.358176164
247.4998	1736485	0.024522395	B_2	0.751679395
247.4998	1736485	0.024522395	B_4-SO_3	0.751679395
254.034	1.01E+07	0.14260169	Z_1-SO_3	-0.01561602
258.029	2354491	0.033249788	C_1-SO_3	-0.346259529
258.491	9691482	0.136861734	B_2+Na	-0.161090715
258.491	9691482	0.136861734	$[B_4+2Na-SO_3]^{2-}$	-0.161090715
265.4988	5.99E+06	0.084532256	Z_2+Na-SO_3	-0.062555839
272.0447	1113743	0.015728121	Y_1-SO_3	-0.511978362
294.0265	2266385	0.032005567	Y_1+Na-SO_3	0.018219446
303.9645	1532401	0.02164035	$[B_4+3Na]^{3-}$	1.157362126
305.4771	6174027	0.087188733	Z_2+Na	0.296812756

306.3736	4.21E+06	0.059409273	$[M-10H+5Na-SO_3]^{5-}$	-0.093230618
316.4682	3.39E+07	0.478943948	$[Z_2+2Na]^{2-}$	-0.116951719
317.4666	1.85E+06	0.026173	$[Y_4+4Na]^{4-}$	0.91866042
320.2925	2084328	0.029434584	$[B_3+3Na]^{3-}$	0.292520118
322.3647	7.08E+09	100	$[M-10H+5Na]^{5-}$	0.726964832
323.3643	2.71E+08	3.82032369	$[^{0,2}X_4+3Na-SO_3]^{3-}$	-0.732664882
324.4654	3403400	0.048062332	$[^{1,5}X_4+4Na]^{4-}$	0.678961455
324.4654	3403400	0.048062332	$[^{2,4}A_5+4Na]^{4-}$	0.678961455
324.9644	5182639	0.073188493	$[Z_3+3Na-SO_3]^{3-}$	0.237092637
325.4735	7939030	0.112113855	$[Y_2+2Na]^{2-}$	-0.167966056
326.296	1697111	0.023966361	$[C_3+3Na]^{3-}$	0.353219163
339.4708	1534878	0.021675329	$[^{2,4}A_5+2Na]^{2-}$	0.302360321
339.4708	1.53E+06	0.021675329	$[^{1,5}X_2+2Na]^{2-}$	0.302360321
339.4708	1534878	0.021675329	$[^{0,2}A_5+4Na-SO_3]^{4-}$	0.302360321
341.9571	1.98E+07	0.280238841	B_1+Na	0.015098385
353.4539	4.51E+06	0.063619197	$[^{3,5}A_5+5Na]^{5-}$	0.912747037
355.9728	1.32E+07	0.186283958	Z_1+Na	-0.125776464
359.9677	2.17E+07	0.306522585	C_1+Na	-0.083760293
364.9476	5.26E+07	0.742157872	$[Y_3+4Na]^{4-}$	-0.041083524
368.2142	1324962	0.018710925	$[^{2,4}X_4+5Na-SO_3]^{5-}$	-1.898186572
368.2142	1324962	0.018710925	$[^{0,4}X_4+5Na]^{5-}$	-1.898186572
368.2142	1324962	0.018710925	$[^{1,5}A_5+5Na-SO3]^{5-}$	-1.898186572
372.2749	3034960	0.042859275	$[Y_3+5Na]^{5-}$	-3.06E-04

373.9834	2.22E+07	0.313339629	Y_1+Na	-0.214145869
374.2793	5315127	0.075059469	$[^{1,5}X_3+4Na]^{4-}$	-0.205156951
383.2185	6931490	0.097885518	$[M-9H+5Na-SO_3]^4$	0.73953567
390.9688	3307261	0.046704671	$[Z_4+4Na]^{4-}$	0.906948756
392.3004	1802024	0.025447927	$[C_4+4Na-SO_3]^{4-}$	1.001263317
395.9658	3052516	0.043107198	$[Y_1+2Na]^{2-}$	-1.352260726
401.9781	5255955	0.074223851	$^{2,4}A_2$+Na	0.334682412
401.9781	5255955	0.074223851	$^{1,5}X_1$+Na	0.334682412
403.2071	3.09E+07	0.436200699	$[M-9H+5Na]^{4-}$	2.199968081
412.9492	1192068	0.016834215	$[B_4+4Na]^{4-}$	0.830011698
418.9534	1390945	0.019642728	$[C_4+4Na]^{4-}$	-0.801247426
420.2765	2573892	0.036348138	$[B_4+5Na]^{5-}$	0.850944557
423.9605	4291079	0.060598009	$[^{2,4}A_2+2Na]^{2-}$	-0.756737951
423.9605	4291079	0.060598009	$[^{1,5}X_1+2Na]^{2-}$	-0.756737951
424.9489	1.75E+07	0.247505052	$[Z_4+5Na]^{5-}$	-0.374194011
426.2806	6558674	0.092620664	$[C_4+5Na]^{5-}$	-0.517982756
430.9524	1.11E+07	0.157087243	$[Y_4+5Na]^{5-}$	-0.318947831
440.2847	4660179	0.065810387	$[^{1,5}X_4+5Na]^{5-}$	-1.815289062
440.2847	4660179	0.065810387	$[^{2,4}A_5+5Na]^{5-}$	-1.815289062
440.9647	1562700	0.022068228	$[B_3+3Na-SO_3]^{3-}$	-1.311950821
447.9717	1151502	0.016261348	$[Z_3+3Na-SO_3]^{3-}$	0.550275832
451.9542	1470005	0.020759202	$[B_3+4Na-SO_3]^{4-}$	1.977622954
451.9542	1470005	0.020759202	$[^{3,5}A_2+2Na]2-$	1.977622954

481.2842	2090998	0.029528777	$[^{0,3}X_4+5Na]^{5-}$	-1.304849955
491.9339	1880838	0.026560927	$[B_3+4Na]^{4-}$	-0.810936185
495.9574	2247086	0.031733030	$[^{2,4}X_4+2Na]^{3-}$	0.041211200
495.9574	2247086	0.031733030	$[^{1,5}A_5+2Na]^{3-}$	0.041211200
497.9606	2081498	0.029394619	$[^{0,2}A_2+2Na]^{2-}$	-0.054014314
498.9416	4913635	0.069389656	$[Z_3+4Na\text{-}SO_3]^{4-}$	-0.548952022
500.9386	7148359	0.100948112	$[C_3+4Na]^{4-}$	0.366144673
507.9476	2024582	0.02859086	$[Y_3+4Na\text{-}SO_3]^{4-}$	-1.952075372
517.9329	4544610	0.064178338	$[^{0,2}X_1+2Na]^{2-}$	-0.494672187
519.9433	3193041	0.045091672	$[^{0,2}A_2+3Na]^{3-}$	-1.50450828
539.9724	1297940	0.018329325	$[B_2+2Na]_{2-}$	-2.337547253
539.9724	1297940	0.018329325	$^{0,3}X_3$	-1.312778209
539.9724	1297940	0.018329325	$[B_4+4Na\text{-}SO_3]^{4-}$	-2.337547253
557.9817	2362800	0.033367126	$[C_2+2Na]^{2-}$	0.004435629
558.9171	6845617	0.096672832	$[Y_3+5Na]^{5-}$	-1.989481088
572.9129	3184656	0.04497326	$[^{1,5}X_3+5Na]^{5-}$	0.951900367
579.9228	1617068	0.022836005	$[^{0,2}X_3+5Na]^{5-}$	-2.637613144
595.9617	1065288	0.015043846	$[Y_4+4Na\text{-}SO_3]^{4-}$	1.598159747
595.9617	1065288	0.015043846	C_4+Na	-2.319392337
597.9496	1214589	0.017152254	$[Z_4+5Na\text{-}SO_3]^{5-}$	-2.103157189
637.9266	1180976	0.016677576	$[Z_4+5Na]^{5-}$	0.234660226
655.9251	4633859	0.065438699	$[Z_2+3Na]^{3-}$	0.681551902
673.9367	1571007	0.022185538	$[Y_2+3Na]^{3-}$	-0.872881682

APPENDIX C

SUPPLEMENTAL DATA FOR CHAPTER 4

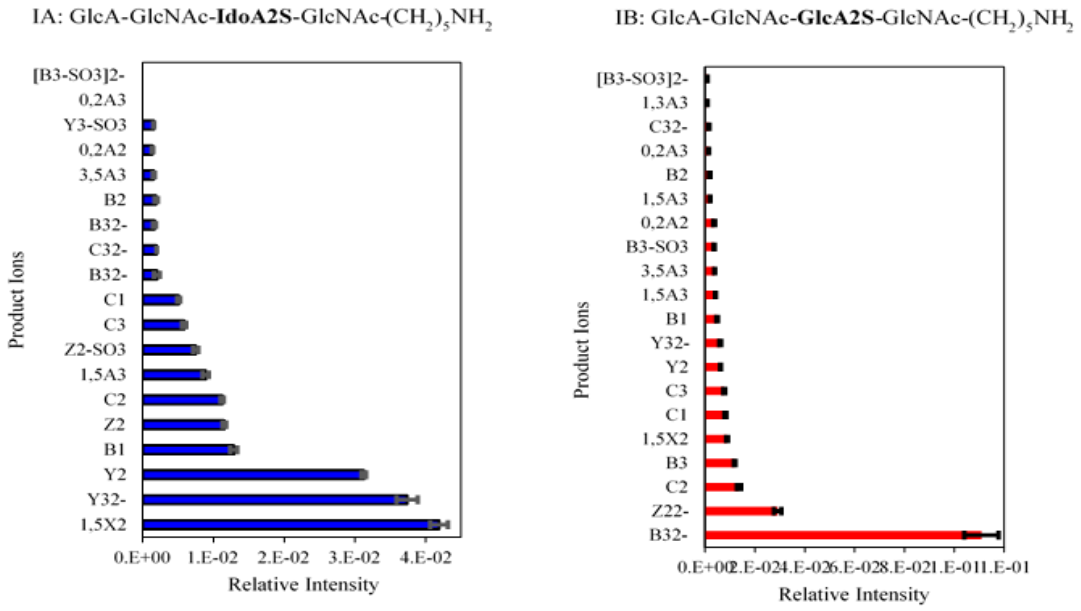

Scheme 1. EDD mass spectrum-to-spectrum product ion variation for $[M-3H]^{2-}$ precursor ion for IA and IB

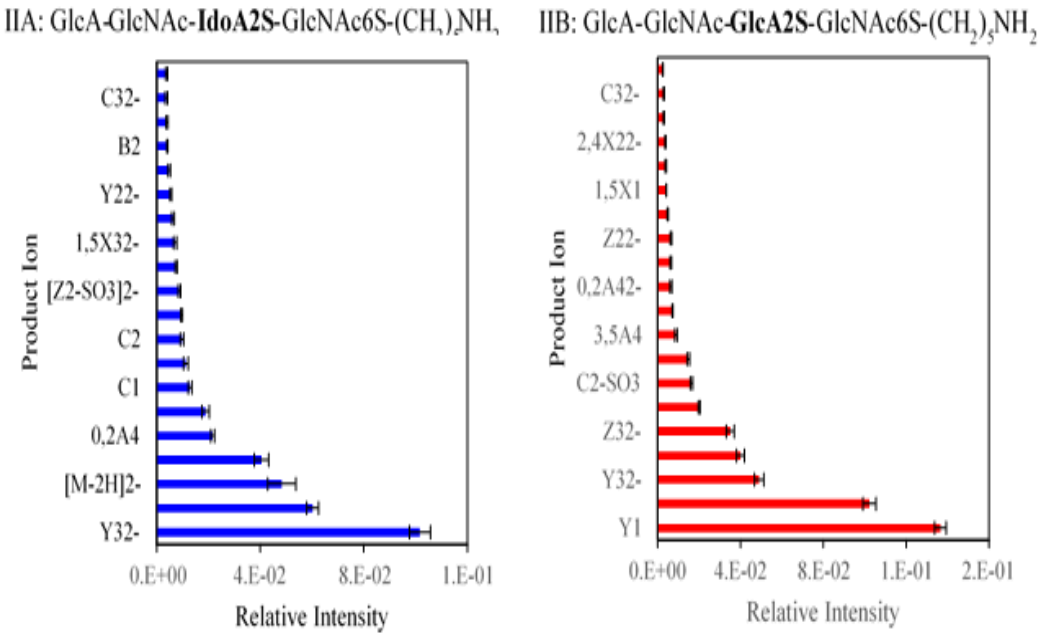

Scheme 2. EDD mass spectrum-to-spectrum product ion variation for $[M-3H]^{3-}$ precursor ion for IIA and IIB

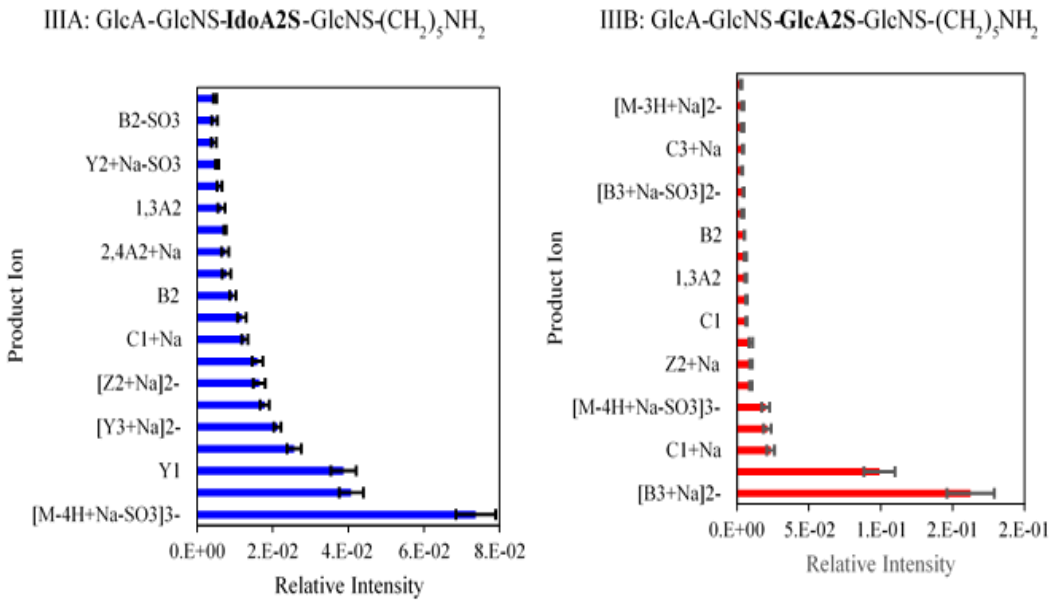

Scheme 3. EDD mass spectrum-to-spectrum product ion variation for IIIA and IIIB

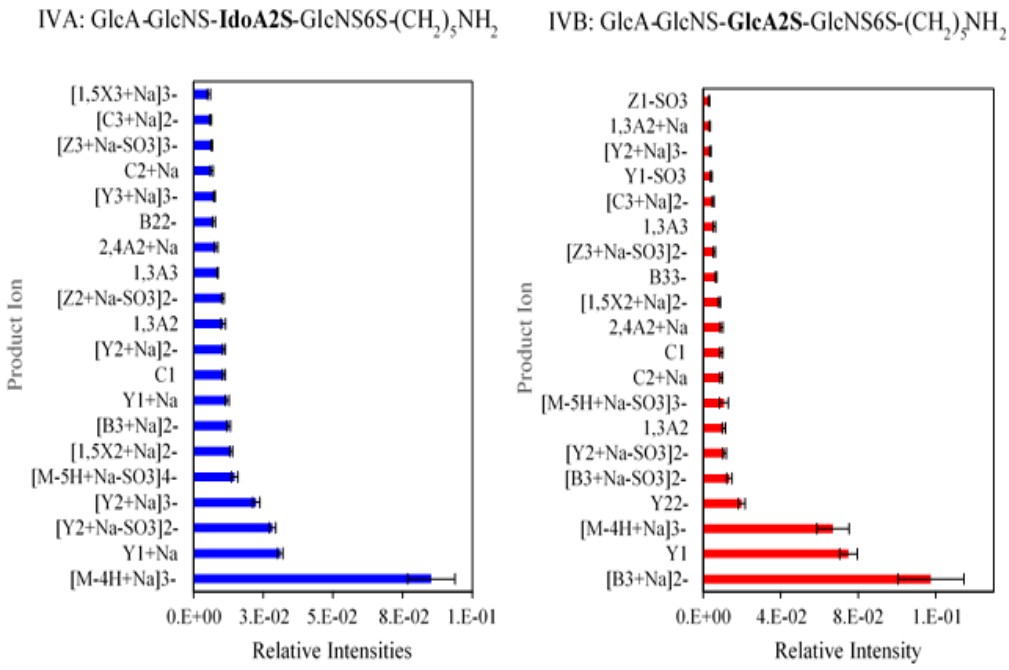

Scheme 4. EDD mass spectrum-to-spectrum product ion variation for IVA and IVB

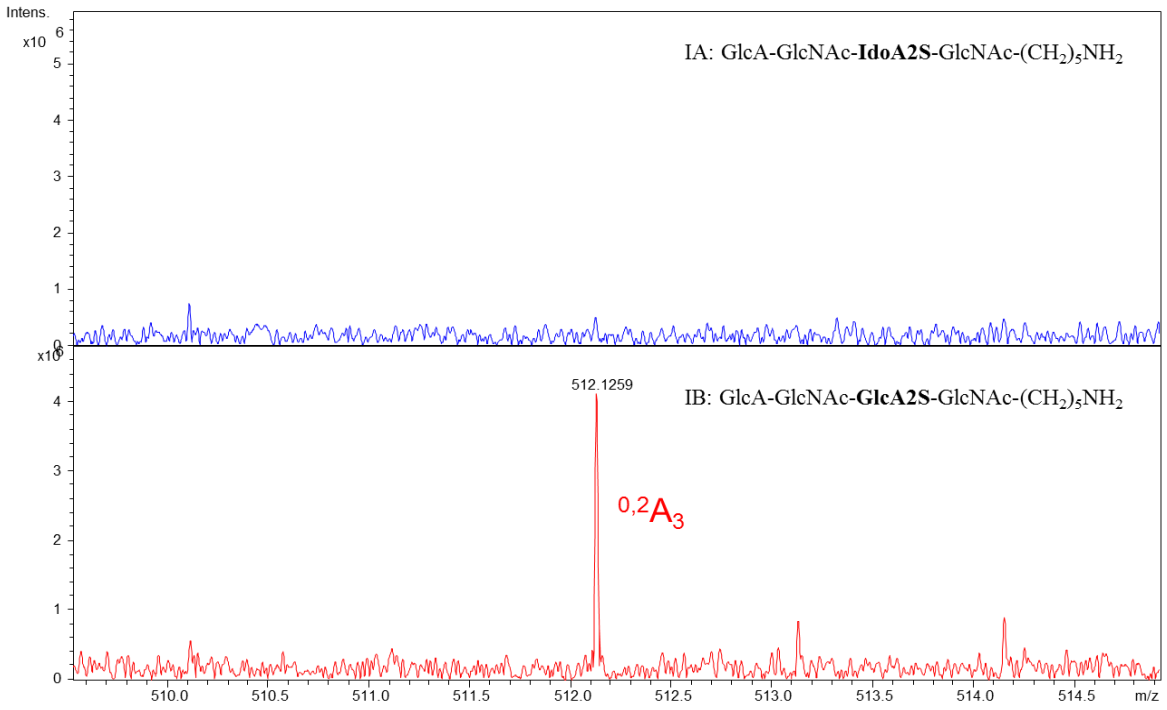

Scheme 5. EDD assignment of stereospecific ion $^{0,2}A_3$, for the $[M-2H]^{2-}$ precursor for IA and IB.

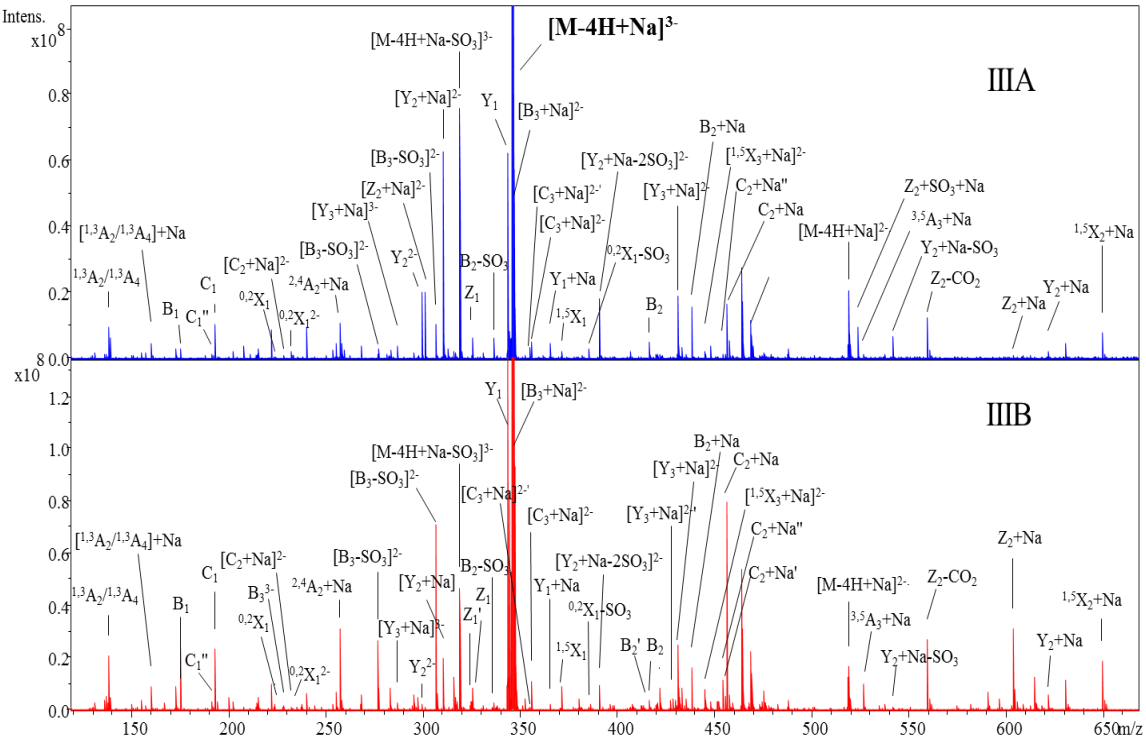

Scheme 6. EDD of the $[M-4H+Na]^{3-}$ precursor for IIIA and IIIB.

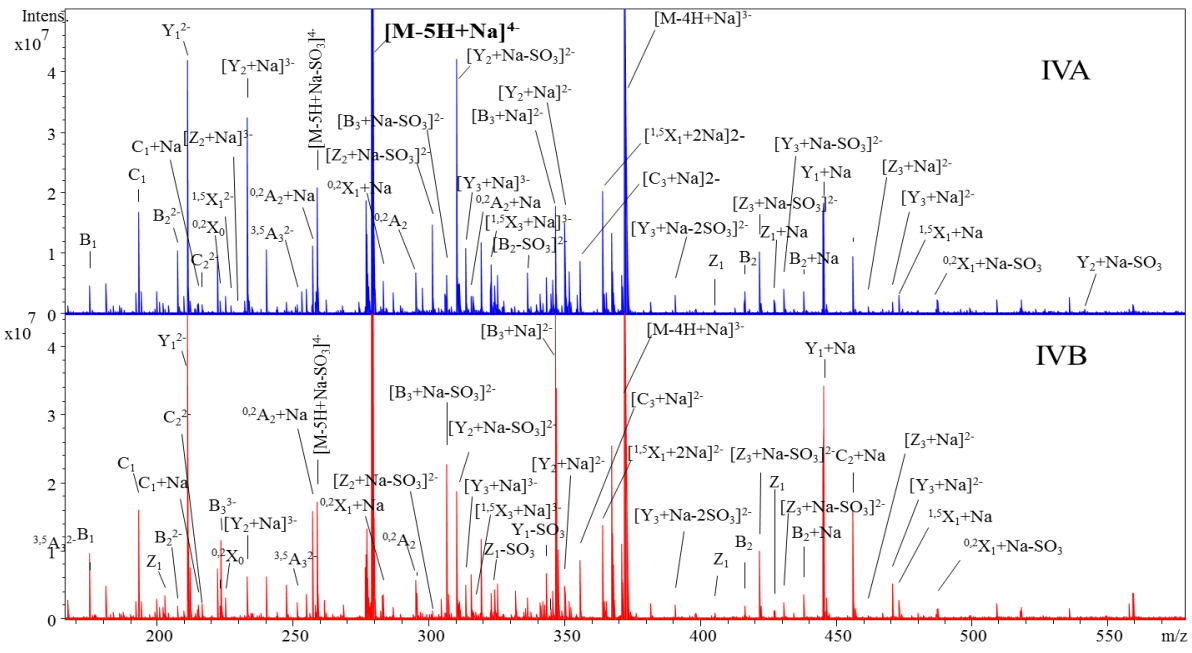

Scheme 7. EDD mass spectra of the $[M-5H+Na]^{4-}$ precursor ion for IVA and IVB.

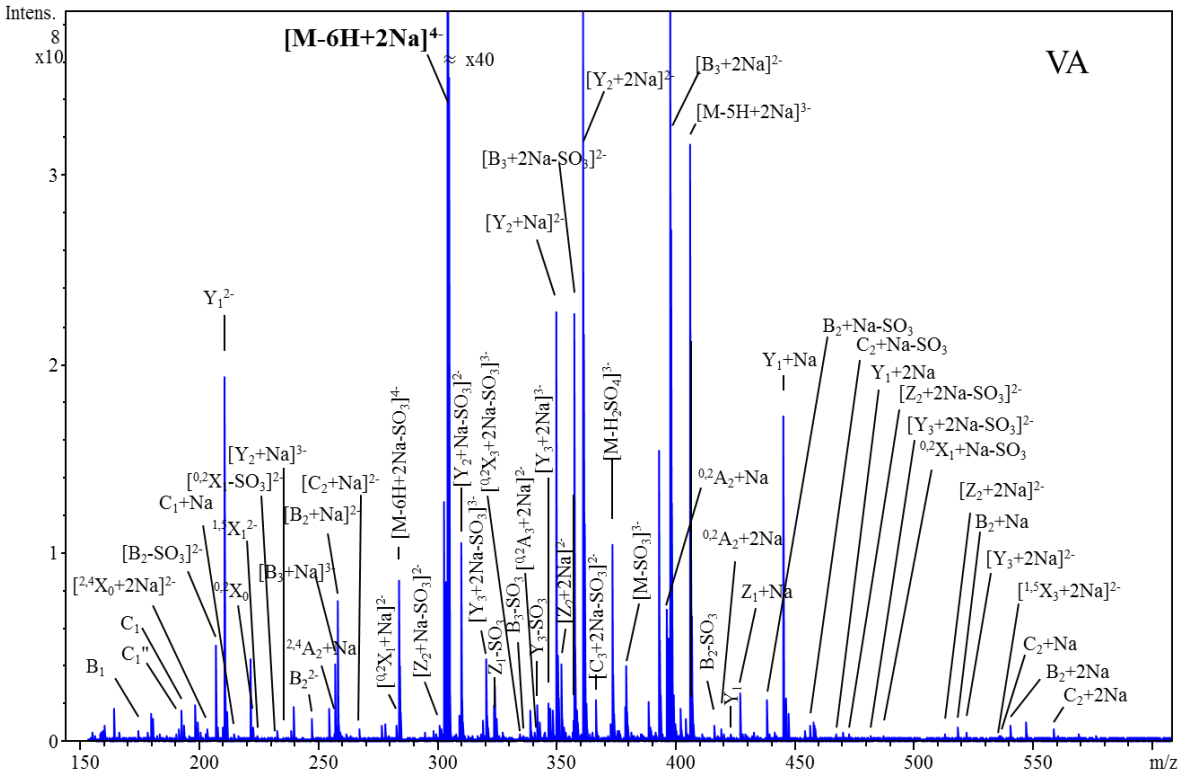

Scheme 8. Annotated EDD mass spectrum for $[M-6H+2Na]^{4-}$ precursor ion for VA.

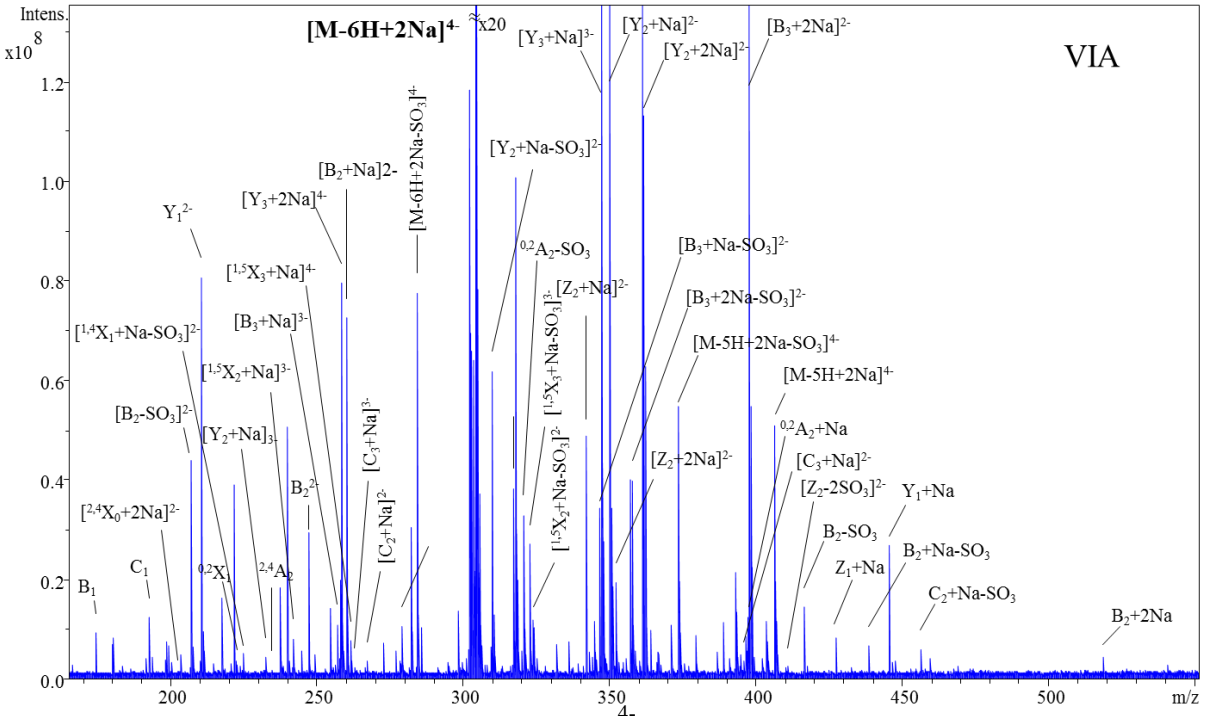

Scheme 9. EDD mass spectrum for $[M-6H+2Na]^{4-}$ precursor ion for VIA.

Supplemental Table 1. Diagnostic ratio (DR) analysis for IA: GlcA-GlcNAc-**IdoA2S**-GlcNAc-$(CH_2)_5NH_2$

Mass to charge	Relative Intensity	Ion
589.1561	0.040905	$^{1,5}X_2$
561.1611	0.030978	Y_2
∑I(IdoA2S)	0.071883	
Mass to charge		Type
543.1507	0.011894	Z_2
396.1148	0.011304	C_2
463.1937	0.007846	Z_2-SO_3
316.543	0.002741	B_3^{2-}
634.0948	0.001923	B_3
∑I(Glc2AS)	0.035708	
DR	**0.5**	

Supplemental Table 2. Diagnostic ratio (DR) analysis for IB: GlcA-GlcNAc-**GlcA2S**-GlcNAc-$(CH_2)_5NH_2$.

Mass to charge	Relative Intensity	Ion
589.1598	0.00903265	$^{1,5}X_2$
561.1643	0.00633442	Y_2
∑I(IdoA2S)	0.01536706	
Mass to charge		Type
543.1536	0.02970089	Z_2
396.1166	0.01396326	C_2
554.1399	0.00373472	B_3-SO_3
2.77E+02	0.00091155	$[B_3$-$SO_3]^{2-}$
634.0978	0.01220159	B_3
3.17E+02	0.11002256	B_3^{2-}
∑I(GlcA2S)	0.17053457	
DR	**11.1**	

Supplemental Table 3. Diagnostic ratio (DR) analysis for IIA: GlcA-GlcNAc-**IdoA2S**-GlcNAc6S-$(CH_2)_5NH_2$.

Mass to charge	Relative Intensity	Ion
334.0525	0.061648	$^{1,5}X_2^{2-}$
669.1119	0.003814	$^{1,5}X_2$
280.0768	0.004874	$[Y_2$-$SO_3]^{3-}$
320.0551	0.005808	Y_2^{2-}

561.1622	0.000842	Y_2-SO_3
641.1167	0.002051	Y_2
∑I(IdoA2S)	0.079036	
Mass to charge		Type
271.0716	0.008601	$[Z_2\text{-}SO_3]^{2-}$
311.0499	0.003614	Z_2^{2-}
463.193	0.002581	Z_2-SO_3
385.1288	0.04294	Y_1
396.1149	0.0101	C_2
276.5643	0.001021	$[B_3\text{-}SO_3]^{2-}$
316.543	0.004247	B_3^{2-}
554.1359	0.001846	B_3-SO_3
634.093	0.002992	B_3
∑I(GlcA2S)	0.077942	
DR	**1.0**	

Supplemental Table 4. Diagnostic ratio (DR) analysis for IIB: GlcA-GlcNAc-**GlcA2S**-GlcNAc6S-$(CH_2)_5NH_2$.

Mass to charge	Relative Intensity	Ion
669.1120	0.001555	$^{1,5}X_2$
334.0527	0.014178	$^{1,5}X_2^{2-}$
641.1168	0.001868	Y_2^{2-}
320.0553	0.003819	Y_2

∑I(IdoA2S)	0.021421	
Type		
543.1464	0.00198	Z_2-SO_3
271.0703	0.001099	$[Z_2\text{-}SO_3]^{2-}$
623.1026	0.00278	Z_2
311.0483	0.006607	Z_2^{2-}
385.1289	0.136354	Y_1
396.1150	0.016735	C_2
276.5647	0.002035	$[B_3\text{-}SO_3]^{2-}$
634.0895	0.001836	B
316.5431	0.104079	B_3^{2-}
∑I(GlcA2S)	0.273505	
DR	**12.8**	

Supplemental Table 5. Diagnostic ratio (DR) analysis for IIIA: GlcA-GlcNS-**IdoA2S**-GlcNS-$(CH_2)_5NH_2$.

Mass to charge	Relative Intensity	Ion
649.0847	0.0171838	$^{1,5}X_2$+Na
259.0714	0.0015996	$[Y_2\text{-}SO_3]^{2-}$
299.05	0.0134743	Y_2^{2-}
310.041	0.0452264	$[Y_2+Na]^{2-}$

541.1328	0.0059167	Y_2+Na-SO_3
621.0897	0.0026221	Y_2+Na
∑I(IdoA2S)	0.0860228	
Mass to charge		Type
250.0661	0.0009182	$[Z_2\text{-}SO_3]^{2-}$
301.0356	0.0182524	Z_2^{2-}
523.1225	0.0093005	Z_2+Na-SO_3
603.0795	0.0023441	Z_2+Na
343.1183	0.043336	Y_1
365.1005	0.0030053	Y_1+Na
456.0436	0.0139317	C_2+Na
346.5072	0.0286709	$[B_3+Na]^{2-}$
614.065	0.001692	B_3+Na-SO_3
∑I(GlcA2S)	0.1214511	
DR	**1.4**	

Supplemental Table 6. Diagnostic ratio (DR) analysis for IIIA: GlcA-GlcNS-**GlcA2S**-GlcNS-$(CH_2)_5NH_2$

Mass to charge	Relative Intensity	Ion

649.0844	0.006986	$^{1,5}X_2$+Na
310.0409	0.005948	$[Y_2+Na]^{2-}$
621.0908	0.001434	Y_2+Na
∑I(IdoA2S)	0.014367	
Mass to charge	Relative Intensity	Type
301.0353	0.000592	Z_2^{2-}
603.0787	0.009677	Z_2+Na
343.1181	0.094812	Y_1
227.5179	0.000601	$[C_2+Na]^{2-}$
456.0434	0.022569	C_2+Na
346.507	0.154192	$[B_3+Na]^{2-}$
306.5286	0.020485	$[B_3+Na\text{-}SO_3]^{2-}$
614.0651	0.004425	B_3+Na-SO_3
∑I(GlcA2S)	0.307353	
DR	**21.4**	

Supplemental Table 7. Diagnostic ratio (DR) analysis for IVA: GlcA-GlcNS-**IdoA2S**-GlcNS6S-$(CH_2)_5NH_2$

Mass to charge	Relative Intensity	Ion
324.0382	0.00374	[1,5X2+Na-SO3]2-
364.0166	0.013995	[1,5X2+Na]2-

729.0412	0.000481	1,5X2+Na
233.0102	2.39E-02	[Y2+Na]3-
310.0406	2.97E-02	[Y2+Na-SO3]2-
350.0192	0.011716	[Y2+Na]2-
∑I(IdoA2S)	8.35E-02	
227.0066	1.12E-03	[Z2+Na]3-
290.0446	3.99E-04	[Z2-SO3]3-
301.0354	1.09E-02	[Z2-SO3+Na]2-
341.0136	2.52E-03	[Z2+Na]2-
523.1209	5.00E-04	[Z2+Na-SO3]2-
211.0336	3.22E-02	Y12-
222.0245	1.95E-03	[Y1+Na]2-
343.1181	4.74E-03	Y1-SO3
365.0998	0.002765	Y1+Na-SO3
445.0573	1.29E-02	Y1+Na
216.5266	1.28E-03	C22-
354.1051	0.000436	C2-SO3
434.0621	9.07E-04	C2
456.0429	7.11E-03	C2+Na
223.3414	3.97E-04	B33-
295.5374	0.001009	[B3-SO3]2-

306.5285	0.004804	[B3+Na-SO3]2-
346.507	0.012674	[B3+Na]2-
∑I(GlcA2S)	0.098641	
DR	**1.2**	

Supplemental Table 8. Diagnostic ratio (DR) analysis for IVB: GlcA-GlcNS-**GlcA2S**-GlcNS6S-$(CH_2)_5NH_2$

Mass to charge	RI	Ion
364.0165	0.008533	$[^{1,5}X_2+Na]^{2-}$
324.0382	0.00273	$[^{1,5}X_2+Na\text{-}SO_3]^{2-}$
350.0189	0.003064	$[Y_2+Na]^{2-}$
233.0101	0.003932	$[Y_2+Na]^{3-}$
310.0406	0.011529	$[Y_2+Na\text{-}SO_3]^{2-}$
∑I(IdoA2S)	0.029788	
Mass to charge		Type
341.0135	0.001545	$[Z_2+Na]^{2-}$
301.0358	0.000822	$[Z_2+Na\text{-}SO_3]^{2-}$
211.0335	0.078156	Y_1^{2-}
222.0245	0.000895	$[Y_1+Na]^{2-}$
445.0572	0.02103	Y_1+Na
343.118	0.00421	$Y_1\text{-}SO_3$
365.0997	0.001644	$Y_1+Na\text{-}SO_3$

216.5268	0.001159	C_2^{2-}
227.5177	0.000337	C_2+Na
434.0617	0.000643	C_2
456.0426	0.009851	C_2+Na
354.1043	0.000542	C_2-SO_3
346.5067	0.122002	$[B_3+Na]^{2-}$
223.3413	0.007206	B_3^{3-}
295.5374	0.002385	$[B_3-SO_3]^{2-}$
306.5284	0.01418	$[B_3+Na-SO_3]^{2-}$
∑I(GlcA2S)	0.266607	
DR	**8.9**	

Supplemental Table 9. Diagnostic ratio (DR) analysis for: GlcA-GlcNS6S-**IdoA2S**-GlcNS6S-$(CH_2)_5NH_2$

Mass to charge	Relative Intensity	Ion
364.0173	0.000455	$[^{1,5}X_2+Na]^{2-}$
310.0411	0.011688	$[Y_2+Na-SO_3]^{2-}$
233.0106	0.000628	$[Y_2+Na]^{3-}$
350.0195	0.025286	$[Y_2+Na]^{2-}$
361.0106	0.11471	$[Y_2+2Na]^{2-}$
∑I(IdoA2S)	0.152767	

Mass to charge		Type
301.0357	0.000888	$[Z_2+Na-SO_3]^{2-}$
341.014	0.000529	$[Z_2+Na]^{2-}$
352.0052	0.004597	$[Z_2+2Na]^{2-}$
365.0999	0.000456	$Y_1+Na-SO_3$
445.0573	0.019189	Y_1+Na
467.039	0.000381	Y_1+2Na
423.0747	0.000427	Y_1
211.0339	0.02148	Y_1^{2-}
456.0438	0.000878	$C_2+Na-SO_3$
536.0004	0.000264	C_2+Na
557.9831	0.00073	C_2+2Na
306.5289	0.000243	$[B_3+Na-2SO_3]^{2-}$
346.5073	0.002283	$[B_3+Na-SO_3]^{2-}$
357.4983	0.02524	$[B_3+2Na-SO_3]^{2-}$
257.3214	0.004605	$[B_3+Na]^{3-}$
386.4852	0.000329	$[B_3+Na]^{2-}$
397.4768	0.135746	[B_3+2Na]2-
$\sum I(GlcA2S)$	0.218264	
DR	**1.4**	

Supplemental Table 10. Diagnostic ratio (DR) analysis for VIA: IdoA-GlcNS6S-**IdoA2S**-GlcNS6S-$(CH_2)_5NH_2$

Mass to charge	Relative Intensity	Type
364.0174	0.001564	$[^{1,5}X_2+Na]^{2-}$
242.3419	0.00052	$[^{1,5}X_2+Na]^{3-}$
324.0382	0.000718	$[^{1,5}X_2+Na\text{-}SO_3]^{2-}$
361.0105	0.088657	$[Y_2+2Na]2-$
350.0193	0.021106	$[Y_2+Na]^{2-}$
233.0102	0.000769	$[Y_2+Na]^{3-}$
310.0408	0.007454	$[Y_2+Na\text{-}SO_3]^{2-}$
$\sum I(IdoA2S)$	0.120789	
Mass to charge	RI	Type
352.0053	0.00239	$[Z_2+2Na]^{2-}$
290.0449	0.000406	$[Z_2\text{-}SO_3]^{2-}$
301.0357	0.000537	$[Z_2+Na\text{-}SO_3]^{2-}$
211.0337	0.009436	Y_1^{2-}
445.0577	0.004097	Y_1+Na
343.1182	0.000889	Y_1-SO3
267.4965	0.000452	$[C_2+Na]^{2-}$
397.4767	0.040324	$[B_3+2Na]^{2-}$
386.4858	0.001039	$[B_3+Na]^{2-}$
257.3213	0.001272	$[B_3+Na]^{3-}$
357.4977	0.005012	$[B_3+2Na\text{-}SO_3]^{2-}$
346.5071	0.003301	$[B_3+Na\text{-}SO3]^{2-}$

$\sum I(GlcA2S)$	0.069156	
DR	**0.6**	

APPENDIX D

SUPPLEMENTAL DATA FOR CHAPTER 5

*

Supplemental Figure 1. Chemical structures for mono-sulfated HS standards (1a-1f)

(a)

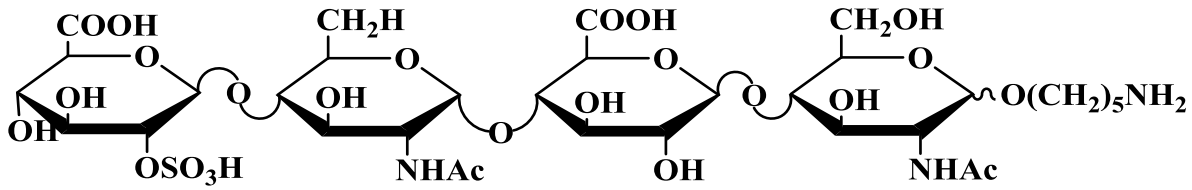

(b)

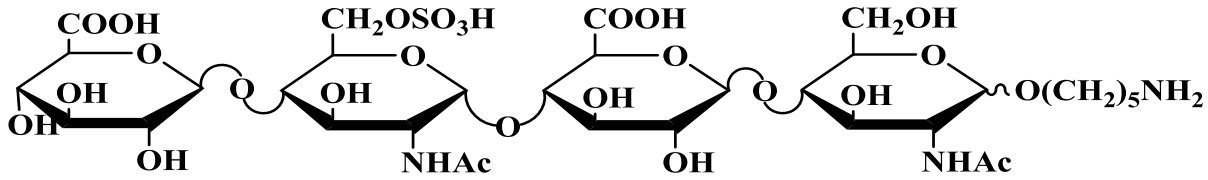

(c)

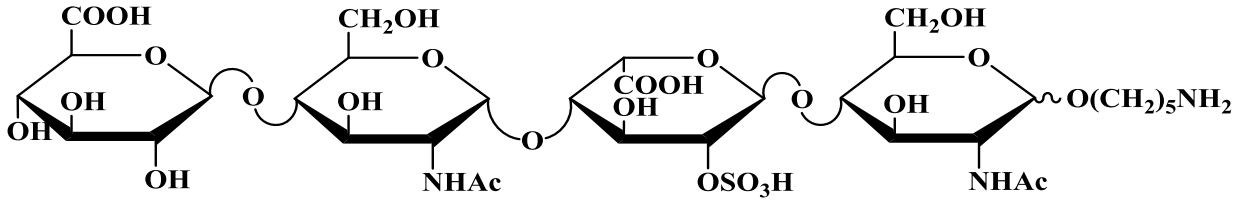

(d)

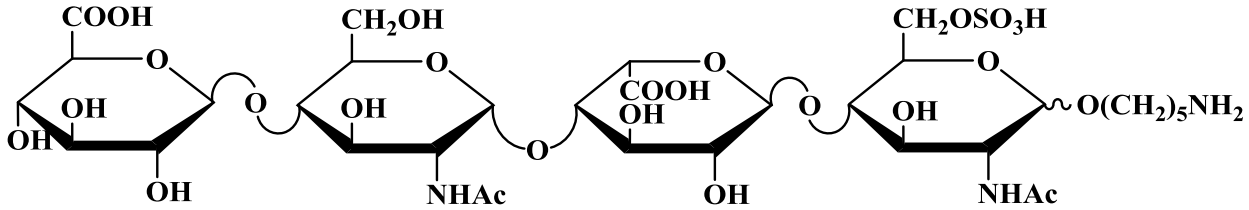

(e)

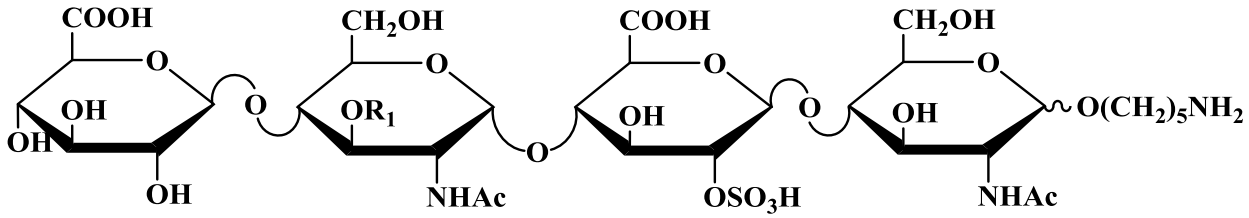

(f)

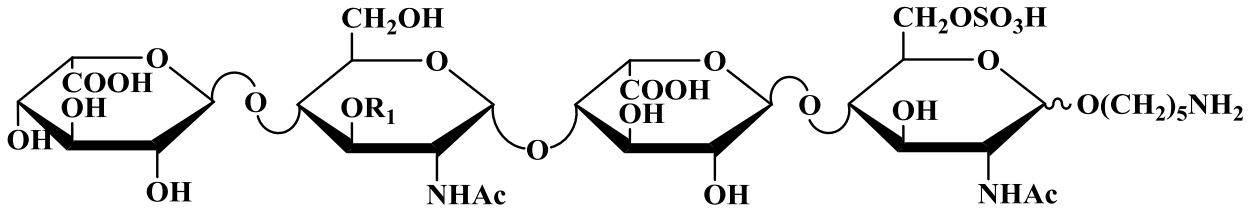

Supplemental Figure 2. Chemical structures for di-sulfated HS standards (2a-2h)

(a)

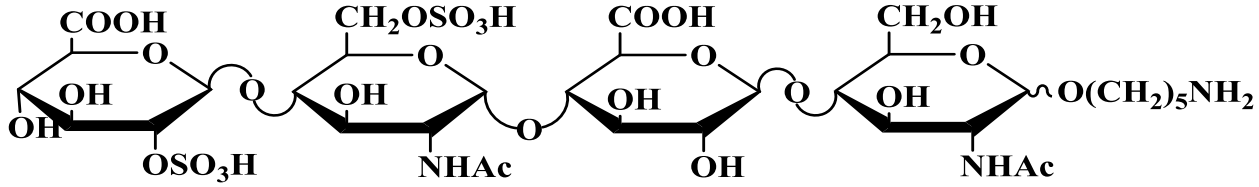

(b)

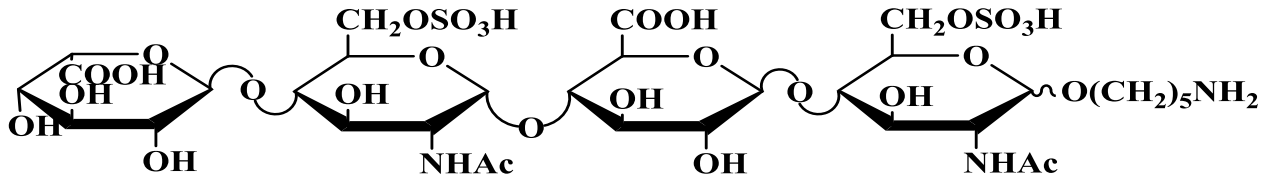

(c)

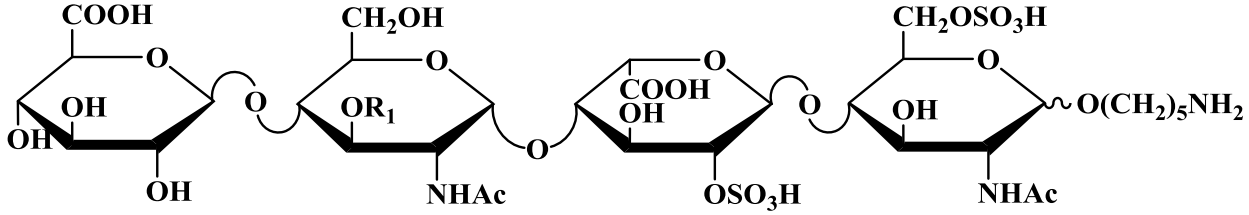

(d)

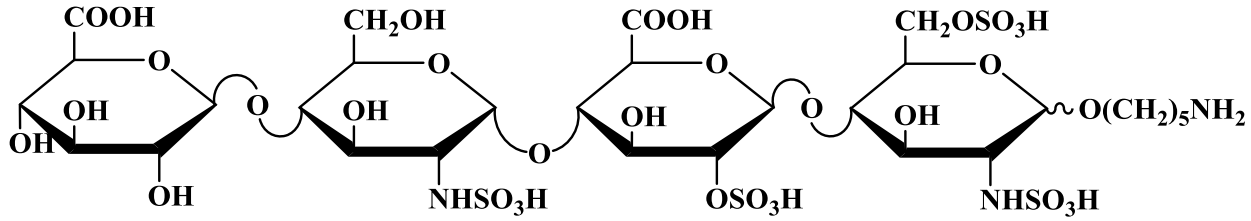
COOH
O
OH
OH
OH
O
CH2OH
O
OH
NHSO3H
O
COOH
O
OH
OSO3H
O
CH2OSO3H
O
OH
O(CH2)5NH2
NHSO3H

(e)

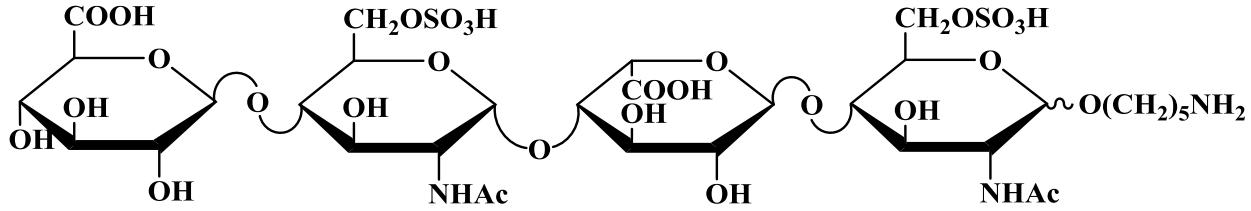
COOH
O
OH
OH
OH
O
CH2OSO3H
O
OH
NHAc
O
COOH
O
OH
OH
O
CH2OSO3H
O
OH
O(CH2)5NH2
NHAc

(f)

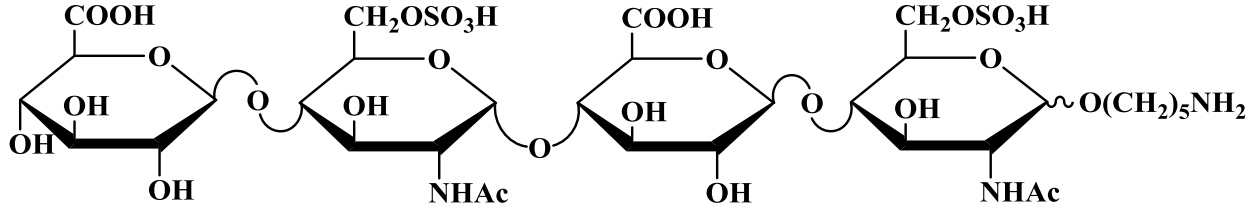
COOH
O
OH
OH
OH
O
CH2OSO3H
O
OH
NHAc
O
COOH
O
OH
OH
O
CH2OSO3H
O
OH
O(CH2)5NH2
NHAc

(g)

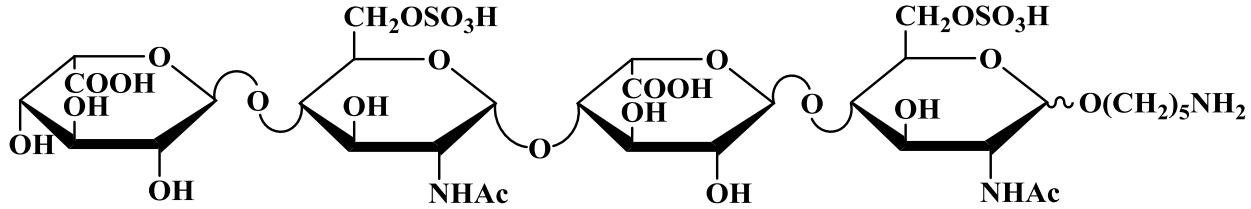
COOH
O
OH
OH
OH
O
CH2OSO3H
O
OH
NHAc
O
COOH
O
OH
OH
O
CH2OSO3H
O
OH
O(CH2)5NH2
NHAc

(h)

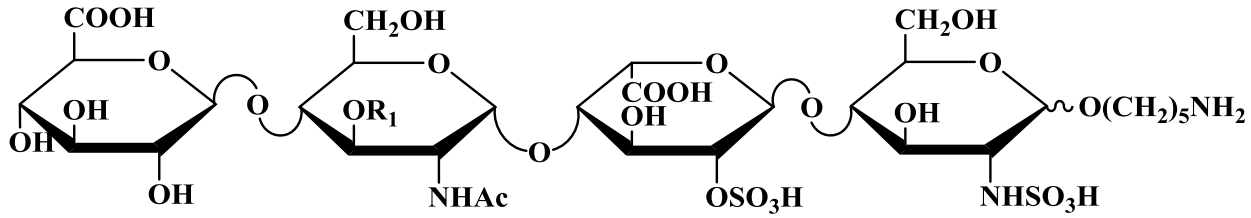
COOH
O
OH
OH
OH
O
CH2OH
O
OR1
NHAc
O
COOH
O
OH
OSO3H
O
CH2OH
O
OH
O(CH2)5NH2
NHSO3H

Supplemental Figure 3. Chemical structures for tri-sulfated HS standards (3a-3j)

(a)

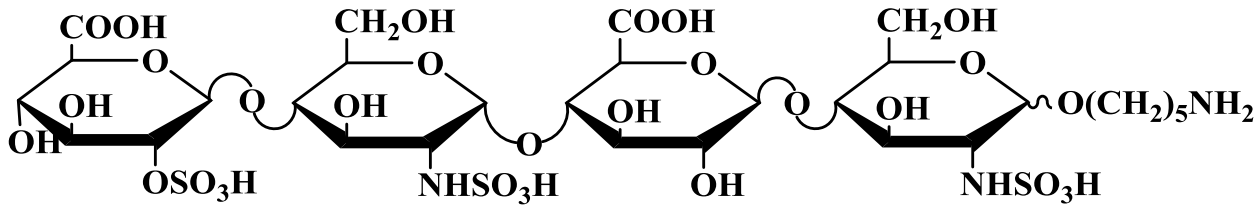

(b)

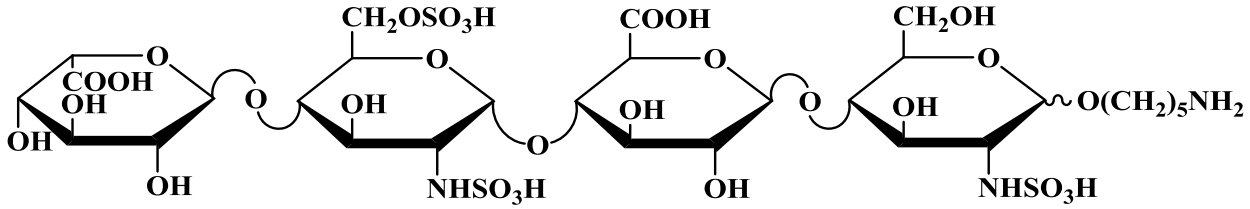

(c)

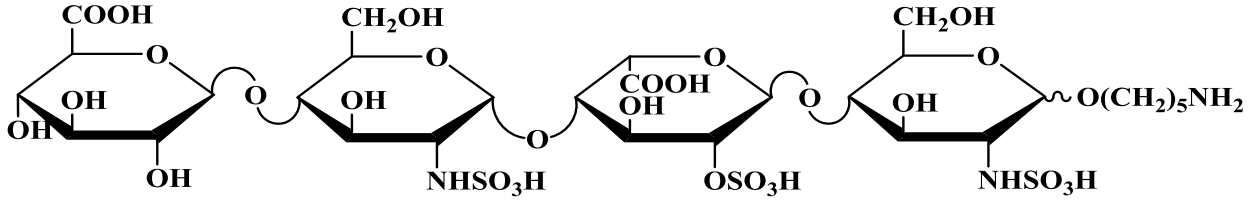

(d)

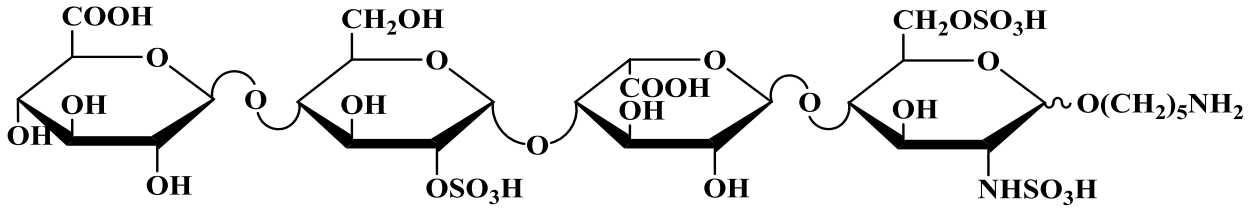

(e)

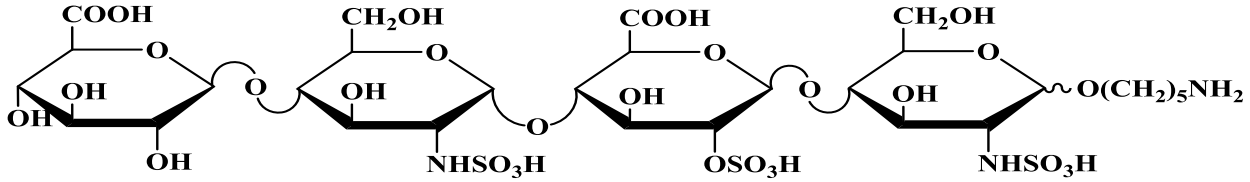

(f)

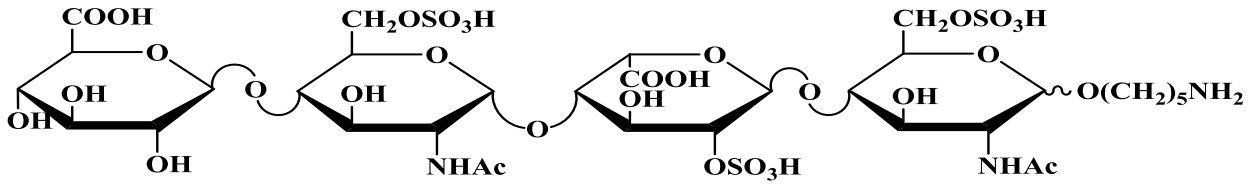

(g)

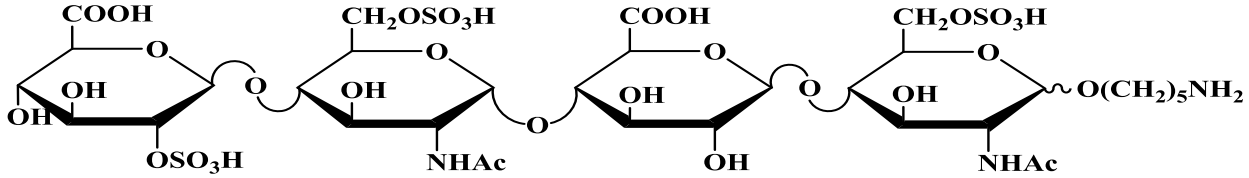

(h)

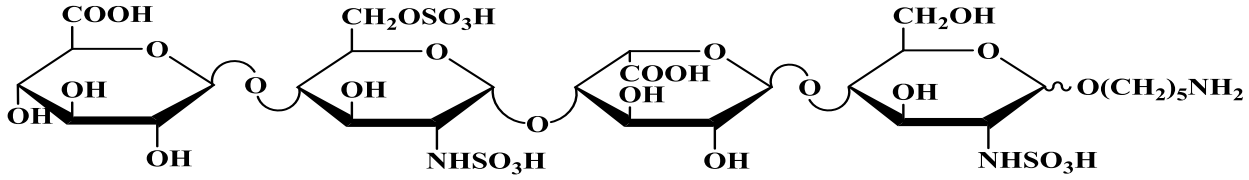

(i)

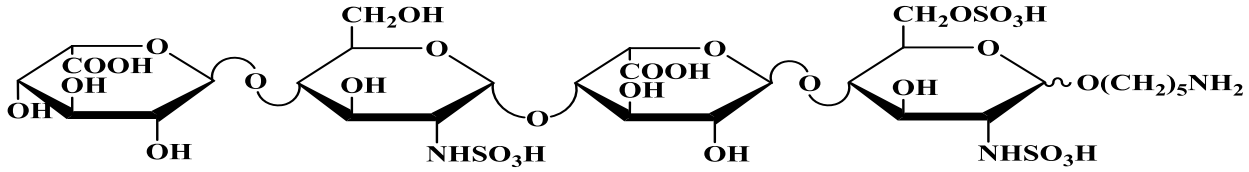

(j)

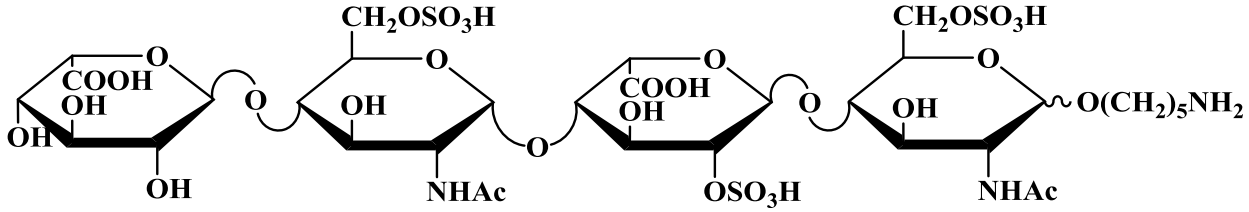

Supplemental Figure 4. Chemical structures for tetra-sulfated HS standards (4a-4i)

(a)

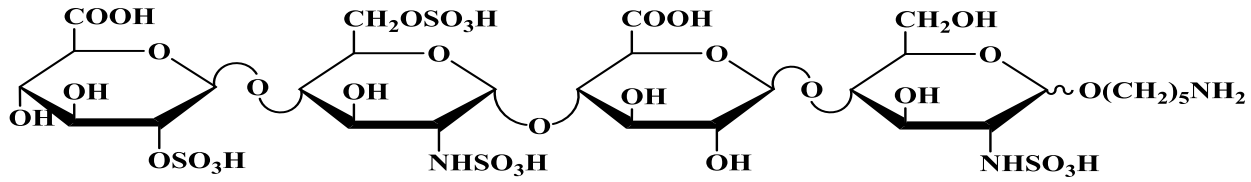

(b)

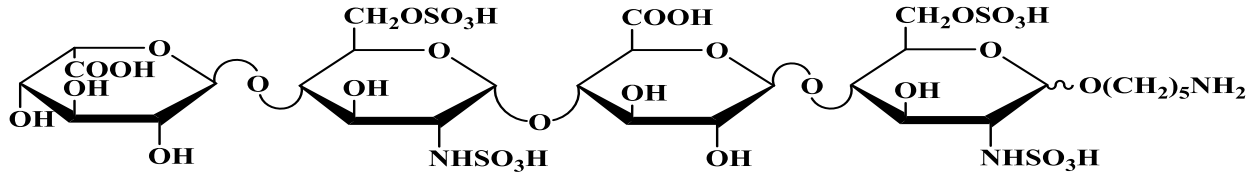

(c)

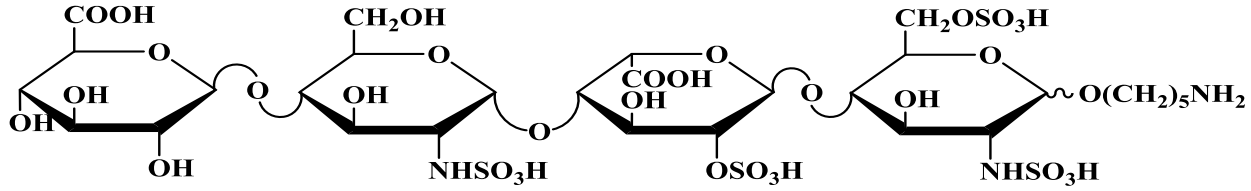

(d)

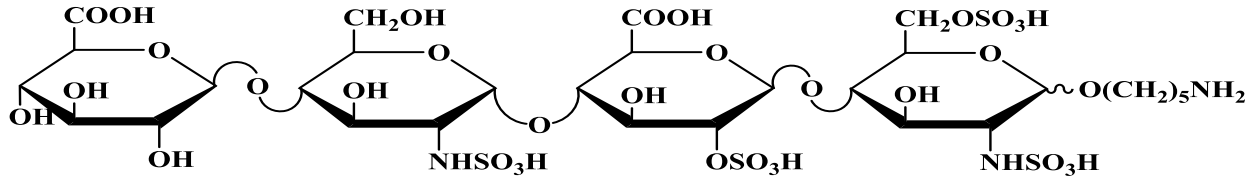

(e)

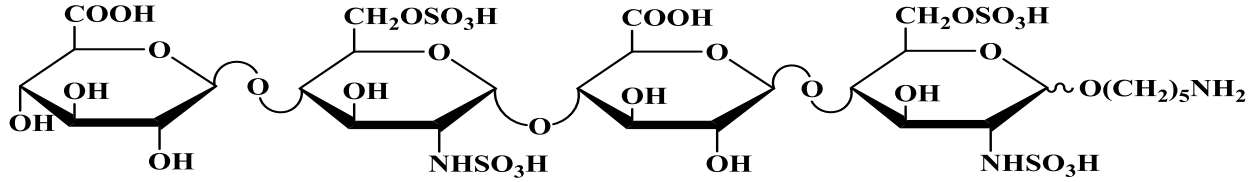

(f)

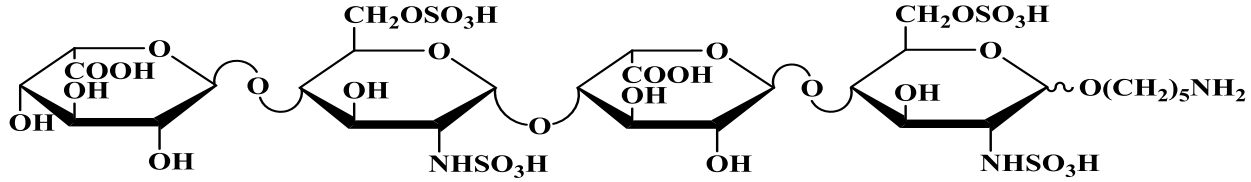

(g)

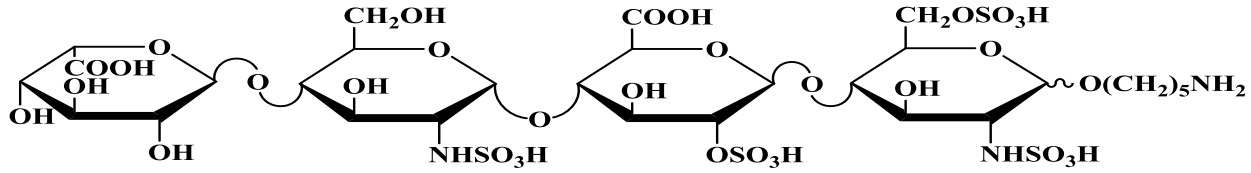

(h)

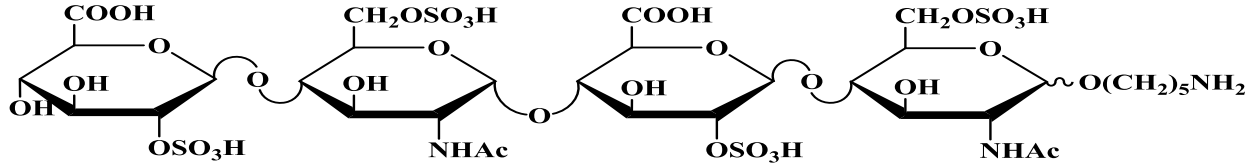

(i)

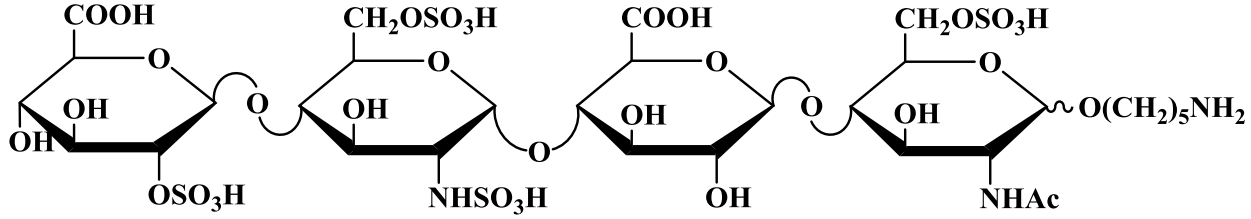

Supplemental Table 1. Diagnostic ratio results for EDD diagnostic ratio results for 1a, for $[M-2H]^{2-}$ precursor ion

Mass to charge	Ions	Intensity	Intensity	Intensity	Diagnostic Ratio
481.2038	Y_2	4953862	4459979	4736759	
∑(IdoA)		4953862	4459979	4736759	
Mass to charge		Intensity	Intensity	Intensity	
463.1935	Z_2	18180694	14825351	18820748	
305.1720	Y_1	13468601	11676351	18172296	
396.1156	C_2-SO_3	11396200	11229495	19052994	

476.0718	C_2	1.3E+08	1.15E+08	1.47E+08	
237.5322	C_2^{2-}	2389162	1972587	2548052	
634.0922	B_3	5774204	4787680	5418335	
316.5428	B_3^{2-}	18307592	17412888	18700824	
∑(GlcA)		2E+08	1.77E+08	2.3E+08	
DR		1.128642	1.120889	1.20892	1.1528 ± 0.0487

Supplemental Table 2. Diagnostic ratio results for EDD fragmentation of $[M-2H]^{2-}$ precursor ion for 1b

Mass to charge	Ion	Intensity	Intensity	Intensity	Diagnostic ratio
481.2038	Y_2	3826594	3401895	3091584	
∑(IdoA)		3826594	3401895	3091584	
Mass to charge		Intensity	Intensity	Intensity	
463.1936	Z_2	13200108	8777935	9727237	
305.1718	Y_1	6298305	4179045	4522439	
237.5322	C_2^{2-}	4228510	3653947	3707224	
396.1149	C_2-SO_3	5390822	4001383	4789525	
476.0717	C_2	1.2E+08	1.11E+08	1.15E+08	
316.5429	B_3^{2-}	21278472	15765723	16803910	
634.0922	B_3	3005581	5648101	3954922	
∑(GlcA)		1.73E+08	1.53E+08	1.58E+08	
DR		1.178828	1.175803	1.231532	1.1953 ± 0.0313

Supplemental Table 3. Diagnostic ratio results for EDD fragmentation of $[M-2H]^{2-}$ precursor ion for 1c

Mass to charge	Ion	Intensity	Intensity	Intensity	Diagnostic ratio
589.1560	$^{1,5}X_2$	75981352	70956120	71628008	
481.2059	$[Y_2\text{-}SO_3]^{2-}$	1924399	1707910	2103669	
561.161	Y_2	58341192	54835952	57124256	
∑(IdoA)		1.36E+08	1.27E+08	1.31E+08	
Mass to charge	Ion	Intensity	Intensity	Intensity	
463.1937	$Z_2\text{-}SO_3$	11434117	10020313	12431328	
543.1507	Z_2	19122436	17559604	19897310	
396.1150	C_2	20399828	19140978	19257978	
554.1363	$B_3\text{-}SO_3$	708409	629737	910967	
316.5429	B_3^{2-}	2950708	2372489	2742307	
634.0935	B_3	3599267	2858662	2873887	
∑(GlcA)		57506356	51952046	57202810	
DR		-0.8517	-0.86703	-0.83649731	-0.8518±0.0153

Supplemental Table 4. Diagnostic ratio results for EDD fragmentation of $[M-2H]^{2-}$ precursor ion for 1d

Mass to charge	Ion	Intensity	Intensity	Intensity	Diagnostic Ratio
589.1561	$^{1,5}X_2$	34064452	78604040	1.46E+08	
561.1612	Y_2	87650456	32484504	54215304	
∑(IdoA)		37891027	1.11E+08	2.00E+08	

Mass to charge	Ion	Intensity	Intensity	Intensity	
463.1941	Z_2-SO_3	14381227	11107665	5735756	
543.1508	Z_2	62147240	52074904	81305416	
385.1292	Y_1	1.14E+08	92183688	1.06E+08	
396.1153	C_2	26298524	20477350	25084380	
554.1374	B_3	23547678	18100076	16959450	
∑(GlcA)		41036558	1.94E+08	2.35E+08	
DR		-0.44249	-0.47712	-0.40834	-0.4427 ± 0.0344

Supplemental Table 5. Diagnostic ratio results for EDD fragmentation of $[M-2H]^{2-}$ precursor ion for 1e

Mass to charge	Ion	Intensity	Intensity	Intensity	Diagnostic Ratio
589.1562	$^{1,5}X_2$	18859728	19324480	18866658	
561.1613	Y_2	14170177	14151433	13597671	
∑(IdoA)		33029905	33475913	32464329	
Mass to charge	Ion	Intensity	Intensity	Intensity	
543.1505	Z_2	67996360	65750260	65171776	
396.1148	C_2	24833928	27427278	27150918	
316.5428	B_3^{2-}	1.92E+08	2.39E+08	2.3E+08	
554.1365	B_3-SO_3	7726079	8649897	8605791	

634.0939	B_3	27101668	29135022	27453156	
∑(GlcA)		3.2E+08	3.7E+08	3.58E+08	
DR		0.685066	0.566572	0.56565	0.6058±0.0687

Supplemental Table 6. Diagnostic ratio results for EDD fragmentation of $[M-2H]^{2-}$ precursor ion for 1f

Mass to charge	Ion	Intensity	Intensity	Intensity	Diagnostic Ratio
589.1562	$^{1,5}X_2$	98733624	29401934	34576320	
561.1613	Y_2	40268916	68868184	82239992	
∑(IdoA)		1.39E+08	98270118	1.17E+08	
Mass to charge	Ion	Intensity	Intensity	Intensity	
385.1292	Y_1	57366876	45159348	46729528	
543.1508	Z_2	43243596	34453864	36506452	
554.1375	B_3	30213758	57744536	23246144	
396.1153	C_2	26809426	20088266	20274656	
∑(GlcA)		1.58E+08	1.57E+08	1.27E+08	
DR		-0.4225	-0.27241	-0.44165	-0.3789 ± 0.0927

Supplemental Table 7. Diagnostic ratio results for EDD fragmentation of $[M-3H]^{3-}$ precursor ion for 2a

Mass to charge	Ion	Intensity	Intensity	Intensity	Diagnostic Ratio
481.2052	Y_2	16893164	58452360	15220988	

∑(IdoA)		16893164	58452360	15220988	
Mass to charge	Ion	Intensity	Intensity	Intensity	
305.1721	Y_1	11606355	26672774	10171876	
463.1944	Z_2	1825369	5508413	1249289	
316.5435	$[B_3\text{-}SO_3]^{2-}$	1148720	3571099	1367998	
356.5216	B_3^{2-}	25366874	82167296	20596796	
476.0723	$C_2\text{-}SO_3$	3197851	9225579	2696663	
237.5322	$[C_2\text{-}SO_3]^{2-}$	2545543	7572881	2531461	
396.1155	$C_2\text{-}2SO_3$	913770	3010048	1032572	
556.0293	C_2	1104824	2609164	1641224	
277.5107	C_2^{2-}	23649902	61248728	20326660	
∑(GlcA)		71359208	2.02E+08	61614539	
DR		0.148618	0.060537	0.130119	0.1108 ± 0.0439

Supplemental Table 8. Diagnostic ratio results for EDD fragmentation of $[M\text{-}3H]^{3-}$ precursor ion for 2b

Mass to charge	Ion	Intensity	Intensity	Intensity	Diagnostic Ion
561.1635	Y_2	3967151	3913552	3650378	

280.0771	Y_2^{2-}	51042728	43887312	43292356	
589.1582	$^{1,5}X_2$	4446280	4110748	4078222	
∑(IdoA)		59456159	51911612	51020956	
Mass to charge	Ion	Intensity	Intensity	Intensity	
305.1725	Y_1-SO_3	2139748	2060722	2130710	
385.1295	Y_1	2.78E+08	235951360	2.41E+08	
463.1962	Z_2-SO_3	1248782	974702	1037232	
543.1507	Z_2	90478400	67026844	75424456	
271.0717	Z_2^{2-}	1.16E+08	104895120	1.02E+08	
554.1387	B_3-SO_3	2720663	2926886	3183758	
634.0954	B_3	3135454	3110907	3061120	
316.5435	B_3^{2-}	3293167	3271514	3272172	
396.1157	$[C_2\text{-}SO_3]^{2-}$	45214664	35790492	37231400	
476.0730	C_2	1.99E+08	151758352	1.62E+08	
237.5323	C_2^{2-}	60920324	54750216	55949996	
∑(GlcA)		8.02E+08	662517115	6.87E+08	
		0.652732	0.6288113	0.651971	0.6445 ± 0.0125

Supplemental Table 9. Diagnostic ratio results for EDD fragmentation of $[M\text{-}3H]^{3-}$ precursor ion for 2c

Mass to charge	Ion	Intensity	Intensity	Intensity	Diagnostic Ratio
334.0527	$^{1,5}X_2^{2-}$	1.16E+08	1.57E+08	1.13E+08	

669.1123	$^{1,5}X_2$	7410978	10212210	7355478	
280.0768	$[Y_2\text{-}SO_3]^{2-}$	8902406	10410245	10296887	
320.0553	Y_2^{2-}	11122452	13116672	10015481	
481.2047	$Y_2\text{-}2SO_3$	2471130	2862044	2582460	
561.1621	$Y_2\text{-}SO_3$	1782634	2036215	1583196	
641.1179	Y_2	4986183	5308680	4320404	
∑(IdoA)		1.52E+08	2.01E+08	1.49E+08	
Mass to charge	Ion	Intensity	Intensity	Intensity	
271.0716	$[Z_2\text{-}SO_3]^{2-}$	23951520	25713974	22351576	
311.0500	Z_2^{2-}	7900344	9618064	8335596	
463.1942	$Z_2\text{-}2SO_3$	4181159	5008681	4255833	
543.1509	$Z_2\text{-}SO_3$	18499390	20356690	18105550	
385.1290	Y_1	1.19E+08	1.32E+08	1.24E+08	
396.1151	C_2	24762044	28903464	24500704	
276.5646	$B_3\text{-}SO_3$	2010021	2168577	2482320	
316.5430	B_3	9315893	9441328	9285729	
554.1361	$B_3\text{-}SO_3$	3761689	4912886	3526783	
634.0936	B_3	7279126	10323493	6943638	
∑(GlcA)		2.21E+08	2.48E+08	2.23E+08	
DR		-0.31613	-0.38591	-0.3013	-0.3345 ± 0.0452

Supplemental Table 10. Diagnostic ratio results for EDD fragmentation of $[M-3H]^{3-}$ precursor ion for 2d

Mass to charge	Ion	Intensity	Intensity	Intensity	Diagnostic Ratio
481.2047	Y_2-SO_3	3931460	1.33E+07	6034545	
561.1611	Y_2	3149911	1.04E+07	5169641	
280.0770	Y_2^{2-}	43970548	1.41E+08	81498664	
589.1563	$^{1,5}X_2$	2640543	7024767	2450717	
∑(IdoA)		62216104	1.71E+08	95153567	
Mass to charge	Ion	Intensity	Intensity	Intensity	
305.1718	Y_1-SO_3	842014	2411961	1147884	
385.1292	Y_1	43873032	1.51E+08	74058000	
463.1930	Z_2-SO_3	1492385	4535612	1868347	
543.1515	Z_2	7169626	2.56E+07	12541788	
271.0717	Z_2^{2-}	20714480	6.59E+07	41429652	
634.0943	B_3	1387186	2.95E+06	1378609	
396.1154	C_2-SO_3	2500403	7684790	4379382	
476.0723	C_2	12205525	4.02E+07	24981498	
237.5323	C_2^{2-}	5686696	1.72E+07	10809529	
∑(GlcA)		1.14E+08	3.17E+08	1.73E+08	
DR		-0.22535	-0.20959	-0.21852	-0.2178 ± 0.0079

Supplemental Table 11. Diagnostic ratio results for EDD fragmentation of $[M-3H]^{3-}$ precursor ion for 2e

Mass to charge	Ion	Intensity	Intensity	Intensity	Diagnostic ratio
334.0529	$^{1,5}X_2^{2-}$	4.77E+07	1.99E+07	3.54E+07	
589.1564	Y_2^{2-}	2563960	871951	1716219	
669.1130	$^{1,5}X_2$	5704086	1753353	5421969	
320.0555	$^{1,5}X_2$-SO_3	1.15E+07	2808579	8822770	
∑(IdoA)		6.75E+07	2.53E+07	5.14E+07	
Mass to charge	Ion	Intensity	Intensity	Intensity	
385.1293	Y_1	6.07E+08	4.19E+08	6.05E+08	
543.1518	Z_2-SO_3	5363064	2481766	4434532	
271.0717	$[Z_2$-$SO_3]^{2-}$	3097429	1578554	2390932	
623.1093	Z_2	1.22E+07	4220742	9379510	
311.0500	Z_2^{2-}	2.28E+07	9395726	1.83E+07	
396.1155	C_2	6.18E+07	3910351	5.28E+07	
276.5646	$[B_3$-$SO_3]^{2-}$	5245960	2575506	4819975	

634.0961	B_3	1865195	2510799	1690066	
554.1363	B_3-SO_3	1937628	861370	5842274	
316.5432	B_3^{2-}	3.05E+08	2.17E+08	3.00E+08	
∑(GlcA)		1031310922	697248056	1004119323	
DR		0.70709	0.96280	0.81374	0.8279 ± 0.1284

Supplemental Table 12. Diagnostic ratio results for EDD fragmentation of $[M-3H]^{3-}$ precursor ion for 2f

Mass to charge	Type	Intensity	Intensity	Intensity	Diagnostic Ratio
589.1576	$^{1,5}X_2$	3283151	3471716	3139461	
280.0768	Y_2^{2-}	24513988	26311380	13704574	
561.1615	Y_2	3655253	3452701	2865757	
∑(IdoA)		31452392	33235797	19709792	
Mass to charge	Type	Intensity	Intensity	Intensity	
271.0715	Z_2^{2-}	50710320	49473280	26766388	
543.1517	Z_2	40955940	39687268	43432528	
305.1715	Y_1-SO_3	865512	1192119	472132	

385.1291	Y_1	1.37E+08	1.41E+08	1.1E+08	
237.5321	C_2^{2-}	48455576	48173372	28511514	
396.1154	C_2-SO_3	9653681	9161724	7758384	
476.0726	C_2	63364480	59542688	58801396	
316.5431	B_3^{2-}	4455608	3469007	1639828	
∑(GlcA)		3.55E+08	3.52E+08	2.77E+08	
		0.576017	0.547444	0.671275	0.5982 ± 0.0645

Supplemental Table 13. Diagnostic ratio results for EDD fragmentation of $[M-3H]^{3-}$ precursor ion for 2g

Mass to charge	Ion	Intensity	Intensity	Intensity	Diagnostic Ratio
589.1563	$^{1,5}X_2$	2075773	3507379	1895389	
481.2043	Y_2-SO_3	6358870	12822163	9123369	
561.1602	Y_2	3744493	7547170	5592472	
280.0762	Y_2^{2-}	91306624	1.47E+08	1.27E+08	
∑(IdoA)		1.03E+08	1.71E+08	1.43E+08	
Mass to charge	Ion	Intensity	Intensity	Intensity	
271.071	Z_2^{2-}	61350300	1.09E+08	85146968	
463.1941	Z_2-SO_3	1632908	3687011	2235616	
543.1515	Z_2	12316772	23856412	15371581	
305.1725	Y_1-SO_3	1381245	2741962	1997523	

385.1292	Y_1	1.09E+08	2E+08	1.42E+08	
237.5316	C_2^{2-}	8543020	14346398	10897323	
396.1157	$[C_2\text{-}SO_3]^{2-}$	10027016	18453904	12379704	
476.0721	C_2	35974820	59953336	41777488	
554.1404	$B_3\text{-}SO_3$	819291	2241754	877586	
634.0931	B_3	752178	2191905	1391712	
∑(GlcA)		2.42E+08	4.37E+08	3.14E+08	
DR		-0.10865	-0.07018	-0.13645	-0.1051 ± 0.0333

Supplemental Table 14. Diagnostic ratio results for EDD fragmentation of $[M\text{-}3H]^{3-}$ precursor ion for 2h

Mass to charge	Ion	Intensity	Intensity	Intensity	Diagnostic Ratio
547.1470	$[^{1,5}X_2\text{-}SO_3]$	2008460	2413573	2456307	
627.1025	$^{1,5}X_2$	3201852	4782503	3862109	
313.0474	$^{1,5}X_2^{2-}$	2.32E+08	2.49E+08	2.36E+08	
519.1504	$Y_2\text{-}SO_3$	3593079	3008591	2589491	
439.1938	$Y_2\text{-}2SO_3$	6037843	4509797	4356351	
599.1073	Y_2	3750195	5696699	4746990	
299.0500	Y_2^{2-}	16019182	14858093	14877801	
∑(IdoA)		2.67E+08	2.84E+08	2.69E+08	
Mass to charge	Ion	Intensity	Intensity	Intensity	
501.1404	$Z_2\text{-}SO_3$	41422232	28799298	33621756	

250.0662	$[Z_2\text{-}SO_3]^{2-}$	9631083	6243205	7782201	
421.1832	$Z_2\text{-}2SO_3$	12292547	7636148	9425286	
263.1613	$Y_1\text{-}SO_3$	2255707	1426679	1613432	
343.1184	Y_1	1.96E+08	1.41E+08	1.61E+08	
396.1151	C_2	34861296	31166476	32000104	
554.1355	$B_3\text{-}SO_3$	1370768	1976731	1361046	
276.5646	$[B_3\text{-}SO_3]^{2-}$	5203213	4073069	4941307	
634.0932	B_3	2354586	3440797	2724808	
316.5431	B_3^{2-}	17792328	13739761	14695594	
∑(GlcA)		3.23E+08	2.4E+08	2.69E+08	
DR		-0.39428	-0.5505	-0.47722	-0.4840 ± 0.0782

Supplemental Table 15. Diagnostic ratio results for EDD fragmentation of $[M\text{-}4H+Na]^{3-}$ precursor ion for 3a

Mass to charge	Ion	Intensity	Intensity	Intensity	Diagnostic Ratio
439.1936	$Y_2\text{-}SO_3$	11994233	27614940	30475332	
541.1327	Y_2+Na	11823909	26886140	29990208	
519.1506	Y_2	19095812	44423932	45720728	
259.0714	Y_2^{2-}	16110788	30352780	35083044	
∑(IdoA)		59024742	1.29E+08	1.41E+08	
Mass to charge	Ion	Intensity	Intensity	Intensity	
365.1003	Y_1+Na	3703404	7579423	9153549	

343.1182	Y_1	94945120	1.84E+08	2.1E+08	
523.1222	Z_2+Na	2516275	6431381	6648484	
501.1401	Z_2	18039988	55170172	43524156	
456.0434	C_2+Na-SO_3	17605438	39149364	44723496	
536.0004	C_2+Na	17630782	46317308	44400076	
267.4962	$[C_2+Na]^{2-}$	7272381	15408505	16894044	
306.5286	$[B_3+Na-SO_3]^{2-}$	6669263	13118642	17605078	
346.5069	$[B_3+Na]^{2-}$	34608984	65420492	62058600	
∑(GlcA)		2.03E+08	4.32E+08	4.55E+08	
DR		0.059323	0.046975	0.030667	0.0457 ± 0.0144

Supplemental Table 16. Diagnostic ratio results for EDD fragmentation of $[M-4H+Na]^{3-}$ precursor ion for 3b

Mass to charge	Ion	Intensity	Intensity	Intensity	Diagnostic Ratio
439.1937	Y_2-SO_3	8180905	7237816	10062591	
541.1321	Y_2+Na	9806904	8957386	12319876	
519.1501	Y_2	5898365	5261595	7427824	
259.0719	Y_2^{2-}	15554930	14821769	18842114	
547.1451	$^{1,5}X_2$	4963987	4563442	6827706	
∑(IdoA)		44405091	40842008	55480111	
Mass to charge	Ion	Intensity	Intensity	Intensity	

365.1004	Y_1+Na	5492316	4830407	6898582	
343.1188	Y_1	1.56E+08	1.41E+08	1.8E+08	
523.1229	Z_2+Na	2204812	1987405	2722462	
501.1414	Z_2	31038696	28077654	38164720	
456.0435	C_2+Na-SO_3	31748904	27882164	38848740	
536.9998	C_2+Na	17626022	16808904	21980836	
267.4967	$[C_2+Na]^{2-}$	36567724	34020928	46415680	
306.5292	$[B_3+Na-SO_3]^{2-}$	14180960	13143426	17458340	
346.5075	$[B_3+Na]^{2-}$	1.05E+08	97056528	1.3E+08	
∑(GlcA)		4E+08	3.64E+08	4.82E+08	
DR		0.477259	0.473372	0.461648	0.4708 ± 0.0081

Supplemental Table 17. Diagnostic ratio results for EDD fragmentation of $[M-4H+Na]^{3-}$ precursor ion for 3c

Mass to charge	Ion	Intensity	Intensity	Intensity	Diagnostic ratio
541.1315	Y_2+Na	9856662	9292695	8543154	
259.0717	$[Y_2\text{-}SO_3]^{2-}$	4098259	3821591	3395278	
621.0876	Y_2+Na^{2-}	9785342	7316703	6403490	
310.0411	$[Y_2+Na]^{2-}$	1.15E+08	1.06E+08	95778104	
299.0501	Y_2^{2-}	42128068	34521588	31013434	
649.0844	$^{1,5}X_2$+Na	53614400	45848120	40419540	
∑(IdoA)		2.35E+08	2.07E+08	1.86E+08	
Mass to charge	Ion	Intensity	Intensity	Intensity	
365.1003	Y_1+Na	5693326	6032984	5595992	
343.1185	Y_1	1.09E+08	1.06E+08	89990552	
523.1212	Z_2+Na-SO_3	11797982	14052412	11844299	
501.1395	$Z_2\text{-}SO_3$	1448346	1844284	1843273	
250.0663	$[Z_2\text{-}SO_3]^{2-}$	1581749	1587757	1725699	
603.0803	Z_2+Na	4832664	4176272	3555205	
301.0358	$[Z_2+Na]^{2-}$	20992844	26043782	24685154	
290.0449	Z_2^{2-}	1675820	26713810	23941784	
346.5072	$[B_3+Na]^{2-}$	88291504	84764336	78459888	

614.0629	B_3+Na-SO_3	5449349	4062907	3657268	
306.5289	[B_3+Na-SO_3]$^{2-}$	16010440	15008053	14069679	
∑(GlcA)		2.67E+08	2.9E+08	2.59E+08	
DR		-0.42117	-0.33042	-0.33167	-0.3611 ± 0.0520

Supplemental Table 18. Diagnostic ratio results for EDD fragmentation of [M-4H+Na]$^{3-}$ precursor ion for 3d

Mass to charge	Ion	Intensity	Intensity	Intensity	Diagnostic ratio
541.1348	Y_2+Na-SO_3	6492467	6577430	6028420	
621.0919	Y_2+Na	3213812	2795273	2816983	
310.0413	[Y_2+Na]$^{2-}$	1.83E+08	170611088	1.62E+08	
299.0502	Y_2^{2-}	25007294	23466500	21454286	
569.1273	$^{1,5}X_2$+Na	2194368	1936356	1816670	
649.0841	$^{1,5}X_2$+Na-SO_3	30688646	28348736	29049820	
∑(IdoA)		2.5E+08	233735383	2.23E+08	
Mass to charge	Ion	Intensity	Intensity	Intensity	
365.1005	Y_1+Na-SO_3	12425520	11288990	9265747	
343.1185	Y_1-SO_3	28828430	26804242	22563066	
445.0576	Y_1+Na	41551360	36544236	33541886	

423.0756	Y_1	2453659	2616985	2332267	
211.0340	Y_1^{2-}	95075128	91683088	89541768	
523.1226	Z_2+Na-SO_3	9314176	8805996	7415197	
501.1403	Z_2-SO_3	4647046	3262143	3513124	
250.0663	$[Z_2\text{-}SO_3]^{2-}$	2656023	2527108	2377356	
603.0784	Z_2+Na	22089904	17999020	18959288	
581.0973	Z_2	5613088	4784932	5119645	
301.0359	$[Z_2+Na]^{2-}$	41036320	38856416	38403680	
290.0448	Z_2^{2-}	2187501	1909187	1823365	
354.1050	C_2-SO_3	2485080	2539524	1899643	
456.0437	C_2+Na	15335923	14617575	13318221	
434.0616	C_2	4699490	3794942	3454300	
534.1087	B_3+Na-SO_3	2224983	2013771	1918878	
614.0654	B_3+Na	22431358	21944404	21886074	
306.5289	$[B_3+Na]^{2-}$	5594591	5760800	4490868	
295.5380	B_3^{2-}	4987682	5107061	4093459	
∑(GlcA)		3.26E+08	302860420	2.86E+08	
DR		-0.36307	-0.364603	-0.36902	-0.3656 ± 0.0031

Supplemental Table 19. Diagnostic ratio results for EDD fragmentation of $[M-4H+Na]^{3-}$ precursor ion for 3e

Mass to charge	Ion	Intensity	Intensity	Intensity	Diagnostic ratio
621.0896	Y_2+Na	1888469	1903033	4678952	
310.0409	$[Y_2+Na]^{2-}$	8223750	11488580	15229283	
299.0501	Y_2^{2-}	1235625	2595031	2224641	
649.0840	$^{1,5}X_2$+Na	6203734	7078469	16308934	
∑(IdoA)		17551578	23065113	38441810	
Mass to charge	Ion	Intensity	Intensity	Intensity	
365.1004	Y_1+Na	1078246	1049903	1433730	
343.1183	Y_1	2.36E+08	2.14E+08	3.94E+08	
501.1401	Z_2-SO_3	642118	661845	752949	
603.0791	Z_2+Na	10416531	10120866	27448318	
581.0987	Z_2	944719	852592	1794242	
456.0441	C_2+Na	31035276	29161124	68107160	
227.5175	$[C_2+Na]^{2-}$	749811	701668	1405314	
614.0659	B_3+Na	3698658	3583628	9884447	
306.5288	$[B_3+Na-SO_3]^{2-}$	28241800	25599212	58021244	
534.1082	B_3+Na-$2SO_3$	397086	676727	1367747	

223.3416	B_3^{3-}	613532	585571	1112285	
346.5071	$[B_3+Na]^{2-}$	4.71E+08	4.38E+08	8.5E+08	
∑(GlcA)		7.85E+08	7.25E+08	1.42E+09	
DR		1.173168	1.020694	1.088954	1.0943 ± 0.0764

Supplemental Table 20. Diagnostic ratio results for EDD fragmentation of $[M-4H+Na]^{3-}$ precursor ion for 3f

Mass to charge	Ion	Intensity	Intensity	Intensity	Diagnostic ratio
691.0945	$^{1,5}X_2+Na$	17507536	15518637	13684399	
583.1431	$Y_2+Na-SO_3$	5372735	5816366	4576154	
663.0997	Y_2+Na	8191180	8211126	6763587	
331.0463	$[Y_2+Na]^{2-}$	90258704	1.12E+08	67247632	
280.0768	Y_2-SO_3	1650504	2006527	1656595	
∑(IdoA)		1.23E+08	1.44E+08	92271772	
Mass to charge	Ion	Intensity	Intensity	Intensity	
565.1329	$Z_2+Na-SO_3$	5934525	5715214	5104254	
543.1526	Z_2-SO_3	3392279	3171412	2984783	
271.0715	$[Z_2-SO_3]^{2-}$	8284767	9546820	6088478	
645.0895	Z_2+Na	13109040	12883620	9870525	

322.0410	$[Z_2+Na]^{2-}$	63966488	73397800	46956024	
311.0499	Z_2^{2-}	2609051	2962832	2098137	
407.1110	Y_1+Na	10811056	10601184	8374953	
385.1289	Y_1	73658992	76793968	56991588	
396.1155	C_1-SO_3	3066497	2909268	2104130	
498.0541	C_2+Na	9651722	9033176	7923431	
476.0718	C_2	9920760	9954576	8303512	
237.5323	C_2^{2-}	3216180	1711809	2461464	
327.5340	$[B_3+Na-SO_3]^{2-}$	6217475	7172050	4310007	
367.5125	$[B_3+Na]^{2-}$	36896064	44746456	28587928	
∑(GlcA)		2.51E+08	2.71E+08	1.92E+08	
DR		-0.16774	-0.20211	-0.15853	-0.1761 ± 0.0230

Supplemental Table 21. Diagnostic ratio results for EDD fragmentation of $[M-4H+Na]^{3-}$ precursor ion for 3g

Mass to charge	Ion	Intensity	Intensity	Intensity	Diagnostic ratio
280.0769	Y_2^{2-}	1834082	2455325	1719038	
583.1434	Y_2+Na	1454227	3248872	2089277	
∑(IdoA)		3288309	5704197	3808315	
Mass to charge	Ion	Intensity	Intensity	Intensity	

407.1112	Y_1+Na	1794712	2953360	2199471	
385.1290	Y_1	34097160	47655608	33663008	
565.1307	Z_2+Na	677272	1269839	1024815	
543.1508	Z_2	7245054	10586461	8466306	
271.0717	Z_2^{2-}	5154713	6714853	5341643	
367.5116	$[B_3+Na]^{2-}$	2055413	2702973	2467188	
498.0539	C_2+Na-SO_3	8436823	11647904	7536828	
578.0105	C_2+Na	5110883	6883860	5442739	
288.5017	$[C_2+Na]^{2-}$	7896249	9851609	9140125	
∑(GlcA)		72468279	1E+08	75282123	
DR		0.866054	0.76784	0.818838	0.8176 ± 0.0491

Supplemental Table 22. Diagnostic ratio results for EDD fragmentation of $[M-4H+Na]^{3-}$ precursor ion for 3h

Mass to charge	Ion	Intensity	Intensity	Intensity	Diagnostic ratio
439.1940	Y_2-SO_3	73672480	65028000	7.36E+07	
541.1328	Y_2+Na	32130974	30079736	3.31E+07	
519.1509	Y_2	22361638	22168882	2.36E+07	
259.0716	Y_2^{2-}	1.53E+08	1.32E+08	1.49E+08	
547.1456	$^{1,5}X_2$	7821058	8952708	8543301	
∑(IdoA)		2.89E+08	2.58E+08	2.88E+08	

Mass to charge	Ion	Intensity	Intensity	Intensity	
421.1842	Z_2-SO_3	2210913	2532787	2115592	
523.1222	Z_2+Na	21054136	18640954	2.14E+07	
501.1400	Z_2	23352196	24622700	2.50E+07	
250.0664	Z_2^{2-}	8151763	24622700	8118707	
263.1617	Y_1-SO_3	2071384	1687059	1546338	
365.1004	Y_1+Na	10727273	9701851	1.02E+07	
343.1184	Y_1	1E+08	88141592	9.81E+07	
456.0435	C_2+Na-SO_3	13325671	11330588	1.25E+07	
536.0008	C_2+Na	15261289	16166002	1.58E+07	
267.4965	$[C_2+Na]^{2-}$	11486631	11232580	1.24E+07	
346.5074	$[B_3+Na]^{2-}$	31426172	29354790	3.23E+07	
∑(GlcA)		2.39E+08	2.2E+08	2.39E+08	
DR		-0.55885	-0.54595	-0.55658	-0.5538 ± 0.0069

Supplemental Table 23. Diagnostic ratio results for EDD fragmentation of $[M-4H+Na]^{3-}$ precursor ion for 3i

Mass to charge	Ion	Intensity	Intensity	Intensity	Diagnostic Ratio
299.0501	Y_2^{2-}	22711064	22432704	27117660	
310.0411	$[Y_2+Na]^{2-}$	2.65E+08	2.69E+08	2.97E+08	
259.0716	$[Y_2-SO_3]^{2-}$	2982683	3231133	2027269	

541.1326	Y_2+Na-SO_3	12234378	11165996	12020393	
∑(IdoA)		3.03E+08	3.06E+08	3.38E+08	
Mass to charge	Ion	Intensity	Intensity	Intensity	
523.1217	Z_2+Na-SO_3	15876294	16283533	19806644	
250.0664	$[Z_2\text{-}SO_3]^{2-}$	2635091	2366032	2671868	
603.0788	Z_2+Na	4697920	5571375	5667516	
301.0358	$[Z_2+Na]^{2-}$	2E+08	2.15E+08	2.31E+08	
290.0449	Z_2^{2-}	3587653	4110679	3902428	
365.1005	Y_1+Na-SO_3	19231044	23070818	24487512	
343.1185	Y_1-SO_3	51000916	52660196	58405440	
445.0573	Y_1+Na	1.17E+08	1.31E+08	1.49E+08	
423.0752	Y_1	2857038	2972521	3721266	
222.0249	$[Y_2+Na]^{2-}$	3103792	3695178	3442705	
211.0339	Y_1^{2-}	1.18E+08	1.21E+08	1.32E+08	
354.1046	C_2-SO_3	27349860	27948186	31377986	
456.0434	C_2+Na	24764114	26596388	30505846	
434.0614	C_2	9680554	10199488	11576688	
534.108	B_3+Na-SO_3	3591842	3942113	4187013	
512.1262	B_3-SO_3	2926105	3627586	3374982	
614.0645	B_3+Na	39492632	37713152	41220480	
306.5289	$[B_3+Na]^{2-}$	7584958	9386479	9673348	
295.5379	B_3^{2-}	16586330	17023792	19131400	

∑(GlcA)		6.69E+08	7.14E+08	7.86E+08	
DR		-0.13245	-0.10893	-0.11043	-0.1173 ± 0.0132

Supplemental Table 24. Diagnostic ratio results for EDD fragmentation of $[M-4H+Na]^{3-}$ precursor ion for 3j

Mass to charge	Ion	Intensity	Intensity	Intensity	Diagnostic Ratio
691.0954	$^{1,5}X_1$+Na	1015891	972927	1354847	
331.0465	$[Y_2+Na]^{2-}$	17749454	13359074	14821590	
583.1435	Y_2+Na-SO_3	861968	596013	425964	
663.0999	Y_2+Na	786312	827770	440294	
∑(IdoA)		20413625	15755784	17042695	
Mass to charge	Ion	Intensity	Intensity	Intensity	
271.0718	Z_2-SO_3	850048	788065	849330	
322.0411	$[Z_2+Na]^{2-}$	15986340	12639379	13185950	
645.0875	Z_2+Na	2071721	1735773	1950565	
385.1291	Y_1	6938938	5373554	5842771	
407.1113	Y_1+Na	1222370	1172261	1170104	
237.5323	C_2^{2-}	618784	653889	770111	
396.1162	C_2-SO_3	483950	690507	583341	
476.0717	C_2	1926725	1796958	1819151	
498.0547	C_2+Na	1276965	1305499	869869	

367.5123	$[B_3+Na]^{2-}$	2685137	1894629	2060139	
∑(GlcA)		34060978	28050514	29101331	
DR		-0.2548	-0.2266	-0.2447	-0.2421 ± 0.0143

Supplemental Table 25. Diagnostic ratio results for EDD fragmentation of $[M-5H+2Na]^{3-}$ precursor ion for 4a

Mass to charge	Ion	Intensity	Intensity	Intensity	Diagnostic ratio
259.071	Y_2^{2-}	4194682	1413910	1592519	
439.194	Y_1-SO_3	8694911	4603584	4769891	
519.151	Y_2+Na	9566041	4544486	4462267	
541.134	Y_2	8800816	5472752	6694714	
∑(IdoA)		3.13E+07	1.6E+07	1.8E+07	
Mass to charge	Ion	Intensity	Intensity	Intensity	
501.14	Z_2	5577845	2392848	2551029	
523.123	Z_2+Na	2737808	1616276	1725454	
343.118	Y_1	51835016	2.4E+07	2.4E+07	
365.001	Y_1+Na	2426596	1556181	1662538	
318.465	$[C_2+2Na]^{2-}$	13017124	8906673	9339472	
456.043	C_2+Na-$2SO_3$	1190608	580495	1644509	

557.982	C_2+2Na-SO_3	3026002	2054282	2251709	
637.938	C_2+2Na	10391923	4785345	5426490	
357.498	[B_3+2Na-SO_3]$^{2-}$	1706093	1699917	1718592	
397.476	[B_3+2Na]$^{2-}$	16758693	9432260	9998721	
∑(GlcA)		1.09E+08	5.7E+07	6.1E+07	
DR		0.06404	0.07312	0.06196	0.06637 ± 0.0059

Supplemental Table 26. Diagnostic ratio results for EDD fragmentation of [M-5H+2Na]$^{3-}$ precursor ion for 4b

Mass to charge	Type	Intensity	Intensity	Intensity	Diagnostic ratio
649.0844	$^{1,5}X_2$+Na	1198220	739222	1483201	
643.0718	Y_2+2Na	884993	946677	1096045	
541.1317	Y_2+Na-SO_3	994223	682001	1222909	
621.0917	Y_2+Na	825598	618416	1058971	
310.0408	[Y_2+Na]$^{2-}$	23898174	22844930	24972094	
∑(IdoA)		27801208	25831246	29833220	
301.036	[Z_2+Na]$^{2-}$	974493	386422	757258	
603.0785	Z_2+Na	2909485	3045122	3316420	
625.059	Z_2+2Na	1865955	1487173	1759098	
211.0338	Y_1^{2-}	3725434	4216062	4904305	

343.1181	Y_1-SO_3	3775916	3848223	4355575	
365.1003	Y_1+Na-SO_3	1840655	1340441	1779961	
445.0573	Y_1+Na	59196748	56396764	64546564	
467.0401	Y_1+2Na	1195511	1290632	854680	
256.5048	C_2^{2-}	963027	1161930	830671	
267.4962	$[C_2+Na]^{2-}$	14441716	14577452	16274848	
456.0434	C_2+Na-SO_3	8721067	8568722	9465473	
536.0007	C_2+Na	3094751	3056347	3720669	
557.9814	C_2+2Na	1700937	1513019	2224199	
306.5285	$[B_3$+Na-$SO_3]^{2-}$	3039091	3336177	3346068	
335.5159	B_3^{2-}	2362227	3093654	2194757	
346.507	$[B_3+Na]^{2-}$	67948824	68468720	74900824	
614.0635	B_3+Na-SO_3	1786233	1656897	2081379	
∑(GlcA)		179542070	1.77E+08	1.97E+08	
DR		0.3329813	0.359794	0.343334	0.3454 ± 0.0135

Supplemental Table 27. Diagnostic ratio results for EDD fragmentation of $[M-5H+2Na]^{3-}$ precursor ion for 4c

Mass to charge	Type	Intensity	Intensity	Intensity	Diagnostic ratio
729.0416	$^{1,5}X_2$+Na	1199995	1805712	1363023	
751.0223	$^{1,5}X_2$+2Na	8444108	11866427	9450798	
310.0411	$[Y_2+Na-SO_3]^{2-}$	4866408	4020658	5457672	
350.0196	$[Y_2+Na]^{2-}$	11800761	8612507	11627181	
361.0106	$[Y_2+2Na]^{2-}$	34741944	26614142	35554332	
643.0729	$[Y_2+2Na-SO_3]^{2-}$	1004943	121868	1312227	
∑(IdoA)		62058159	53041314	64765233	
301.0358	$[Z_2+Na-SO_3]^{2-}$	8962030	6959545	9283306	
341.0137	$[Z_2+Na]^{2-}$	772239	1006991	821888	
352.0053	$[Z_2+2Na]^{2-}$	18859134	14005386	18421128	
603.0777	$Z_2+Na-SO_3$	701063	879527	1211262	
625.0616	$Z_2+2Na-SO_3$	2990833	2214531	2921459	
705.0169	Z_2+2Na	1148492	1513624	1165264	
211.0339	Y_1^{2-}	3128457	2967939	3081004	
343.1183	Y_1-SO_3	1838421	3038332	1645814	

365.1001	Y_1+Na-SO_3	1070276	1452156	1015593	
445.0574	Y_1+Na	13798141	14880494	15063420	
456.0431	C_2+Na	7695948	9431812	8163885	
306.5291	[B_3+Na-SO_3]$^{2-}$	1025784	1235046	979390	
346.5073	[B_3+Na]$^{2-}$	7424013	6053076	8196562	
614.0633	B_3+Na-SO_3	1713832	2442810	1693888	
716.0033	B_3+2Na	865475	793564	648315	
∑(GlcA)		71994138	68874833	74312178	
DR		-0.41262	-0.36367	-0.4174	-0.3979 ± 0.0297

Supplemental Table 28. Diagnostic ratio results for EDD fragmentation of [M-5H+2Na]$^{3-}$ precursor ion for 4d

Mass to charge	Type	Intensity	Intensity	Intensity	Diagnostic ratio
324.0393	[$^{1,5}X_2$+Na-SO_3]$^{2-}$	696434	754709	630759	
364.0166	[$^{1,5}X_2$+Na]$^{2-}$	1153170	1354303	1410117	
375.0077	[$^{1,5}X_2$+2Na]$^{2-}$	2625171	2384608	2718783	
671.0664	$^{1,5}X_2$+2Na-SO_3	2156896	2256530	2608878	
751.0221	$^{1,5}X_2$+2Na	3899136	4440243	4152667	
495.5197	[$^{1,5}X_2$+2Na]$^{2-}$	3771398	4454511	4122977	

350.0194	$[Y_2+Na]^{2-}$	5250633	5602884	6008155	
361.0105	$[Y_2+2Na]^{2-}$	35922532	3.92E+07	4E+07	
310.0412	$[Y_2+2Na-SO_3]^{2-}$	4943014	5355231	4822614	
643.0717	$Y_2+2Na-SO_3$	1964410	2311969	2288181	
∑(IdoA)		62382794	68114988	68852095	
Mass to charge	Type	Intensity	Intensity	Intensity	
301.0359	$[Z_2+Na-SO_3]^{2-}$	1398569	1240314	1297616	
341.0147	$[Z_2+Na]^{2-}$	626406	779404	851502	
352.0052	$[Z_2+2Na]^{2-}$	5805828	6460995	5793197	
603.0762	$Z_2+Na-SO_3$	1018255	973494	582061	
625.0636	$Z_2+2Na-SO_3$	1172434	1416280	1588792	
705.017	Z_2+2Na	2238261	2451692	2498172	
343.1184	Y_1-SO_3	7914286	8168837	8662354	
211.0339	Y_1^{2-}	15249004	1.59E+07	1.6E+07	
343.1184	Y_1-SO_3	7914286	8168837	8662354	
365.1005	$Y_1+Na-SO_3$	5230122	5773301	5678404	
222.0247	Y_1^{2-}	517586	1016526	671150	
445.0573	Y_1	84398400	9.32E+07	9.1E+07	
467.0388	Y_1+2Na	3230766	3787288	3622845	
456.0433	C_2+Na	20463914	2.45E+07	2.3E+07	

295.5379	$[B_3\text{-}SO_3]^{2-}$	1850174	1826873	1669217	
306.5288	$[B_3+Na\text{-}SO_3]^{2-}$	9339436	1.06E+07	1.1E+07	
346.5073	$[B_3+Na]^{2-}$	68871208	7.51E+07	7.3E+07	
357.4988	$[B_3+2Na]^{2-}$	754277	710893	801072	
636.046	$B_3+2Na\text{-}SO_3$	918701	1048382	1493647	
716.0031	B_3+2Na	1556756	1451001	1420777	
614.0628	$B_3+Na\text{-}SO_3$	1623777	1012002	1517170	
∑(GlcA)		242092446	265586119	2.61E+08	
DR		0.1117952	0.113841433	0.101494	0.1090 ± 0.0066

Supplemental Table 29. Diagnostic ratio results for EDD fragmentation of $[M\text{-}5H+2Na]^{3-}$ precursor ion for 4e

Mass to charge	Type	Intensity	Intensity	Intensity	Diagnostic ratio
649.0872	$^{1,5}X_2+Na$	3471211	3201469	2747070	
310.0413	$[Y_2+Na]^{2-}$	8187911	12990223	13282343	
∑(IdoA)		11659122	16191692	16029413	
Mass to charge	Type	Intensity	Intensity	Intensity	
603.0773	Z_2+Na	1822586	1546780	1457331	
211.0341	Y_1^{2-}	876137	1157631	1179961	
343.1187	$Y_1\text{-}SO_3$	2966505	2254860	2876901	

365.1008	Y_1+Na-SO_3	1169263	1089303	933694	
445.057	Y_1+Na	33924312	40634352	41504900	
467.0408	Y_1+2Na	659638	701482	6584130	
267.4966	$[C_2+Na]^{2-}$	6584130	9485387	10265702	
456.0429	C_2+Na-SO3	2091750	2121245	2699517	
535.9999	C_2+Na	1207995	1423563	1212212	
557.9816	C_2+2Na	1024824	1123182	1544626	
306.5284	$[B_3+Na-SO_3]^{2-}$	711992	1971198	2374325	
346.5073	$[B_3+Na]^{2-}$	29539070	42221076	42246936	
∑(GlcA)		82578202	105730059	114880235	
DR		0.3730783	0.337785	0.3782064	0.3630 ± 0.0220

Supplemental Table 30. Diagnostic ratio results for EDD fragmentation of $[M-5H+2Na]^{3-}$ precursor ion for 4f

Mass to charge	Ion	Intensity	Intensity	Intensity	Diagnostic ratio
541.1308	Y_2+Na-SO_3	1051640	1345199	537674	
621.0887	Y_2+Na	1493422	1152307	844796	
643.0728	Y_2+2Na	1122508	744326	406429	
310.0410	$[Y_2+Na]^{2-}$	22469200	33014140	21713260	
299.0502	Y_2^{2-}	1162502	1773116	902141	
649.0852	$^{1,5}X_2$+Na	3953852	3242480	1942913	

∑(IdoA)		31253124	41271568	26347213	
Mass to charge	Ion	Intensity	Intensity	Intensity	
365.1002	Y_1+Na-SO_3	1859985	2420895	1189409	
343.1183	Y_1-SO_3	4985872	7951448	4001566	
445.0591	Y_1+Na	17683254	23659024	13914581	
467.0407	Y_1+2Na	1085593	1571967	815349	
423.0753	Y_1	1470693	1591050	1413595	
211.0340	Y_1^{2-}	4927760	6918603	4217780	
523.1223	Z_2+Na-SO_3	1551369	1595637	1225651	
603.0768	B_3+Na-SO_3	2833127	2148827	1727312	
625.0600	Z_2+2Na-2SO_3	7078502	7141195	4880039	
301.0356	$[Z_2+2Na]^{2-}$	6929320	10067999	5599519	
290.0449	Z_2^{2-}	1033112	1502146	820018	
456.0432	C_2+Na-SO_3	5675267	7993177	4578391	
536.0003	C_2+Na	3852101	3563516	2380388	
557.9815	C_2+2Na	2405144	2961318	1933785	
267.4963	$[C_2+Na]^{2-}$	3767821	3638998	2588707	
614.0640	B_3+Na-SO_3	1634622	2089059	1442869	
346.5071	$[B_3+Na]^{2-}$	10053438	14713078	10258414	
357.4981	$[B_3+2Na]^{2-}$	4926859	7243626	4498042	
∑(GlcA)		83753839	1.09E+08	67485415	

DR		-0.04901	-0.05626	-0.06865	-0.0580 ± 0.010

Supplemental Table 31. Diagnostic ratio results for EDD fragmentation of $[M-5H+2Na]^{3-}$ precursor ion for 4g

Mass to charge	Ion	Intensity	Intensity	Intensity	Diagnostic ratio
751.0234	$^{1,5}X_2+2Na$	6471279	4620628	19249286	
310.041	$[Y_2+Na-SO_3]^{2-}$	2789328	2883881	12465444	
350.0194	$[Y_2+Na]^{2-}$	6469536	6009930	29454074	
361.0104	$[Y_2+2Na]^{2-}$	1.5E+07	1.4E+07	77267256	
∑(IdoA)		30779487	27462715	138436060	
Mass to charge	Ion	Intensity	Intensity	Intensity	
445.0573	Y_1	9404970	9181430	29771918	
306.529	$[B_3+Na-SO_3]^{2-}$	580121	462801	1628497	
301.0357	$[Z_2+Na--SO_3]^{2-}$	2460998	2316199	9095460	
352.0051	$[Z_2+2Na]^{2-}$	1.2E+07	1.3E+07	68388928	
625.0624	$Z_2+2Na-SO_3$	1331946	1521457	4357626	
211.0337	Y_1^{2-}	3206567	2506172	7287609	
343.1188	Y_1-SO_3	1842893	1803170	3833694	
354.1039	C_2+Na	1710613	2017566	4045603	
434.0607	C_2	711867	877973	2357441	
456.0438	C_2+Na	3585068	3356300	8086379	

346.5073	$[B_3+Na]^{2-}$	5144408	4977452	19718614	
614.0648	$B_3+Na-SO_3$	850041	683948	2699157	
∑(GlcA)		43097496	42808299	161270926	
DR		-0.33093	-0.28434	-0.410814	-0.342 ± 0.0640

Supplemental Table 32. Diagnostic ratio results for EDD fragmentation of $[M-5H+Na]^{4-}$ precursor ion for 4h

Mass to charge	Type	Intensity	Intensity	Intensity	Diagnostic ratio
334.0528	$^{1,5}X_2^{2-}$	955223	650815	1002196	
345.0441	$^{1,5}X_2+Na$	783458	837877	680078	
691.098	$[^{1,5}X_2+Na]^{2-}$	1196952	5102210	500153	
213.0343	Y_2^{3-}	1387923	1427869	1475201	
280.0768	$[Y_2-SO_3]^{2-}$	2797623	3243543	2813301	
320.0554	Y_2^{2-}	6932348	314.707	7579344	
331.0462	$[Y_2+Na]^{2-}$	2.6E+07	2.9E+07	3E+07	
∑(IdoA)		39822773	39923747	44523445	
Mass to charge	Ion	Intensity	Intensity	Intensity	
271.0706	$[Z_2-SO_3]^{2-}$	754742	1193766	992298	
311.0501	Z_2^{2-}	5650282	4665712	4122502	
322.041	$[Z_2+Na]^{2-}$	1.9E+07	2.3E+07	2.1E+07	
645.0901	Z_2+Na	3139058	2628950	1737143	

385.1291	Y_1	1.2E+07	1.5E+07	1.4E+07	
407.1105	Y_1+Na	1642378	2629451	1967804	
277.5118	C_2^{2-}	868397	1041008	1491622	
288.5021	$[C_2+Na]^{2-}$	1134893	1285271	1394074	
498.0531	C_2+Na-SO_3	910686	1543444	1393011	
578.013	C_2+Na	1856905	1401130	814680	
367.5123	$[B_3+Na-SO_3]^{2-}$	2059375	2222824	1247816	
407.4909	$[B_3+Na]^{2-}$	1145267	1065767	1967804	
∑(GlcA)		49804644	57487861	52241655	
DR		-0.37998	-0.31878	-0.40769	-0.3688 ± 0.0455

Supplemental Table 33. Diagnostic ratio results for EDD fragmentation of $[M-5H+Na]^{4-}$ precursor ion for 4i

Mass to charge	Type	Intensity	Intensity	Intensity	Diagnostic Ratio
611.1382	$^{1,5}X_2$+Na	798696	1152657	914125	
589.1569	$^{1,5}X_2$	593701	73216	395737	
481.2053	Y_2-SO_3	1844981	2414555	1690455	
561.1615	Y_2	1484432	1638215	880023	
583.1438	Y_2+Na	2434406	3187925	1980871	
280.0768	Y_2^{2-}	1.27E+08	1.62E+08	1.16E+08	
∑(IdoA)		134156216	170466568	121861211	

135.9926	C_2^{2-}	604587	419701	421271	
204.6472	$[C_2+Na]^{3-}$	1724020	2306964	1599117	
267.4965	$[C_2+Na-SO_3]^{2-}$	6088346	7179674	5391552	
307.4746	$[C_2+Na]^{2-}$	11714436	15449015	11925317	
456.0438	$C_2+Na-2SO_3$	2885529	3571635	2839526	
271.0716	Z_2^{2-}	10947536	15085654	10359285	
565.1317	Z_2+Na	2155324	3237440	1846839	
192.0607	Y_1^{2-}	518752	747647	618479	
385.1292	Y_1	43756768	54963880	40428128	
407.111	Y_1+Na	5853122	7633493	5520832	
346.507	$[B_3+Na-SO_3]^{2-}$	3762336	4414270	2916271	
386.4854	$[B_3+Na]^{2-}$	2780012	3376198	2567595	
∑(GlcA)		92790768	118385571	86434212	
DR		-0.637227	-0.635462	-0.626301	-0.6372 ± 0.0059

Mass List for all tetrasaccharides are arranged according to product ion types for easy identification of diagnostic ions

Supplemental Table 34. Mass list for 1a, $[M-2H]^{2-}$ precursor ion

Mass to charge	Type	Intensity	Intensity	Intensity
329.0183	$^{3,5}A_2$	13436226	9726875	11114866
546.0772	$^{3,5}A_3$	13252187	1944245	12354879
272.5349	$^{3,5}A_3^{2-}$	3418125	1.03E+07	2412958
226.9867	$^{1,5}A_1$	48367924	3.56E+07	41439664
430.066	$^{1,5}A_2$	3017058	1831368	2743897
606.0982	$^{1,5}A_3$	2949382	1823394	2587924
138.9707	$^{1,3}A_1$	2167716	2164924	2892422
295.0672	$^{0,2}A_2$-SO_3	5584512	5134771	9717899
375.0238	$^{0,2}A_2$	30435614	2.29E+07	30513548
187.0083	$^{0,2}A_2^{2-}$	2206893	2037813	3260839
512.1256	$^{0,2}A_3$-SO_3	2926058	2273449	1942323
592.0826	$^{0,2}A_3$	64947420	4.84E+07	58065824
463.1935	Z_2	18180694	1.48E+07	18820748
305.172	Y_1	13468601	1.17E+07	18172296
481.2038	Y_2	4953862	4459979	4736759
684.282	Y_3	2243618	1564303	1790380
193.0354	C_1-SO_3	7679704	7342090	11769528
272.9922	C_1	10939761	7957538	11483529
652.1038	C_3	4487254	2893906	3377188

325.5483	C_3^{2-}	1588298	1321766	1449702
396.1149	C_2-SO_3	11396200	1.12E+07	19052994
476.0718	C_2	130335080	1.15E+08	147178240
237.5322	C_2^{2-}	2389162	1972587	2548052
175.0249	B_1-SO_3	3784274	2787060	4026302
254.9816	B_1	20464778	1.80E+07	30349696
634.0922	B_3	5774204	4787680	5418335
316.5428	B_3^{2-}	18307592	1.74E+07	18700824
378.1042	B_2-SO_3	6074502	4962519	8365978
458.061	B_2	2557316	2050295	2961689
228.5268	B_2^{2-}	2568759	2237731	3675593

Supplemental Table 35. Mass list for 1b, $[M-2H]^{2-}$ precursor ion

Mass to charge	Type	Intensity	Intensity	Intensity
329.0185	$^{3,5}A_2$	4284341	5972692	4970030
272.5349	$^{3,5}A_3^{2-}$	5288929	5035581	4331408
546.0771	$^{3,5}A_3$	10221850	11118582	10091672
792.2343	$^{1,5}X_3$	11304080	10923962	10797308
430.0661	$^{1,5}A_2$	34828788	40078680	36639108
633.1819	$^{1,4}X_2$	11584176	13201087	12879230
187.0082	$^{0,2}A_2^{2-}$	1985402	1434372	2252575
295.067	$^{0,2}A_2$-SO_3	2033590	1202198	2342331
375.0239	$^{0,2}A_2$	12828680	14951018	13691641

512.1254	$^{0,2}A_3$-SO_3	1884463	2077894	2200792
592.0826	$^{0,2}A_3$	33850096	39578840	35703912
463.1936	Z_2	13200108	8777935	9727237
746.2303	Z_3	50356364	50746292	52200232
305.1718	Y_1	6298305	4179045	4522439
381.6163	Y_3^{2-}	5566312	2806797	3304655
481.2038	Y_2	3826594	3401895	3091584
764.2406	Y_3	1.74E+08	1.68E+08	1.76E+08
193.0354	C_1	5949009	5616593	6187842
237.5322	C_2^{2-}	4228510	3653947	3707224
325.5481	C_3^{2-}	2006934	1520720	1909881
396.1149	C_2-SO_3	5390822	4001383	4789525
476.0717	C_2	1.2E+08	1.11E+08	1.15E+08
652.1036	C_3	12702226	12878903	12658970
175.0248	B_1	2289877	1963750	1754563
228.5269	B_2^{2-}	2084317	1879798	2020292
316.5429	B_3^{2-}	21278472	15765723	16803910
378.1038	B_2-SO_3	2778888	2374452	3136941
458.061	B_2	10460594	12136480	11000460
634.0922	B_3	3005581	5648101	3954922

Supplemental Table 36. Mass list for 1c, $[M-2H]^{2-}$ precursor ion

Mass to charge	Type	Intensity	Intensity	Intensity
708.13	$^{3,5}A_4$	3960562	3570284	4105607
466.1202	$^{3,5}A_3$	2919234	2863134	2948856
792.2357	$^{1,5}X_3$	14729892	13333422	14006717
589.1560	$^{1,5}X_2$	75981352	70956120	71628008
606.0985	$^{1,5}A_3$	15686776	14929562	15398149
295.067	$^{0,2}A_2$	2267083	1977812	2149494
463.1937	Z_2-SO_3	11434117	10020313	12431328
543.1507	Z_2	19122436	17559604	19897310
746.2301	Z_3	55782500	51098512	52817640
381.6167	Y_3^{2-}	61711896	55143924	65828820
481.2059	$[Y_2\text{-}SO_3]^{2-}$	1924399	1707910	2103669
561.161	Y_2	58341192	54835952	57124256
684.2843	Y_3-SO_3	2052620	2183665	2116049
764.2413	Y_3	172169312	161544704	1.76E+08
193.0354	C_1	8563274	7784544	9144521
325.5482	C_3^{2-}	3765727	3547045	3140814
396.115	C_2	20399828	19140978	19257978
652.1008	C_3	12336112	12761586	11974259
175.0248	B_1	20927004	17497670	21120648
316.5429	B_3^{2-}	2950708	2372489	2742307

378.1046	B_2	2751274	2502634	3372956
634.0935	B_3	3599267	2858662	2873887
554.1363	B_3-SO_3	708409	629737	910967

Supplemental Table 37. Mass list for 1d, $[M-2H]^{2-}$ precursor ion

Mass to charge	Type	Intensity	Intensity	Intensity
708.1323	$^{3,5}A_4$	2020992	1636812	3825933
466.121	$^{3,5}A_3$	2582051	3142912	3654324
738.1415	$^{2,5}A_4$	3649753	3.07E+06	5.77E+06
325.1079	$^{2,4}X_0$	5382524	4603399	9.34E+06
792.2356	$^{1,5}X_4$	1.16E+07	1.09E+07	1.84E+07
589.1561	$^{1,5}X_2$	8.77E+07	7.86E+07	1.46E+08
413.124	$^{1,5}X_1$	3.93E+07	3.71E+07	6.13E+07
427.1404	$^{0,2}X_1$	5278222	4.14E+06	5.17E+06
295.0674	$^{0,2}A_2$	6465858	5.45E+06	4.20E+06
754.1353	$^{0,2}A_4$	4400716	3.24E+06	7.46E+06
512.1261	$^{0,2}A_3$	2024293	1.95E+06	3.38E+06
367.1184	Z_1	5.30E+07	4.78E+07	9.51E+07
463.1941	Z_2-SO_3	1.44E+07	1.11E+07	5.74E+06
543.1508	Z_2	6.21E+07	5.21E+07	8.13E+07
746.2301	Z_3	2.36E+07	2.09E+07	3.73E+07
381.617	Y_3^{2-}	5.14E+07	3.63E+07	3.05E+07

385.1292	Y_1	1.14E+08	9.22E+07	1.06E+08
561.1612	Y_2	3.41E+07	3.25E+07	5.42E+07
684.284	Y_3-SO_3	4359345	2.82E+06	2004799
764.2413	Y_3	1.14E+08	9.92E+07	1.09E+08
193.0354	C_1	1.59E+07	1.38E+07	1.59E+07
396.1153	C_2	2.63E+07	2.05E+07	2.51E+07
572.1479	C_3	7852971	6.71E+06	1.27E+07
175.0248	B_1	2.02E+07	17181670	1.11E+07
378.1047	B_2	6071337	5119370	7054814
554.1374	B_3^{2-}	2.35E+07	18100076	1.70E+07

Supplemental Table 38. Mass list for 1e, $[M-2H]^{2-}$ precursor ion

Mass to charge	Type	Intensity	Intensity	Intensity
466.1204	$^{3,5}A_3$	9258155	9278186	8894991
792.237	$^{1,5}X_4$	19458582	21205990	20200214
589.1562	$^{1,5}X_2$	18859728	19324480	18866658
302.5452	$^{1,5}A_3^{2-}$	5264730	4655255	4458332
606.099	$^{1,5}A_3$	9171905	9773996	9136041
138.9707	$^{1,3}A_1$	2210370	2447444	2159266
295.067	$^{0,2}A_2$	5271872	6711872	6219881
512.1265	$^{0,2}A_3$	3660899	3859024	3607435
543.1505	Z_2	67996360	65750260	65171776

746.2307	Z_3	66822464	67597464	67188824
381.6166	Y_3^{2-}	12205501	13605678	13992851
561.1613	Y_2	14170177	14151433	13597671
764.2421	Y_3	53538196	55436252	54541332
193.0353	C_1	13901131	18047946	16335187
325.5481	C_3^{2-}	4180683	3821758	3761776
396.1148	C_2	24833928	27427278	27150918
652.1036	C_3	19295032	20389830	20521456
175.0248	B_1	9028621	11029749	10739540
316.5428	B_3^{2-}	1.92E+08	2.39E+08	229861216
378.1043	B_2	2817446	3266066	2898724
554.1365	B_3-SO_3	7726079	8649897	8605791
634.0939	B_3	27101668	29135022	27453156

Supplemental Table 39. Mass list for 1f, $[M-2H]^{2-}$ precursor ion

Mass to charge	Type	Intensity	Intensity	Intensity
708.1287	$^{3,5}A_4$	2603993	1854698	2456689
466.1211	$^{3,5}A_3$	5208071	3663329	4742282
792.2356	$^{1,5}X_3$	14628845	9894642	1835586
589.1562	$^{1,5}X_2$	98733624	68868184	82239992
413.1241	$^{1,5}X_1$	27980874	19914906	23900970
427.1408	$^{0,2}X_2$	2315761	2037411	2108218

295.0673	$^{0,2}A_2$	8314981	5844047	4822074
754.1359	$^{0,2}A_4$	3938080	2611794	2508711
512.1265	$^{0,2}A_3$	2286307	1431615	2166608
367.1185	Z_1	27441324	18344746	23979300
543.1508	Z_2	43243596	34453864	36506452
746.2299	Z_3^{2-}	30583546	22263986	25011282
381.6169	Y_3^{2-}	3317790	2496851	3090448
385.1292	Y_1	57366876	45159348	46729528
561.1613	Y_2	40268916	29401934	34576320
764.2406	Y_3	74867800	63050980	62926004
193.0354	C_1	13342981	8889682	8789495
396.1153	C_2	26809426	20088266	20274656
572.1478	C_3	4537660	3117556	3993233
175.0248	B_1	4339692	2933228	2845255
378.1047	B_2	10259728	6916056	6244765
554.1375	B_3	30213758	57744536	23246144

Supplemental Table 40. Mass list for 2a, $[M-3H]^{3-}$ precursor ion

Intensity	Type	Intensity	Intensity	Intensity
312.5136	$^{3,5}A_3$	1433123	2911206	1274875
235.0459	$^{2,4}A_2$-SO_3	524861	1045141	390739
254.5078	$^{1,5}A_3$	423018	1543471	651794
226.9867	1,5A1	6188499	17516212	7036902
138.9706	$^{1,3}A_1$	7340656	23551332	5708639
187.0083	$[^{0,2}A_2$-$2SO_3]^{2-}$	3181894	10726090	3823986
226.9867	$^{0,2}A_2^{2-}$	6188499	17516212	7036902
295.0673	$^{0,2}A_2$-$2SO_3$	792450	2792770	815889
375.0247	$^{0,2}A_2$-SO_3	1627157	4974239	2147060
335.5163	$^{0,2}A_3$	1712571	3794698	1968022
463.1944	Z_2	1825369	5508413	1249289
746.2325	Z_3	5053441	10800346	5003729
305.1721	Y_1	11606355	26672774	10171876
381.6168	Y_3^{2-}	12540829	46072244	10156834
481.2052	Y_2	16893164	58452360	15220988
764.2456	Y_3	5053441	1763667	1031206
193.0353	C_1-SO_3	1827215	6376027	1502298
237.5322	$[C_2$-$SO_3]^{2-}$	2545543	7572881	2531461
272.9924	C_1	2751908	6704973	3245593
277.5107	C_2^{2-}	23649902	61248728	20326660
365.527	C_3^{2-}	1272730	3118593	1239551

396.1155	C_2-2SO_3	913770	3010048	1032572
476.0727	C_2-SO_3	3197851	9225579	2696663
556.0293	C_2	1104824	2609164	1641224
175.0248	B_1	2168886	6830924	1679280
228.5269	$[B_2\text{-}SO_3]^{2-}$	9298817	28189652	9192398
254.9817	B_1	7563902	21674812	6933691
268.5054	B_2^{2-}	23722534	67227752	20188312
316.5434	$[B_3\text{-}SO_3]^{2-}$	1148720	3571099	1367998
356.5216	B_3^{2-}	25366874	82167296	20596796
378.1049	B_2-2SO_3	1006450	3404232	1012237
458.0619	B_2-SO_3	3626845	9603274	3303169

Supplemental Table 41. Mass list for 2b, $[M\text{-}3H]^{3-}$ precursor ion

Mass to charge	Type	Intensity	Intensity	Intensity
329.0193	$^{3,5}A_2$	2621842	2309726	2882243
393.54	$^{3,5}A_4^{2-}$	2097303	1903412	1665985
272.535	$^{3,5}A_3^{2-}$	1092199	1226606	1134021
546.0791	$^{3,5}A_3$	6682052	5778519	6705200
325.1077	$^{2,4}X_0$	2163365	1646526	1851132
391.585	$^{2,4}X_2^{2-}$	2465859	2719581	2581216
235.0461	$^{2,4}A_2$	4337817	4358333	3941279
258.5374	$^{2,4}A_4^{2-}$	2132332	1722658	1250763

438.1266	$^{2,4}A_4$-SO_3	1255952	983073	1107360
589.1582	$^{1,5}X_2$	4446280	4110748	4078222
413.1246	$^{1,5}X_1$	12490953	11523924	11332234
435.5931	$^{1,5}X_3^{2-}$	14441967	12987597	12855073
430.0673	$^{1,5}A_2$	20571896	18235674	19969920
444.0638	$^{1,5}A_4$	1756797	1681787	1683750
606.0982	$^{1,5}A_3$	2669901	2251780	2591304
138.9706	$^{0,4}A_2$	14164506	12200141	12843370
427.1405	$^{0,2}X_1$	26119194	20905616	20982272
442.6009	$^{0,2}X_3$	4039898	3302302	3284796
187.0084	$^{0,2}A_2^{2-}$	54421368	47557328	49110104
295.0675	$^{0,2}A_2$-SO_3	18632128	15648690	16180789
375.0247	$^{0,2}A_2$	22063370	19546282	19559768
170.037	$[^{0,2}A_3$-$SO_3]^{3-}$	2347609	2931647	4615227
592.0856	$^{0,2}A_3$	2295111	2341340	2239949
271.0717	Z_2^{2-}	1.16E+08	1.05E+08	1.02E+08
367.1189	Z_1	24023064	22298044	22409242
412.5902	Z_3^{2-}	6574090	6433803	6241769
463.1962	Z_2-SO_3	1248782	974702	1037232
543.1525	Z_2	90478400	67026844	75424456
280.0771	Y_2^{2-}	51042728	43887312	43292356
280.7277	Y_3^{3-}	43116896	38147840	38188796
305.1725	Y_1-SO_3	2139748	2060722	2130710

385.1295	Y_1	2.78E+08	2.36E+08	2.41E+08
421.5955	Y_3^{2-}	1.09E+08	85428064	89105200
561.1635	Y_2	3967151	3913552	3650378
193.0354	C_1	32031806	27212362	28280596
237.5323	C_2^{2-}	60920324	54750216	55949996
396.1157	C_2-SO_3	45214664	35790492	37231400
476.073	C_2	1.99E+08	1.52E+08	1.62E+08
652.108	C_3	3201375	2418979	2362325
175.0248	B_1	18974152	18352452	18312224
228.527	B_2^{2-}	54145360	45349324	46375840
316.5435	B_3^{2-}	3293167	3271514	3272172
378.1051	B_2-SO_3	45905756	38390312	40051752
458.0623	B_2	58343688	45056664	47350928
554.1387	B_3-SO_3	2720663	2926886	3183758
634.0954	B_3	3135454	3110907	3061120

Supplemental Table 42. Mass list for 2c, $[M-3H]^{3-}$ precursor ion

Mass to charge	Type	Intensity	Intensity	Intensity
393.5396	$^{3,5}A_4$	11350148	14504291	11030887
249.0616	$^{3,5}A_2$	3794451	4844149	4333636
466.1207	$^{3,5}A_3$	3112665	3552505	3798220
391.5847	$^{2,4}X_2$	5662833	6974684	5620073
117.0193	$^{2,4}A_2$	1785343	1881912	1477407

669.1123	$^{1,5}X_2$	7410978	10212210	7355478
334.0527	$^{1,5}X_2^{2-}$	1.16E+08	1.57E+08	1.13E+08
413.1238	$^{1,5}X_1$	9524131	10832582	9471354
435.5925	$^{1,5}X_3$	13892856	16819810	13228666
302.5456	$^{1,5}A_3$	3520522	4407570	3438413
138.9706	$^{1,3}A_1$	10230613	11560870	10535709
427.1397	$^{0,2}X_1$-SO_3	9328769	9751206	8590003
253.0446	$^{0,2}X_1$	1461748	1736839	2002378
442.5996	$^{0,2}X_3^{2-}$	4321862	5332627	5004513
416.5424	$^{0,2}A_4^{2-}$	42019412	55481164	38866420
295.0672	$^{0,2}A_2$	10854747	11886829	10755838
170.0368	$^{0,2}A_3^{3-}$	1739666	1500019	7003748
367.1183	Z_1	24201378	28575318	22159140
543.1509	Z_2-SO_3	18499390	20356690	18105550
271.0716	$[Z_2\text{-}SO_3]^{2-}$	23951520	25713974	22351576
463.1942	Z_2-$2SO_3$	4181159	5008681	4255833
746.2313	Z_3-SO_3	3903717	4419722	3305192
311.05	Z_2^{2-}	7900344	9618064	8335596
412.5896	Z_3^{2-}	4976328	6581690	4673350
385.129	Y_1	1.19E+08	1.32E+08	1.24E+08
561.1621	Y_2-SO_3	1782634	2036215	1583196
280.0768	$[Y_2\text{-}2SO_3]^{2-}$	8902406	10410245	10296887
481.2047	Y_2-$2SO_3$	2471130	2862044	2582460

764.2411	Y_3-2SO_3	4656264	5973302	4583887
381.6167	Y_3-SO_3	41307908	47506028	42225264
641.1179	Y_2	4986183	5308680	4320404
320.0553	Y_2^{2-}	11122452	13116672	10015481
280.7276	Y_3^{3-}	5495906	5839423	5227143
421.595	Y_3^{2-}	2.2E+08	2.62E+08	2.08E+08
652.104	C_3	6659362	8571112	6615147
325.5484	C_3^{2-}	6609974	6307658	7108567
396.1151	C_2	24762044	28903464	24500704
193.0354	C_1	42342648	45591132	42446056
554.1361	B_3-SO_3	3761689	4912886	3526783
276.5646	[B_3-SO_3]$^{2-}$	2010021	2168577	2482320
634.0936	B_3	7279126	10323493	6943638
316.543	B_3^{2-}	9315893	9441328	9285729
378.1045	B_2	12963348	14164153	12480096
175.0248	B_1	9757516	10457740	9082857

Supplemental Table 43. Mass list for 2d, [M-3H]$^{3-}$ precursor ion

Mass to charge	Type	Intensity	Intensity	Intensity
262.0241	$^{3,5}A_4^{3-}$	625389	1180702	324166
329.0185	$^{3,5}A_2$	936219	3415798	1152719
393.5391	$^{3,5}A_4$	886093	1607873	901362
546.0777	$^{3,5}A_3$	6468559	19922766	8878974
391.5846	$^{2,4}X_2^{2-}$	1804402	5685678	2322166

439.622	$[^{2,4}X_3\text{-}SO_3]^{2-}$	739756	1566261	417083
589.1563	$^{1,5}X_2$	2640543	7024767	2450717
413.1239	$^{1,5}X_1$	6301924	24611498	11343921
435.5926	$^{1,5}X_3^{2-}$	1916018	5311606	2733715
138.9705	$^{0,4}A_1$	3304528	8813950	6092146
427.1395	$^{0,2}X_1$	4065879	11474377	5320816
442.5998	$^{0,2}X_3^{2-}$	1646457	3563601	2144419
187.0083	$^{0,2}A_2^{2-}$	4273035	12593102	8403465
295.0673	$^{0,2}A_2\text{-}SO_3$	840665	3747673	1732350
375.0245	$^{0,2}A_2$	2166484	8818102	4545041
271.0717	Z_2^{2-}	20714480	65920348	41429652
367.1185	Z_1	8235406	31091486	14553196
412.5899	Z_3^{2-}	6397335	15870143	8714601
463.193	$Z_2\text{-}SO_3$	1492385	4535612	1868347
543.1515	Z_2	7169626	25582480	12541788
280.077	Y_2^{2-}	43970548	1.41E+08	81498664
280.7277	Y_3^{3-}	4069645	9555567	5932649
305.1718	$Y_1\text{-}SO_3$	842014	2411961	1147884
381.6174	$[Y_3\text{-}SO_3]^{2-}$	592475	1692583	1068408
385.1292	Y_1	43873032	1.51E+08	74058000
421.5952	Y_3^{2-}	15199365	36955524	26300584
481.2047	$Y_2\text{-}SO_3$	3931460	13267948	6034545
561.1611	Y_2	3149911	10425351	5169641

193.0354	C_1	6783990	19384940	12002436
237.5323	C_2^{2-}	5686696	17216060	10809529
325.5485	C_3^{2-}	800693	1190130	657374
396.1154	C_2-SO_3	2500403	7684790	4379382
476.0723	C_2	12205525	40184704	24981498
175.0248	B_1	3627576	10152664	6202314
228.527	B_2^{2-}	3182757	10789885	6861092
378.1047	B_2-SO_3	9197253	28487602	18111860
458.0618	B_2	14788148	46792020	28732822
634.0943	B_3	1387186	2947346	1378609

Supplemental Table 44. Mass list for 2e, $[M-3H]^{3-}$ precursor ion

Mass to charge	Type	Intensity	Intensity	Intensity
249.0616	$^{3,5}A_2$	4019100	1898242	3269202
393.5403	$^{3,5}A_4^{2-}$	29499370	11212873	24167392
466.1212	$^{3,5}A_3$	6116105	3052005	5045965
117.0192	$^{2,4}A_2$	2166346	1222186	1753459
391.5848	$^{2,4}X_2^{2-}$	11430339	4346128	9657261
334.0529	$^{1,5}X_2^{2-}$	47684208	19886212	35433116
589.1564	$^{1,5}X_2$-SO_3	2563960	871951	1716219
669.1130	$^{1,5}X_2$	5704086	1753353	5421969
413.1242	$^{1,5}X_1$	15951114	6657880	12857099
435.5928	$^{1,5}X_3^{2-}$	14121942	5504928	11690282

302.5457	$^{1,5}A_3$	5275969	2943714	4879100
138.9706	$^{1,3}A_1$	11596684	7757057	12122019
401.5374	$^{0,3}A_4^{2-}$	2782103	997823	1983152
427.1399	$^{0,2}X_1$	1859690	1198840	1687443
442.6009	$^{0,2}X_3^{2-}$	4758530	1675634	3144635
295.0673	$^{0,2}A_2$	25430046	16612956	22768562
416.5429	$^{0,2}A_4^{2-}$	29680206	8842506	22860674
376.5651	$[^{0,2}A_4\text{-}SO_3]^{2-}$	2134010	622963	1378118
271.0717	$[Z_2\text{-}SO_3]^{2-}$	3097429	1578554	2390932
311.05	Z_2^{2-}	22837844	9395726	18274178
367.1186	Z_1	28537222	11302170	20952110
412.5901	Z_3^{2-}	124933920	45798188	98704176
543.1518	$Z_2\text{-}SO_3$	5363064	2481766	4434532
623.1093	Z_2	12228549	4220742	9379510
746.2359	$Z_3\text{-}SO_3$	4560323	1356240	3478906
280.7273	Y_3^{3-}	2624621	1374220	2098568
320.0555	Y_2^{2-}	11527683	4986274	8822770
385.1293	Y_1	607204480	418512896	604887360
421.5954	Y_3^{2-}	165125088	65530380	135569712
641.1205	Y_2	6867400	2808579	5120556
193.0353	C_1	73373464	45545732	64188976
325.5485	C_3^{2-}	6850733	4193238	5647986
396.1155	C_2	61829440	36576476	52830960

652.1037	C_3	6457834	2639065	5259741
175.0248	B_1	9895051	6461344	8031619
276.5647	$[B_3\text{-}SO_3]^{2-}$	5245960	3910351	4819975
316.5432	B_3^{2-}	304745888	217199376	299569536
378.1048	B_2	9838445	6845108	9232129
554.1363	$B_3\text{-}SO_3$	6820640	2510799	1690066
634.0961	B_3	1937628	861370	5842274

Supplemental Table 45. Mass list for 2f, $[M\text{-}3H]^{3-}$ precursor ion

Mass to charge	Type	Intensity	Intensity	Intensity
329.0193	$^{3,5}A_2$	1169673	1126042	1077951
272.535	$^{3,5}A_3^{2-}$	1420996	1038458	760599
546.0785	$^{3,5}A_3$	4593221	4733588	3584542
391.5845	$^{2,4}X_2^{2-}$	2852211	1965187	1492881
258.5373	$^{2,4}A_3^{2-}$	1223278	1422837	806058
589.1576	$^{1,5}X_2$	3283151	3471716	3139461
413.124	$^{1,5}X_1$	7364870	7400088	5146482
435.5926	$^{1,5}X_3$	6283759	5992812	4597731
430.0666	$^{1,5}A_2$	3057054	2584220	453214
444.0638	$^{1,5}A_4^{2-}$	2212441	1812291	2251636
138.9705	$^{0,4}A_2$	8436629	8609626	3568462
427.1399	$^{0,2}X_1$	10977989	12898537	8979800
442.6009	$^{0,2}X_3^{2-}$	1180483	1595147	929097

187.0082	$^{0,2}A_2^{2-}$	29028410	29272360	13551302
295.0672	$^{0,2}A_2$-SO_3	2852968	2892288	1799683
375.0243	$^{0,2}A_2$	15463825	15099366	13983369
592.0849	$^{0,2}A_3$	2821220	3203800	2622129
271.0715	Z_2^{2-}	50710320	49473280	26766388
367.1186	Z_1	12155999	11845782	8504810
412.5898	Z_3^{2-}	8809666	8199691	5517441
543.1517	Z_2	40955940	39687268	43432528
280.0768	Y_2^{2-}	24513988	26311380	13704574
280.7274	Y_3^{3-}	5769718	5805452	3239412
305.1715	Y_1-SO_3	865512	1192119	472132
385.1291	Y_1	1.37E+08	1.41E+08	1.1E+08
421.595	Y_3^{2-}	18349716	16585141	11853790
561.1615	Y_2	3655253	3452701	2865757
193.0353	C_1	14123663	14885751	6838985
237.5321	C_2^{2-}	48455576	48173372	28511514
396.1154	C_2-SO_3	9653681	9161724	7758384
476.0726	C_2	63364480	59542688	58801396
175.0247	B_1	4384311	4443582	1992785
228.5268	B_2^{2-}	15777938	17051976	8092012
316.5431	B_3^{2-}	4455608	3469007	1639828
378.1046	B_2-SO_3	7411261	7653413	6239802
458.0617	B_2	17850652	17811004	13252686

Supplemental Table 46. Mass list for 2g, $[M-3H]^{3-}$ precursor ion

Mass to charge	Type	Intensity	Intensity	Intensity
329.019	$^{3,5}A_2$	1581586	2964251	1795119
546.077	$^{3,5}A_3$	2328344	6047929	3043751
117.0189	$^{2,4}A_2$	911162	1334839	1245758
325.1082	$^{2,4}X_1$	1025305	1824666	1244754
391.5848	$^{2,4}X_2^{2-}$	1050721	2783278	2085936
235.0461	$^{2,4}A_2$	1763149	3618383	2144769
117.0189	$^{2,4}A_2^{2-}$	911162	1334839	1245758
589.1563	$^{1,5}X_2$	2075773	3507379	1895389
413.1241	$^{1,5}X_1$	7068606	1.40E+07	9707612
435.5923	$^{1,5}X_3^{2-}$	2082805	4124073	2457783
269.0543	$^{1,5}A_4$-SO_3	2515911	2742384	2604522
430.0666	$^{1,5}A_2$	6151447	1.36E+07	8907465
606.1018	$^{1,5}A_3$	729753	1965651	798280
138.9704	$^{0,4}A_2$	1.07E+07	1.63E+07	12816767
427.14	$^{0,2}X_1$	6690497	1.25E+07	8015773
442.6001	$^{0,2}X_3^{2-}$	1191738	2.40E+06	1225656
295.0675	$^{0,2}A_2$-SO_3	6195276	1.10E+07	7270794
375.0243	$^{0,2}A_2$	4416316	7298814	5088121
187.0078	$^{0,2}A_2^{2-}$	7738598	1.41E+07	11486864
367.1186	Z_1	1.18E+07	2.27E+07	16355682
463.194	Z_2-SO_3	1632908	3687011	2235616

543.1504	Z_2	1.23E+07	2.39E+07	15371581
271.0718	Z_2^{2-}	6.14E+07	1.09E+08	85146968
412.5898	Z_3^{2-}	6335955	9072636	7430592
305.1725	Y_1-SO_3	1381245	2741962	1997523
385.1292	Y_1	1.09E+08	2.00E+08	1.42E+08
481.2043	Y_2-SO_3	6358870	1.28E+07	9123369
561.1602	Y_2	3744493	7547170	5592472
280.0762	Y_2^{2-}	9.13E+07	1.47E+08	1.27E+08
381.6172	$[Y_3$-$SO_3]^{2-}$	1777003	2317856	1644541
280.7277	Y_3^{3-}	2.40E+07	3.82E+07	31706602
421.5947	Y_3^{2-}	7.28E+07	1.01E+08	82065440
325.5478	C	822634	955878	787118
396.1148	C_2-SO_3	1.00E+07	1.85E+07	12379704
476.0718	C_2	3.60E+07	6.00E+07	41777488
237.5323	C_2^{2-}	8543020	1.43E+07	10897323
193.0354	C_1	1.52E+07	2.77E+07	18929382
554.1363	B_3-SO_3	819291	2241754	877586
634.0931	B_3	752178	2191905	1391712
378.104	B_2-SO_3	6.44E+07	9.78E+07	79782800
458.0614	B_2	5.18E+07	8.88E+07	61987544
228.527	B_2^{2-}	9466420	1.51E+07	13848651
175.0248	B_1	1.89E+07	3.13E+07	24279332

Supplemental Table 47. Mass list for 2h, $[M-3H]^{3-}$ precursor ion

Mass to charge	Type	Intensity	Intensity	Intensity
249.0618	$^{3,5}A_2$	2606825	2184222	2314953
466.121	$^{3,5}A_3$	2925157	2343954	2998707
370.5792	$^{2,4}X_2$	8893946	7649259	9330297
235.0462	$^{2,4}A_2$	1407763	1062987	1138972
117.0193	$^{2,4}A_2^{2-}$	4345239	3551408	3674516
438.1258	$^{2,4}A_3$	2778622	1757626	1763670
547.147	$[^{1,5}X_2\text{-}SO_3]^{2-}$	2008460	2413573	2456307
627.1025	$^{1,5}X_2$	3201852	4782503	3862109
313.0474	$^{1,5}X_2^{2-}$	2.32E+08	2.49E+08	2.36E+08
371.1132	$^{1,5}X_1$	13165855	12868573	13144080
374.609	$^{1,5}X_3\text{-}SO_3$	2395920	2023263	2366535
414.5873	$^{1,5}X_3$	26867350	27028522	25097532
302.5456	$^{1,5}A_3$	1392313	1020366	1168388
137.9866	$^{1,3}A_2$	4567462	3120292	3555916
138.9706	$^{1,3}A_1$	13807556	8540340	10248340
223.0759	$^{0,2}X_0$	3386159	2257461	2230949
340.5688	$^{0,2}X_2$	4182089	3183020	3004299
385.1291	$^{0,2}X_1$-SO3	22219004	13832533	17028420
232.0392	$^{0,2}X_2$	7102250	4989494	6196831
421.5947	$^{0,2}X_3^{2-}$	4161789	5411991	4534173

295.0673	$^{0,2}A_2$	14893086	11183250	12179266
325.1078	Z_1	30709620	41884264	36519688
501.1404	Z_2-SO_3	41422232	28799298	33621756
250.0662	$[Z_2\text{-}SO3]^{2-}$	9631083	6243205	7782201
421.1832	Z_2-$2SO_3$	12292547	7636148	9425286
351.6059	$[Z_3\text{-}SO_3]^{2-}$	1735726	991081	1337409
290.0447	Z_2^{2-}	8951083	6386202	7897569
391.5844	Z_3^{2-}	12741263	14796792	14301805
263.1613	Y_1-SO_3	2255707	1426679	1613432
343.1184	Y_1	1.96E+08	1.41E+08	1.61E+08
519.1504	Y_2-SO_3	3593079	3008591	2589491
259.0716	$[Y_2\text{-}SO_3]^{2-}$	17174934	11674326	14782764
439.1938	Y_2-$2SO_3$	6037843	4509797	4356351
360.6114	$[Y_3\text{-}SO_3]^{2-}$	1.3E+08	86975832	1.05E+08
642.2733	Y_3-$2SO_3$	2100503	1024713	1772947
599.1073	Y_2	3750195	5696699	4746990
299.05	Y_2^{2-}	16019182	14858093	14877801
266.724	Y_3^{3-}	14802051	9626302	12083741
400.5898	Y_3^{2-}	3.66E+08	3.1E+08	3.17E+08
572.1488	C_3-SO_3	3761424	4564991	3721380
652.1036	C_3	24545506	35273536	28989608
325.5482	C_3^{2-}	22672108	18396212	22408040
396.1151	C_2	34861296	31166476	32000104

193.0354	C_1	56956608	40170060	46060664
554.1355	B_3-SO_3	1370768	1976731	1361046
276.5646	$[B_3\text{-}SO_3]^{2-}$	5203213	4073069	4941307
634.0932	B_3	2354586	3440797	2724808
316.5431	B_3^{2-}	17792328	13739761	14695594
378.1046	B_2	14859884	10971101	12500551
175.0248	B_1	26089024	19668372	20817302

Supplemental Table 48. Mass list for 3a, $[M\text{-}4H+Na]^{3-}$ precursor ion

Mass to charge	Type	Intensity	Intensity	Intensity
302.4989	$[^{3,5}A_3+Na]^{2-}$	1296317	3532304	3259765
526.05	$^{3,5}A_3$+Na-SO_3	574866	1740049	1410033
606.0059	$^{3,5}A_3$+Na	2682316	8034884	5530886
167.9887	$[^{2,4}A_2+Na]^{2-}$	7222455	14595523	20050722
257.028	$^{2,4}A_2$+Na-SO_3	1604500	3370492	3873326
336.9848	$^{2,4}A_2$	14708487	30636918	35915760
288.5016	$[^{2,4}A_3+Na]^{2-}$	6032714	11081107	13616555
404.5729	$[^{1,5}X_3+Na]^{2-}$	2671910	6684575	6106927
371.1133	$^{1,5}X_1$	4905833	14099756	11514096
226.9865	$^{1,5}A_1$	1011505	2694547	2546427
453.0199	$[^{1,5}A_4+Na]^{2-}$	4366834	15685561	12201267
138.9707	$^{1,3}A_1$	4709786	8578739	10372421

160.9527	$^{1,3}A_1$+Na	1423735	3027669	3271940
137.9867	$^{1,3}A_2$	10067876	19861122	23107076
159.9686	$^{1,3}A_2$+Na	4000497	8548664	9526759
300.7029	$[^{0,2}X_3+Na]^{3-}$	735562	567777	
223.0755	$^{0,2}X_0$	893006	1647876	1885095
385.1288	$^{0,2}X_1$	5354427	12439857	13591553
197.999	$[^{0,2}A_2+Na]^{2-}$	699677	1130616	1919601
295.0672	$^{0,2}A_2$-SO_3	1354071	2544935	2659832
375.0241	$^{0,2}A_2$	2818648	6018072	7678707
397.0062	$^{0,2}A_2$+Na	2404487	5854855	6620127
325.1076	Z_1	4769412	14055604	12245965
501.1401	Z_2	18039988	55170172	43524156
523.1222	Z_2+Na	2516275	6431381	6648484
764.1495	Z_3+Na	2778751	9505578	6701809
259.0714	Y_2^{2-}	16110788	30352780	35083044
343.1182	Y_1	94945120	183540160	2.1E+08
365.1003	Y_1+Na	3703404	7579423	9153549
390.5751	$[Y_3+Na]^{2-}$	10190402	22539358	23153272
439.1936	Y_2-SO_3	11994233	27614940	30475332
519.1506	Y_2	19095812	44423932	45720728
541.1327	Y_2+Na	11823909	26886140	29990208
782.1541	Y_3+Na	1513671	4019651	3787008
193.0354	C_1-SO_3	3211882	6676691	8036518

267.4962	$[C_2+Na]^{2-}$	7272381	15408505	16894044
272.9922	C_1	9935768	18757676	19567312
294.9742	C_1+Na	9985806	24763668	25518666
344.5216	C_3^{2-}	1017832	1031898	1312024
355.512	$[C_3+Na]^{2-}$	2063729	4787591	5685269
456.0434	$C_2+Na\text{-}SO_3$	17605438	39149364	44723496
536.0004	C_2+Na	17630782	46317308	44400076
632.0763	$C_3+Na\text{-}SO_3$	949108	2994561	1889174
712.0343	C_3+Na	1836496	6544140	5074494
175.0248	$B_1\text{-}SO_3$	3226444	6764392	6989816
247.5	B_2^{2-}	2218656	3853958	3546246
254.9816	B_1	9073984	18352314	20172108
258.491	$[B_2+Na]^{2-}$	55768516	103936808	1.21E+08
276.9636	B_1+Na	7663161	16520707	19009724
306.5286	$[B_3+Na\text{-}SO3]^{2-}$	6669263	13118642	17605078
346.5069	$[B_3+Na]^{2-}$	34608984	65420492	62058600
416.0512	$B_2\text{-}SO_3$	880681	2356010	2347185
438.0327	$B_2+Na\text{-}SO_3$	10385348	22807600	27756008
517.9896	B_2+Na	4923296	12684475	13147943

Supplemental Table 49. Mass list for 3b, $[M-4H+Na]^{3-}$ precursor ion

Mass to charge	Type	Intensity	Intensity	Intensity
223.0758	$^{0,2}X_0$	1166141	877998	1410666
526.0481	$^{3,5}A_3$+Na-SO_3	2043188	1803875	2683811
606.0045	$^{3,5}A_3$+Na	8641429	7813316	10129546
302.4994	[$^{3,5}A_3$+Na]2-	3315940	2580831	3721313
257.0284	$^{2,4}A_2$+Na	3168406	3003445	4289856
235.0462	$^{2,4}A_2$	5003937	4080141	6296988
404.5733	$^{1,5}X_3$+Na-SO_3	2817507	2679748	2880190
444.5512	$^{1,5}X_3$+Na	12247588	11650109	17028676
547.1451	$^{1,5}X_2$	4963987	4563442	6827706
371.1135	$^{1,5}X_1$	12934848	10927500	15253567
159.9685	$^{1,3}A_2$+Na	3297442	2834955	3761150
137.9864	$^{1,3}A_2$	13630839	12599873	15300000
160.9525	$^{1,3}A_1$+Na	4570000	3933225	5265356
138.9704	$^{1,3}A_1$	12768480	11145720	15369239
451.5597	[$^{0,2}X_3$+Na]$^{2-}$	2844572	2278796	3742319
385.1298	$^{0,2}X_1$	9368524	6593882	11850472
397.0064	$^{0,2}A_2$+Na	43409692	38028064	52479192
375.0242	$^{0,2}A_2$	1872356	1472244	1845878
197.9995	[$^{0,2}A_2$+Na]$^{2-}$	1139773	1742727	1354313
652.0103	$^{0,2}A_3$+Na	2479832	2275906	2586184
325.1081	Z_1	10936856	10170320	14413413

523.1211	Z_2+Na	2204812	1987405	2722462
501.1398	Z_2	31038696	28077654	38164720
764.1464	$[Z_3+Na-SO_3]^{2-}$	2401943	1759261	2340788
421.5488	$[Z_3+Na]^{2-}$	5290249	5350121	7358968
365.1004	Y_1+Na	5492316	4830407	6898582
343.1187	Y_1	1.56E+08	1.41E+08	1.8E+08
439.1937	Y_2-SO_3	8180905	7237816	10062591
541.1321	Y_2+Na	9806904	8957386	12319876
519.1501	Y_2	5898365	5261595	7427824
259.0719	Y_2^{2-}	15554930	14821769	18842114
390.5758	$[Y_3+Na-SO_3]^{2-}$	28294484	27096560	36210944
286.7004	$[Y_3+Na]^{3-}$	38461128	37001908	49066484
430.5537	$[Y_3+Na]^{2-}$	76520272	72677504	94836496
632.073	C_3+Na-SO_3	2053909	2097142	2815521
712.0291	C_3+Na	3958926	3659355	5564591
355.513	$[C_3+Na]^{2-}$	4062126	3462177	5643413
456.0435	C_2+Na-SO_3	31748904	27882164	38848740
535.9998	C_2+Na	17626022	16808904	21980836
267.4967	$[C_2+Na]^{2-}$	36567724	34020928	46415680
215.0176	C_1+Na	1655522	1340492	1755530
193.0355	C_1	6621445	5776325	7579619
306.5292	$[B_3+Na-SO_3]^{2-}$	14180960	13143426	17458340
346.5075	$[B_3+Na]^{2-}$	1.05E+08	97056528	1.3E+08

438.033	B_2+Na-SO_3	19026214	16978296	23544824
416.0512	B_2-SO_3	1418245	1214588	1336081
207.5218	$[B_2\text{-}SO_3]^{2-}$	4899965	4486133	5153271
336.0946	B_2-2SO_3	1488467	1149106	1515006
517.9895	B_2+Na	5653592	5524762	6697961
258.4914	$[B_2+Na]^{2-}$	18353146	18274574	22510906
247.5002	B_2^{2-}	1811276	1743661	1656579
175.0248	B_1	6572079	6514844	7538099

Supplemental Table 50. Mass list for 3c, $[M-4H+Na]^{3-}$ precursor ion

Mass to charge	Type	Intensity	Intensity	Intensity
526.0482	$^{3,5}A_3$+Na	6325660	6177450	5228130
257.0281	$^{2,4}A_2$+Na	1.80E+07	17148488	1.59E+07
371.1134	$^{1,5}X_1$	4881856	4790737	3948909
649.0819	$^{1,5}X_2$+Na	5.36E+07	45848120	4.04E+07
444.5509	$^{1,5}X_3$+Na	1.24E+07	10219498	9376419
160.9525	$^{1,3}A_3$+Na	2047511	2099742	1850493
138.9704	$^{1,3}A_3/^{1,3}A_2$	1.13E+07	10995292	9723097
159.9684	$^{1,3}A_2$+Na	8563459	9499477	8480213
137.9864	$^{1,3}A_2$	1.63E+07	18173986	1.58E+07
385.1288	$^{0,2}X_1$-SO_3	4585378	5234053	4025406
487.0655	$^{0,2}X_1$+Na	3806452	2799484	2853629

232.0393	$^{0,2}X_1^{2-}$	2694772	3268881	2467571
223.076	$^{0,2}X_0$	1759071	1367138	1152263
370.5332	$[^{0,2}X_2+Na]^{2-}$	1590411	1376969	1424052
451.5583	$[^{0,2}X_3+Na]^{2-}$	2776002	2792743	2486643
295.0671	$^{0,2}A_2$	2856583	2443787	1915385
325.108	Z_1	1.58E+07	13877774	1.14E+07
523.1212	$Z_2+Na\text{-}SO_3$	1.18E+07	14052412	1.18E+07
501.1395	$Z_2\text{-}SO_3$	1448346	1844284	1843273
250.0663	$[Z_2\text{-}SO_3]^{2-}$	1581749	1587757	1725699
764.1452	$Z_3+Na\text{-}SO_3$	2207030	1940467	1830435
381.5701	$[Z_3+Na\text{-}SO_3]_{2-}$	1480397	1492003	2026119
603.0772	Z_2+Na	4832664	4176272	3555205
301.0358	$[Z_2+Na]^{2-}$	2.10E+07	26043782	2.47E+07
290.0449	Z_2^{2-}	1675820	842553	1255236
421.5483	$[Z_3+Na]^{2-}$	1.40E+07	11345574	1.03E+07
365.1003	Y_1+Na	5693326	6032984	5595992
343.1185	Y_1	1.09E+08	1.06E+08	9.00E+07
541.1315	$Y_2+Na\text{-}SO_3$	9856662	9292695	8543154
259.0717	$[Y_2\text{-}SO3]^{2-}$	4098259	3821591	3395278
390.5754	$[Y_3\text{-}SO3]^{2-}$	2.45E+07	26866992	2.69E+07
621.0876	Y_2+Na	9785342	7316703	6403490
310.0412	$[Y_2+Na]^{2-}$	1.15E+08	1.06E+08	9.58E+07
299.0501	Y_2^{2-}	4.21E+07	34521588	3.10E+07

286.7003	$[Y_3+Na]^{3-}$	3462393	3928728	4095327
430.5535	$[Y_3+Na]^{2-}$	6.50E+07	56532016	5.72E+07
456.043	C_2+Na	2.80E+07	26713810	2.39E+07
434.06	C_2	1538126	1538743	1.14E+06
632.0766	C_2+Na-SO3	3460652	2797829	3141723
315.5342	$[C_2+Na-SO_3]^{2-}$	2616541	2538117	2335885
712.0338	C_3+Na	1.12E+07	10430136	9709534
355.5127	[C_3+Na]2-	5863184	6234512	4749426
215.0175	C_1+Na	2964833	3090054	2283381
193.0354	C_1	2.06E+07	20849102	1.84E+07
336.0941	B_2-SO_3	1.27E+07	12513297	1.11E+07
438.0324	B_2+Na	3.62E+07	34036428	3.11E+07
416.0505	B_2	1.52E+07	13643862	1.25E+07
207.5217	B_2^{2-}	8210831	7933658	7126378
614.0629	B_3+Na-SO_3	5449349	4062907	3657268
306.5289	$[B_3+Na-SO_3]^{2-}$	1.60E+07	15008053	1.41E+07
346.5072	$[B_3+Na]^{2-}$	8.83E+07	84764336	7.85E+07
175.0248	B_1	5120295	5059434	4189024

Supplemental Table 51. Mass list for 3d, $[M-4H+Na]^{3-}$ precursor ion

Mass to charge	Type	Intensity	Intensity	Intensity
504.0671	$^{3,5}A_3$+Na	3019730	2690718	2748338

257.0282	$^{2,4}A_2$+Na	1.14E+07	1.01E+07	8213772
473.0524	$^{1,5}X_1$+Na	5812013	4696040	4903205
569.1273	$^{1,5}X_2$+Na-SO_3	2194368	1936356	1816670
627.1034	$^{1,5}X_2$	1499001	977963	1025673
649.0841	$^{1,5}X_2$+Na	3.07E+07	2.83E+07	2.90E+07
444.5515	[$^{1,5}X_3$+Na]$^{2-}$	1.02E+07	8619555	9951654
137.9865	$^{1,3}A_3$	1.49E+07	1.45E+07	1.23E+07
159.9686	$^{1,3}A_2$+Na	6296114	6040000	5494977
138.9706	$^{0,4}A_2$	2.98E+06	2920000	5494977
232.0394	$^{0,2}X_1^{2-}$	2205156	2033670	1718240
385.1294	$^{0,2}X_1$+Na-SO_3	4824626	3948057	3374799
487.0671	$^{0,2}X_1$+Na	5280689	4994736	4338843
223.0759	$^{0,2}X_0$	1661972	1391414	1014644
451.5587	[$^{0,2}X_3$+Na]$^{2-}$	2298181	1867811	2363613
295.0675	$^{0,2}A_2$	4519518	4108080	3554585
250.0663	[Z_2-SO_3]$^{2-}$	2656023	2527108	2377356
290.0448	Z_2^{2-}	2187501	1909187	1823365
301.0359	[Z_2+Na]$^{2-}$	4.10E+07	3.89E+07	3.84E+07
325.108	Z_1-SO_3	6167100	5703414	4577611
405.0652	Z_1	2633426	1870574	1889972
421.5483	[Z_3+Na]$^{3-}$	7926106	6180164	7905881
427.0473	Z1+Na	1.19E+07	9440449	9507397
501.1403	Z_2-SO_3	4647046	3262143	3513124

523.1226	Z_2+Na-SO_3	9314176	8805996	7415197
581.0973	Z_2	5613088	4784932	5119645
603.0784	Z_2+Na	2.21E+07	1.80E+07	1.90E+07
211.034	Y_1^{2-}	9.51E+07	9.17E+07	8.95E+07
259.0718	$[Y_2\text{-}SO_3]^{2-}$	1.40E+06	1.33E+06	1514001
222.0249	$[Y_1+Na]^{2-}$	1333350	1614592	1269641
286.7004	$[Y_3+Na]^{3-}$	4463719	5138932	5050166
621.0919	Y_2+Na	3213812	2795273	2816983
299.0502	Y_2^{2-}	2.50E+07	2.35E+07	2.15E+07
310.0413	$[Y_2+Na]^{2-}$	1.83E+08	1.71E+08	1.62E+08
343.1185	$Y_1\text{-}SO_3$	2.88E+07	2.68E+07	2.26E+07
365.1005	Y_1+Na-SO_3	1.24E+07	1.13E+07	9265747
390.5757	$[Y_3+Na\text{-}SO_3]^{2-}$	1.12E+07	1.20E+07	1.21E+07
423.0756	Y_1	2453659	2616985	2332267
430.5537	$[Y_3+Na]^{2-}$	6.26E+07	5.63E+07	5.91E+07
445.0576	Y_1+Na	4.16E+07	3.65E+07	3.35E+07
541.1329	Y_2+Na-SO_3	6492467	6577430	6028420
621.0893	Y_2+Na	3213812	2795273	2816983
193.0355	C_1	2.84E+07	2.57E+07	2.33E+07
215.0173	C_1+Na	2012768	1782210	1576689
354.105	$C_2\text{-}SO_3$	2485080	2539524	1899643
434.0616	C_2	4699490	3794942	3454300
456.0437	C_2+Na	1.53E+07	1.46E+07	1.33E+07

552.1188	C_3+Na-SO3	2835352	2459962	2528621
632.0754	C_3+Na	2928760	2817722	3192715
175.0248	B_1	6210414	5182627	4645872
207.5217	B_2^{2-}	4325153	4618663	4261016
295.538	B_3^{2-}	4987682	5107061	4093459
306.5289	$[B_3+Na]^{2-}$	5594591	5760800	4490868
336.0941	B_2-SO_3	2.21E+07	1.99E+07	1.84E+07
416.0509	B_2	2.84E+07	2.67E+07	2.61E+07
438.033	B_2+Na	3.08E+07	2.83E+07	2.79E+07
534.1087	B_3+Na-SO_3	2224983	2013771	1918878
614.0654	B_3+Na	2.24E+07	2.19E+07	2.19E+07

Supplemental Table 52. Mass list for 3e, $[M-4H+Na]^{3-}$ precursor ion

Mass to charge	Type	Intensity	Intensity	Intensity
526.0487	$^{3,5}A_3$	3010492	2970918	7201154
235.0468	$^{2,4}A_2$	758916	633646	1140940
257.028	$^{2,4}A_2$+Na	12824724	11666714	22327536
371.1133	$^{1,5}X_1$	2986423	2797993	5687020
649.084	$^{1,5}X_2$+Na	6203734	7078469	16308934
444.5514	$[^{1,5}X_2+Na]^{2-}$	2915743	2899876	8072554
138.9707	$^{1,3}A_3$	2320185	2461135	4091779
160.9526	$^{1,3}A_3$+Na	798811	795148	1138333
159.9686	$^{1,3}A_2$	4517123	9528111	9033248

137.9867	$^{1,3}A_2$+Na	10147960	3858490	20047048
451.5575	[$^{0,2}X_3$+Na]2-	1284551	1412567	3549947
317.0493	$^{0,2}A_2$+Na	1858728	1123073	2553187
295.0671	$^{0,2}A_2$	2444163	1787281	4624740
325.1078	Z_1	3334939	2942248	6102916
501.1401	Z_2-SO_3	642118	661845	752949
603.0791	Z_2	10416531	10120866	27448318
581.0987	Z_2+Na	944719	852592	1794242
421.5484	[Z_2+Na]$^{2-}$	3290354	3685826	9303588
365.1004	Y_1+Na	1078246	1049903	1433730
343.1183	Y_1	2.36E+08	2.14E+08	3.94E+08
390.5752	[Y_3+Na-SO_3]$^{2-}$	3016976	3548503	5834638
621.0896	Y_2+Na	1888469	1903033	4678952
310.0409	[Y_2+Na]$^{2-}$	8223750	11488580	15229283
299.0501	Y_2^{2-}	1235625	2595031	2224641
286.7002	[Y_3+Na]$^{3-}$	701579	586520	1305708
430.5537	[Y_3+Na]$^{2-}$	9516300	11406181	26579844
456.0434	C_2+Na	31035276	29161124	68107160
227.5177	[C_2+Na]$^{2-}$	749811	701668	1405314
315.5331	[C_3+Na-SO_3]$^{2-}$	759287	1130534	1608119
712.0322	C_2+Na	4593818	4628571	11641135
355.5126	[C_3+Na]$^{2-}$	2921537	3109662	3923885
215.0173	C_1	2203653	1899537	4065745

193.0355	B_1	9302481	9073122	18685114
336.094	B_2-SO_3	1592005	2079289	2630860
438.0328	B_2+Na	7308309	7202464	15007184
416.0505	B_2	2946551	2945410	6993843
614.075	B_3+Na-SO_3	3698658	3583628	9884447
306.5288	$[B_3\text{-}SO_3]^{2-}$	28241800	25599212	58021244
534.1082	B_3+Na-2SO_3	397086	676727	1367747
223.3416	B_3^{3-}	613532	585571	1112285
346.5071	$[B_3+Na]^{2-}$	4.71E+08	4.38E+08	8.5E+08
175.0248	B_1	1704274	2069228	3837495
207.5217	B_2^{2-}	443695	581021	1428241

Supplemental Table 53. Mass list for 3f, $[M\text{-}4H+Na]^{3-}$ precursor ion

Mass to charge	Type	Intensity	Intensity	Intensity
568.0588	$^{3,5}A_3$+Na	3169551	2422242	2228943
351.0009	$^{3,5}A_2$+Na	2159655	1822259	2091665

444.5089	$[^{3,5}A_4+Na]^{2-}$	4891406	4469457	3324023
442.554	$[^{2,4}X_2+Na]^{2-}$	4755477	3960611	3941326
257.0281	$^{2,4}A_2+Na$	3508733	3228143	2881128
413.1237	$^{1,5}X_1$	6090364	4910386	4909060
691.0945	$^{1,5}X_2+Na$	17507536	15518637	13684399
446.5833	$[^{1,5}X_3+Na\text{-}SO_3]^{2-}$	2545274	2625983	2038363
486.5617	$[^{1,5}X_3+Na]^{2-}$	39274812	35181864	30604678
628.0798	$^{1,5}A_3+Na\text{-}SO_3$	4117619	3770481	3438442
160.9526	$^{1,3}A_3+Na/^{0,4}A_2+Na$	8104938	6574874	6871212
138.9707	$^{1,3}A_3/^{0,4}A_2$	24637250	20293468	20551604
427.1399	$^{0,2}X_1\text{-}SO_3$	4982853	4313170	3984259
529.0777	$^{0,2}X_1$	6985964	6780871	5758091
493.5694	$^{0,2}X_1+Na$	5876353	5251705	4848329
397.0061	$[^{0,2}X_3+Na]^{2-}$	33578612	32889646	25239330
187.0084	$^{0,2}A_2{}^{2-}$	4437149	4287618	3400626
367.1183	Z_1	22942552	22689908	17156974
565.1326	$Z_2+Na\text{-}SO_3$	5934525	5715214	5104254
543.1507	$Z_2\text{-}SO_3$	3392279	3171412	2984783
271.0715	[Z2-SO3]2-	8284767	9546820	6088478
645.0895	Z_2+Na	13109040	12883620	9870525
322.041	$[Z_2+Na]^{2-}$	63966488	73397800	46956024
311.0499	$Z_2{}^{2-}$	2609051	2962832	2105316

463.5589	$[Z_3+Na]^{2-}$	45149060	41034844	35881832
407.111	Y_1+Na	10811056	10601184	8374953
385.1289	Y_1	73658992	76793968	56991588
583.1431	$Y_2+Na-SO_3$	5372735	5816366	4576154
280.0768	Y_2-SO_3	1612667	2006527	1656595
432.5861	$[Y_3+Na-SO_3]^{2-}$	52780484	64327400	42255544
663.0997	Y_2+Na	8191180	8211126	6763587
331.0463	$[Y_2+Na]^{2-}$	90258704	1.12E+08	67247632
314.7072	$[Y_3+Na]^{3-}$	98007576	1.29E+08	69716480
472.5642	$[Y_3+Na]^{2-}$	2.94E+08	3.06E+08	2.39E+08
396.1151	C_2-SO_3	3066497	2909268	2104130
498.0541	C_2+Na	9651722	9033176	7923431
476.0718	C_2	9920760	9954576	8303512
237.5323	C_2^{2-}	3216180	3867490	2461464
193.0355	C_1	10660580	9661762	8262612
376.5178	$[C_3+Na]^{2-}$	7079357	6756462	7146252
378.1045	B_2-SO_3	12129939	12724233	9339102
480.0432	B_2+Na	10741470	10695881	8327224
458.0612	B_2	11168538	12222701	9511880
228.527	B_2^{2-}	4084066	4514636	2739833
175.0249	B_1	11886065	12372981	8846988
327.5341	$[B_3+Na-SO_3]^{2-}$	6217475	7172050	4310007
367.5125	$[B_3+Na]^{2-}$	36896064	44746456	28587928

Supplemental Table 54. Mass list for 3g, $[M-4H+Na]^{3-}$ precursor ion

Mass to charge	Type	Intensity	Intensity	Intensity
336.9851	$^{2,4}A_2$+Na	3417203	4847579	2758559
413.1238	$^{1,5}X_1$	1608340	2223040	1882518
446.5844	$^{1,5}X_3$+Na	622413	675123	480865
226.9869	$^{1,5}A_1$	852491	1488901	1647938
160.9525	$^{1,3}A_1$+Na	2296731	3230019	2307444
138.9704	$^{1,3}A_1$	8029150	12317395	8680865
427.1399	$^{0,2}X_1$	4841438	6787362	4099093
397.0062	$^{0,2}A_2$+Na-SO_3	7411468	9952519	6488470
375.0244	$^{0,2}A_2$-SO_3	1.19E+07	12348125	8358974
476.9631	$^{0,2}A_2$+Na	1005086	1344587	1131254
237.9778	$[^{0,2}A_2+Na]^{2-}$	1.16E+07	16038270	1.17E+07
304.011	$^{0,2}A_4^{3-}$	439893	601867	600414
367.1185	Z_1	2407576	3587273	3840246
565.1307	Z_2+Na	677272	1269839	1024815
543.1508	Z_2	7245054	10586461	8466306
271.0717	Z_2^{2-}	5154713	6714853	5341643
407.1112	Y_1+Na	1801977	2953360	2199471
385.129	Y_1	3.41E+07	47655608	3.37E+07
583.1434	Y_2+Na	1454227	2455325	1719038

280.0769	Y_2^{2-}	1834082	3248872	2089277
432.5861	$[Y_3+Na]^{2-}$	4.88E+07	70124392	5.48E+07
498.0539	$C_2+Na-SO_3$	8436823	11647904	7536828
578.0105	C_2+Na	5110883	6883860	5442739
288.5017	$[C_2+Na]^{2-}$	7896249	9851609	9140125
193.035	C_1-SO_3	439641	775949	571811
294.9744	C_1+Na	2655221	3547251	2843194
272.9926	C_1	552966	732516	715787
754.0424	C_3+Na	826815	1312474	1456792
480.0434	$B_2+Na-SO_3$	2628770	3385264	2510635
458.061	B_2-SO_3	1140784	1160266	935430
228.5269	$[B_2-SO_3]^{2-}$	1038608	1467071	1357059
279.4964	$[B_2+Na]^{2-}$	8893122	13669957	1.01E+07
268.5056	B_2^{2-}	1768710	2174860	1728934
175.0248	B_1-SO_3	1272124	1818593	1078689
276.9637	B_1+Na	2093508	2645530	1708147
254.9818	B_1	1.20E+07	16575485	1.26E+07
367.5125	$[B_3+Na]^{2-}$	2055413	2702973	2467188

Supplemental Table 55. Mass list for 3h, $[M-4H+Na]^{3-}$ precursor ion

Mass to charge	Type	Intensity	Intensity	Intensity
606.0057	$^{3,5}A_3$+Na	3884920	5619448	4673371
302.4992	$[^{3,5}A_3+Na]^{2-}$	4010437	3928219	4389697
351.0008	$^{3,5}A_2$+Na	3266190	2449029	3015898
257.0281	$^{2,4}A_2$+Na	4317422	4214081	4781087
235.046	$^{2,4}A_2$	1377512	618442	953035
371.1135	$^{1,5}X_1$	9420831	11566907	10869621
547.1456	$^{1,5}X_2$	7821058	8952708	8543301
404.5736	$[^{1,5}X_3+Na-SO_3]^{2-}$	2023562	2317250	2078062
444.5512	$[^{1,5}X_3+Na]^{2-}$	26877990	32703042	31578272
159.9685	$^{1,3}A_2$+Na	6783930	5399747	6397605
137.9865	$^{1,3}A_2$	19424796	14705326	16897360
160.9525	$^{0,4}A_2$+Na	5293285	4101298	4766958
138.9705	$^{0,4}A_2$	19539516	14923148	18503894
385.1293	$^{0,2}X_1$	17988174	13585778	16005194
223.0758	$^{0,2}X_0$	1780263	1297227	1367068
451.5592	$[^{0,2}X_3+Na]^{2-}$	2394590	3101538	2978839
397.0064	$^{0,2}A_2$+Na	32952532	27725024	31627098
375.0243	$^{0,2}A_2$	1290004	1172636	1063417
187.0083	$^{0,2}A_2^{2-}$	3619599	3423691	3371081
325.1079	Z_1	13904978	13556640	13745227
421.1842	Z_2-SO_3	2210913	2532787	2115592

523.1222	Z_2+Na	21054136	18640954	21437256
501.14	Z_2	23352196	24622700	25037994
250.0664	Z_2^{2-}	8151763	6566651	8118707
764.148	Z_3+Na-SO_3	1687668	1734864	1676258
381.5703	[Z_3+Na-SO_3]$^{2-}$	2583531	2302867	3009855
280.6969	[Z_3+Na]$^{3-}$	2005756	1320185	1644791
421.5489	[Z_3+Na]$^{2-}$	2773846	3065659	3775661
263.1617	Y_1-SO_3	2071384	1687059	1546338
365.1004	Y_1+Na	10727273	9701851	10161977
343.1185	Y_1	1E+08	88141592	98129144
439.194	Y_2-SO_3	73672480	65028000	73628064
541.1328	Y_2+Na	32130974	30079736	33083882
519.1509	Y_2	22361638	22168882	23573136
259.0716	Y_2^{2-}	1.53E+08	1.32E+08	1.49E+08
390.5757	[Y_3+Na-SO_3]$^{2-}$	19298164	15803088	18971006
286.7003	[Y_3+Na]$^{3-}$	24656940	20612384	22657142
430.5538	[Y_3+Na]$^{2-}$	82910376	1.01E+08	95888368
456.0435	C_2+Na-SO_3	13325671	11330588	12457711
536	C_2+Na	15261289	16166002	15843977
267.4965	[C_2+Na]$^{2-}$	11486631	11232580	12357585
215.0175	C_1+Na	2231751	1620724	1727799
193.0354	C_1	17416506	14955259	17084164
632.0752	C_3+Na-SO_3	3192977	3883421	3240696

712.0307	C_3+Na	4188929	4889268	4885867
355.5128	$[C_3+Na]^{2-}$	7300344	6416185	7624321
344.5213	C_3^{2-}	1434300	586033	1237405
438.033	B_2+Na-SO_3	1.02E+08	89928728	1.01E+08
416.0511	B_2	3906121	2329204	2791307
207.5216	$[B_2-SO_3]^{2-}$	30025370	24545446	29398638
336.0938	B_2-2SO_3	4184413	2594492	3774248
517.9901	B_2+Na	16546667	14209308	16575340
258.4911	$[B_2+Na]^{2-}$	1.27E+08	1.1E+08	1.24E+08
247.5002	B_2^{2-}	7240663	5784942	7392239
175.0248	B_1	9064512	7069957	7618775
346.5074	$[B_3+Na]^{2-}$	31426172	29354790	32269380

Supplemental Table 56. Mass list for 3i, $[M-4H+Na]^{3-}$ precursor ion

Mass to charge	Type	Intensity	Intensity	Intensity
235.0461	$^{2,4}A_2$	6095704	5708069	7662294
257.0282	$^{2,4}A_2$+Na	14672342	15986492	16973246
473.0523	$^{1,5}X_1$+Na	2877967	3652474	2861360
159.9685	$^{1,3}A_2$+Na	5515815	5499487	6395495
232.0393	$^{0,2}X_1^{2-}$	3575836	4303758	5586101
385.1291	$^{0,2}X_1$-SO_3	6427921	7118606	9067832
487.0678	$^{0,2}X_1$+Na	6866344	8967269	11023825

223.0758	$^{0,2}X_0$	2296951	2046143	2498658
295.0674	$^{0,2}A_2$	41433516	42379640	49449228
250.0664	$[Z_2\text{-}SO_3]^{2-}$	2635091	2366032	2671868
290.0449	Z_2^{2-}	3587653	4110679	3902428
301.0358	$[Z_2+Na]^{2-}$	2E+08	2.15E+08	2.31E+08
325.1079	$Z_1\text{-}SO_3$	9311903	11120148	12070221
381.5703	$[Z_3+Na\text{-}SO3]^{2-}$	4131877	4438224	4609380
421.5488	$[Z_3+Na]^{2-}$	2219367	1968444	2042850
427.0471	Z_1	4721492	5890587	6141419
523.1217	$Z_2+Na\text{-}SO_3$	15876294	16283533	19806644
603.0788	Z_2+Na	4697920	5571375	5667516
764.1458	$Z_3+Na\text{-}SO_3$	3428790	3760238	4022335
211.0339	Y_1^{2-}	1.18E+08	1.21E+08	1.32E+08
222.0249	$[Y_1+Na]^{2-}$	3103792	3695178	3442705
259.0716	$[Y_2\text{-}SO_3]^{2-}$	2982683	3231133	2027269
286.7002	$[Y_3+Na]^{3-}$	27341288	30398538	29660670
299.0501	Y_2^{2-}	22711064	22432704	27117660
310.0411	$[Y_2+Na]^{2-}$	2.65E+08	2.69E+08	2.97E+08
343.1185	$Y_1\text{-}SO_3$	51000916	52660196	58405440
365.1005	$Y_1+Na\text{-}SO_3$	19231044	23070818	24487512
390.5755	$[Y_3+Na\text{-}SO_3]^{2-}$	44748240	46556800	48740900
423.0752	Y_1	2857038	2972521	3721266
430.554	$[Y_3+Na]^{2-}$	37740152	40615264	40682688

445.0573	Y_1	1.17E+08	1.31E+08	1.49E+08
541.1326	Y_2+Na-SO_3	12234378	11165996	12020393
193.0355	C_1	35000056	37425912	40897796
354.1046	C_2-SO_3	27349860	27948186	31377986
434.0614	C_2	9680554	10199488	11576688
456.0434	C_2+Na	24764114	26596388	30505846
552.1182	C_3+Na-SO_3	2780743	3392515	3633203
632.0738	C_3+Na	3208123	3043455	3168508
175.0248	B_1	12790164	12459665	13889165
207.5217	B_2^{2-}	5238247	5830423	5456656
295.5379	B_3^{2-}	16586330	17023792	19131400
306.5289	$[B_3+Na]^{2-}$	7584958	9386479	9673348
336.094	B_2-SO_3	58436740	62339492	68799808
416.051	B_2	38637960	39947732	42546548
438.0329	B_2+Na	39685360	38687232	42480700
512.1262	B_3-SO_3	2926105	3627586	3374982
534.108	B_3+Na-SO_3	3591842	3942113	4187013
614.0645	B_3+Na	39492632	37713152	41220480

Supplemental Table 57. Mass list for sample 3j, $[M-4H+Na]^{3-}$ precursor ion

Mass to charge	Type	Intensity	Intensity	Intensity
444.5104	$[^{3,5}A_4+Na]^{2-}$	788890	1200049	939722
442.5558	$[^{2,4}X_2+Na]^{2-}$	823807	900547	769384
691.0954	$^{1,5}X_1+Na$	1015891	972927	1354847
486.5615	$[^{1,5}X_3+Na]^{2-}$	2151788	2053585	2111592
430.0667	$^{1,5}A_2$	3902633	4179090	3687985
160.9525	$^{0,4}A_2+Na$	925476	585084	774294
138.9705	$^{0,4}A_2$	2586993	2436402	2257371
529.079	$^{0,2}X_1+Na$	886699	777055	593506
397.0063	$^{0,2}A_2+Na$	2590631	1667005	1884989
375.0256	$^{0,2}A_2$	1520748	1444189	1420448
187.0084	$^{0,2}A_2^{2-}$	873446	465976	586258
367.1185	Z_1	3421583	1730409	2440125
271.0718	Z_2-SO_3	850048	788065	849330
645.0875	Z_2+Na	2071721	1735773	1950565
322.0411	$[Z_2+Na]^{2-}$	15986340	12639379	13185950
463.5592	$[Z_3+Na]^{2-}$	3633086	3953809	3370321
407.1113	Y_1+Na	1222370	1172261	1170104
385.1291	Y_1	6938938	5373554	5842771
583.1435	Y_2+Na-SO_3	861968	596013	425964
432.5861	Y_3+Na-SO_3	11031441	8664174	8733028
663.0999	Y_2+Na	786312	827770	440294

331.0465	$[Y_2+Na]^{2-}$	17749454	13359074	14821590
314.7072	$[Y_3+Na]^{3-}$	37570076	34213648	31679210
472.5643	$[Y_3+Na]^{2-}$	35891788	34504852	32550248
396.1162	C_2-SO_3	483950	690507	583341
498.0547	C_2+Na	1276965	1305499	869869
476.0717	C_2	1926725	1796958	1819151
237.5323	C_2^{2-}	618784	653889	770111
193.0354	C_1	1547574	1278828	1307186
378.1047	B_2-SO_3	5176692	3918043	4344764
480.0442	B_2+Na	1025582	1278828	973459
458.0609	B_2	2279949	1305499	1930339
228.527	B_2^{2-}	1337653	649989	718136
367.5123	$[B_3+Na]^{2-}$	2685137	1894629	2060139
175.0248	B_1	5440769	5335352	4515866

Supplemental Table 58. Mass list for 4a, $[M-5H+2Na]^{3-}$ precursor ion

Mass to charge	Type	Intensity	Intensity	Intensity
353.4684	$[^{3,5}A_3+2Na]^{2-}$	1350838	572190	818213
707.9439	$^{3,5}A_3$+Na	5985812	2503094	2585923

336.9848	$^{2,4}A_2$+Na	5166719	2464495	2682282
358.9668	$^{2,4}A_2$+2Na	5908698	3949326	3728809
455.5426	$[^{1,5}X_3$+Na$]^{2-}$	1493522	756534	567232
371.113	$^{1,5}X_1$	7792552	4135482	919433
226.9867	$^{1,5}A_1$	2370559	708456	4262898
138.9707	$^{0,4}A_2$	19461674	4516089	681378
160.9526	$^{0,4}A_2$+Na	1670028	648414	4671313
137.9866	$^{1,3}A_2$	11275462	2923121	663856
159.9686	$^{1,3}A_2$+Na	1111538	473107	573210
385.1289	$^{0,2}X_1$	4912989	2180018	2424389
226.9867	$^{0,2}A_2^{2-}$	2370559	708456	681378
397.0058	$^{0,2}A_2$+Na-SO_3	1468743	992334	946515
498.9445	$^{0,2}A_2$+2Na	6822110	5020310	5113979
325.1075	Z_1	12401274	2642894	2755742
432.5392	$[Z_2$+Na-$SO_3]^{2-}$	1335506	1119629	959482
501.1397	Z_2	5577845	2392848	2551029
523.1214	Z_2+Na	2737808	1616276	1725454
381.5701	$[Z_3$+Na-$SO_3]^{2-}$	756421	1369650	1221497
259.0715	$[Y_2$+Na$]^{2-}$	4194682	1413910	1592519
343.1181	Y_1	51835016	23900596	24298912
365.1006	Y_1+Na	2426596	1556181	1662538
390.5755	Y_3+Na-SO_3	1478714	1292028	1266442
439.1934	Y_2-SO_3	8694911	4603584	4769891

441.5446	$[Y_3+2Na]^{2-}$	38577688	23672398	27733664
519.1504	Y_2	9566041	5472752	4462267
541.1325	Y_2+Na	8800816	4544486	6694714
193.0354	C_1-SO_3	1334325	289089	459659
272.9922	C_1	8265476	2734635	2901567
294.9742	C_1+Na	2439967	1531161	1346570
318.4656	$[C_2+2Na]^{2-}$	13017124	8906673	9339472
406.482	$[C_3+2Na]^{2-}$	1389651	1453082	1710402
456.0435	$C_2+Na-2SO_3$	1190608	580495	424502
557.9822	$C_2+2Na-SO_3$	3026002	2054282	2251709
637.9386	C_2+Na	10391923	4785345	5426490
175.0248	B_1-SO_3	3585099	515887	913909
254.9816	B_1	25873168	6524091	7060511
258.491	$[B_2+Na-SO_3]^{2-}$	4048969	2996880	4124915
276.9636	B_1+Na	3399772	2029151	2251933
298.4694	$[B_2+Na]^{2-}$	5724471	2778168	3111794
309.4604	$[B_2+2Na]^{2-}$	32016876	21886986	22292362
357.4977	$[B_3+Na-SO_3]^{2-}$	1706093	1699917	1718592
397.4763	$[B_3+Na]^{2-}$	16758693	9432260	9998721
438.0328	$B_2+Na-2SO_3$	1384240	812086	677558
517.9894	$B_2+Na-SO_3$	1118099	915547	1135953
539.9719	$B_2+2Na-SO_3$	2454430	1881521	1778480

Supplemental Table 59. Mass list for 4b, $[M-5H+2Na]^{3-}$ precursor ion

Mass to charge	Type	Intensity	Intensity	Intensity
302.499	$[^{3,5}A_3+Na]2-$	2159664	1825191	2339414
606.0057	$[^{3,5}A_3+Na]-$	4153275	4157815	5452485
539.5293	$[^{2,4}X_3+2Na]^{2-}$	928952	1050731	1105085
235.0457	$^{2,4}A_2$	1285433	928631	1387061
473.0521	$^{1,5}X_1+Na$	6160080	6192316	7861274
649.0844	$^{1,5}X_2+Na$	1198220	739222	1483201
330.011	$[^{1,5}X_3+2Na]^{3-}$	1008140	990450	1316543
455.542	$[^{1,5}X_3+2Na-SO_3]^{2-}$	2064156	2016972	1868959
495.5203	$[^{1,5}X_3+Na]^{2-}$	5808289	5484634	6814024
332.5094	$[^{1,5}A_3+Na]^{2-}$	1078976	1356622	1080351
137.9868	$^{1,3}A_2$	3512973	3323376	3821861
138.9708	$^{0,4}A_2$	6031271	6399267	7683151
160.9527	$^{0,4}A_2+Na$	1359456	1361377	1665620
487.0683	$^{0,2}X_1$	1605997	945924	2253262
502.5293	$^{0,2}X_3+2Na$	735149	1104772	876730
462.5491	$[^{0,2}X_3+2Na-SO_3]^{2-}$	886258	684427	888314
375.0236	$^{0,2}A_2$	1333706	1681775	1851522
397.0062	$^{0,2}A_2+Na$	9380697	9101665	10803940
301.036	$[Z_2+Na]^{2-}$	974493	386422	757258

325.1077	Z_1-SO_3	1635492	1479514	1739729
405.0652	Z_1	843480	1017476	547003
427.047	Z_1+Na	1910689	2593958	3273144
432.539	$[Z_3+2Na-SO_3]^{2-}$	1181718	1780200	1573096
472.5175	$[Z_3+2Na]^{2-}$	11947792	11693389	14450973
603.0785	Z_2+Na	2909485	3045122	3316420
625.059	Z_2+2Na	1865955	1487173	1759098
211.0338	Y_1^{2-}	3725434	4216062	4904305
310.0408	Y_2+Na	23898174	22844930	24972094
320.6796	$[Y_3+Na]^{3-}$	37923068	37593356	39810912
343.1181	Y_1-SO_3	3775916	3848223	4355575
365.1003	Y_1+Na-SO_3	1840655	1340441	1779961
441.5451	$[Y_3+2Na-SO_3]^{2-}$	33052364	30616524	33790844
445.0573	Y_1+Na	59196748	56396764	64546564
467.0401	Y_1+2Na	1195511	1290632	854680
481.523	$[Y_3+2Na]^{2-}$	8675999	8610769	11426174
643.0718	Y_2+2Na	884993	946677	1096045
541.1317	Y_2+Na-SO_3	994223	682001	1222909
621.0917	Y_2+Na	825598	618416	1058971
193.0354	C_1	2979126	2264585	3012113
256.5048	C_2^{2-}	963027	1161930	830671
267.4962	$[C_2+Na]^{2-}$	14441716	14577452	16274848
456.0434	C_2+Na-SO_3	8721067	8568722	9465473

536.0007	C_2+Na	3094751	3056347	3720669
557.9814	C_2+2Na	1700937	1513019	2224199
175.0249	B_1	3227813	3241375	3301338
207.5218	$[B_2\text{-}SO_3]^{2-}$	763700	828533	973148
247.4999	B22-	3008353	2748803	2376457
258.4911	$[B_2+Na]^{2-}$	1894521	1881999	2090112
306.5285	$[B_3+Na\text{-}SO_3]^{2-}$	3039091	3336177	3346068
335.5159	B_3^{2-}	2362227	3093654	2194757
336.0938	B_2-2SO_3	1133715	1018440	1255977
346.507	$[B_3+Na]^{2-}$	67948824	68468720	74900824
416.0507	$B_2\text{-}SO_3$	1839494	1701121	1922935
438.0327	B_2+Na-SO_3	10357244	10348482	10776430
517.9901	B_2+Na	3603649	3654895	3815365
614.0635	B_3+Na-SO_3	1786233	1656897	2081379

Supplemental Table 60. Mass list for 4c, $[M\text{-}5H+2Na]^{3-}$ precursor ion

Mass to charge	Type	Intensity	Intensity	Intensity
526.0486	$^{3,5}A_3$+Na	1035868	1400286	1101798
332.5099	$^{1,5}A_3$+Na	868821	977186	755105
257.0279	$^{2,4}A_2$+Na	2306836	4492564	2612503
473.0527	$^{1,5}X_1$+Na	2023873	1998406	1850752
729.0416	$^{1,5}X_2$+Na	1199995	1805712	1363023

751.0223	$^{1,5}X_2$+2Na	8444108	11866427	9450798
495.5209	$[^{1,5}X_3$+2Na$]^{2-}$	4915058	7863262	5126964
138.9705	$^{0,4}A_2$	2201737	2870125	2204178
137.9865	$^{1,3}A_2$	3130283	5064495	3322959
159.9685	$^{1,3}A_2$+Na	1390504	2215710	1397544
487.0672	$^{0,2}X_1$+Na-SO_3	1842601	2330989	2209140
283.0082	$[^{0,2}X_1$+Na$]^{2-}$	1191119	1060065	1367728
190.0133	$[^{0,2}A_3$+Na$]^{3-}$	1795568	1119261	915774
295.0669	$^{0,2}A_2$	867522	1393298	794975
301.0358	$[Z_2$+Na-$SO_3]^{2-}$	8962030	6959545	9283306
325.1078	Z_1-SO_3	1433797	2227023	1409572
341.0137	$[Z_2$+Na$]^{2-}$	772239	1006991	821888
352.0053	$[Z_2$+2Na$]^{2-}$	18859134	14005386	18421128
427.0467	Z_1+Na	5544788	6781209	5688008
472.5182	$[Z_3$+2Na$]^{2-}$	3662870	5509751	4469967
603.0777	Z_2+Na-SO_3	701063	879527	1211262
625.0616	Z_2+2Na-SO_3	2990833	2214531	2921459
705.0169	Z_2+2Na	1148492	1513624	1165264
211.0339	Y_1^{2-}	3128457	2967939	3081004
310.0411	$[Y_2$+Na-$SO_3]^{2-}$	4866408	4020658	5457672
320.6798	$[Y_3$+2Na$]^{3-}$	33233052	21165622	33907556
343.1183	Y_1-SO_3	1838421	3038332	1645814
350.0196	$[Y_2$+Na$]^{2-}$	11800761	8612507	11627181

361.0106	$[Y_2+2Na]^{2-}$	34741944	26614142	35554332
365.1001	$Y_1+Na-SO_3$	1070276	1452156	1015593
379.5841	$[Y_3+Na-2SO_3]^{2-}$	11276787	14372268	12993474
441.5449	$[Y_3+Na-SO_3]^{2-}$	21526144	13496805	21991226
445.0574	Y_1+Na	13798141	14880494	15063420
481.5232	$[Y_3+2Na]^{2-}$	84428280	64659476	85101312
643.0729	$[Y_2+2Na-SO_3]^{2-}$	1004943	121868	1312227
193.0354	C_1	4803759	7560434	5412906
456.0431	C_2+Na	7695948	9431812	8163885
712.0322	C_3+Na	1394327	1752412	1615348
734.0156	C_3+2Na	1648858	2011737	1659372
175.0248	B_1	5048745	5621932	4495785
306.5291	$[B_3+Na-SO_3]^{2-}$	1025784	1235046	979390
336.0939	B_2-SO_3	3346756	3459841	2957272
346.5073	$[B_3+Na]^{2-}$	7424013	6053076	8196562
416.0506	B_2	5465319	5271876	5668521
438.0329	B_2+Na	11051382	10569571	10573188
614.0633	$B_3+Na-SO_3$	1713832	2442810	1693888
716.0033	B_3+2Na	865475	793564	648315

Supplemental Table 61. Mass list for 4d, $[M-5H+2Na]^{3-}$ precursor ion

Mass to charge	Type	Intensity	Intensity	Intensity

526.0486	$^{3,5}A_3$+Na	3280405	3548744	3816024
396.1132	$^{2,4}A_3$-SO_3	639372	756301	665559
235.0462	$^{2,4}A_2$	1042209	1133372	1313753
257.0281	$^{2,4}A_2$+Na	22182328	2.42E+07	23832022
225.0311	$^{1,5}X_1^{2-}$	911030	803227	617918
473.0523	$^{1,5}X_1$+Na	4725607	5013449	5201886
324.0393	$[^{1,5}X_2$+Na-$SO_3]^{2-}$	696434	754709	630759
364.0166	$[^{1,5}X_2$+Na$]^{2-}$	1153170	1354303	1410117
375.0077	$[^{1,5}X_2$+2Na$]^{2-}$	2625171	2384608	2718783
671.0664	$^{1,5}X_2$+2Na-SO_3	2156896	2256530	2608878
751.0221	$^{1,5}X_2$+2Na	3899136	4440243	4152667
455.5421	$[^{1,5}X_3$+2Na-$SO_3]^{2-}$	4465714	4252384	4412062
495.5197	$[^{1,5}X_2$+2Na$]^{2-}$	3771398	4454511	4122977
332.51	$[^{1,5}A_3$+Na$]^{2-}$	701077	1323733	1228607
138.9707	$^{0,4}A_3$	10225003	1.16E+07	11454811
160.9527	$^{0,4}A_3$+Na	1952094	2363267	2211112
137.9867	$^{1,3}A_3$	12556273	1.35E+07	12989646
159.9687	$^{1,3}A_3$+Na	6332419	6688890	6860247
232.0392	$[^{0,2}X_1$-$SO_3]^{2-}$	984822	711713	627624
283.0087	$[^{0,2}X_1$+Na$]^{2-}$	2531096	2961695	2998361
487.0677	$^{0,2}X_1$+Na-SO_3	4631255	4775645	4705724
589.007	$^{0,2}X_1$+2Na	743053	1084882	1090656

223.076	$^{0,2}X_0$	1823661	1909149	1904975
381.5236	$[^{0,2}X_2+2Na-SO_3]^{2-}$	1703224	1819719	2090694
462.5503	$[^{0,2}X_3+2Na-SO_3]^{2-}$	2921195	2766567	2756802
502.528	$[^{0,2}X_3+2Na]^{2-}$	949231	1130660	506371
190.0136	$[^{0,2}A_3+Na]^{3-}$	1541010	1949509	1044976
295.0672	$^{0,2}A_2$	1576542	1936684	2051218
317.0489	$^{0,2}A_2+Na$	1371450	1731322	1678515
301.0359	$[Z_2+Na-SO_3]^{2-}$	1398569	1240314	1297616
325.1078	Z_1-SO_3	6756599	6850005	7454355
341.0147	$[Z_2+Na]^{2-}$	626406	779404	851502
352.0052	$[Z_2+2Na]^{2-}$	5805828	6460995	5793197
421.5479	$[Z_3+Na-SO_3]^{2-}$	1008815	883806	1118751
427.0468	Z_1	6513789	6597558	6746432
432.5393	$[Z_3+2Na-SO_3]^{2-}$	3333571	3624636	2792805
472.5169	$[Z_3+2Na]^{2-}$	3200758	2795987	3546491
603.0762	$Z_2+Na-SO_3$	1018255	973494	582061
625.0636	$Z_2+2Na-SO_3$	1172434	1416280	1588792
705.017	Z_2+2Na	2238261	2451692	2498172
211.0339	Y_1^{2-}	15249004	1.59E+07	16073473
310.0412	$[Y_2+2Na-SO_3]^{2-}$	4943014	5355231	4822614
320.6797	$[Y_3+2Na]^{3-}$	4998191	4158849	3957601

343.1184	Y_1-SO_3	7914286	8168837	8662354
350.0194	$[Y_2+Na]^{2-}$	5250633	5602884	6008155
361.0105	$[Y_2+2Na]^{2-}$	35922532	3.92E+07	40088964
365.1005	Y_1+Na-SO_3	5230122	5773301	5678404
441.5448	$[Y_3+2Na-SO_3]^{2-}$	26384878	3.05E+07	30279322
222.0247	Y_1^{2-}	517586	1016526	671150
445.0573	Y_1	84398400	9.32E+07	91264864
467.0388	Y_1+2Na	3230766	3787288	3622845
481.5228	$[Y_3+Na]^{2-}$	7919705	9129316	9551812
643.0717	Y_2+2Na-SO_3	1964410	2311969	2288181
193.0355	C_1	11771184	1.38E+07	13679495
215.0174	C_1+Na	3064094	3223596	2580862
355.5125	[C_3+Na]2-	844078	1193429	839574
366.5032	$[C_3+2Na]^{2-}$	1902678	1981680	2140586
456.0433	C_2+Na	20463914	2.45E+07	23150184
654.0558	C_3+2Na-SO_3	1859443	1891189	2114889
734.0149	C_3+2Na	790009	1079562	840988
175.0249	B_1	2703710	2796207	2884660
295.5379	$[B_3-SO_3]^{2-}$	1850174	1826873	1669217
306.5288	$[B_3+Na-SO_3]^{2-}$	9339436	1.06E+07	10778313
336.094	B_2-SO_3	3196958	3339484	3643534
346.5073	$[B_3+Na]^{2-}$	68871208	7.51E+07	72857952
357.4988	$[B_3+2Na]^{2-}$	754277	710893	801072

416.0508	B_2	3586193	3838907	4042313
438.0328	B_2+Na	8712041	9523748	10363745
636.046	B_3+2Na-SO_3	918701	1048382	1493647
716.0031	B_3+2Na	1556756	1451001	1420777
614.0628	B_3+Na-SO_3	1623777	1012002	1517170

Supplemental Table 62. Mass list for 4e, $[M-5H+2Na]^{3-}$ precursor ion

Mass to charge	Type	Intensity	Intensity	Intensity
302.4991	$[^{3,5}A_3+Na]^{2-}$	1049126	1062165	929990
606.0044	$^{3,5}A_3$+Na	1129521	948736	909153
257.0283	$^{2,4}A_2$+Na	670398	461935	567837
473.052	$^{1,5}X_1$+Na	1926880	1969710	1432579
649.0872	$^{1,5}X_2$+Na	3471211	3201469	2747070
495.52	$[^{1,5}X_3+2Na]^{2-}$	4250396	3808660	3578009
332.51	$[^{1,5}A_3+Na]^{2-}$	786909	636872	439813
137.9865	$^{1,3}A_2$	2025306	1779197	1793244
159.9686	$^{1,3}A_2$+Na	710400	428991	504967
138.9705	$^{0,4}A_2$	2824143	1853230	2246339
160.9526	$^{0,4}A_2$+Na	506524	461331	528424
397.0062	$^{0,2}A_2$+Na	5825552	5591150	6761151
325.1078	Z_1-SO_3	656327	535785	762716
427.0466	Z_1+Na	1439998	1750614	1550625
472.5174	$[Z_3+2Na]^{2-}$	7557976	5184294	5424669

603.0773	Z_2+Na	1822586	1546780	1457331
211.0341	Y_1^{2-}	876137	1157631	1179961
310.0413	$[Y_2+Na]^{2-}$	8187911	12990223	13282343
320.6797	$[Y_3+2Na]^{3-}$	981215	1769629	2331439
343.1187	Y_1-SO_3	2966505	2254860	2876901
365.1008	Y_1+Na-SO_3	1169263	1089303	933694
441.5451	$[Y_3+2Na-SO3]^{2-}$	2696446	6723802	7204883
445.057	Y_1+Na	33924312	40634352	41504900
481.5223	$[Y_3+2Na]^{2-}$	2057799	1332147	1530928
193.0353	C_1	835627	601849	636587
267.4966	$[C_2+Na]^{2-}$	6584130	9485387	10265702
456.0429	C_2+Na-SO3	2091750	2121245	2699517
535.9999	C_2+Na	1207995	1423563	1212212
557.9816	C_2+2Na	1024824	1123182	1544626
175.0249	B_1	592743	754840	582094
258.491	$[B_2+Na]^{2-}$	910637	1427287	1287370
306.5284	$[B_3+Na-SO_3]^{2-}$	711992	1971198	2374325
346.5073	$[B_3+Na]^{2-}$	29539070	42221076	42246936
438.0325	B_2+Na-SO_3	5123891	6365798	6190604
517.9896	B_2+Na	1333429	1317020	859165

Supplemental Table 63. Mass list for 4f, $[M-5H+2Na]^{3-}$ precursor ion

Mass to charge	Type	Intensity	Intensity	Intensity
606.0054	$^{3,5}A_3$+Na	3806096	3088745	1730145
302.4992	$[^{3,5}A_3$+Na$]^{2-}$	1469394	1408906	946261
539.5297	$[^{2,4}X_3$+2Na$]^{2-}$	1413037	1377949	800121
235.0463	$^{2,4}A_2$	758739	1490494	339610
473.0517	$^{1,5}X_1$+Na	5238959	4464813	2874318
649.0852	$^{1,5}X_2$+Na	3953852	3242480	1934252
455.5418	$[^{1,5}X_3$+2Na-$SO_3]^{2-}$	1185170	1413304	693494
330.0117	$[^{1,5}X_3$+2Na$]^{3-}$	705021	697263	400153
495.5205	$[^{1,5}X_3$+2Na$]^{2-}$	7308995	5439494	3750942
332.5086	$^{1,5}A_3$	754068	459994	410770
503.9911	$[^{1,5}A_4$+2Na$]^{2-}$	1851012	943501	848252
539.5297	$[^{1,3}X_3$+2Na$]^{2-}$	1413037	1377149	800121
159.9685	$^{1,3}A_2$+Na	869075	1056744	483212
137.9865	$^{1,3}A_2$	1639609	2630461	1548110
160.9525	$^{0,4}A_2$+Na	876160	1383238	530302
138.9705	$^{0,4}A_2$	4238176	5462835	2927984
517.5345	$[^{0,3}X_3$+Na$]^{2-}$	1175218	791886	700426
385.1298	$^{0,2}X_1$-SO_3	892481	704088	598491
487.0675	$^{0,2}X_2$+Na	2573936	3166793	2118578

502.5284	$[^{0,2}X_3+2Na]^{2-}$	2299410	1312719	861651
397.0061	$^{0,2}A_2$	6335327	9602490	5539272
325.1075	Z_1-SO_3	1572149	2323770	1228304
427.0466	Z_1+Na	6007408	6051350	3921028
405.0642	Z_1	1423726	1363250	602001
523.1223	Z_2+Na-SO_3	1551369	1595637	1225651
603.0768	Z_2+Na	2833127	2148827	1724997
625.06	Z_2+2Na	7078502	7141195	4880039
301.0356	$[Z_2+Na]^{2-}$	6929320	10067999	5599519
290.0449	Z_2^{2-}	1033112	1502146	820018
432.5393	$[Z_3+2Na-SO_3]^{2-}$	1532437	1617236	867747
314.6763	$[Z_3+2Na]^{3-}$	1671216	1579343	693065
472.5176	$[Z_3+2Na]^{2-}$	15789410	11545859	7435445
365.1002	Y_1+Na-SO_3	1859985	2420895	1189409
343.1183	Y_1-SO_3	4985872	7951448	4001566
445.0571	Y_1+Na	17683254	23659024	13914581
467.0376	Y_1+2Na	1085593	1571967	815349
423.0747	Y_1	1470693	1591050	1413595
211.0338	Y_1^{2-}	4927760	6918603	4217780
541.1308	Y_2+Na-SO_3	1051640	1331136	640944
621.0887	Y_2+Na	1493422	1152307	844796
643.0728	Y_2+2Na	1122508	744326	405829
310.041	$[Y_2+Na]^{2-}$	22469200	33014140	21713260

299.0502	Y_2^{2-}	1162502	1773116	902141
441.5448	$[Y_3+2Na-SO_3]^{2-}$	13875304	16330991	12052785
320.6796	[Y3+2Na]3-	64338072	71615648	55821468
481.5232	$[Y_3+2Na]^{2-}$	43178468	42074484	27672992
456.0432	$C_2+Na-SO_3$	5675267	7993177	4578391
536.0003	C_2+Na	3852101	3563516	2380388
557.9815	C_2+2Na	2405144	2961318	1933785
267.4963	[C2+Na]2-	3767821	3638998	2588707
734.0112	$[C_3+2Na]^{2-}$	1198440	1064844	650844
193.0354	C_1	1411925	1961503	1228263
438.0328	$B_2+Na-SO_3$	9608544	13667227	8688275
416.0521	B_2-SO3	738334	1063717	985865
517.9897	B_2+Na	4515435	5389265	3008121
539.9721	B_2+2Na	1327430	1784100	1060242
258.4909	$[B_2+Na]^{2-}$	1914874	2496523	1486437
614.064	$B_3+Na-SO_3$	1634622	2089059	1442869
346.5071	$[B_3+Na]^{2-}$	10053438	14713078	10258414
357.4981	$[B_3+2Na]^{2-}$	4926859	7243626	4498042
175.0248	B_1	4691455	7116659	4181947

Supplemental Table 64. Mass list for 4g, $[M-5H+2Na]^{3-}$ precursor ion

Mass to charge	Ion	Intensity	Intensity	Intensity
235.0458	$^{2,4}A_2$	1030409	1229563	2187701
257.028	$^{2,4}A_2$+Na	2689442	3203856	3932352
751.0234	$^{1,5}X_2$+2Na	6471279	4620628	19249286
495.5208	$[^{1,5}X_3+2Na]^{2-}$	3805305	3035525	10877226
138.9706	$^{0,4}A_2$	3240383	3077794	5132025
137.9866	$^{0,3}A_2$	3348167	3519986	7076238
159.9685	$^{0,4}A_2$+Na	1999268	1518543	2306939
283.0091	$[^{0,2}X_1+Na]^{2-}$	679078	967626	2081630
487.0656	$^{0,2}X_1$+Na-SO3	982685	1190013	2207435
190.0134	$^{0,2}A_3^{3-}$	1210089	800810	1934578
295.0672	$^{0,2}A_2$	3267332	3188541	7714463
301.0357	$[Z_2+Na--SO3]^{2-}$	2460998	2316199	9095460
325.1078	Z_1-SO_3	1503008	1532047	2669139
352.0051	$[Z_2+2Na]^{2-}$	12268004	13103831	68388928
427.0465	Z_1+Na	3283420	3034856	9711016
472.5176	$[Z_3+2Na]^{2-}$	2716962	2760397	8887796
625.0624	Z_2+2Na-SO_3	1331946	1521457	4357626
211.0337	Y_1^{2-}	3206567	2506172	7287609
310.041	$[Y_2+Na-SO_3]^{2-}$	2789328	2883881	12465444
320.6798	$[Y_3+Na]^{3-}$	7264913	8075400	55106104

343.1188	Y_1-SO_3	1842893	1803170	3833694
350.0194	$[Y_2+Na]^{2-}$	6469536	6009930	29454074
361.0104	$[Y_2+2Na]^{2-}$	15049344	13948276	77267256
365.0999	Y_1+Na-SO_3	826361	591257	1469022
379.5839	$[Y3-2SO_3]^{2-}$	11471940	11414471	20956102
441.5452	$[Y_3+2Na-SO_3]^{2-}$	4398698	3981720	25809430
445.0573	Y_1	9404970	9181430	29771918
306.529	$[B_3+Na-SO_3]^{2-}$	580121	462801	1628497
481.5236	$[Y_3+2Na]^{2-}$	6278980	6005294	33589328
193.0354	C_1	5735467	5573187	11713730
354.1039	C_2+Na	1710613	2017566	4045603
434.0607	C_2	711867	877973	2357441
456.0438	C_2+Na	3585068	3356300	8086379
175.0248	B_1	3258914	2749990	7292058
336.0939	B_2-SO_3	4246162	3791343	10279680
346.5073	$[B_3+Na]^{2-}$	5144408	4977452	19718614
416.0508	B_2	4598641	3938988	12861164
438.033	B_2+Na	7039556	6235889	22019906
614.0648	B_3+Na-SO_3	850041	683948	2699157

Supplemental Table 65. Mass list for 4h, $[M-5H+Na]^{4-}$ precursor ion

Mass to charge	Type	Intensity	Intensity	Intensity
323.5048	$[^{3,5}A_3+Na]^{2-}$	785230	777884	582630
322.6558	$[^{3,5}A_4+Na]^{3-}$	1389511	1415646	616267
442.5538	$[^{2,4}X_2+Na]^{2-}$	2330515	1646692	1083362
336.9849	$^{2,4}A_2+Na$	1441066	2338390	1908303
413.1234	$^{1,5}X_1$	1480325	1136825	917841
334.0528	$^{1,5}X_2^{2-}$	955223	650815	1002196
345.0441	$^{1,5}X_2+Na$	783458	837877	680078
691.098	$[^{1,5}X_2+Na]^{2-}$	1196952	5102210	500153
316.7116	$^{1,5}X_3^{3-}$	915136	610412	905585
446.5851	$[^{1,5}X_3+Na\text{-}SO_3]^{2-}$	1147684	634974	680078
486.5634	$[^{1,5}X_3+Na]^{2-}$	2000989	1641239	953124
393.4933	$[^{1,5}A_3+Na]^{2-}$	1619199	1255495	1517375
708.0374	$^{1,5}A_3+Na\text{-}SO_3$	1560342	890720	531427
254.508	$^{1,5}A_2$	2123399	1537060	717389
226.987	$^{1,5}A_1$	1933583	1869720	1305765
138.9706	$^{1,3}A_3/^{0,4}A_2$	17139282	4723723	23020492
160.9525	$^{1,3}A_3+Na/^{0,4}A_2+Na$	3175584	23692250	4681124
253.0446	$^{0,2}X_1^{2-}$	1368752	2096930	1521725
529.0799	$^{0,2}X_1+Na$	1223277	1265305	725864
226.987	$^{0,2}A_2^{2-}$	1933583	1869720	1305765

237.9778	$[^{0,2}A_2+Na]^{2-}$	2267149	3039390	3188611
337.9912	$[^{0,2}A_4+Na]^{3-}$	14253575	9643333	4748814
397.006	$^{0,2}A_2+Na\text{-}SO_3$	2063976	2313880	2468677
271.0706	$[Z_2\text{-}SO_3]^{2-}$	754742	1193766	992298
311.0501	Z_2^{2-}	5650282	4665712	4122502
322.041	$[Z_2+Na]^{2-}$	18877010	23221350	21279026
367.1184	Z_1	11416510	11941409	9422920
463.5595	$[Z_3+Na]^{2-}$	6839928	4671585	1650817
645.0901	Z_2+Na	3139058	2628950	1737143
213.0343	Y_2^{3-}	1387923	1427869	1475201
280.0768	$[Y_2\text{-}SO_3]^{2-}$	2797623	3243543	2813301
307.3799	Y_3^{3-}	4542814	5198757	4747999
314.7071	$[Y_3+Na]^{3-}$	35525020	40968280	42259836
320.0554	Y_2^{2-}	6932348	314.7071	7579344
331.0462	$[Y_2+Na]^{2-}$	25769246	28661118	30473172
385.1291	Y_1	11765651	14589188	13833875
407.1105	Y_1+Na	1642378	2629451	1967804
432.5879	$[Y_3+Na\text{-}SO_3]^{2-}$	980040	1431813	458239
472.5645	$[Y_3+Na\text{-}SO_3]^{2-}$	2145386	2334260	1595799
193.0355	$C_1\text{-}SO_3$	647019	1095452	1062080
272.9923	C_1	977288	1518673	489371
277.5118	C_2^{2-}	868397	1041008	1491622
288.5021	$[C_2+Na]^{2-}$	1134893	1285271	1394074

294.9744	C_1+Na	2258485	1970559	1986058
416.4966	$[C_3+Na]^{2-}$	2487047	2320370	1037721
498.0531	C_2+Na-SO_3	910686	1543444	1393011
578.013	C_2+Na	1856905	1401130	814680
175.0248	B_1-SO_3	2271741	2938742	2442893
228.5269	B_2-SO_3	7838213	8879348	8149124
254.9817	B_1	11414815	14048083	12996723
268.5054	B_2^{2-}	7886756	8685465	7949080
276.9636	B_1+Na	3291855	5083127	4241916
279.4964	$[B_2+Na]^{2-}$	4785582	5782640	5901930
367.5123	$[B_3+Na-SO_3]^{2-}$	2059375	2222824	1247816
407.4909	$[B_3+Na]^{2-}$	1145267	1065767	1967804
458.0613	B_2-SO_3	2097676	2127898	1053392
480.044	B_2+Na-SO_3	2310728	2163421	2162538

Supplemental Table 66. Mass list for 4i, $[M-5H+Na]^{4-}$ precursor ion

Mass to charge	Type	Intensity	Intensity	Intensity
342.4775	$[^{3,5}A_3+Na]^{2-}$	1434290	1959210	1355126
164.0055	$[^{3,5}A_2-SO_3]^{2-}$	1041250	1405202	865069
214.9748	$[^{3,5}A_2+Na]^{2-}$	1215350	1095174	837462
351.0014	$^{3,5}A_2$+Na-SO_3	1393518	1765333	1397784
231.2373	$[^{3,5}A_4+Na]^{4-}$	900235	875806	369657
282	$[^{3,5}A_4+Na-SO_3]^{3-}$	1259599	1079150	882810

308.6529	$[^{3,5}A_4+Na]^{3-}$	2208175	2511501	2000414
325.1085	$^{2,4}X_0$	1481430	1690682	1241330
235.0459	$^{2,4}A_2$-SO_3	1559001	1525774	1368832
336.985	$^{2,4}A_2$+Na	2533322	3353329	2531737
413.1234	$^{1,5}X_1$	2189359	2971709	2070673
611.1382	$^{1,5}X_2$+Na	798696	1152657	914125
589.1569	$^{1,5}X_2$	593701	73216	395737
310.0352	$[^{1,5}X_3+Na]^{3-}$	5342714	7134668	5598454
425.5781	$[^{1,5}X_3+Na-SO_3]^{2-}$	567628	1115614	919203
465.5569	$[^{1,5}X_3+Na]^{2-}$	5749788	6698332	4958843
226.9868	$^{1,5}A_1$	2369625	2774377	2143280
168.9812	$^{1,4}A_1$	1142175	1729962	941771
190.963	$^{1,4}A_1$+Na	1490671	1516281	1239687
137.9866	$^{1,3}A_2$	11042352	12479291	9201944
159.9686	$^{1,3}A_2$+Na	4204167	5022994	3860341
160.9526	$^{1,3}A_3$+Na/$^{0,4}A_2$+Na	4644111	5781021	3806966
138.9706	$^{1,3}A_3/^{0,4}A_2$	27319530	33185860	24377956
427.1399	$^{0,2}X_1$	4698089	5895175	4471831
255.7675	$[^{0,2}X_3+Na]^{4-}$	1385501	1339984	1322643
314.7068	$[^{0,2}X_3+Na-SO_3]^{3-}$	776482	732330	708899
187.0081	$^{0,2}A_2$-SO_3	711857	944801	637867
226.9868	$^{0,2}A_2$	2369625	2774377	2143280
237.9778	$[^{0,2}A_2+Na]^{2-}$	2593053	2975694	2505950

397.0067	$^{0,2}A_2$+Na-SO_3	4855252	5606124	4347392
476.963	$^{0,2}A_2$+Na	2779839	3425361	2326749
271.0716	Z_2^{2-}	10947536	15085654	10359285
294.7004	$[Z_3+Na]^{3-}$	2116201	2411483	1771621
367.1184	Z_1	4952137	6366546	5259995
402.5763	$[Z_3+Na-SO_3]^{2-}$	1530529	1430788	942487
565.1317	Z_2+Na	2155324	3237440	1846839
192.0607	Y_1^{2-}	518752	747647	618479
280.0768	Y_2^{2-}	1.27E+08	1.62E+08	1.16E+08
300.7035	$[Y_3+Na]^{3-}$	45529992	58291192	41193588
385.1292	Y_1	43756768	54963880	40428128
407.111	Y_1+Na	5853122	7633493	5520832
451.5597	$[Y_3+Na]^{2-}$	774571	1074279	860825
481.2053	Y_2-SO_3	1844981	2414555	1690455
561.1615	Y_2	1484432	1638215	880023
583.1438	Y_2+Na	2434406	3187925	1980871
135.9926	C_2^{2-}	604587	419701	421271
193.0354	C_1-SO_3	9284493	11310409	8435880
204.6472	$[C_2+Na]^{3-}$	1724020	2306964	1599117
263.3246	$[C_3+Na]^{3-}$	2099108	1765733	1195118
267.4965	$[C_2+Na-SO_3]^{2-}$	6088346	7179674	5391552
272.9923	C_1-SO_3	21634434	27491488	20483082
294.9743	C_1+Na	15972485	19843552	15415935

307.4746	$[C_2+Na]^{2-}$	11714436	15449015	11925317
355.512	$[C_3+Na-SO_3]^{2-}$	1045970	1008115	425070
395.4917	$[C_3+Na]^{2-}$	2092804	2588080	1656991
456.0438	$C_2+Na-2SO_3$	2885529	3571635	2839526
175.0248	B_1-SO_3	4974416	6105023	4088244
198.6438	$[B_2+Na]^{3-}$	8785666	11701043	7789772
207.5217	$[B_2-2SO3]^{2-}$	716257	480242	565983
247.5	$[B_2-2SO_3]^{2-}$	7189932	6290958	9115275
254.9817	B_1	13581352	16316972	13294333
258.491	$B_2+Na-SO_3$	70131816	85627536	64084124
276.9637	B_1	11367042	14713952	10811804
287.478	B_2^{2-}	826990	929852	1022501
298.4693	$[B_2+Na]^{2-}$	36583224	49107144	35383112
346.507	$[B_3+Na-SO_3]^{2-}$	3762336	4414270	2916271
386.4854	$[B_3+Na]^{2-}$	2780012	3376198	2567595
416.0504	B_2-2SO_3	802299	855523	598260
438.0328	$B_2+Na-2SO_3$	2742004	3429761	2604654
517.9901	$B_2+Na-SO_3$	3906398	4922208	3801642

APPENDIX E

SUPPLEMENTAL DATA FOR CHAPTER 7

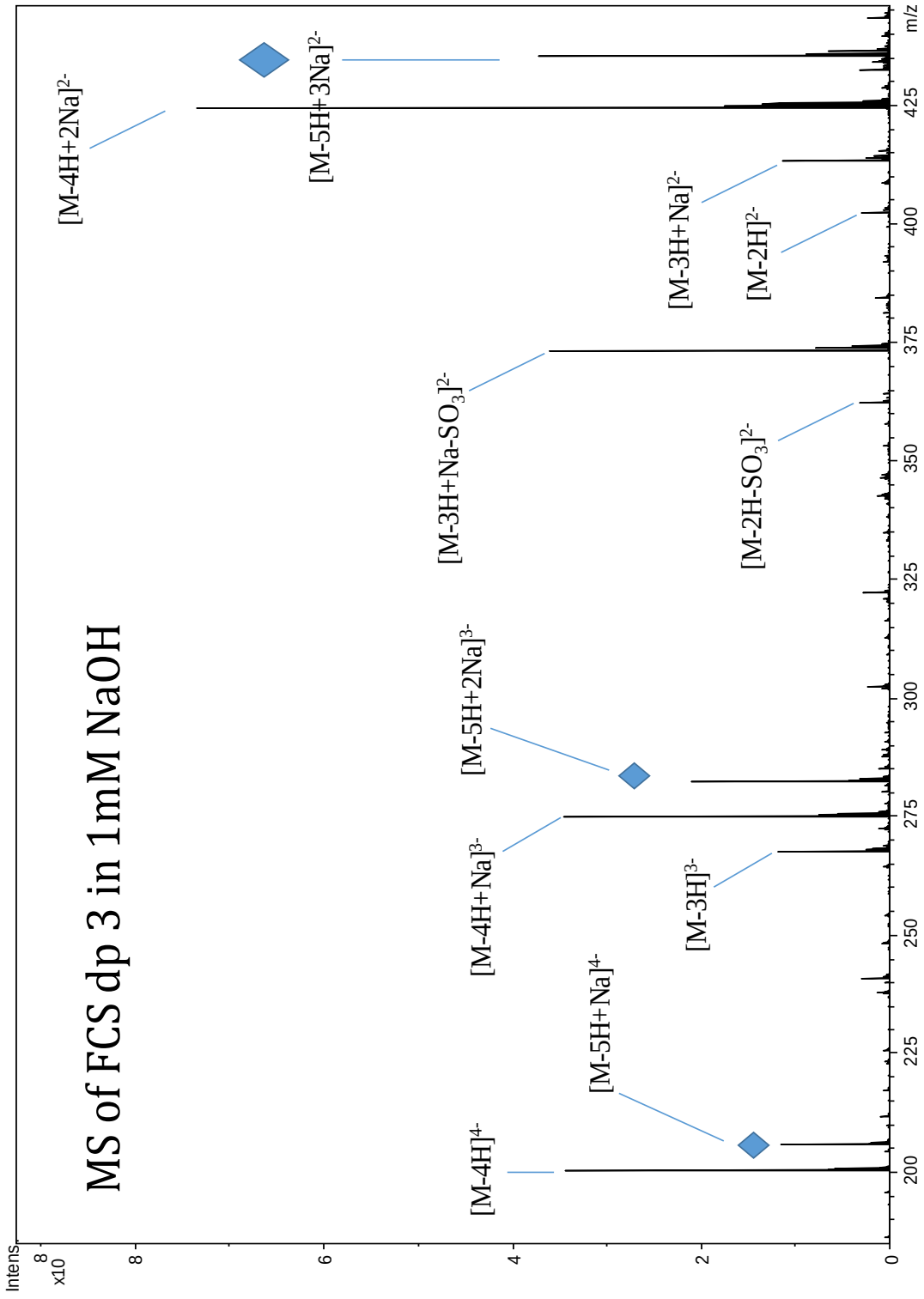

Supplementary Figure 1. ESI MS of FCS dp3

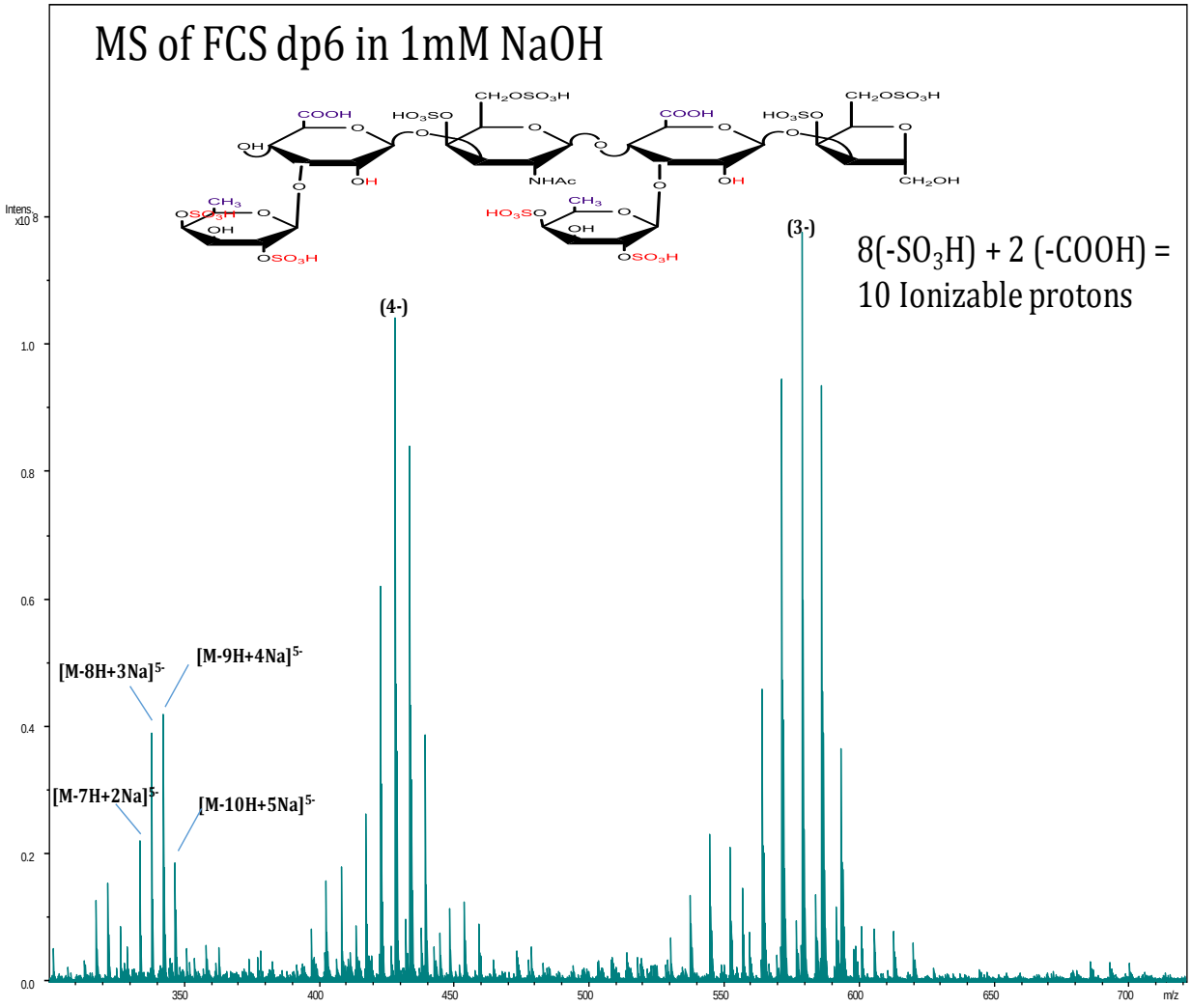

Supplementary Figure 2. ESI MS of FCS dp6

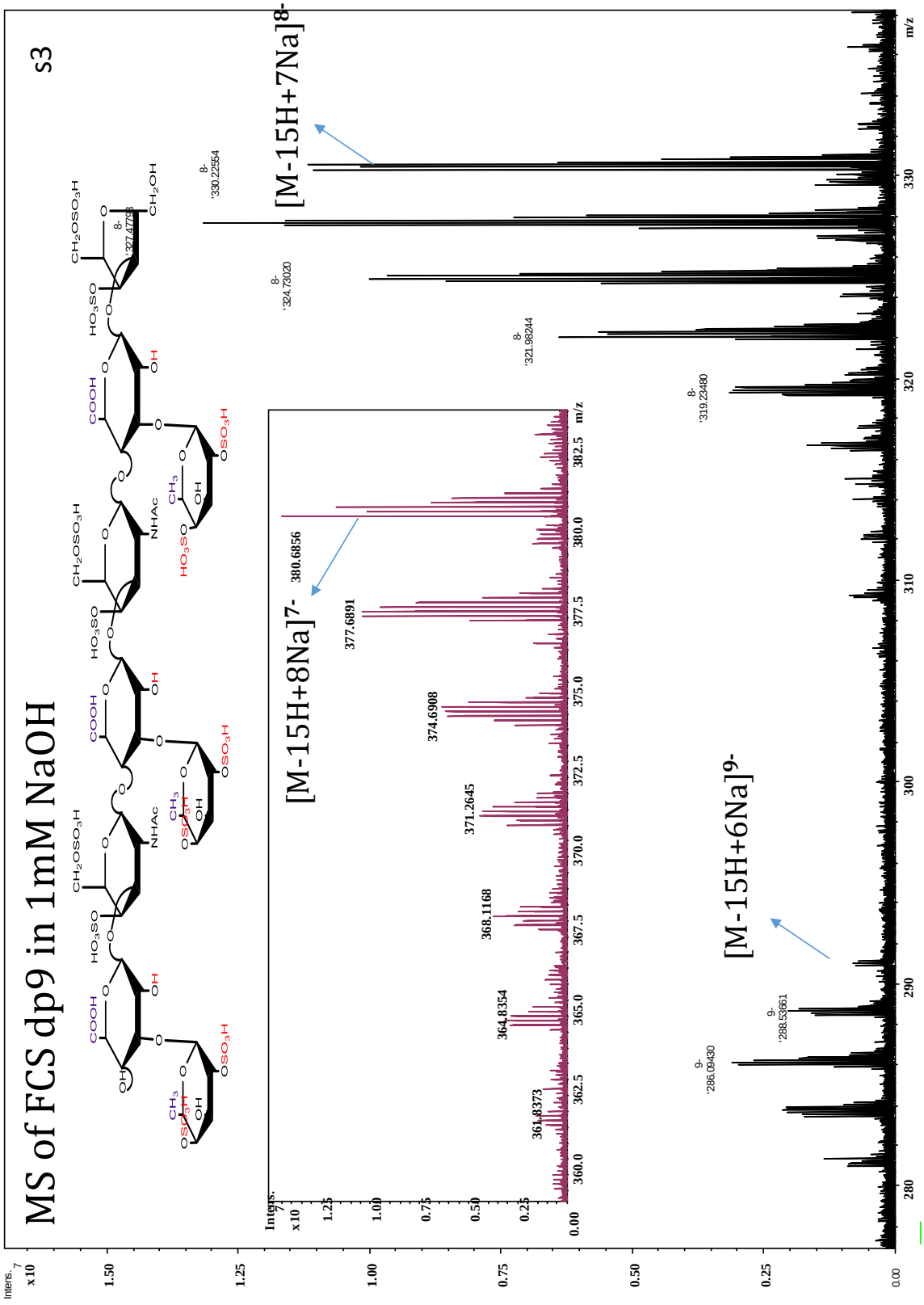

Supplementary Figure 3. ESI MS of FCS dp9

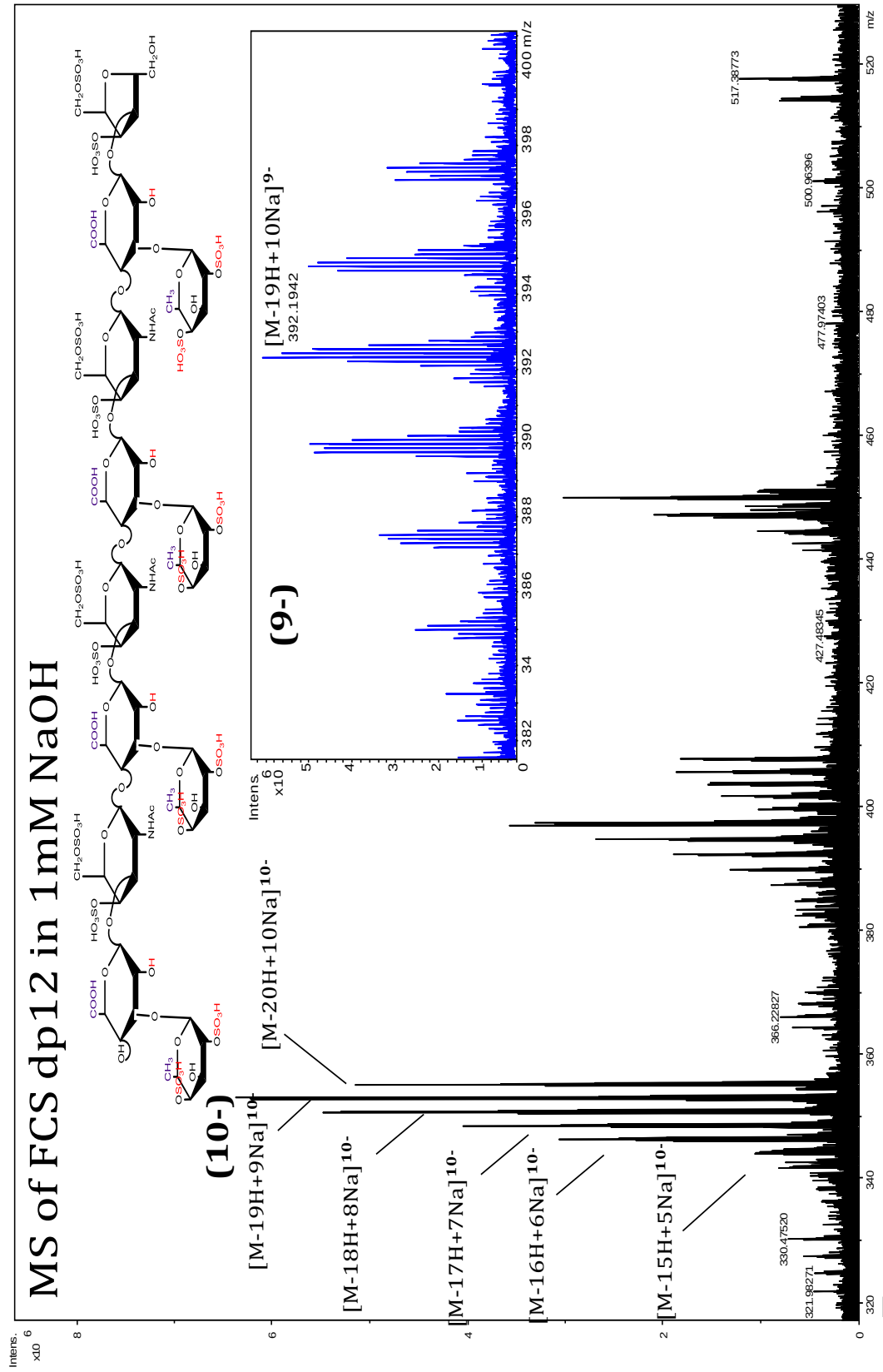

Supplementary Figure 3. ESI MS of FCS dp12

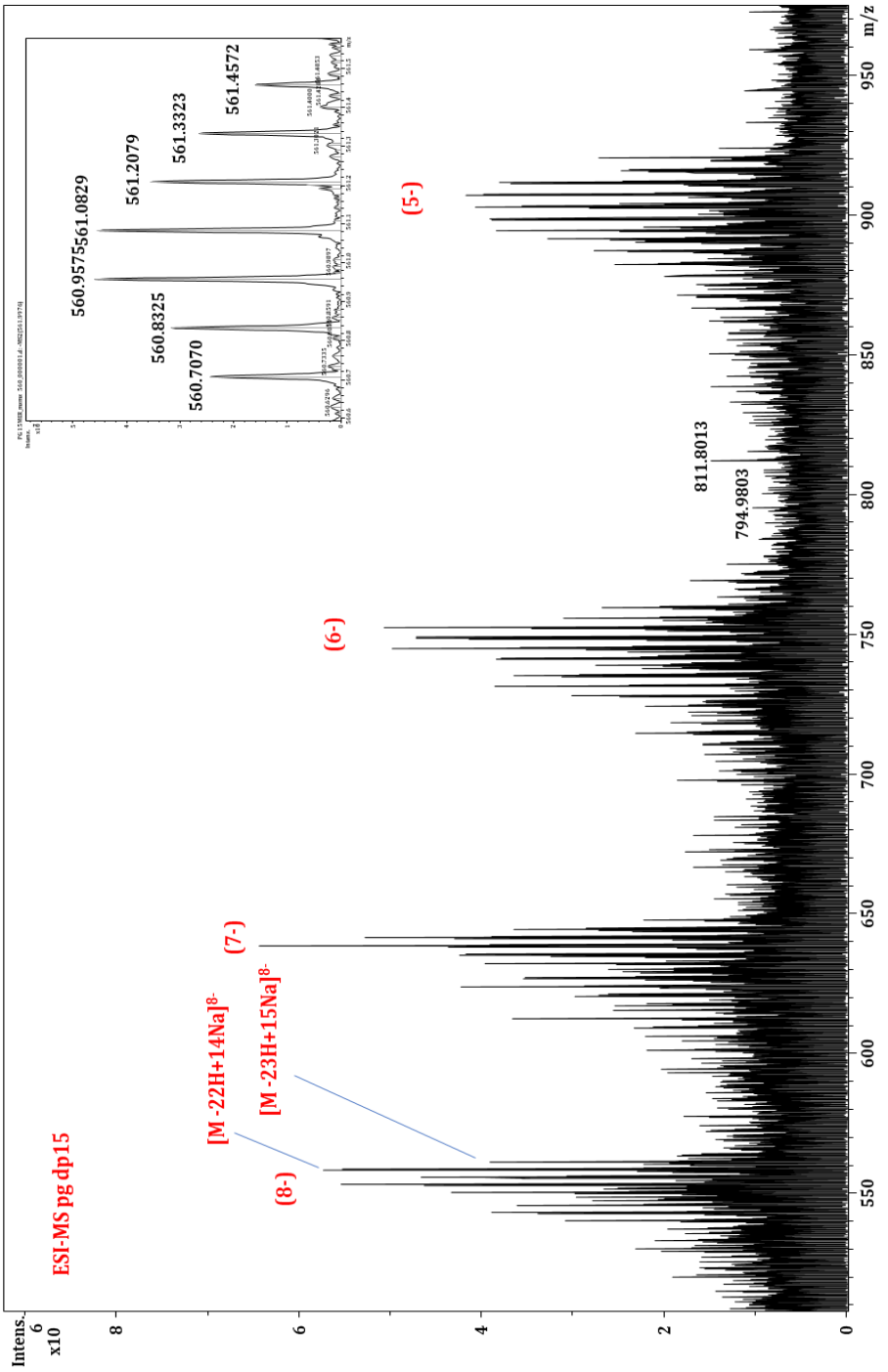

Supplementary Figure 5. ESI MS of FCS pg dp15; insert shows isotopic distribution of the selected molecular ion $[M-22H+14Na]^{8-}$.

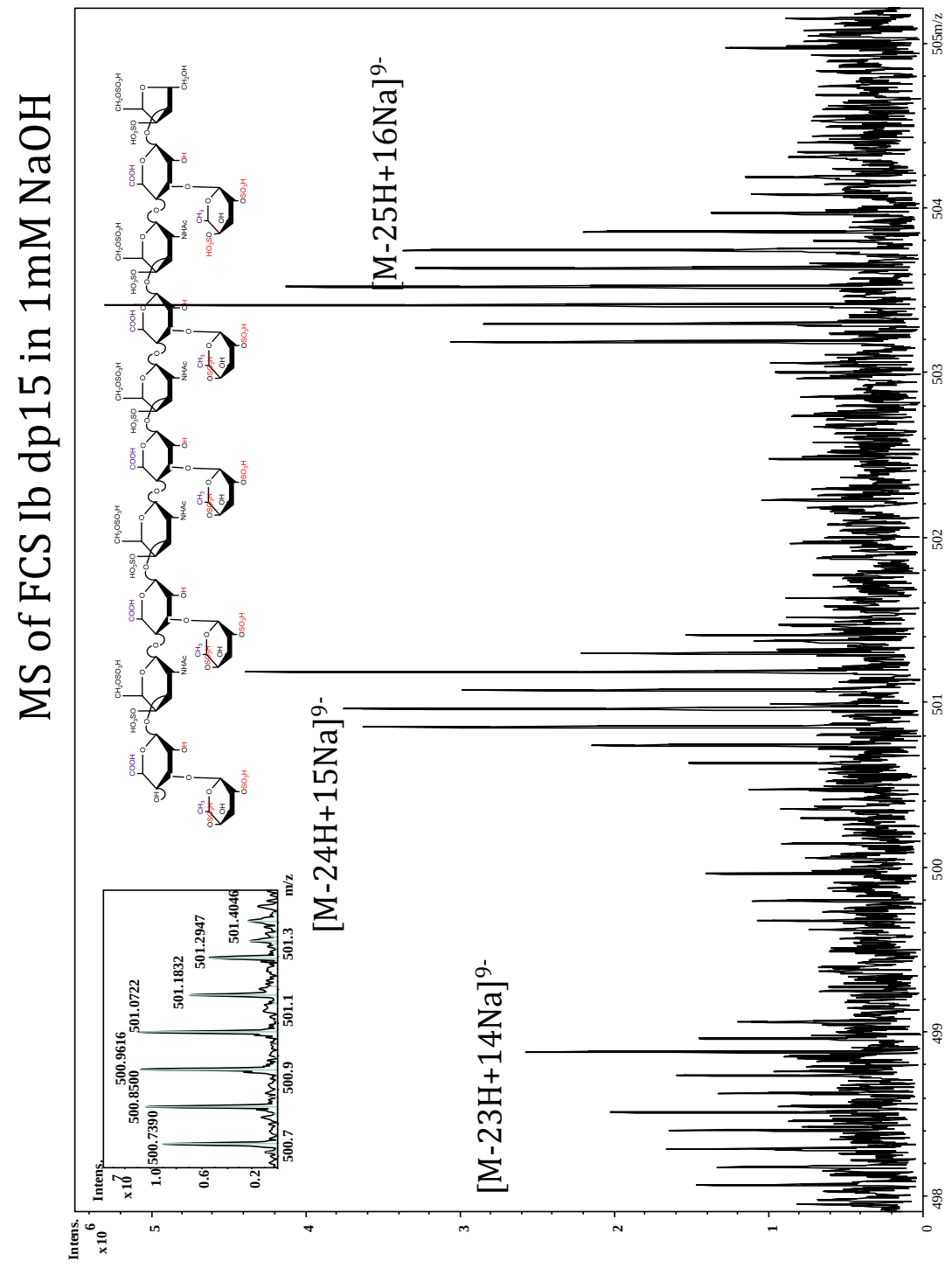

Supplementary Figure 6. ESI MS of FCS Ib dp15; insert shows isotopic distribution of the selected molecular ion $[M-24H+15Na]^{9-}$.

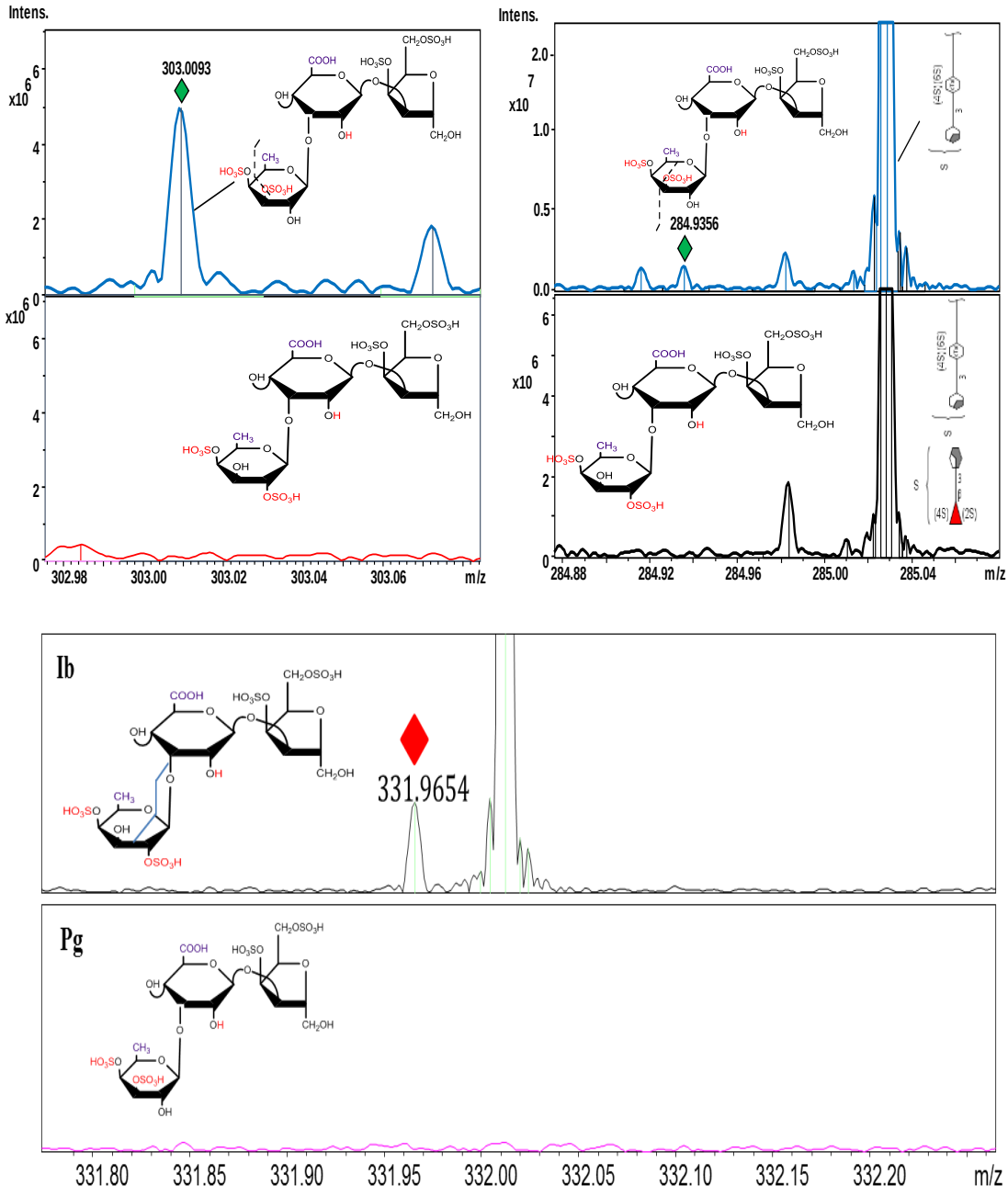

Supplementary Figure 7. Expanded diagnostic ration region for the MS/MS comparison of FCS pg dp3 and FCS Ib dp3.

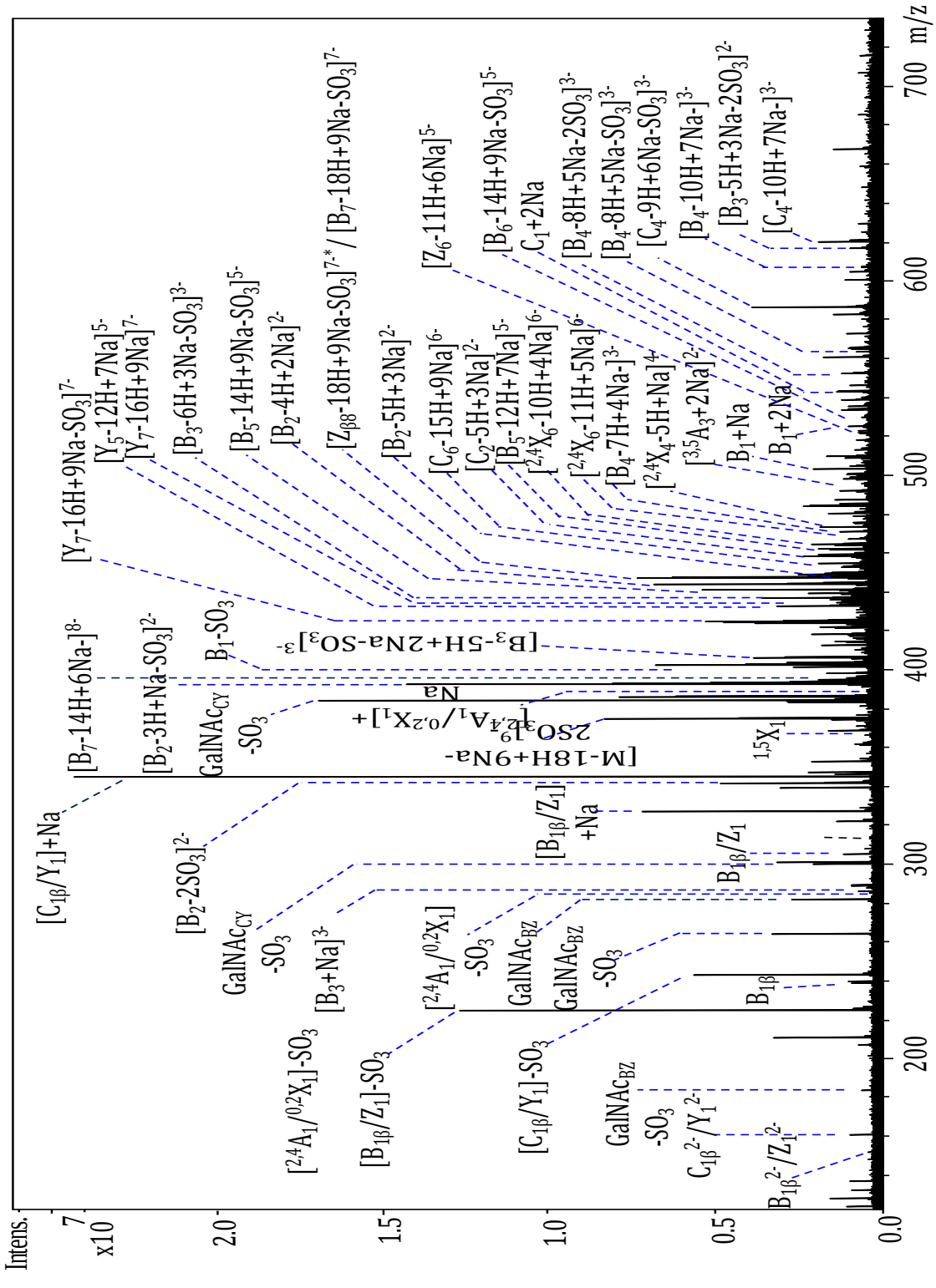

Supplementary Figure. MS/MS spectra annotations for Pg dp 12

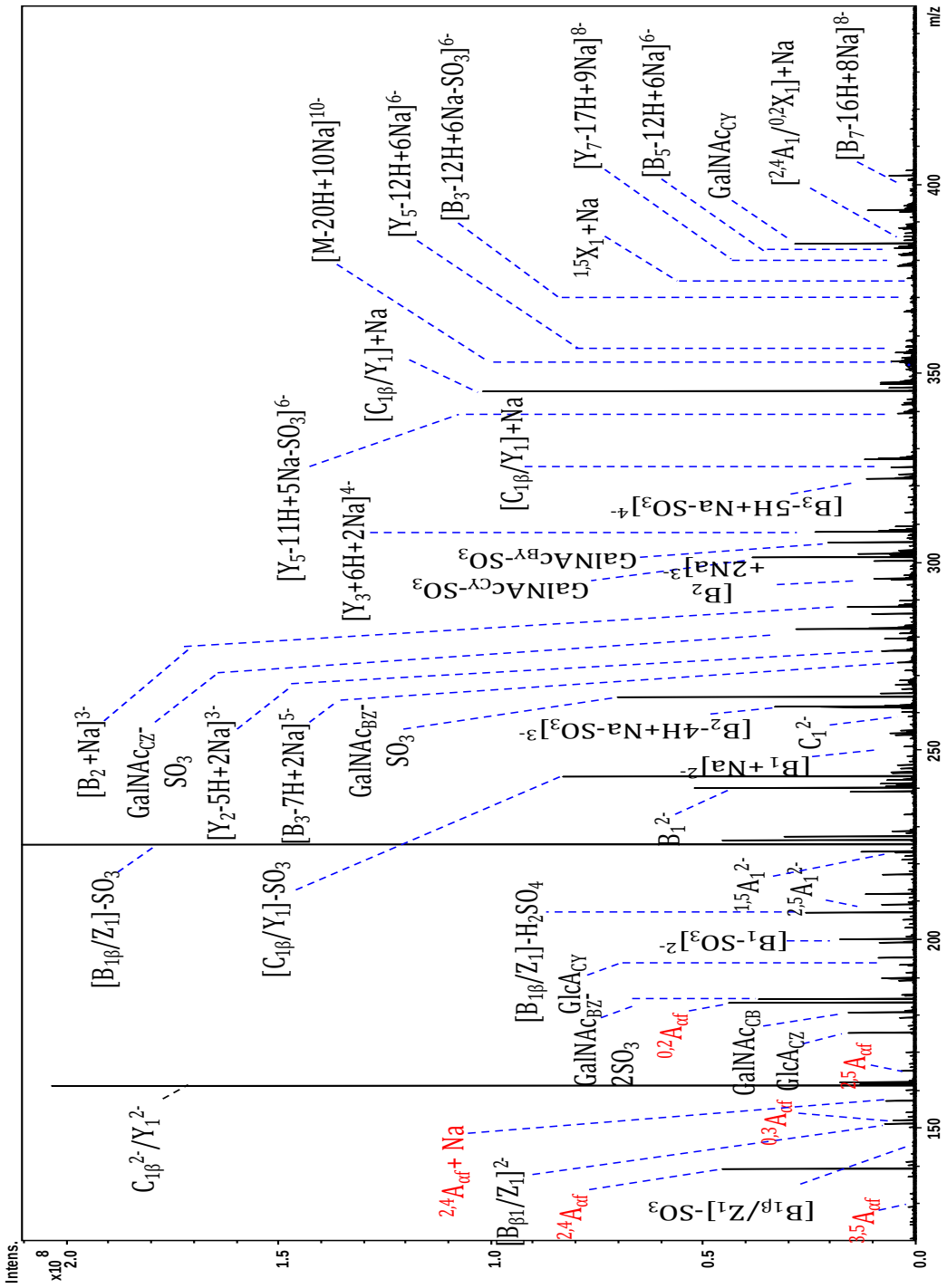

Supplementary Figure MS/MS spectra annotations for Ib dp 12.

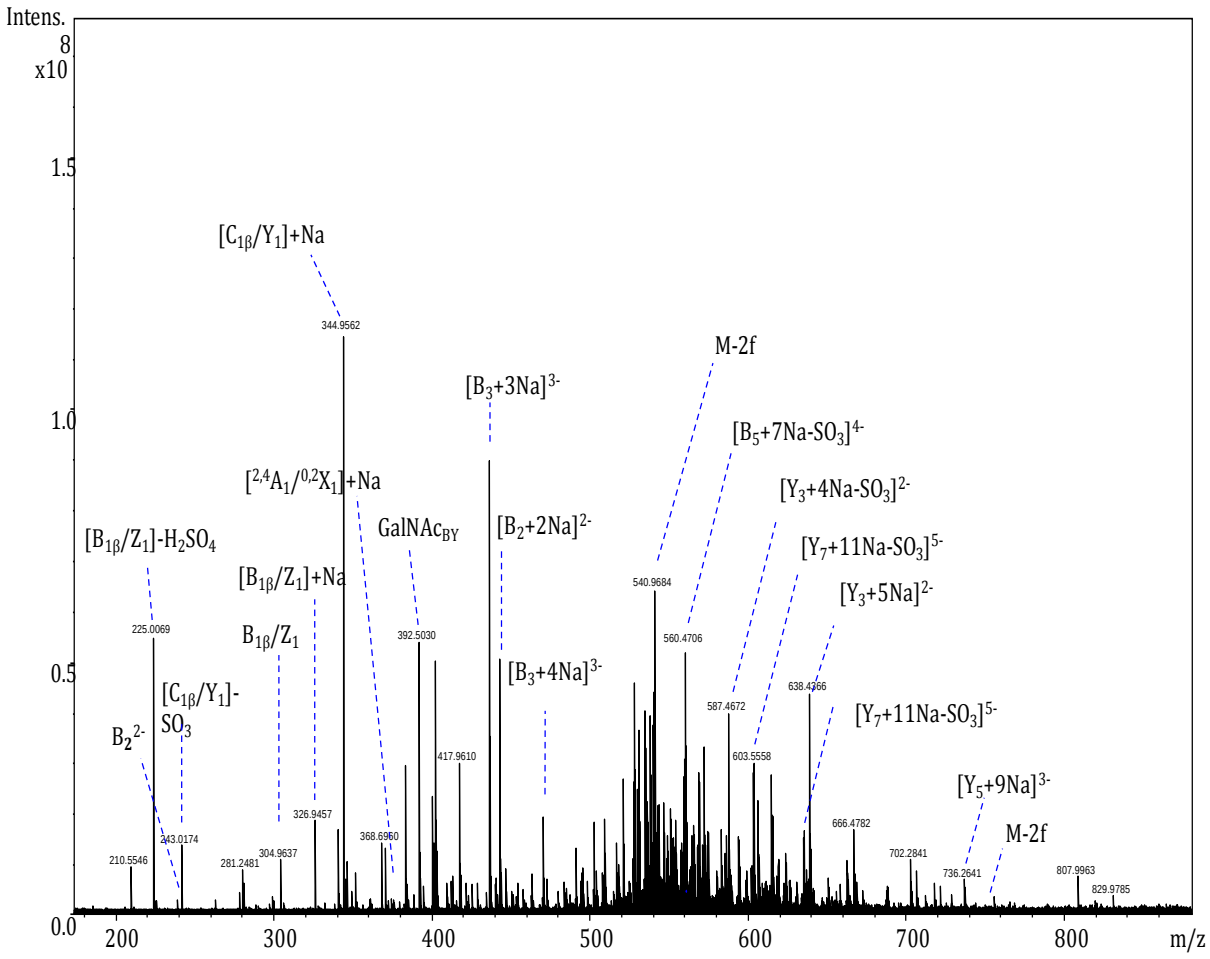

Supplementary Figure. MS/MS spectra annotations for Pg dp 15.

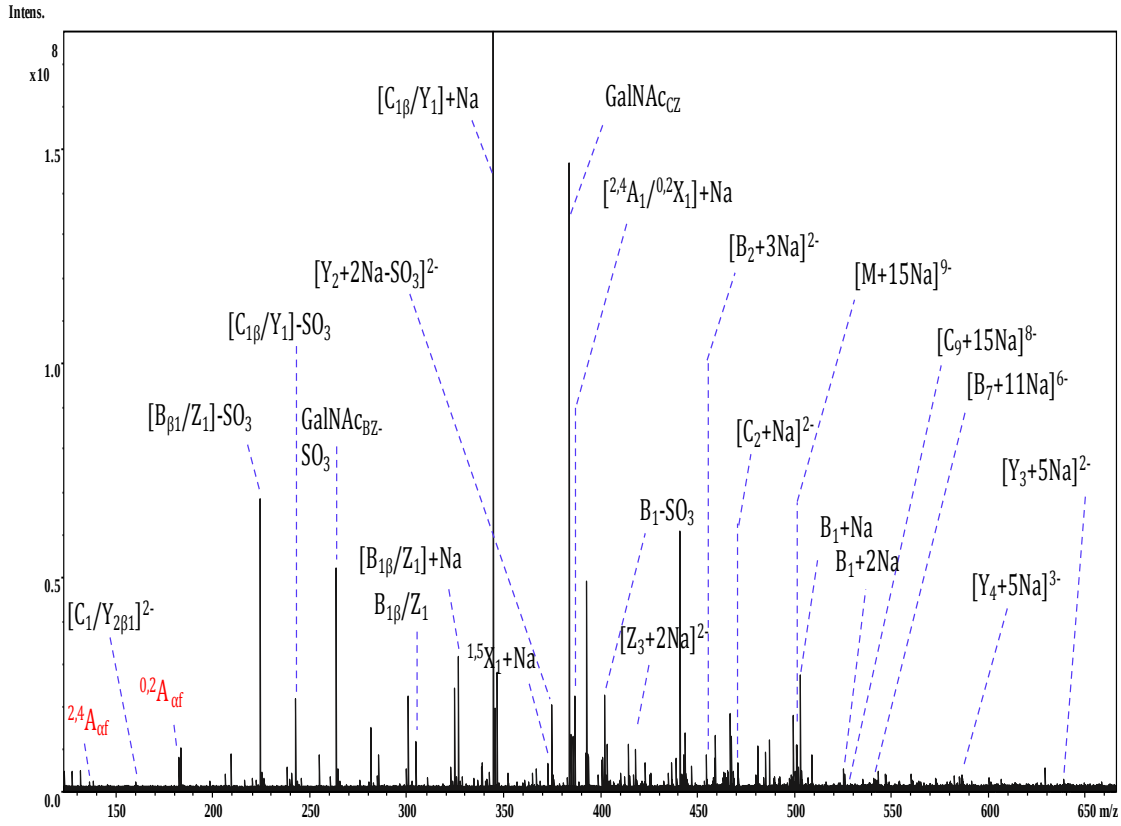

Supplementary Figure. MS/MS spectra annotations for Ib dp 15.

Pg dp3 m/z 434

Mass to Charge	Intensity	Type	Accuracy PPM	Ion Structure
182.9964	4735698	$^{0,2}A_{\alpha f}$-SO_3	2.635275885	
225.0074	3.57E+07	Z_1-SO_3	0.208579807	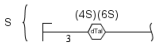
225.0074	3.57E+07	$B_{\beta f}$-SO_3	0.208579807	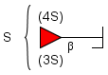
243.0179	2.57E+07	Y_1-SO_3	0.4592995	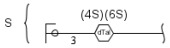
243.0179	2.57E+07	$C_{\beta f}$-SO_3	0.4592995	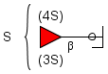
246.9892	2426515	Z_1+Na-SO_3	0.775620958	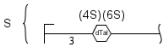
246.9892	2426515	$B_{\beta f}$+Na-SO_3	0.775620958	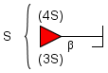
264.9999	2.76E+08	Y_1+Na-SO_3	0.212286872	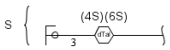
264.9999	2.76E+08	$C_{\beta f}$+Na-SO_3	0.212286872	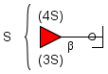
270.9201	1767539	$^{1,4}A_{\alpha f}$+Na	-0.40094478	
285.023	993557	$B_1{}^{3,5}X_{\beta f}$+Na	-0.701038162	
285.0287	7329414	$^{0,2}X_1$-SO_3	-0.433977351	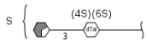
285.0287	7329414	$^{2,4}A_1$-SO_3	-0.433977351	
285.0287	7329414	$^{1,3}A_1$-SO_3	-0.433977351	
298.9514	899351	$^{1,5}A_{\alpha f}$+Na	-0.362921866	
304.9643	7119925	Z_1	-0.126283634	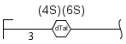
304.9643	7119925	$B_{\beta f}$	-0.126283634	
306.9176	4826932	$^{0,2}A_{\alpha f}$+2Na	-0.045360709	
307.0105	2095193	$^{0,2}X_1$+Na-SO_3	0.068212651	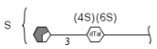
307.0105	2095193	$^{2,4}A_1$+Na-SO_3	0.068212651	
307.0105	2095193	$^{1,3}A_1$+Na-SO_3	0.068212651	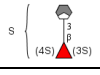

321.9973	851833	$[^{0,4}X_{\beta f}+2Na-2SO_3]^{2-}$	0.96439318	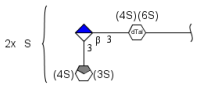
323.0052	853826	$^{2,5}X_1+Na-SO_3$	0.729288569	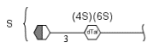
326.9462	5.65E+08	Z_1+Na	0.018737027	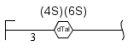
326.9462	5.65E+08	$B_{\beta f}+Na$	0.018737027	
327.0028	800406	$B_1{}^{0,3}X_{\beta f}$	-0.136133391	
337.0212	3562753	$^{1,4}A_1+Na-SO_3$	-0.339361441	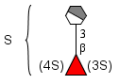
344.9568	2.80E+09	Y_1	-0.084613494	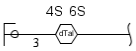
344.9568	2.80E+09	$C_{\beta f}$	-0.084613494	
346.9702	8343895	$[^{0,3}X_{\beta f}+2Na]^{2-}$	1.543265099	
348.9283	7812848	Z_1+2Na	-0.427698183	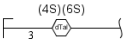
348.9283	7812848	$B_{\beta f}+2Na$	-0.427698183	
351.0006	9284221	$^{1,4}X_1+Na-SO_3$	-0.711719581	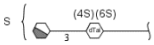
365.0167	824240	$^{2,5}A_1+Na-SO_3$	-1.917035577	
366.9388	1.99E+08	Y_1+2Na	-0.230419896	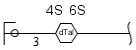
366.9388	1.99E+08	$C_{\beta f}+2Na$	-0.230419896	
372.952	1.81E+08	$^{1,5}X_1+Na$	-0.843449023	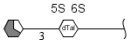
372.9673	7126981	$[^{0,4}X_{\beta f}+3Na-SO_3]^{2-}$	-0.830826188	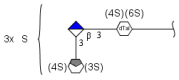
372.9831	1465195	$^{1,4}X_1+2Na-SO_3$	-2.158746603	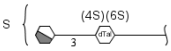
381.0111	5.95E+07	$^{2,4}X_1+Na-SO_3$	-0.485886107	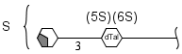
381.0111	5.95E+07	$^{1,3}X_1+Na-SO_3$	-0.485886107	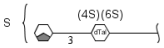
381.0111	5.95E+07	$^{0,2}A_1+Na-SO_3$	-0.485886107	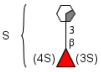
381.0111	5.95E+07	$C_1{}^{1,3}X_{\beta f}+Na$	-0.485886107	
386.9673	8.73E+08	$^{0,2}X_1+Na$	0.091733849	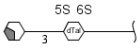
386.9673	8.73E+08	$^{2,4}A_1+Na$	0.091733849	

386.9673	8.73E+08	$^{1,3}A_1$+Na	0.091733849	
394.9806	4714873	[M-5H+3Na-SO_3]$^{2-}$	-1.272204255	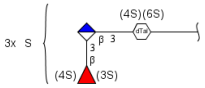
401.0397	9783128	$Z_{\beta f}$-SO_3	-0.411630071	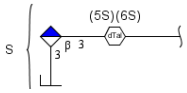
401.0397	9783128	B_1-SO_3	-0.411630071	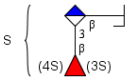
402.9624	2397252	$^{2,5}X_1$+Na	-0.371945373	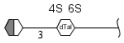
408.9495	1.03E+08	$^{0,2}X_1$+2Na	-0.537631175	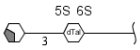
408.9495	1.03E+08	$^{2,4}A_1$+2Na	-0.537631175	
408.9495	1.03E+08	$^{1,3}A_1$+2Na	-0.537631175	
416.9775	1500582	$^{1,4}A_1$+Na	0.959725645	
419.0502	1240362	$Y_{\beta f}$-SO_3	-0.239575116	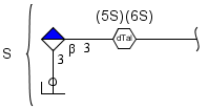
419.0502	1240362	C_1-SO_3	-0.239575116	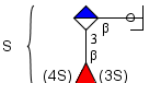
423.0217	2.41E+07	$Z_{\beta f}$+Na-SO_3	-0.521112747	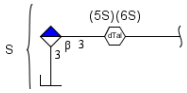
423.0217	2.41E+07	B_1+Na-SO_3	-0.521112747	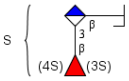
424.9442	2.09E+07	$^{2,5}X_1$+2Na	-0.012335738	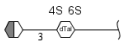
434.9577	5.25E+09	[M-5H+3Na]$^{2-}$	1.850253484	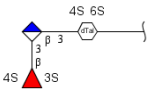
438.9603	2.07E+07	$^{1,4}A_1$+2Na	-1.03694571	
452.9379	2404569	$^{1,4}X_1$+2Na	2.670079055	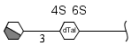
460.9677	5.65E+07	$^{2,4}X_1$+Na	0.063839614	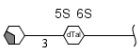
460.9677	5.65E+07	$^{1,3}X_1$+Na	0.063839614	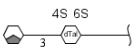
460.9677	5.65E+07	$^{0,2}A_1$+Na	0.063839614	

466.955	1.04E+07	$^{2,5}A_1$+2Na	-0.515158848	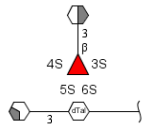
482.95	5.04E+08	$^{2,4}X_1$+2Na	-0.674881458	
482.95	5.04E+08	$^{1,3}X_1$+2Na	-0.674881458	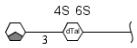
482.95	5.04E+08	$^{0,2}A_1$+2Na	-0.674881458	
488.9366	4549145	$^{2,5}A_1$+3Na	0.212874225	
496.9648	1682764	$^{1,5}A_1$+2Na	1.054662221	
502.9784	9.30E+07	$Z_{\beta f}$+Na	-0.210517987	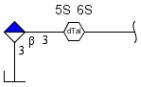
502.9784	9.30E+07	B_1+Na	-0.210517987	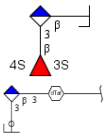
520.9883	1959348	$Y_{\beta f}$+Na	1.07257687	
520.9883	1959348	C_1+Na	1.07257687	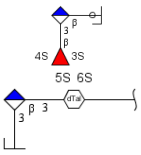
524.9602	7.87E+07	$Z_{\beta f}$+2Na	0.073818929	
524.9602	7.87E+07	B_1+2Na	0.073818929	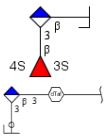
542.9704	6.08E+08	$Y_{\beta f}$+2Na	0.743020246	
542.9704	6.08E+08	C_1+2Na	0.743020246	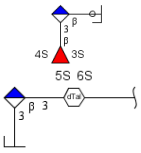
546.9419	2470316	$Z_{\beta f}$+3Na	0.518135473	
546.9419	2470316	B_1+3Na	0.518135473	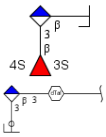
564.9524	7244274	$Y_{\beta f}$+3Na	0.616115623	
564.9524	7244274	C_1+3Na	0.616115623	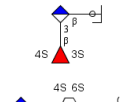
570.9658	1246419	$^{1,5}X_{\beta f}$+2Na	-0.143511222	
584.9813	7526957	$^{0,2}X_{\beta f}$+2Na	0.116455005	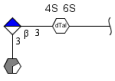
689.0296	721731	[M-3H+2Na-2SO_3]	-1.288411993	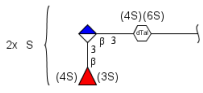

Pg dp 3 m/z 282

Mass to Charge	Intensity	Type	Accuracy PPM	Ion Structure
151.9785	2213629	Z_1^{2-}	-0.049164849	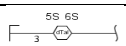
151.9785	2213629	$B_{\beta f}^{2-}$	-0.049164849	
152.9861	1214720	${}^{0,3}A_{\alpha f}$	1.422089981	
160.9526	1127600	${}^{2,4}A_{\alpha f}$+Na-SO_3	0.075388655	
160.9838	1.86E+07	Y_1^{2-}	1.08626593	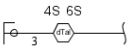
160.9838	1.86E+07	$C_{\beta f}^{2-}$	1.08626593	
171.9747	3357787	Y_1+Na^{2-}	0.274400827	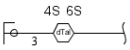
171.9747	3357787	$C_{\beta f}$+Na^{2-}	0.274400827	
175.0248	1308516	$C_1Z_{2\beta f}$	0.066024929	
175.0248	1308516	$B_1Y_{2\beta f}$	0.066024929	
182.997	5519605	${}^{0,2}A_{\alpha f}$ – SO_3	-0.097018037	
193.0354	1781191	$C_1Y_{2\beta f}$	-0.641115235	
200.0161	3918530	$[Z_{2\beta f}$-$SO_3]^{2-}$	-0.853710423	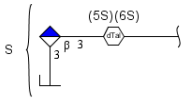

200.0161	3918530	$[B_1\text{-}SO_3]^{2-}$	-0.853710423	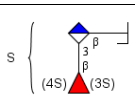
209.0216	5810266	$[Y_{2\beta f}\text{-}SO_3]^{2-}$	-0.901404448	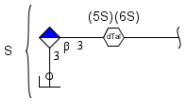
209.0216	5810266	$[C_1\text{-}SO_3]^{2-}$	-0.901404448	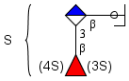
209.0371	1186490	$[^{2,5}X_{\beta f}+Na]^{2-}$	-1.835645443	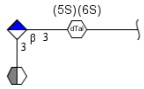
214.3504	1307770	$[M\text{-}3H\text{-}2SO_3]^{3-}$	-1.446065259	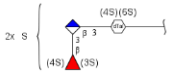
225.0074	1.37E+08	$Z_1\text{-}SO_3$	0.653009925	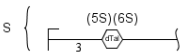
225.0074	1.37E+08	$B_{\beta f}\text{-}SO_3$	0.653009925	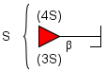
239.9946	1.00E+07	$Z_{2\beta f}^{2-}$	-0.681173376	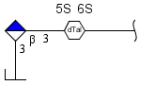
239.9946	1.00E+07	B_1^{2-}	-0.681173376	
241.0023	6828999	$[M\text{-}3H\text{-}SO_3]^{3-}$	-0.159525382	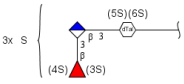
243.018	8.07E+07	$Y_1\text{-}SO_3$	-0.363684845	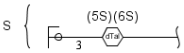
243.018	8.07E+07	$C_{\beta f}\text{-}SO_3$	-0.363684845	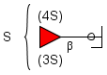

246.9895	2.05E+07	Z_1+Na-SO_3	-0.843881686	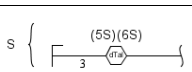
246.9895	2.05E+07	$B_{\beta f}$+Na-SO_3	-0.843881686	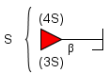
248.3298	3143686	[M-4H+Na-SO_3]$^{3-}$	-0.497590972	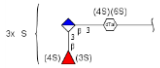
250.9855	2.84E+07	[$Z_{2\beta f}$+Na]$^{2-}$	-0.761633033	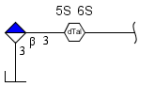
250.9855	2.84E+07	[B_1+Na]$^{2-}$	-0.761633033	
255.0122	1462417	$B_1^{2,5}X_{\beta f}$+Na	0.139216869	
259.9907	4.98E+08	[$Y_{2\beta f}$+Na]$^{2-}$	-0.418537726	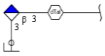
259.9907	4.98E+08	[C_1+Na]$^{2-}$	-0.418537726	
260.006	4026855	[$^{2,5}X_{\beta f}$+2Na-SO_3]$^{2-}$	0.368756875	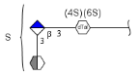
265	7.35E+07	Y_1+Na-SO_3	-0.165071698	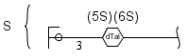
265	7.35E+07	$C_{\beta f}$+Na-SO_3	-0.165071698	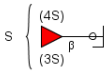
270.9201	9068252	$^{1,4}A_1$+Na	-0.770057013	
282.0506	3.23E+07	[M-2H-3SO_3]$^{2-}$	-0.829670279	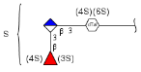

282.3091	9.44E+09	$[M-5H+2Na]^{3-}$	0.576783863	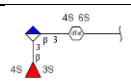
283.0436	1199961	$B_1{}^{2,4}X_{\beta f}+Na$	-0.227420793	
283.0436	1199961	$B_1{}^{1,3}X_{\beta f}+Na$	-0.227420793	
284.9356	1479085	$^{0,2}A_{\alpha f}+Na$	0.145436372	
285.0228	5861823	$B_1{}^{3,5}X_{\beta f}+Na$	6.60E-04	
296.0013	3787273	$[^{0,3}X_{\beta f}+Na-SO_3]^{2-}$	0.188749171	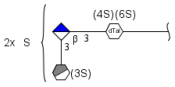
298.9515	1112277	$^{1,5}A_{\alpha f}+Na$	-0.697424164	
303.0094	4963099	$[^{2,4}X_{\beta f}+Na]^{2-}$	-0.393050643	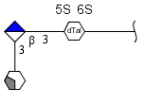
303.0094	4963099	$[^{1,3}X_{\beta f}+Na-SO_3]^{2-}$	-0.393050643	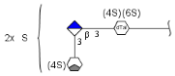
304.9643	2.89E+07	Z_1	-1.110004243	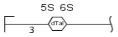
304.9643	2.89E+07	$B_{\beta f}$	-1.110004243	
321.0827	1530259	$Z_{\beta f}$	0.063422912	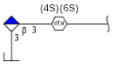
321.0827	1530259	B_1	0.063422912	

322.028	1945407	$[M-2H-2SO_3]^{2-}$	2.401247717	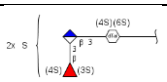
322.9749	1424266	Y_1	-0.847823873	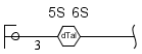
322.9749	1424266	$C_{\beta f}$	-0.847823873	
326.9462	1.69E+09	Z_1+Na	-0.898844307	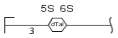
326.9462	1.69E+09	$B_{\beta f}$+Na	-0.898844307	
327.0029	2199589	$B_1{}^{0,3}X_{\beta f}$	-0.441941035	
339.093	3030471	$Y_{\beta f}$	0.840624843	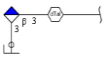
339.093	3030471	C_1	0.840624843	
344.9567	3.13E+09	Y_1+Na	0.495169537	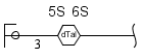
344.9567	3.13E+09	$C_{\beta f}$+Na	0.495169537	
346.9703	1.12E+07	$[^{0,3}X_{\beta f}$+2Na$]^{2-}$	1.255055548	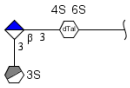
348.9283	4865995	Z_1+2Na	-0.427698183	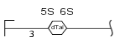

348.9283	4865995	$B_{\beta f}$+2Na	-0.427698183	
366.939	8.87E+07	Y_1+2Na	-0.775469493	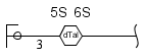
366.939	8.87E+07	$C_{\beta f}$+2Na	-0.775469493	
401.0396	1.36E+08	$Z_{\beta f}$-SO_3	0.336425797	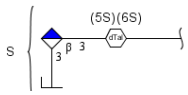
401.0396	1.36E+08	B_1-SO_3	0.336425797	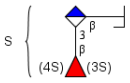
419.0498	1.37E+07	$Y_{\beta f}$-SO_3	-0.478209895	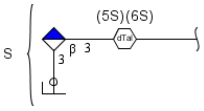
419.0498	1.37E+07	C_1-SO_3	-0.478209895	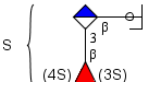
423.0213	4.08E+07	$Z_{\beta f}$+Na-SO_3	-0.048323785	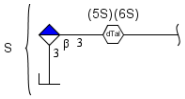
423.0213	4.08E+07	B_1+Na-SO_3	-0.048323785	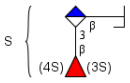
502.9777	1.29E+07	$Z_{\beta f}$+Na	-0.210517987	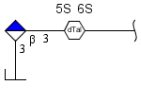
502.9777	1.29E+07	B_1+Na	-0.210517987	

Pg dp 3 205

Mass to charge	Intensity	Type	Accuracy PPM	Ion Structure
129.4916	473100	$[Y_{1\beta}+Na]^{4-}$	1.21533752	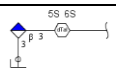
129.4916	473100	$[C_1+Na]^{4-}$	1.21533752	
137.9811	596675	$^{1,5}A_{\alpha f}{}^{2-}$	-0.469506331	
138.9705	469152	$^{2,4}A_{\alpha f}$-SO_3	1.205262988	
150.0081	443046	$[^{2,5}X_1$-$SO_3]^{2-}$	0.048310725	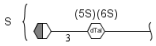
151.9785	2.66E+07	$Z_1{}^{2-}$	-0.049164849	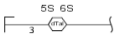
151.9785	2.66E+07	$B_{\beta f}{}^{2-}$	-0.049164849	
160.9838	5.17E+07	$Y_1{}^{2-}$	-0.156096452	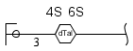
160.9838	5.17E+07	$C_{\beta f}{}^{2-}$	-0.156096452	
165.6639	877557	$Y_{2\beta f}{}^{3-}$	1.330601698	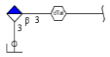
165.6639	877557	$C_1{}^{2-}$	1.330601698	
168.9812	3.08E+07	$^{1,4}A_{\alpha f}-SO_3$	0.190447221	
174.9813	520924	$^{1,5}X_1{}^{2-}$	-0.387572844	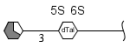
175.0248	7589225	$C_1Z_{2\beta f}$	0.066024929	
175.0248	7589225	$B_1Y_{2\beta f}$	0.066024929	

181.9891	4107527	$^{0,2}X_1^{2-}$	-0.235101993	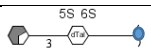
181.9891	4107527	$^{2,4}A_1^{2-}$	-0.235101993	
182.997	1.07E+07	$^{0,2}A_{\alpha f} - SO_3$	-0.64347503	
189.9865	2312419	$^{2,5}X_1^{2-}$	0.0764528	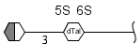
192.9798	2040872	$[^{0,2}X_1+Na]^{2-}$	1.189414643	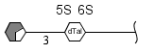
192.9798	2040872	$[^{2,4}A_1+Na]^{2-}$	1.189414643	
193.0354	1580572	$C_1Y_{2\beta f}$	-0.123075871	
194.343	7241325	$^{2,4}X_{2\beta f}{}^{3-}$	0.241384219	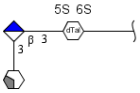
196.9943	1570267	$^{1,4}A_1^{2-}$	0.200802764	
197.0068	693933	$C_1Z_{2\beta f}+Na$	-0.222357807	
197.0068	693933	$B_1Y_{2\beta f}$	-0.222357807	
197.0125	1158688	$^{1,5}A_{\alpha f}-SO_3$	0.163999746	
Mass to charge	Intensity	Type	Accuracy PPM	Ion Structure
200.0161	3.72E+07	$Z_{2\beta f}-SO_3^{2-}$	0.14620823	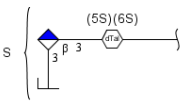

200.0161	3.72E+07	B_1-SO_3^{2-}	0.14620823	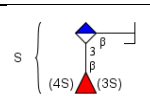
205.0719	1315234	$^{0,2}X_1$	-0.67416355	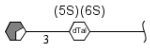
205.0719	1315234	$^{2,4}A_1$	-0.674163549	
205.9845	2.31E+09	$[M-5H+Na]^{4-}$	0.688673177	
207.9857	627028	$[^{1,4}A_1+Na]^{2-}$	-1.866109064	
209.0214	6726480	$[Y_{2\beta f}$-$SO_3]^{2-}$	0.055434515	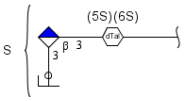
209.0214	6726480	$[C_1$-$SO_3]^{2-}$	0.055434515	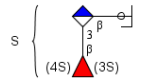
209.0371	1186490	$[^{2,5}X_{\beta f}+Na]^{2-}$	-1.835645443	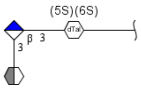
210.9918	1191113	$^{2,5}A_1^{2-}$	-0.014844179	
216.3229	572715	$^{0,3}X_{\beta f}^{3-}$	2.473502959	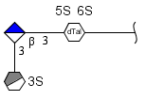
218.9894	3955741	$^{2,4}X_1^{2-}$	-0.665881545	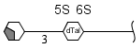
218.9894	3955741	$^{0,2}A_1^{2-}$	-0.665881545	
225.0074	4.45E+08	Z_1-SO_3	0.208579807	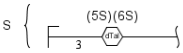
225.0074	4.45E+08	$B_{\beta f}$-SO_3	0.208579807	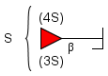
225.9971	6383493	$^{1,5}A_1^{2-}$	-0.091987906	

229.9803	2108564	$[^{2,4}X_1+Na]^{2-}$	-0.319601288	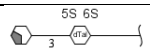
229.9803	2108564	$[^{0,2}A1+Na]^{2-}$	-0.319601288	
239.9946	1.89E+08	$Z_{2\beta f}^{2-}$	-0.264497618	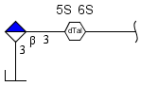
239.9946	1.89E+08	B_1^{2-}	-0.264497618	
241.0023	4.82E+07	$[M-3H-SO_3]^{3-}$	0.255408351	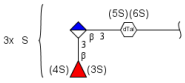
243.018	2.48E+08	Y_1-SO_3	0.047807158	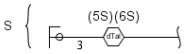
243.018	2.48E+08	$C_{\beta f}-SO_3$	0.047807158	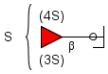
246.9895	1.13E+07	$Z_1+Na-SO_3$	-0.439006516	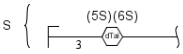
246.9895	1.13E+07	$B_{\beta f}+Na-SO_3$	-0.439006516	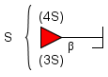
248.9999	2885233	$Y_{\beta f}^{2-}$	-0.325843504	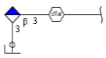
248.9999	2885233	C_1^{2-}	-0.325843504	
250.9855	1.86E+07	$[Z_{2\beta f}+Na]^{2-}$	0.035225142	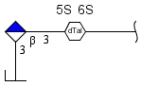
250.9855	1.86E+07	$[B_1+Na]^{2-}$	0.035225142	
259.9907	7.64E+08	$[Y_{2\beta f}+Na]^{2-}$	0.350720237	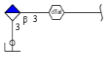
259.9907	7.64E+08	$[C_1+Na]^{2-}$	0.350720237	

265	2.13E+07	Y_1+Na-SO_3	-0.165071698	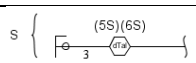
265	2.13E+07	$C_{\beta f}$+Na-SO_3	-0.165071698	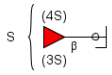
270.9201	1411140	$^{1,4}A_1$+Na	-0.40094478	
271.0129	1520599	$^{1,5}X_1$	0.096821959	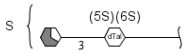
274.982	3.27E+08	$[M-4H+Na]^{3-}$	-0.189277844	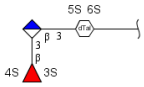
285.0287	1.27E+07	$^{0,2}X_1$-SO_3	-0.433977351	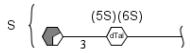
285.0287	1.27E+07	$^{2,4}A_1$-SO_3	-0.433977351	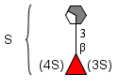
292.0176	872510	$^{2,4}X_{\beta f}^{2-}$	2.084062741	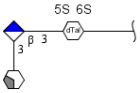
298.9515	1112277	$^{1,5}A_{\alpha f}$+Na	-0.697424164	
301.0236	1603815	$^{2,5}X_1$-SO_3	-0.362343683	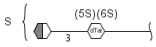
303.0094	2210692	$[^{2,4}X_{\beta f}$+Na$]^{2-}$	-0.723073278	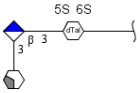
304.9643	4.38E+07	Z_1	-0.126283634	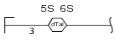
304.9643	4.38E+07	$B_{\beta f}$	-0.126283634	
315.0391	9782023	$^{1,4}A_1$-SO_3	0.130110834	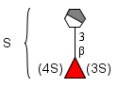
322.9749	7110174	Y_1	-0.22858123	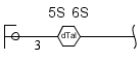

322.9749	7110174	$C_{\beta f}$	-0.22858123	
323.0054	2492328	$^{2,5}X_{\beta f}$+Na-SO_3	0.110103422	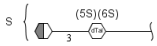
326.9462	2.30E+07	Z_1+Na	0.018737027	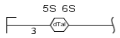
326.9462	2.30E+07	$B_{\beta f}$	0.018737027	
343.0342	2698427	$^{2,5}A_1$-SO_3	-0.4209143	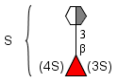
344.9567	3.67E+08	Y_1+Na	0.205277938	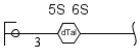
344.9567	3.67E+08	$C_{\beta f}$+Na	0.205277938	
364.9851	591111	$^{0,2}X_1$	0.796909243	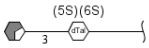
364.9851	591111	$^{2,4}A_1$	0.796909243	
372.9516	8839686	$^{1,5}X_1$+Na	0.229075301	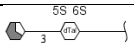
373.0446	6720657	$^{1,5}A_1$-SO_3	0.054411724	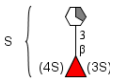
381.011	9895787	$^{2,4}X_1$+Na-SO_3	-0.22342662	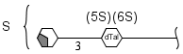
381.011	9895787	$^{0,2}A_1$+Na-SO_3	-0.22342662	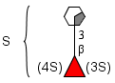
386.9672	6.44E+07	$^{0,2}X_1$+Na	0.350153708	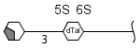
386.9672	6.44E+07	$^{2,4}A_1$+Na	0.350153708	
401.0396	7.76E+07	$Z_{\beta f}$-SO_3	-0.162278239	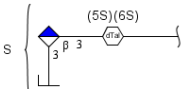
401.0396	7.76E+07	B_1-SO_3	-0.162278239	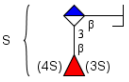

416.9779	5618035	$^{1,4}A_1$+Na	4.41E-04	
419.0498	1128063	$Y_{\beta f}$-SO_3	0.714965142	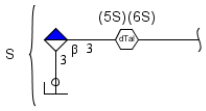
419.0498	1128063	C_1-SO_3	0.714965142	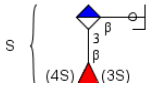
423.0213	4576912	$Z_{\beta f}$+Na-SO_3	0.424465624	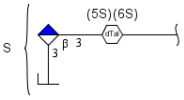
423.0213	4576912	B_1+Na-SO_3	0.424465624	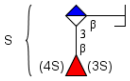
444.9726	1.59E+07	$^{2,5}A_1$+Na	0.482739836	
474.9834	6514866	$^{1,5}A_1$+Na	-0.043176246	
502.9777	1084875	$Z_{\beta f}$+Na	1.18119352	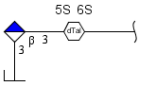
502.9777	1084875	B_1+Na	1.18119352	

Ib dp 3 434

Mass to charge	Intensity	Type	Accuracy PPM	Structure
138.9705	757365	$^{2,4}A_{\alpha f}$	1.205262988	
160.9523	557021	$^{2,4}A_{\alpha f}$ + Na	1.442252671	
182.9966	8319349	$^{0,2}A_{\alpha f}$	1.10518945	
225.0072	2.42E+07	Z_1-SO_3	0.786339037	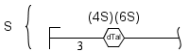
225.0072	2.42E+07	$B_{1\beta}$-SO_3	0.786339037	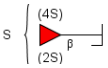
239.9946	493576	$Z_{2\beta}^{2-}$	-0.514503115	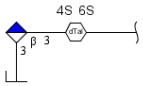
239.9946	493576	B_1^{2-}	-0.514503115	
243.0178	1.12E+07	Y_1-SO_3	0.788493617	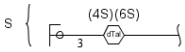
243.0178	1.12E+07	$C_{1\beta}$-SO_3	0.788493617	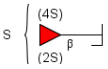
259.9911	613347	$[Y_{2\beta}+Na]^{2-}$	-1.264720119	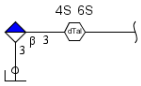
259.9911	613347	$[C_1+Na]^{2-}$	-1.264720119	
264.9998	1.69E+07	Y_1+Na-SO_3	0.476438041	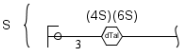
264.9998	1.69E+07	$C_{1\beta}$+Na-SO_3	0.476438041	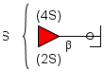
271.0122	364900	$^{1,5}X_1$-SO_3	2.42144018	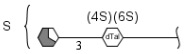

285.0284	798942	$^{0,2}X_1$-SO_3	0.302790784	
285.0284	798942	$^{2,4}A_1$-SO_3	0.302790784	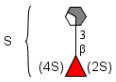
298.9515	408329	$^{1,5}A_{\alpha f}$ + Na	-0.965025841	
304.9641	5282509	Z_1	0.299995897	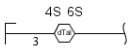
304.9641	5282509	$B_{1\beta}$	0.299995897	
326.9461	4.16E+07	Z_1 + Na	0.324597846	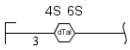
326.9461	4.16E+07	$B_{1\beta}$ + Na	0.324597846	
344.9566	3.22E+08	Y_1+Na	0.263256244	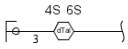
344.9566	3.22E+08	$C_{1\beta}$+Na	0.263256244	
346.9703	1195943	$[^{2,4}X_{\beta f}$+2Na$]^{2-}$	1.168592715	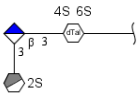
348.9280	1481826	Z_1 + Na	0.432077678	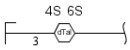
348.9280	1481826	$B_{1\beta}$ + Na	0.432077678	
351.0005	581020	$^{1,4}X_1$+Na-SO_3	-0.398329928	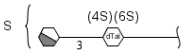
366.9387	1.94E+07	Y_1+2Na	-0.012399891	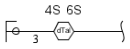
366.9387	1.94E+07	$C_{1\beta}$+2Na	-0.012399891	
372.9517	1.46E+07	$^{1,5}X_1$+Na	-0.065869118	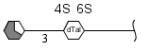
381.0109	3490022	$^{2,4}X_1$+Na-SO_3	0.039033004	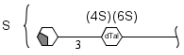

381.0109	3490022	$^{0,2}A_1$+Na-SO_3	0.039033004	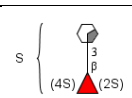
386.96736	6.18E+07	$^{0,2}X_1$+Na	-0.063318002	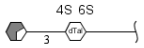
386.96736	6.18E+07	$^{2,4}A_1$+Na	-0.063318002	
401.03958	3878778	$Z_{1\beta}$-SO_3	-0.112407858	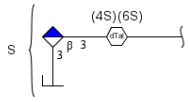
401.03958	3878778	B_1-SO_3	-0.112407858	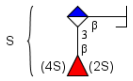
408.94937	1.09E+07	$^{0,2}X_1$+2Na	-0.219743584	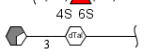
408.94937	1.09E+07	$^{2,4}A_1$+2Na	-0.219743583	
423.02153	2204132	$Z_{1\beta}$+Na-SO_3	-0.119242158	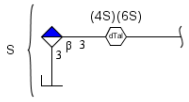
423.02153	2204132	B_1+Na-SO_3	-0.119242158	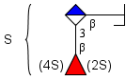
424.94437	1641024	$^{2,5}X_1$+2Na	-0.412388097	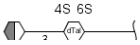
438.95939	4878100	$^{1,4}A_1$+2Na	1.036136851	
441.03123	2137194	$Y_{2\beta}$+ Na-SO_3	1.846227534	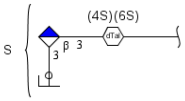
441.03123	2137194	C_1+Na-SO_3	1.846227534	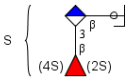
460.96774	2526556	$^{2,4}X_1$+Na	-0.02293436	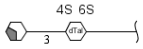

460.96774	2526556	$^{0,2}A_1$+Na	-0.02293436	
466.95476	578068	$^{2,5}A_1$+2Na	-0.001190694	
482.9499	1.98E+07	$^{2,4}X_1$+2Na	-0.467820782	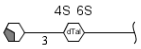
482.9499	1.98E+07	$^{0,2}A_1$+2Na	-0.467820782	
502.97819	4583382	$Z_{1\beta}$+Na	0.206995059	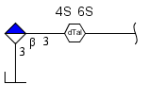
502.97819	4583382	B_1+Na	0.206995059	
524.96087	4957187	$Z_{2\beta}$+2Na	-1.202466767	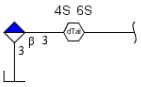
524.96087	4957187	B_1+2Na	-1.202466767	
542.97065	7228288	$Y_{2\beta}$+2Na	0.28258986	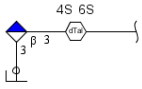
542.97065	7228288	C_1+2Na	0.28258986	
564.95401	465325	$Y_{2\beta}$+3Na	-2.233675623	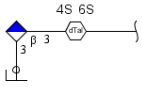
564.95401	465325	C_1+3Na	-2.233675623	
584.98177	670763	$^{0,2}X_{2\beta}$-SO_3	-0.68698893	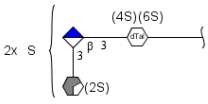

Ib dp 3 282

Mass to charge	Intensity	Type	Accuracy PPM	Structure
138.9707	1623989	$^{2,4}A_{\alpha f}$	-0.233891029	
151.9783	465102	Z_1^{2-}	1.266812433	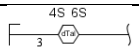
151.9783	465102	$B_{1\beta}^{2-}$	1.266812433	
152.9862	342147	$^{0,3}A_{\alpha f}$	0.768435323	
157.0143	501241	$GlcA_{BZ}$	-0.338376823	
160.9527	1422239	$^{2,4}A_{\alpha f}$ + Na	-0.545911935	
160.9838	1.35E+07	Y_1^{2-}	-0.156096452	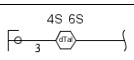
160.9838	1.35E+07	$C_{1\beta}^{2}$	-0.156096452	
165.664	319886	$Y_{2\beta}^{3-}$	0.726969448	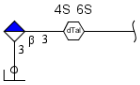

165.664	319886	C_1^{3-}	0.726969448	
168.9815	247395	$^{1,4}A_1$+Na-SO_3	-1.584895388	
175.0249	1480349	$GlcA_{CZ}$	-0.505322386	
175.0249	1480349	$GlcA_{BY}$	-0.505322386	
182.9969	5542940	$^{0,2}A_{\alpha f}$	-0.097018037	
193.0353	655719	$GlcA_{CY}$	0.39496403	
197.007	309813	$GlcA_{CZ}$	-1.237549935	
197.007	309813	$GlcA_{BY}$	-1.237549935	
200.0161	3279072	$[Z_{2\beta}$-$SO_3]^2$	0.14620823	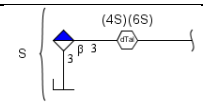
200.0161	3279072	$[B_1$-$SO_3]^{2-}$	0.14620823	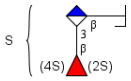
209.0212	842113	$[Y_{2\beta}$-$SO_3]^2$	1.01227531	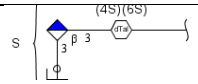
209.0212	842113	$[C_1$-$SO_3]^{2-}$	1.01227531	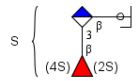
211.0077	390348	$[Z_{2\beta}$+Na-$SO_3]^2$	-2.836090816	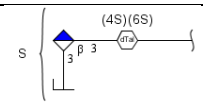
211.0077	390348	$[B_1$+Na-$SO_3]^{2-}$	-2.836090816	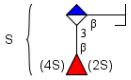

225.0074	1.02E+08	Z_1-SO_3	0.208579807	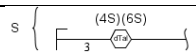
225.0074	1.02E+08	$B_{1\beta}$-SO_3	0.208579807	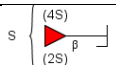
239.9945	1.10E+07	$Z_{2\beta}^{2-}$	0.152178487	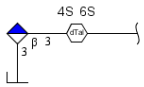
239.9945	1.10E+07	B_1^{2-}	0.152178487	
243.018	2.29E+07	Y_1-SO_3	0.047807158	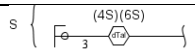
243.018	2.29E+07	$C_{1\beta}$-SO_3	0.047807158	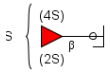
246.9895	1457033	Z_1+Na-SO_3	-0.439006516	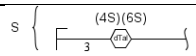
246.9895	1457033	$B_{1\beta}$+Na-SO_3	-0.439006516	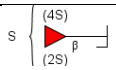
250.9855	1861924	$[Z_{2\beta}+Na]^{2-}$	0.035225142	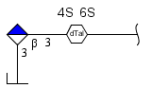
250.9855	1861924	$[B_1+Na]^{2-}$	0.035225142	
259.9908	1.87E+07	$[Y_{2\beta}+Na]^{2-}$	-0.033908892	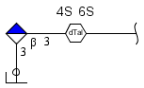
259.9908	1.87E+07	$[C_1+Na]^{2-}$	-0.033908892	
264.9999	9644279	Y_1+Na-SO_3	0.212286872	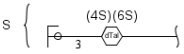
264.9999	9644279	$C_{1\beta}$+Na-SO_3	0.212286872	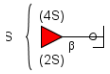
280.9961	333735	$[^{0,2}X_{\beta f}$+Na-$SO_3]^{2-}$	-0.094211272	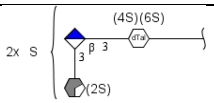

298.951	1011062	$^{1,5}A_{\alpha f}$+Na	0.975089563	
304.9642	1.12E+07	Z_1	0.201623666	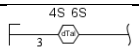
304.9642	1.12E+07	$B_{1\beta}$	0.201623666	
326.9462	2.38E+07	Z_1 + Na	0.018737027	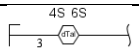
326.9462	2.38E+07	$B_{1\beta}$ + Na	0.018737027	
331.9654	1667067	$[^{0,2}X_{\beta f}$+2Na$]^{2-}$	0.160028726	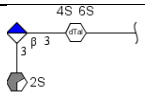
344.9567	3.61E+08	Y_1+Na	0.205277938	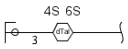
344.9567	3.61E+08	$C_{1\beta}$+Na	0.205277938	
346.9702	1377603	$[^{0,3}X_{\beta f}$+2Na$]^{2-}$	1.543265099	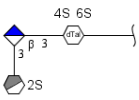
348.9276	547200	Z_1 + 2Na	1.578447792	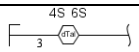
348.9276	547200	$B_{1\beta}$ + 2Na	1.578447792	
353.979	800695	$[^{2,4}X_{\beta f}$+2Na]2-	-1.241601903	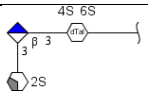
366.9387	1.32E+07	Y_1+2Na	0.042105125	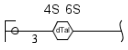
366.9387	1.32E+07	$C_{1\beta}$+2Na	0.042105125	
401.0396	8791207	$Z_{1\beta}$-SO_3	-0.162278239	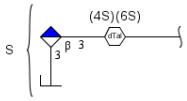

401.0396	8791207	B_1-SO_3	-0.162278239	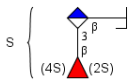
419.0497	1254891	$Y_{1\,\beta}$ -SO_3	0.953600492	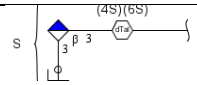
419.0497	1254891	C_1-SO_3	0.953600492	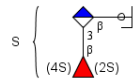
423.0214	3170034	$Z_{1\beta}$+Na-SO3	0.188070863	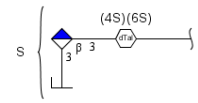
423.0214	3170034	B_1+Na-SO_3	0.188070863	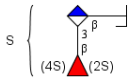
441.0316	1838627	Y_1+Na-SO_3	1.007283832	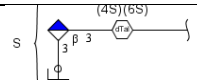
441.0316	1838627	C_1+Na-SO_3	1.007283832	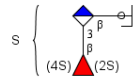
502.9782	3747757	$Z_{2\beta}$+Na	0.187113477	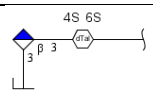
502.9782	3747757	B_1+Na	0.187113477	
524.9613	530186	$Z_{2\beta}$+2Na	-2.021573781	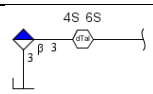
524.9613	530186	B_1+2Na	-2.021573781	
542.9707	6371434	$Y_{2\beta}$+2Na	0.190503834	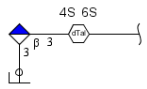
542.9707	6371434	C_1+2Na	0.190503834	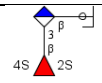

Ib dp 3 205

Mass to charge	Intensity	Type	Accuracy PPM	Structure
151.9785	1937439	Z_1^{2-}	-0.049164849	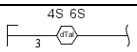
151.9785	1937439	$B_{1\beta}^{2-}$	-0.049164849	
152.9863	664493	${}^{0,3}A_{\alpha f}$	0.11478152	
160.9527	2337516	${}^{2,4}A_{\alpha f}$ + Na	-0.545911935	
160.9838	9.12E+07	Y_1^{2-}	-0.156096452	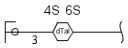
160.9838	9.12E+07	$C_{1\beta}^{2}$	-0.156096452	
168.9812	5696860	${}^{1,4}A_1$+Na-SO_3	0.190447221	
171.9748	743435	$[Y_1+Na]^{2-}$	-0.307079875	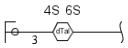
171.9748	743435	$[C_1+Na]^{2-}$	-0.307079875	
179.0108	2736856	$[{}^{2,4}X_1$-$SO_3]^{2-}$	0.262000952	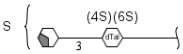
179.0108	2736856	$[{}^{0,2}A_1$-$SO_3]^{2-}$	0.262000952	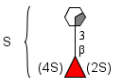
181.989	9985338	${}^{0,2}X_1^{2-}$	0.314381638	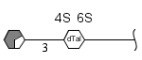
181.989	9985338	${}^{2,4}A_1^{2-}$	0.314381638	

182.9968	2.75E+07	$^{0,2}A_{\alpha f}$	0.449439553	
189.9865	3565765	$^{2,5}X_1^{2-}$	0.0764528	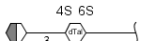
190.9633	1059859	$^{1,4}A_{\alpha F}$+Na-SO_3	-0.645045409	
192.9798	3396651	$[^{0,2}X_1$+Na$]^{2-}$	1.189414643	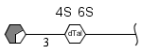
192.9798	3396651	$[^{2,4}A_1$+Na$]^{2-}$	1.189414643	
196.9945	1805321	$^{1,4}A_1^{2-}$	-0.814454211	
197.0125	2509739	$^{1,5}A_{\alpha F}$-SO_3	0.163999746	
200.0161	2.14E+07	$[Z_{2\beta}$-$SO_3]^2$	0.14620823	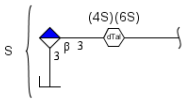
200.0161	2.14E+07	$[B_1$-$SO_3]^{2-}$	0.14620823	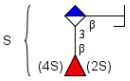
207.9855	666461	$[^{1,4}A_1$+Na$]^{2-}$	-0.904505362	
218.9894	2622930	$^{2,4}X_1^2$	-0.665881545	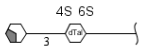
218.9894	2622930	$^{0,2}A_1^{2-}$	-0.665881545	
225.0075	4.56E+08	Z_1-SO_3	-0.235849916	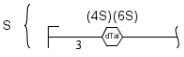
225.0075	4.56E+08	$B_{1\beta}$-SO_3	-0.235849916	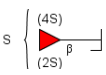

225.9971	5256183	$^{1,5}A_1^{2-}$	-0.091987906	
239.9945	2.41E+07	$Z_{2\beta}^{2-}$	0.152178487	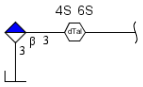
239.9945	2.41E+07	B_1^{2-}	0.152178487	
243.018	8.38E+07	Y_1-SO_3	0.047807158	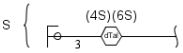
243.018	8.38E+07	$C_{1\beta}$-SO_3	0.047807158	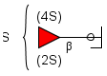
246.9894	1.54E+07	Z_1+Na-SO_3	-0.034131019	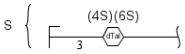
246.9894	1.54E+07	$B_{1\beta}$+Na-SO_3	-0.034131019	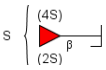
250.9855	3080011	$[Z_{2\beta}+Na]^{2-}$	0.035225142	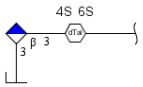
250.9855	3080011	$[B_1+Na]^{2-}$	0.035225142	
259.9908	9.16E+07	$[Y_{2\beta}+Na]^{2-}$	-0.033908892	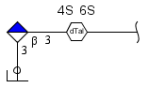
259.9908	9.16E+07	$[C_1+Na]^{2-}$	-0.033908892	
264.9999	1.01E+07	Y_1+Na-SO_3	0.212286872	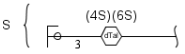
264.9999	1.01E+07	$C_{1\beta}$+Na-SO_3	0.212286872	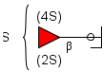
271.0129	1649350	$^{1,5}X_1$-SO_3	0.096821959	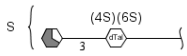
285.0287	6464948	$^{0,2}X_1$-SO_3	-0.433977351	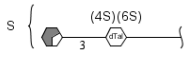

285.0287	6464948	$^{2,4}A_1$-SO_3	-0.433977351	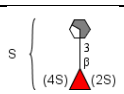
304.9642	1.51E+07	Z_1	0.201623666	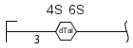
304.9642	1.51E+07	$B_{1\beta}$	0.201623666	
307.0102	1146954	$^{0,2}X_1$+Na-SO_3	1.045378948	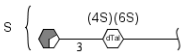
307.0102	1146954	$^{2,4}A_1$+Na-SO_3	1.045378948	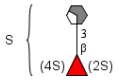
315.0388	1159011	$^{1,4}A_1$-SO_3	1.082374615	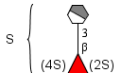
322.9748	2250017	Y_1	0.081040378	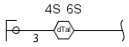
322.9748	2250017	$C_{1\beta}$	0.081040378	
323.0045	1025613	$^{2,5}X_1$+Na-SO_3	2.896442619	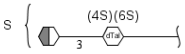
326.9462	1.81E+07	Z_1 + Na	0.018737027	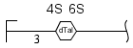
326.9462	1.81E+07	$B_{1\beta}$ + Na	0.018737027	
344.9568	2.21E+08	Y_1+Na	-0.084613494	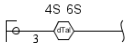
344.9568	2.21E+08	$C_{1\beta}$+Na	-0.084613494	
365.0163	3974384	$^{2,5}A_1$+Na-SO_3	-0.821196204	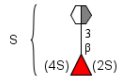
372.9517	9084897	$^{1,5}X_1$+Na	-0.039055996	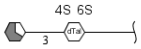
386.9674	1.09E+08	$^{0,2}X_1$+Na	-0.166685876	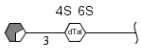

386.9674	1.09E+08	$^{2,4}A_1$+Na	-0.166685876	
401.039	2181672	$Z_{1\beta}$-SO_3	1.333835363	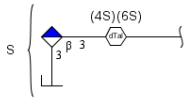
401.039	2181672	B_1-SO_3	1.333835363	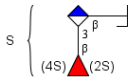
416.9782	7510223	$^{1,4}A_1$+Na	-0.719020803	
423.0212	2334018	$Z_{1\beta}$+Na-SO3	0.660860496	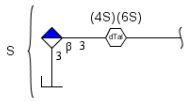
423.0212	2334018	B_1+Na-SO_3	0.660860496	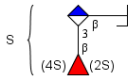
444.973	6127107	$^{2,5}A_1$+Na	-0.416191544	
474.9835	1.02E+07	$^{1,5}A_1$+Na	-0.253709866	

Pg dp6 $[M-9H+3Na]^{6-}$

Mass to charge	Intensity	Type	Accuracy PPM	Ion Structure
136.9915	2124990	$^{3,5}A_{\alpha f}$	-0.708525712	

138.9707	3.92E+07	$^{2,4}A_{\alpha f}$ -SO_3	-0.233891029	
145.0506	1230829	$B_{\beta f}$ -$2SO_3$	0.223204868	
145.0506	1230829	Z_1	0.223204868	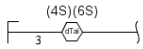
150.008	1791338	$[^{2,5}X_2$-$SO_3]^{2-}$	0.71494187	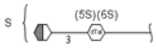
151.9785	1.81E+08	$B_{\beta f}^{2-}$	-0.049164849	
151.9785	1.81E+08	Z_1^{2-}	-0.049164849	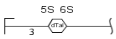
152.9862	3225081	$^{0,3}A_{\alpha f}$	0.768435323	
157.0142	1.27E+07	GlcA	0.298508033	
160.9526	1.32E+07	$^{2,4}A_{\alpha f}$+Na -SO_3	0.075388655	
160.9838	3.43E+08	$C_{\beta f}^{2-}$	-0.156096452	
160.9838	3.43E+08	Y_1^{2-}	-0.156096452	
163.0611	1984213	$C_{\beta f}$	0.595249265	
163.0611	1984213	Y_1	0.595249265	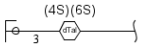
165.6642	1824872	C_1^{3-}	-0.480292866	

167.002	1321589	$^{2,5}A_{\alpha f}$ -SO_3	-0.193865942	
168.9812	1.42E+07	$^{1,4}A_{\alpha f}$-SO_3	0.190447221	
174.9812	1418274	$^{1,5}X_1^{2-}$	0.183916901	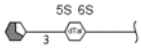
175.0248	4.08E+07	$B_1Y_{\beta f}$	0.066024929	
178.6681	1145398	$B_2Y_{\beta f}^{3-}$/$C_2Z_{\beta f}^{3-}$	-1.939657947	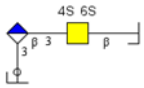
180.4892	2.54E+07	$B_2Y_3^{2-}$/ $C_2Z_3^{2-}$	0.135129969	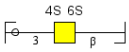
181.9891	44154030	$^{2,4}A_1^{2-}$	-0.235101993	
181.9891	4154030	$^{0,2}X_1^{2-}$	-0.235101993	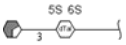
182.9969	4.38E+07	$^{0,2}A_{\alpha f}$-SO_3	-0.097018037	
184.0615	3.50E+07	B_2Z_3	0.170665783	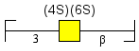
189.4945	3.76E+07	$C_2Y_3^{2-}$	0.035528736	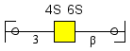
190.963	2771031	$^{1,4}A_{\alpha f}$+Na-SO_3	0.925938533	
193.0353	2.92E+07	$C_1Y_{4\beta f}$	0.39496403	
197.0067	2490439	$B_1Y_{4\beta f}$ / $C_1Z_{4\beta f}$	0.28523903	

197.0125	4228347	$^{1,5}A_{\alpha f}$-SO_3	0.16400000	
200.0161	5.44E+07	B_1^{2-}	0.14620823	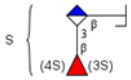
207.9852	1785398	$[^{1,4}A_1+Na]^{2-}$	0.537903659	
208.0002	3785331	$[^{1,5}A_1+2Na-SO_3]^{2-}$	2.002743267	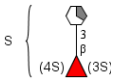
208.3466	2425169	$[Z_2-2SO_3]^{3-}$	- 0.151318364	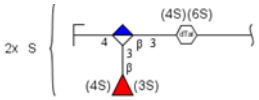
209.0214	1.92E+07	$[C_1-SO_3]^{2-}$	0.055434515	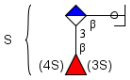
210.9918	7277628	$^{2,5}A_1^{2-}$	- 0.014844179	
214.3501	4142890	$[Y_2-SO_3]^{3-}$	-0.04648781	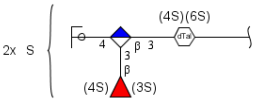
214.7444	3527534	C_2^{4-}	0.566381475	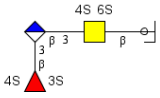
219.9897	4007477	$[Y_{4\beta f}Y_{2\beta f}+3Na]^{5-}$	0.210899874	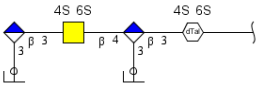
220.24	2327710	$[C_2+Na]^{4-}$	0.035355748	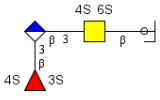
225.0074	1.29E+09	$B_{\beta f}$-SO_3	0.208579807	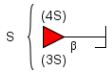
225.0074	1.29E+09	Z_1-SO_3	0.208579807	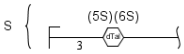

227.3537	1.53E+07	$[B_2\text{-}2SO_3]^{3-}$	0.101373616	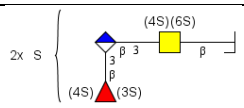
228.5268	4.56E+07	$B_2Y_{4\beta f}{}^{2-}$ /$C_2Z_{4\beta f}{}^{2-}$	0.26738877	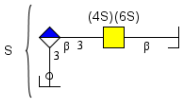
231.2696	1563083	$[Y_3\text{-}3SO_3]^{4-}$	0.843994412	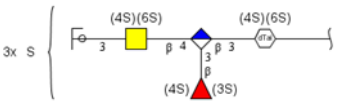
232.4099	1257281	$[B_3\text{-}2SO_3]^{5-}$	0.638687939	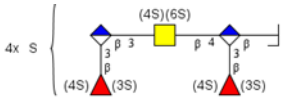
232.4099	1257281	$[Z_{4\beta f}\text{-}2SO_3]^{5-}$	0.638687939	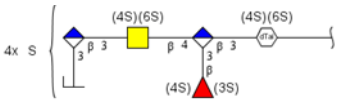
232.9736	1668028	$[^{2,5}A_1+2Na]^{2-}$	0.607390709	
233.3572	2.32E+07	$[C_2\text{-}SO_3]^{3-}$	0.191164732	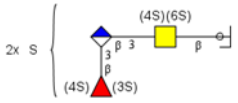
234.2607	1.10E+07	$[Z_{4\beta f}Y_{2\beta f}\text{-}SO_3]^{4-}$	- 0.005063803	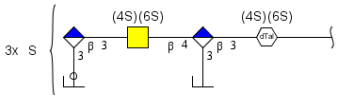
234.9989	4454889	$[Z_2\text{-}SO_3]^{3-}$	- 0.255354387	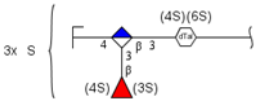
236.0121	6484978	$[C_3\text{-}2SO_3]^{5-}$	0.260048531	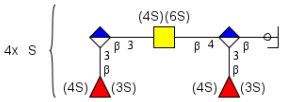
237.5321	1.00E+07	$[C_2Y_{4\beta f}\text{-}SO_3]^{2-}$	0.18291633	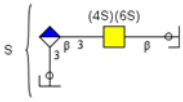
239.9945	1.85E+08	$B_1{}^{2-}$	0.152178487	

241.0023	3.17E+07	$[Y_2\text{-}SO_3]^{3-}$	0.255408351	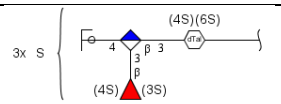
241.5811	2331442	$[Y_3+2Na]^{5-}$	0.61037308	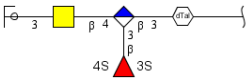
241.9803	8078802	$[B_3Z_1+Na]^{2-}$	-0.303752	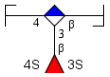
242.3261	6.12E+07	$[Z_2+Na\text{-}SO_3]^{3-}$	0.22643592	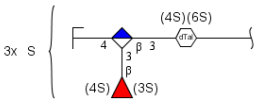
243.018	6.30E+08	$C_{\beta f}\text{-}SO_3$	0.047807158	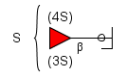
243.018	6.30E+08	$Y_1\text{-}SO_3$	0.047807158	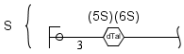
246.9894	9431378	$B_{\beta f}+Na\text{-}SO_3$	-0.034131019	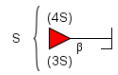
246.9894	9431378	$Z_1+Na\text{-}SO_3$	-0.034131019	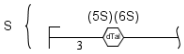
247.5041	4811456	$[M\text{-}6H\text{-}2SO_3]^{6-}$	0.315389388	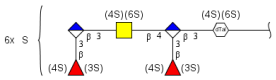
248.3297	6725149	$[Y_2+Na\text{-}SO_3]^{3-}$	-0.094900717	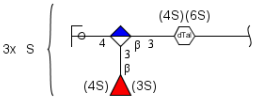
248.4014	1.07E+07	$[B_3\text{-}SO_3]^{5-}$	0.045686538	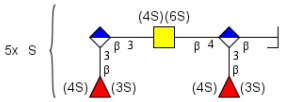
248.9998	6623068	C_1^{2-}	0.075763113	
249.7471	1375873	$Z_{4\beta f}Z_{2\beta f}^{4-}$	0.64577827	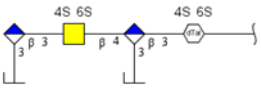

250.9855	8869936	$[B_1+Na]^{2-}$	0.035225142	
251.2591	6291143	$[Y_3-2SO_3]^{4-}$	- 0.402655068	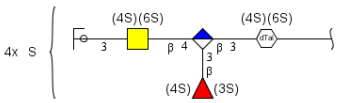
252.0035	5.36E+07	$[C_3-2SO_3]^{5-}$	0.096370884	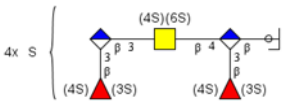
252.7979	4379972	$[B_3+Na-SO_3]^{5-}$	- 0.394480334	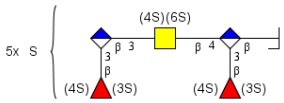
254.006	6.02E+07	$[B_2-SO_3]^{3-}$	- 0.021391883	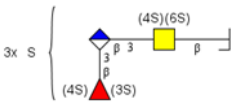
254.2499	1.44E+07	$Z_{4\beta f}Y_{2\beta f}^{4-}$	0.009647005	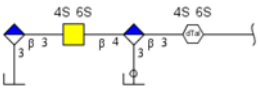
255.2889	1688181	$[C_3-4SO_3]^{4-}$	- 1.122068958	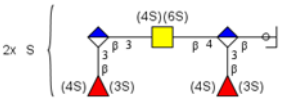
256.7545	1.45E+07	$[Y_3+Na-2SO_3]^{4-}$	- 0.058465383	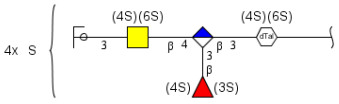
258.7526	1.34E+07	$Y_{4\beta f}Y_{2\beta f}^{4-}$	- 0.217875106	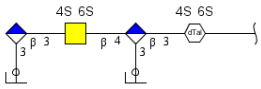
259.379	1598977	$Z_{4\beta f}Y_{2\beta f}^{3-}$ / $Y_{4\beta f}Z_{2\beta f}^{3-}$	- 0.716358431	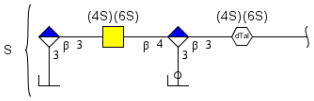
259.5001	1655922	$B_2Z_{4\beta f}^{2-}$	-0.43915012	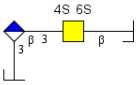
259.7453	6708510	$[Z_{4\beta f}Y_{2\beta f}+Na]^{4-}$	0.341150542	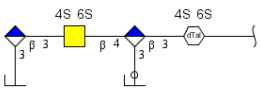

259.9908	2.11E+07	$[C_1+Na]^{2-}$	-0.033908892	
260.0095	1.74E+07	$[C_2-SO_3]^{3-}$	0.062029785	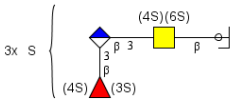
260.7964	9102089	$[C_3+2Na-SO_3]^{5-}$	-0.375231407	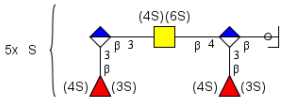
261.3333	4.61E+07	$[B_2+Na-SO_3]^{3-}$	0.036144137	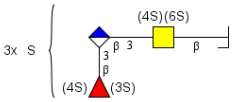
262.9846	2500362	$[Y_2+3Na-SO_3]^{3-}$	-1.117206103	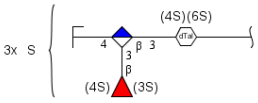
264.0183	9.00E+07	$B_2Z_3-SO_3$	0.174112931	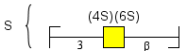
264.248	2543190	$[Y_{4\beta f}Y_{2\beta f}+Na]^{4-}$	0.112711354	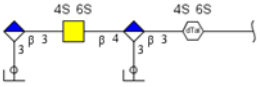
264.9999	1.92E+07	$C_{\beta f}+Na-SO_3$	0.212286872	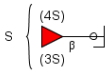
264.9999	1.92E+07	$Y_1+Na-SO_3$	0.212286872	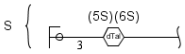
265.1927	2604526	$[Y_{4\beta f}+3Na-SO_3]^{5-}$	-0.033678906	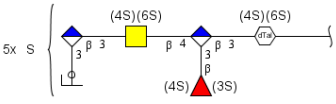
267.3368	2.59E+07	$[C_2+Na-SO_3]^{3-}$	0.115987274	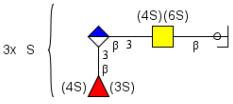
267.9949	3008961	C_3^{5-}	-0.047773297	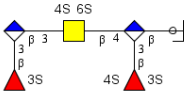

268.1577	1639379	[M-8H+2Na-2SO$_3$]$^{6-}$	-0.265892669	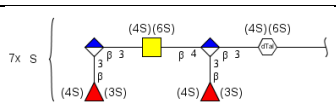
268.5053	5.90E+07	$B_2Y_{4\beta f}^{2-}$	-0.117750003	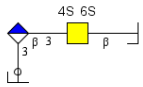
268.7891	1431906	[B$_3$+Na]$^{5-}$	0.235081705	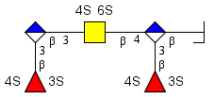
268.9784	1.10E+07	[Z$_2$+Na]$^{3-}$	0.098111967	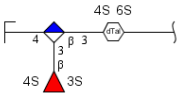
269.6201	6954702	[M-6H+Na-4SO$_3$]$^{5-}$	0.118922143	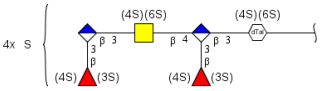
269.7435	1.89E+07	[Y $_{4\beta f}$Y$_{2\beta f}$+2Na]$^{4-}$	0.059105224	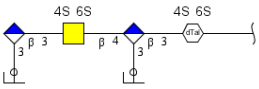
270.0047	1628021	[^{2,4}A$_2$-SO$_3$]$^{2-}$	1.485929689	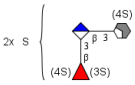
270.7752	9.29E+07	[B$_3$-3SO$_3$]$^{4-}$	-0.088576243	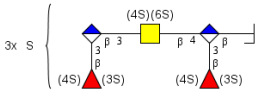
271.013	3708879	^{1,5}X$_1$-SO$_3$	-0.272164066	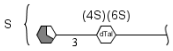
271.7753	1486259	[C$_3$+3Na-4SO$_3$]$^{4-}$	-0.838829908	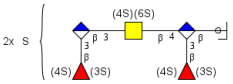
271.7753	1486259	[Y$_{\beta f}$+3Na-4SO$_3$]$^{4-}$	-0.838829908	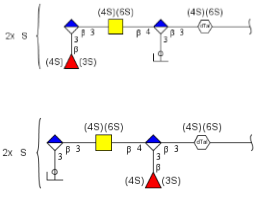

271.8213	9.43E+08	[M-9H+3Na-SO_3]$^{6-}$	-0.0509949	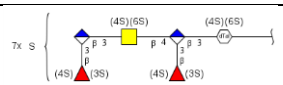
273.0451	1481634	[Z_2-3SO_3]$^{2-}$	-0.059887543	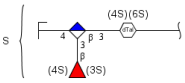
273.1855	3645094	[B_3+2Na]$^{5-}$	0.190767812	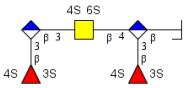
273.1855	3645094	[$Z_{\beta f}$+2Na]$^{5-}$	0.190767812	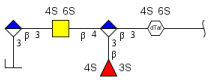 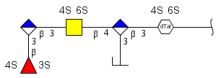
275.239	3660948	[$Y_{4\beta f}Y_{2\beta f}$+3Na]$^{4-}$	0.007639724	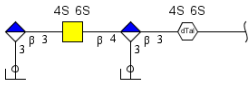
275.2779	3922978	[C_3-3SO_3]$^{4-}$	-0.300833267	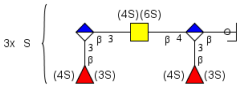
276.3057	3.94E+07	[Z_2+2Na]$^{3-}$	0.149361136	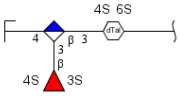
276.7438	3512105	[Y_3+Na-SO_3]$^{4-}$	-0.402438104	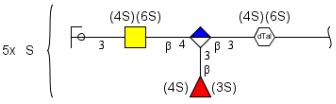
277.5817	1837644	[B_3+3Na]$^{5-}$	0.868366323	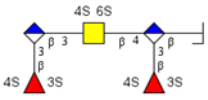
279.4962	1.96E+07	[$B_2Y_{4\beta f}$+Na]$^{2-}$ / [$C_2Z_{4\beta f}$+Na]$^{2-}$	0.145628098	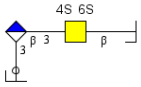
280.7733	3757626	[C_3+Na-3SO_3]$^{4-}$	0.011919759	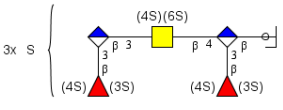

281.184	4.43E+08	$[C_3+3Na]^{5-}$	0.191973228	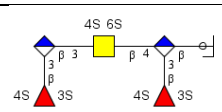
281.992	7174916	$[C_2+3Na-SO_3]^{3-}$	- 1.912230371	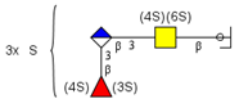
282.0289	1.84E+08	B_2Y_3-SO_3 / C_2Z_3-SO_3	0.037779816	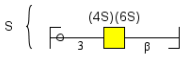
282.043	6227348	$[Y_3-4SO_3]^{3-}$	0.759502393	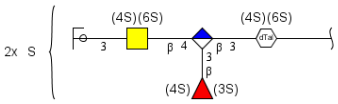
282.0503	2056214	$[Y_2-3SO_3]^{2-}$	0.233968906	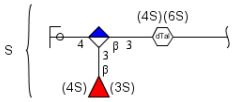
282.2392	4.39E+07	$[Y_3+2Na-SO_3]^{4-}$	- 0.089331142	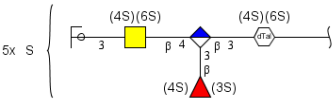
282.3092	1.58E+07	$[Y_2+2Na]^{3-}$	0.222562118	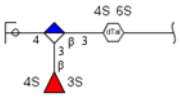
284.9357	1696106	$^{0,2}A_{\alpha f}$+Na	- 0.205520052	
285.0285	1.43E+08	$^{2,4}A_1$-SO_3	0.267706562	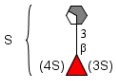
285.0285	1.43E+08	$^{0,2}X_1$-SO_3	0.267706562	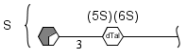
285.1474	4.50E+07	$[M-9H+3Na]^{6-}$	0.076794785	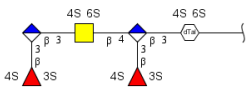
286.0003	5.72E+07	B_2Z_3+Na-SO_3	- 0.032842623	

286.0311	2.96E+08	$[Z_{4\beta f}Y_{2\beta f}\text{-}2SO_3]^{3-}$	-0.049958437	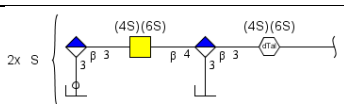
287.9855	3.31E+07	$[B_2+Na]^{3-}$	0.281140312	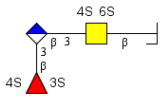
288.5015	1.85E+07	$[C_2Y_{4\beta f}+Na]^{2-}$	0.07988	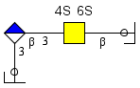
290.7643	8.08E+07	$[B_3\text{-}2SO_3]^{4-}$	0.273949553	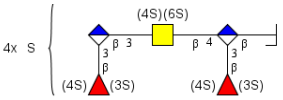
291.7645	1789805	$[C_3+3Na\text{-}3SO_3]^{4-}$	-0.768888093	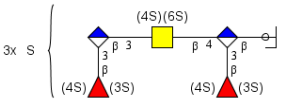
293.3584	1.33E+07	$[Y_{4\beta f}Z_{2\beta f}+Na\text{-}2SO_3]^{3-}/[Z_{4\beta f}Y_{2\beta f}+Na\text{-}2SO_3]^{3-}$	0.002010055	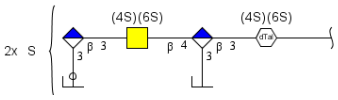
293.9891	5481892	$[C_2+Na]^{3-}$	0.008593289	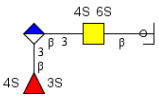
295.267	2408340	$[C_3\text{-}2SO_3]^{4-}$	0.070533619	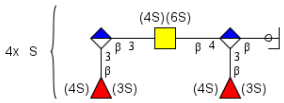
295.313	7627904	$[B_2+2Na]^{3-}$	-0.352698098	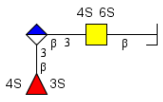
296.2598	6.87E+07	$[B_3+Na\text{-}SO_3]^{4-}$	0.222150457	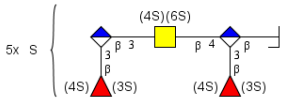
300.7628	1740664	$[C_3+Na\text{-}2SO_3]^{4-}$	-0.974237007	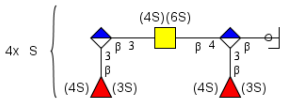

301.023	1547223	$^{2,5}X_1$-SO_3	1.630858771	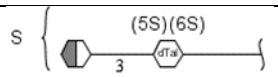
301.3164	7.34E+07	$[C_2+2Na]^{3-}$	0.057765414	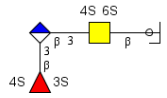
301.5558	1.02E+07	$[B_2-3SO_3]^{2-}$	0.051431609	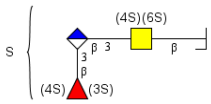
301.7554	3.93E+07	$[B_3+2Na-2SO_3]^{4-}$	-0.159156224	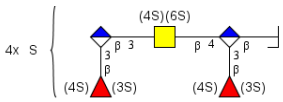
302.692	5527590	$[Z_3-3SO_3]^{3-}$	-0.118374453	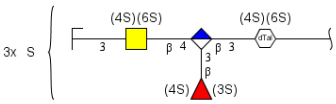
304.0108	6149469	$B_2Y_3+Na-SO_3$	0.181878407	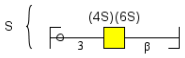
304.9643	5.94E+07	$B_{\beta f}$	-0.126283634	
304.9643	5.94E+07	Z_1	-0.126283634	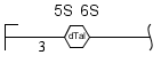
306.2582	1784293	$[C_3+Na-2SO_3]^{4-}$	-0.675425997	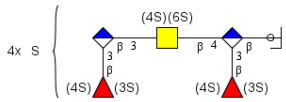
307.7238	7.34E+08	$[Y_3+3Na]^{4-}$	0.209882206	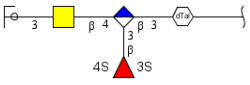
308.6957	4509324	$[Y_3-3SO_3]^{3-}$	-0.694110737	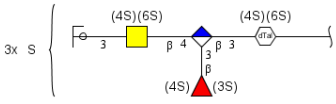
310.561	3369835	$[C_2-3SO_3]^{2-}$	0.315083027	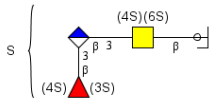

312.6833	5.10E+07	$[Y_{4\beta f}\ Z_{2\beta f}\text{-}SO_3]^{3-}$	0.183025445	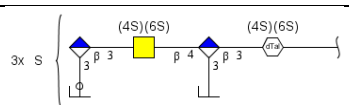
313.0235	2.37E+07	$[Z_2\text{-}2SO_3]^{2-}$	- 0.028988239	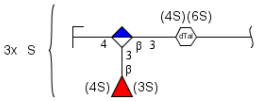
314.0069	2113883	$[Z_{4\beta f}Z_{2\beta f}\text{+}Na]^{3-}$	0.797900725	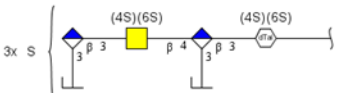
315.0391	2.66E+07	$^{1,4}A_1\text{-}SO_3$	0.130110834	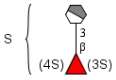
316.0228	1893132	$[Y_3\text{+}Na\text{-}3SO_3]^{3-}$	0.001931295	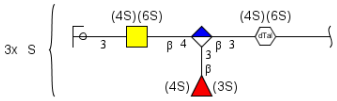
320.0107	2.04E+07	$[Y_{4\beta f}Z_{2\beta f}\text{+}Na\text{-}SO_3]^{3-}$	- 0.087158544	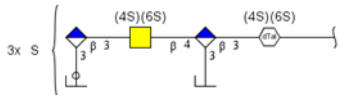
320.24	2506125	$^{2,4}X_3^{4-}$	0.455162534	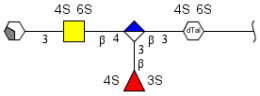
321.7446	6.80E+07	$[B_3\text{+}2Na\text{-}SO_3]^{4-}$	- 0.137958027	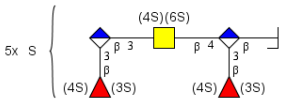
322.0283	2291111	$[Y_2\text{-}2SO_3]^{2-}$	1.469650338	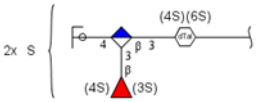
322.9747	3463759	$C_{\beta f}$	0.390662179	
322.9747	3463759	Y_1	0.390662179	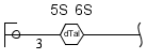
324.0144	1.61E+07	$[Z_2\text{+}Na\text{-}2SO_3]^{2-}$	0.195191942	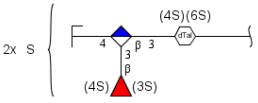

326.387	5.12E+07	[M-8H+3Na-SO_3]$^{5-}$	-0.004128228	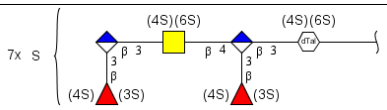
326.9462	1.32E+08	$B_{\beta f}$+Na	0.018737027	
326.9462	1.32E+08	Z_1+Na	0.018737027	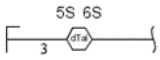
327.24	4.33E+07	[B_3+3Na-SO_3]$^{4-}$	0.127650196	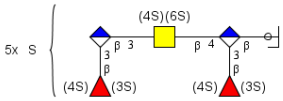
327.338	1.25E+07	[$Y_{4\beta f}$ $Z_{2\beta f}$+2Na-SO_3]$^{3-}$	-0.039751979	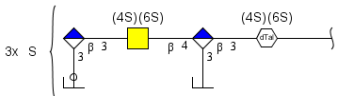
331.7427	1.45E+08	[C_3+3Na-SO_3]$^{4-}$	-0.051414093	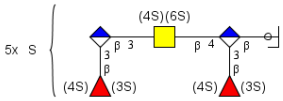
334.717	5851368	[B_3-4SO_3]$^{3-}$	0.165253035	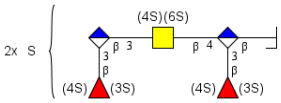
337.0206	1413257	$^{1,4}A_1$+Na-SO_3	1.440944559	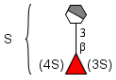
341.5343	7.41E+07	[B_2-2SO_3]$^{2-}$	-0.22607539	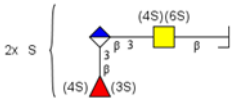
341.9939	3826391	$^{2,4}X_2^{3-}$	-2.673602268	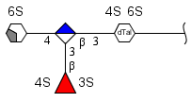
342.3785	1430512	[M-8H+3Na]$^{5-}$	-0.404336721	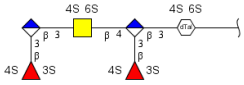
344.9568	1.45E+08	$C_{\beta f}$+Na	-0.084613494	

344.9568	1.45E+08	Y_1+Na	-0.084613494	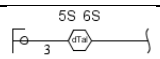
347.2293	2.06E+07	$[B_3+3Na]^{4-}$	-0.157212395	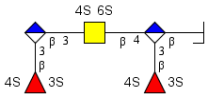
350.5396	2.03E+07	$[C_2-2SO_3]^{2-}$	-0.270638467	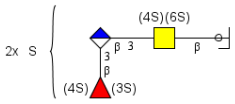
351.7318	1.13E+07	$[C_3+3Na]^{4-}$	0.24616128	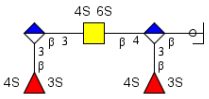
351.7318	1.13E+07	$[Y_{4\beta f}+3Na]^{4-}$	0.24616128	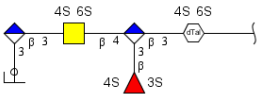
352.5252	1.45E+07	$[B_2+Na-2SO_3]^{2-}$	-0.013881277	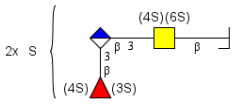
353.9903	4420485	$[Y_{4\beta f}\,Z_{2\beta f}+2Na]^{3-}$	-0.11721696	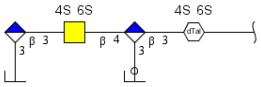
361.5305	1.51E+07	$[C_2+Na-2SO_3]^{2-}$	-0.062375097	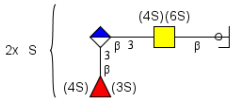
367.3211	1.58E+07	$[Y_{4\beta f}Y_{2\beta f}+Na]^{2-}$	-0.013754542	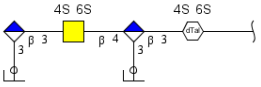
368.6966	1.74E+07	$[B_3+Na-3SO_3]^{3-}$	0.113130959	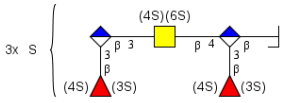
372.9515	4328366	$^{1,5}X_1$+Na	0.497206741	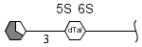
374.9838	1.11E+07	$[Z_2+2Na-SO_3]^{2-}$	0.114250269	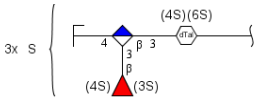

376.6542	1386952	$[Y_3+2Na-SO_3]^{3-}$	1.21736861	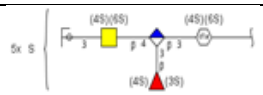
383.0291	1.18E+07	$B_3Z_2-SO_3$	-0.338788881	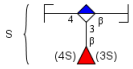
383.0291	1.18E+07	$Z_2Z_{2\beta f}-SO_3$	-0.338788881	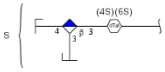
383.9677	5.81E+07	B_2Y_3+Na /C_2Z_3+Na	-0.078524834	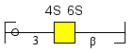
386.9672	4499161	$^{2,4}A_1+Na$	0.350153708	
386.9672	4499161	$^{0,2}X_1+Na$	0.350153708	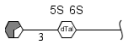
387.9399	1420821	B_2Z_3+2Na	-2.191574004	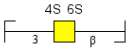
392.5035	3372403	$[B_3Y_3+Na-SO_3]^{2-}$	0.260849903	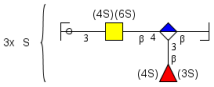
392.5035	3372403	$[B_2+Na-SO_3]^{2-}$	0.260849903	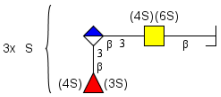
392.5035	3372403	$[Z_3Y_{2\beta f}+Na-SO_3]^{2-}$	0.260849903	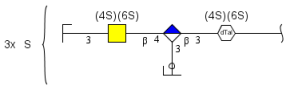
400.4865	1755480	$^{0,2}A_1Y_2^{2-}$	-1.860236238	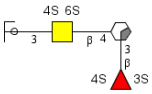
401.0395	9912581	B_1-SO_3	0.087073717	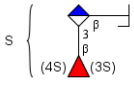

401.9784	8278005	C_2Y_3+Na	- 0.411626595	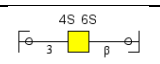
403.4944	2419895	$[B_2+2Na-SO_3]^{2-}$	0.432976269	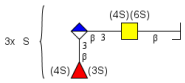

FCS Ib dp 6

Mass to charge	Intensity	Type	Accuracy PPM	Ion Structure
136.9914	2161578	$^{3,5}A_{\alpha f}$	0.021446602	
138.9706	5.76E+07	$^{0,4}A_1$	0.485685462	
138.9706	5.76E+07	$^{2,4}A_{\alpha f}$	0.485685462	
145.0506	837475	$B_{\beta f}$	0.223204868	
145.0506	837475	Z_1	0.223204868	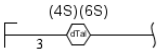
150.008	610349	$[^{2,5}X_1-SO_3]^{2-}$	0.71494187	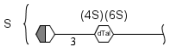
151.9785	3858589	$B_{\beta f}^{2-}$	-0.049164849	
151.9785	3858589	Z_1^{2-}	-0.049164849	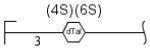
152.9863	2515822	$^{0,3}A_{\alpha f}$	0.11478152	

157.0142	6860123	$B_1Z_{4\beta f}$	0.298508033	
160.9526	2.78E+07	$^{2,4}A_{\alpha f}$+Na	0.075388655	
160.9838	1.22E+08	$C_{\beta f}^{2-}$	-0.156096452	
160.9838	1.22E+08	Y_1^{2-}	-0.156096452	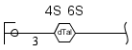
163.0611	2925525	$C_{\beta f}$	0.595249265	
163.0611	2925525	Y_1	0.595249265	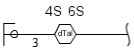
167.0017	831600	$^{2,5}A_{\alpha f}$	1.602522609	
168.9811	1533827	$^{1,4}A_{\alpha f}$-SO_3	0.782229492	
171.9747	1182285	$[C_{\beta f}+Na]^{2-}$	0.274400827	
171.9747	1182285	$[Y_1+Na]^{2-}$	0.274400827	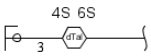
174.9812	680218	$^{1,5}X_1^{2-}$	0.183916901	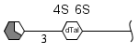
175.0248	2.06E+07	$B_1Y_{4\beta f}$	0.066024929	
175.0248	2.06E+07	$C_1Z_{4\beta f}$	0.066024929	
178.9962	2683940	$B_1Z_{4\beta f}$+Na	-0.047442348	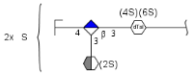
180.4892	9421104	$B_2Y_3^{2-}$	0.135129969	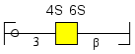

180.4892	9421104	$C_2Z_3^{2-}$	0.135129969	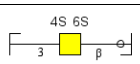
181.9891	2345207	$^{2,4}A_1^{2-}$	-0.235101993	
181.9891	2345207	$^{0,2}X_1^{2-}$	-0.235101993	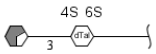
182.9945	5424422	$[C_1\ ^{0,3}X_{\beta f}+Na]^{2-}$	-2.764083073	
182.9969	7.84E+07	$^{0,2}A_{\alpha f}$	-0.097018037	
184.0616	1.24E+08	B_2Z_3	-0.372630685	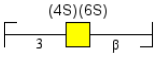
189.4945	3255076	$C_2Y_3^{2-}$	0.035528736	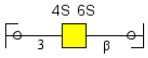
190.9632	4134018	$^{1,4}A_{\alpha f}$+Na-SO_3	-0.121384644	
193.0354	3.28E+07	$C_1Y_{4\beta f}$	-0.123075871	
196.0002	1523352	$[Y_{4\beta f}\ Z_{2\beta f}$+2Na-$SO_3]^{5-}$	-1.624387118	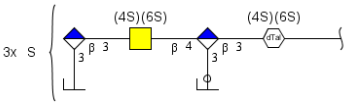
197.0068	1.42E+07	$B_1Y_{4\beta f}$+Na	-0.222357807	
197.0068	1.42E+07	$C_1Z_{4\beta f}$+Na	-0.222357807	
197.0124	823399	$^{1,5}A_{\alpha f}$-SO_3	0.671582093	
200.0162	1.67E+07	B_1-SO_3	-0.353751346	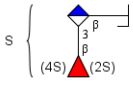

200.0162	1.67E+07	$Z_{2\beta f}Y_2\text{-}SO_3^{2-}$	-0.353751346	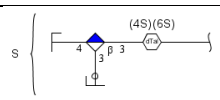
200.0162	1.67E+07	$Y_{2\beta f}Z_2\text{-}SO_3^{2-}$	-0.353751346	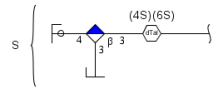
200.4894	892000	Y_2^{4-}	-1.218535743	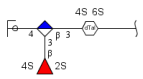
202.0723	759163	B_2Y_3	-1.009049731	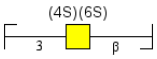
202.0723	759163	C_2Z_3	-1.009049731	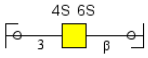
205.9844	1503894	$[Y_2+Na]^{4-}$	1.174147168	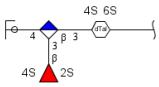
205.9844	1503894	$[Z_3^{0,4}X_{\beta f}+4Na\text{-}3SO_3]^{5-}$	-2.215700801	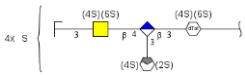
206.9774	1534177	$[Z_2+2Na]^{4-}$	0.419582041	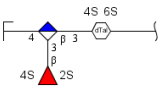
207.9853	1.35E+07	$[C_3{}^{2,4}X_2+3Na]^{5-}$	1.060273972	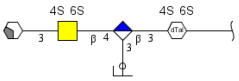
208.0002	2232881	$^{1,5}A_1+2Na\text{-}SO_3$	2.002743267	
209.0213	8068563	$[C_3Y_2\text{-}SO_3]^{2-}$	0.533854684	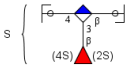
209.0213	8068563	$[C_1\text{-}SO_3]^{2-}$	0.533854684	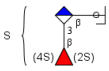
209.3316	1874262	$[^{2,4}A_3Z_3\text{-}SO_3]^{3-}$	2.64396616	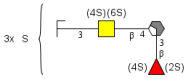
210.9919	1644117	$^{2,5}A_1{}^{2-}$	-0.488796015	

218.0129	818667	$[B_3+4Na-2SO_3]^{5-}$	-0.099418888	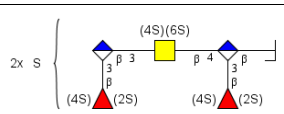
219.9897	4350595	$[Y_{4\beta f}Y_{2\beta f}+3Na]^{5-}$	0.210899874	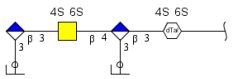
225.0074	9.58E+08	$B_{\beta f}$-SO_3	0.208579807	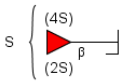
225.0074	9.58E+08	Z_1-SO_3	0.208579807	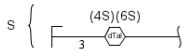
227.3535	1381488	$[B_2-2SO_3]^{3-}$	0.981061064	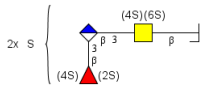
232.9437	2586124	$^{3,5}A_2$	-2.437859449	
232.9744	1378811	$[^{2,5}A_1+2Na]^{2-}$	-2.826465054	
233.3572	1307412	$[C_2-2SO_3]^{3-}$	0.191164732	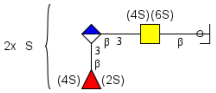
236.9878	1114948	$[^{1,5}A_1+Na]^{2-}$	1.061362652	
237.5322	1558253	$[C_2Y_{4\beta f}$-$SO_3]^{2-}$	-0.2380793	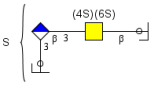
239.9946	5.95E+07	B_1^{2-}	-0.264497618	
242.3262	1.52E+07	$[Z_2+Na-SO_3]^{3-}$	-0.186231067	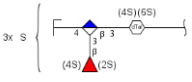
243.0181	3.07E+08	$C_{\beta f}$-SO_3	-0.363684845	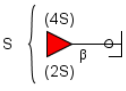

243.0181	3.07E+08	Y_1-SO_3	-0.363684845	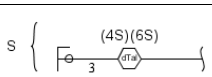
246.9894	6554776	$B_{\beta f}$+Na-SO_3	-0.034131019	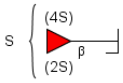
246.9894	6554776	Z_1+Na-SO_3	-0.034131019	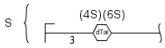
248.3297	6204680	$[Y_2$+Na-$SO_3]^{3-}$	-0.094900717	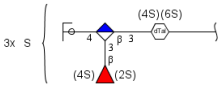
248.401	893947	$[B_3$-$SO_3]^{5-}$	1.655986087	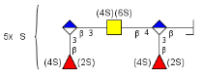
248.401	893947	$[Z_{\beta f}$-$SO_3]^{5-}$	1.655986087	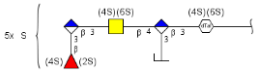
248.9386	836582	$^{1,4}A_{\alpha f}$	-2.222483777	
250.9855	5316778	$[B_3Y_2$+Na$]^{2-}$	0.035225142	
254.006	4584459	$[B_2$-$SO_3]^{3-}$	-0.021391883	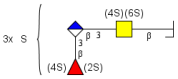
256.7545	2842915	$[Y_3$+Na-$2SO_3]^{4-}$	-0.058465383	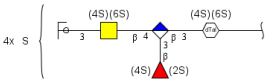
259.7453	924003	$[Y_{4\beta f}Z_{2\beta f}$+Na$]^{4-}$	0.341150542	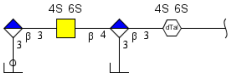
259.9909	2.72E+07	$[C_1$+Na$]^{2-}$	-0.418537726	
260.0092	961378	$[C_3Y_3$-$SO_3]^{3-}$	1.215835183	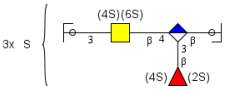
260.0092	961378	$[C_2$-$SO_3]^{3-}$	1.215835183	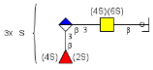

260.0092	961378	$[Y_3Y_{2\beta f}\text{-}SO_3]^{3-}$	1.215835183	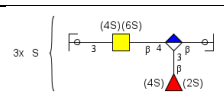
260.797	894489	$[C_3+2Na\text{-}SO_3]^{5-}$	-2.675870505	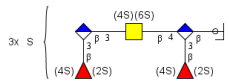
260.797	894489	$[Y_{\beta f}+2Na\text{-}SO_3]^{5-}$	-2.675870505	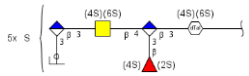 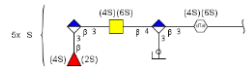
261.3334	2.39E+07	$[B_3Y_3+Na\text{-}SO_3]^{3-}$	-0.34650884	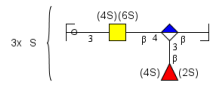
261.3334	2.39E+07	$[B_2+Na\text{-}SO_3]^{3-}$	-0.34650884	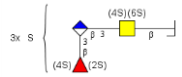
261.3334	2.39E+07	$[Y_3Z_{2\beta f}+Na\text{-}SO_3]^{3-}$	-0.34650884	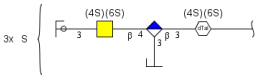
262.9844	2748944	$[Y_2+3Na\text{-}SO_3]^{3-}$	-0.356705569	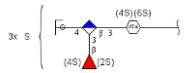
264.0107	1.02E+07	$[^{0,2}X_2+3Na\text{-}2SO_3]^{3-}$	1.411315274	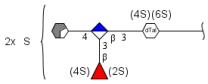
264.0184	3.40E+08	$B_2Z_3\text{-}SO_3$	-0.204648616	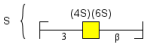
265	7.12E+07	$C_{\beta f}+Na\text{-}SO_3$	-0.165071698	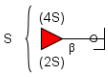
265	7.12E+07	$Y_1+Na\text{-}SO_3$	-0.165071698	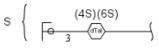
267.3369	1.19E+07	$[C_2+Na\text{-}SO_3]^{3-}$	-0.258072617	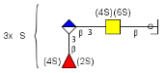
268.9783	2185711	$[Z_2+Na]^{3-}$	0.469889207	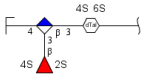

269.7435	1136262	$[Y_{4\beta f}Y_{2\beta f}+2Na]^{4-}$	0.059105224	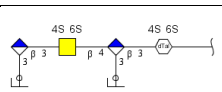
270.7752	1908905	$[B_3\text{-}3SO_3]^{4-}$	-0.088576243	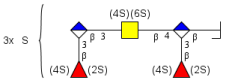
271.0131	6618889	$^{1,5}X_1\text{-}SO_3$	-0.641149819	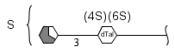
273.1861	1163515	$[B_3+2Na]^{5-}$	-2.005537617	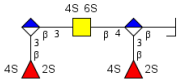
273.1861	1163515	$[Z_{\beta f}+2Na]^{5-}$	-2.005537617	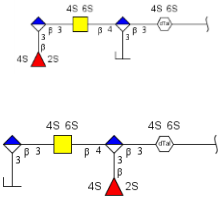
276.3058	1.43E+08	$[Z_2+2Na]^{3-}$	-0.212556764	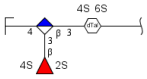
280.7735	1052986	$[C_3+Na\text{-}3SO_3]^{4-}$	-0.700398186	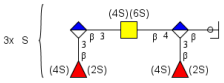
280.7735	1052986	$[Y_{\beta f}+Na\text{-}3SO_3]^{4-}$	-0.700398186	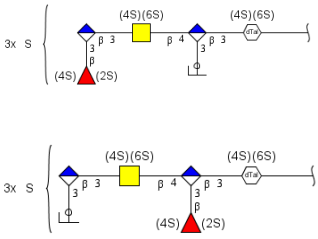
281.1842	6045869	$[C_3+3Na]^{5-}$	-0.519304427	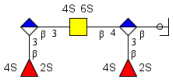
281.1842	6045869	$[Y_{\beta f}+3Na]^{5-}$	-0.519304427	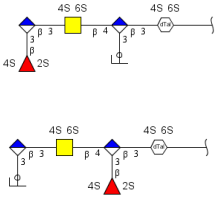

282.029	6.08E+07	B_2Y_3-SO_3	-0.316793663	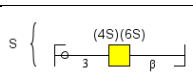
282.2392	1.81E+07	$[Y_3+2Na-SO_3]^{4-}$	-0.089331142	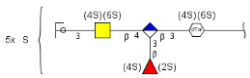
282.3093	2.24E+07	$[Y_2+2Na]^{3-}$	-0.131659377	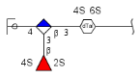
285.0285	4707449	$^{2,4}A_1$-SO_3	0.267706562	
285.0285	4707449	$^{0,2}X_1$-SO_3	0.267706562	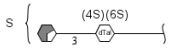
286.0003	1.22E+08	B_2Z_3-SO_3	-0.032842623	
287.9857	6705762	$[B_2+Na]^{3-}$	-0.413338811	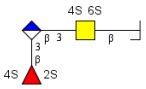
288.5017	1.06E+07	$[C_2Y_{4\beta f}+Na]^{2-}$	-0.613356871	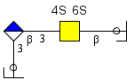
290.0079	5351146	$[M-7H+2Na-SO_3]^{5-}$	-0.055506764	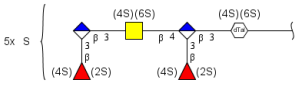
290.7645	2543143	$[B_3-2SO_3]^{4-}$	-0.413892514	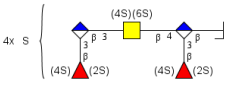
290.7645	2543143	$[Z_{\beta f}-2SO_3]^{4-}$	-0.413892514	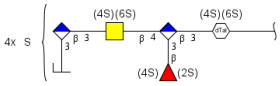
				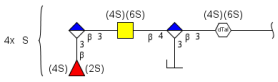
293.9892	985583	$[Y_3Y_{2\beta f}+Na]^{3-}$	-0.331555263	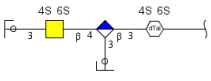
295.2679	1380334	$[C_3-2SO_3]^{4-}$	-2.977545985	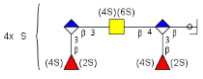

295.2679	1380334	$[Y_{\beta f}\text{-}2SO_3]^{4-}$	-2.977545984	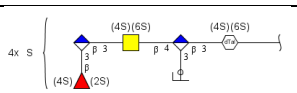 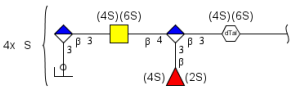
295.3131	8156065	$[B_2+2Na]^{3-}$	-0.691321629	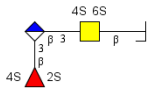
296.26	1.32E+07	$[B_3+Na\text{-}2SO_3]^{4-}$	-0.452932391	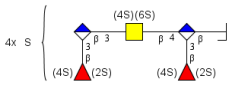
296.26	1.32E+07	$[Z_{\beta f}+Na\text{-}2SO_3]^{4-}$	-0.452932391	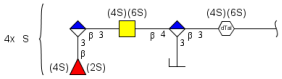 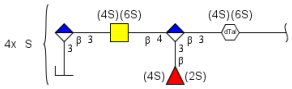
298.9513	5042737	$^{1,5}A_{\alpha f}+Na$	-0.028419345	
299.3616	1414512	$[Y_{4\beta f}Y_{2\beta f}+Na\text{-}2SO_3]^{3-}$	1.076128891	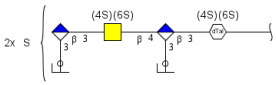
300.0396	2.43E+07	$C_2Y_3\text{-}SO_3$	-0.415475158	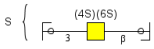
300.7625	3427787	$[C_3+Na\text{-}2SO_3]^{4-}$	0.023226798	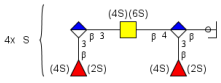
301.3166	1.24E+07	$[C_2+2Na]^{3-}$	-0.605988297	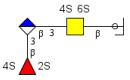
301.556	1459185	$[B_2\text{-}3SO_3]^{2-}$	-0.611795156	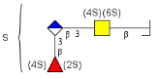
301.7555	9856884	$[B_3+2Na\text{-}2SO_3]^{4-}$	-0.490550297	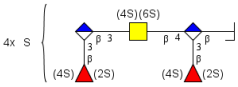

301.7555	9856884	$[Z_{\beta f}+2Na-2SO_3]^{4-}$	-0.490550297	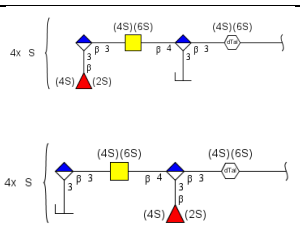
304.9644	6.58E+07	$B_{\beta f}$	-0.454190719	
304.9644	6.58E+07	Z_1	-0.454190719	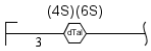
307.724	2.08E+07	$[Y_3+3Na]^{4-}$	-0.440050987	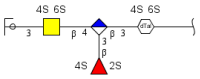
307.7307	1477374	$[^{2,5}X_3+4Na-SO_3]^{4-}$	2.654701822	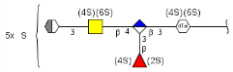
308.6962	1043737	$[Y_3-3SO_3]^{3-}$	-2.313825049	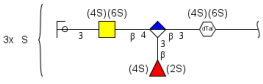
310.3958	1.96E+07	$[M-8H+3Na-2SO_3]^{5-}$	-0.529190794	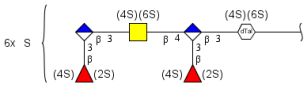
313.0237	7348779	$[Z_2-2SO_3]^{2-}$	-0.667917477	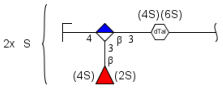
320.0108	9542218	$[Z_{4\beta f}Y_{2\beta f}+Na-SO_3]^{3-}$	-0.39964797	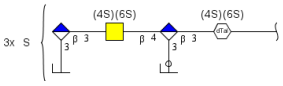
320.0108	9542218	$[Y_{4\beta f}Z_{2\beta f}+Na-SO_3]^{3-}$	-0.39964797	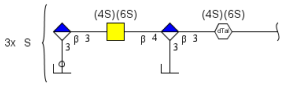
320.752	1472146	$[C_3+Na-SO_3]^{4-}$	-0.902177539	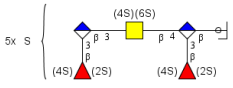

320.752	1472146	$[Y_{\beta f}+Na-SO_3]^{4-}$	-0.902177539	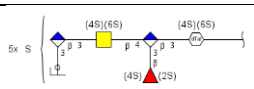
				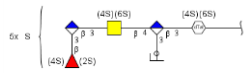
321.7447	1.44E+07	$[B_3+2Na-SO_3]^{4-}$	-0.448763414	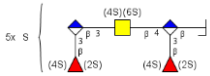
321.7447	1.44E+07	$[Z_{\beta f}+2Na-SO_3]^{4-}$	-0.448763414	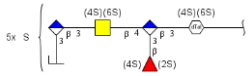
				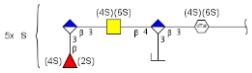
324.0146	1.31E+07	$[Z_2+Na-2SO_3]^{2-}$	-0.422064314	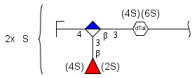
326.5898	3915742	$[^{1,5}A_3Z_{4\beta f}]^{2-}$	2.794243727	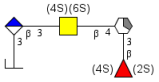
326.9463	6.90E+07	$B_{\beta f}+Na$	-0.287123604	
326.9463	6.90E+07	Z_1+Na	-0.287123604	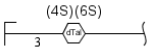
327.2325	2074018	$[^{2,5}A_3+2Na]^{4-}$	-0.337910354	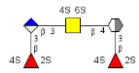
327.2401	2.79E+07	$[B_3+3Na-SO_3]^{4-}$	-0.177935864	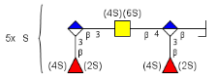
327.2401	2.79E+07	$[Z_{\beta f}+3Na-SO_3]^{4-}$	-0.177935864	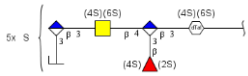
				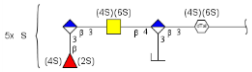
327.3381	1.40E+07	$[Y_{4\beta f}Z_{2\beta f}+2Na-SO_3]^{3-}$	-0.3452465	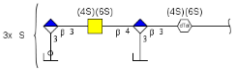

330.7835	2.08E+08	[M-9H+4Na-SO_3]$^{5-}$	-0.339859152	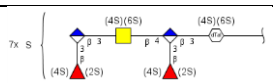
331.7428	2.09E+07	[C_3+3Na-SO_3]$^{4-}$	-0.352852421	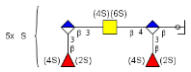
331.7428	2.09E+07	[$Y_{βf}$+3Na-SO_3]$^{4-}$	-0.352852421	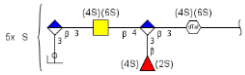
				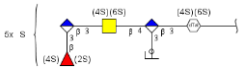
332.0018	1040838	[Z_3+4Na-3SO_3]$^{3-}$	-1.735875127	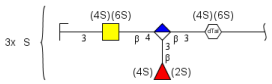
333.3419	2100366	[$Y_{βf}Y_{βf}$+2Na-SO_3]$^{3-}$	-1.17432082	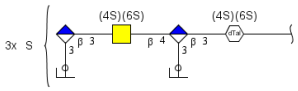
334.7172	1290369	[B_3-4SO_3]$^{3-}$	-0.432266403	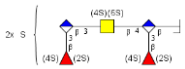
336.4811	1109274	[$^{3,5}A_3Z_{4βf}$+3Na]$^{2-}$	-0.520104993	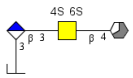
337.0213	6146095	$^{1,4}A_1$+Na-SO_3	-0.636078491	
341.5343	1.21E+07	[B_2-2SO_3]$^{2-}$	-0.22607539	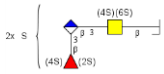
344.9568	8.96E+08	$C_{βf}$+Na	-0.084613494	
344.9568	8.96E+08	Y_1+Na	-0.084613494	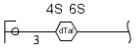
345.9965	1073491	[Z_2+3Na-2SO_3]$^{2-}$	-0.266236797	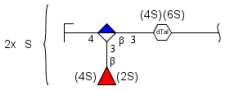
347.2292	1.14E+07	[B_3+3Na]$^{4-}$	0.130781772	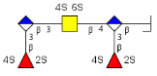

347.2292	1.14E+07	$[Z_{\beta f}+3Na]^{4-}$	0.130781772	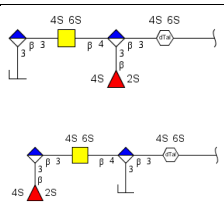
348.9283	2734915	$B_{\beta f}+2Na$	-0.427698183	
348.9283	2734915	Z_1+2Na	-0.427698183	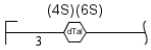
350.0022	3421624	$[Y_3+2Na-2SO_3]^{3-}$	0.534306165	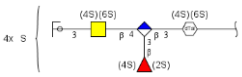
350.5395	4633384	$[C_2-2SO_3]^{2-}$	0.014636011	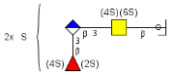
351.1711	1.06E+08	$[M-10H+5Na]^{5-}$	0.112250125	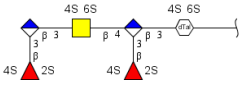
351.2217	3049447	$[^{1,5}A_3+5Na]^{4-}$	-0.600547318	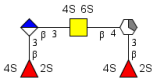
351.7711	2.61E+07	$[M-4H-3SO_3]^{4-}$	-1.132363489	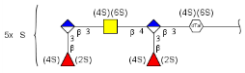
352.5252	2.90E+07	$[B_2+Na-2SO_3]^{2-}$	-0.013881277	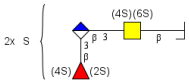
352.7244	1522029	$[B_3+4Na]^{4-}$	0.940027823	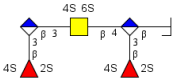
352.7244	1522029	$[Z_{\beta f}+4Na]^{4-}$	0.940027824	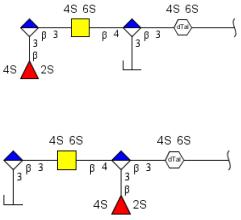

353.9904	1.03E+07	$[Z_{4\beta f}Y_{2\beta f}+2Na]^{3-}$	-0.399710463	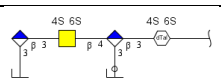
357.2273	1.42E+08	$[C_3+4Na]^{4-}$	0.203630154	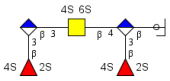
357.2273	1.42E+08	$[Y_{\beta f}+4Na]^{4-}$	0.203630154	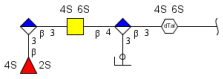
				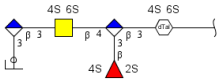
361.3174	6846805	$[B_3Y_{2\beta f}+3Na]^{3-}$	0.479870791	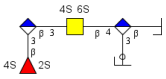
361.3174	6846805	$[Z_{4\beta f}Y_{2\beta f}+3Na]^{3-}$	0.479870791	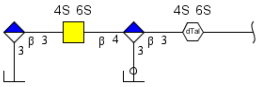
361.3695	2411048	$[B_3\text{-}3SO_3]^{3-}$	-0.479200191	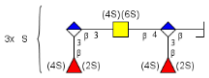
361.5305	1.31E+07	$[C_2+Na\text{-}2SO_3]^{2-}$	-0.062375097	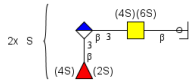
363.993	3664122	$[Z_2+Na\text{-}SO_3]^{2-}$	-0.355712885	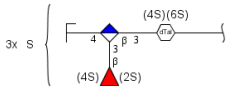
366.9386	2.59E+07	$C_{\beta f}+2Na$	0.314630295	
366.9386	2.59E+07	Y_1+2Na	0.314630295	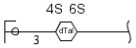
367.3209	5946782	$[Y_{4\beta f}Y_{2\beta f}+4Na]^{4-}$	0.53072849	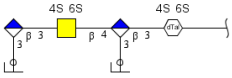
368.6965	1.10E+07	$[B_3+Na\text{-}3SO_3]^{3-}$	0.384356781	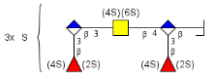

368.6965	1.10E+07	$[Z_{\beta f}+Na-3SO_3]^{3-}$	0.384356781	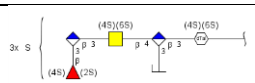
				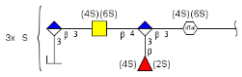
374.9838	2.72E+08	$[Z_2+Na-SO_3]^{2-}$	0.114250269	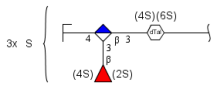
375.9714	3504074	$[Z_{4\beta f}Y_{2\beta f}+4Na]^{4-}$	2.136184649	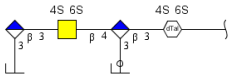
376.024	2523242	$[B_3+2Na-3SO_3]^{3-}$	-0.115443872	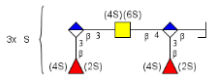
376.024	2523242	$[Z_{\beta f}+2Na-3SO_3]^{3-}$	-0.115443873	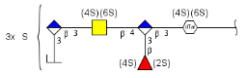
				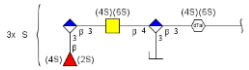
377.9774	974452	$[Z_3+3Na-SO_3]^{3-}$	2.782823347	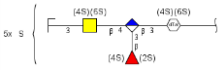
383.9677	3.10E+08	B_2Y_3+Na	-0.078524834	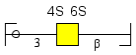
386.9673	7.94E+07	$^{2,4}A_1+Na$	0.091733849	
386.9673	7.94E+07	$^{0,2}X_1+Na$	0.091733849	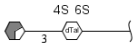
387.9394	4520865	B_2Z_3+2Na	-0.902715734	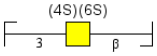
392.5033	4094878	$[B_2+Na-SO_3]^{2-}$	0.770399892	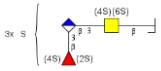
401.0393	2.21E+07	B_1-SO_3	0.585778002	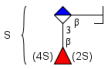
401.9784	2.25E+07	C_2Y_3+Na	-0.411626595	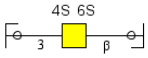

402.6759	8081558	$[B_3+2Na-2SO_3]^{3-}$	0.814821547	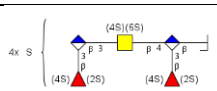
403.4942	2.85E+07	$[B_2+2Na-SO_3]^{2-}$	0.928646558	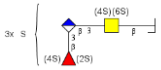
404.6303	1758362	$[Z_3+3Na]^{3-}$	1.046295841	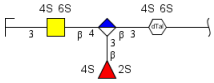
405.0103	6880584	$B_3Z_2+Na-SO_3$	1.518163859	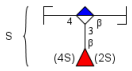
405.0103	6880584	$Z_2Z_{2\beta f}+Na-SO_3$	1.518163859	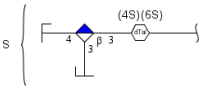
405.9493	6606138	B_2Y_3+2Na	0.774695263	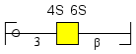
405.9493	6606138	C_2Z_3+2Na	0.774695263	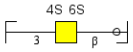
408.9486	2545746	$^{2,4}A_1+2Na$	1.663133215	
408.9486	2545746	$^{0,2}X_1+2Na$	1.663133215	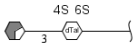
410.0031	7722091	$[B_3+3Na-2SO_3]^{3-}$	1.08045118	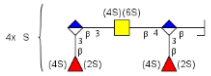
412.4995	1.77E+07	$[C_2+2Na-SO_3]^{2-}$	0.865568322	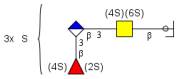
414.962	1.90E+07	$[Z_2+2Na]^{2-}$	0.602753987	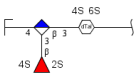
416.9778	9.25E+07	$^{1,4}A_1+Na$	0.240262191	
417.9614	2.22E+07	$[Y_3+4Na]^{3-}$	0.382342325	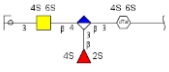

419.0499	3068991	C_1-SO_3	0.476329907	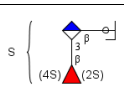
425.9533	3417303	$[Z_2+3Na]^{2-}$	-0.182088037	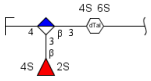
429.5501	925552	$[Y_{4\beta f}Z_{2\beta f}-2SO_3]^{2-}$	0.388270192	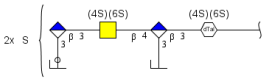
434.9585	3666311	$[Y_2+3Na]^{2-}$	0.010994152	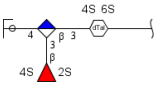
436.6559	1979290	$[B_3+3Na-SO_3]^{3-}$	-0.195790324	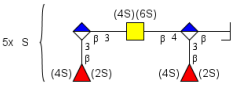
436.6559	1979290	$[Z_{\beta f}+3Na-SO_3]^{3-}$	-0.195790324	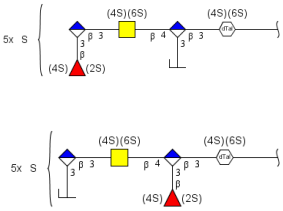
438.9597	4.09E+07	$^{1,4}A_1+2Na$	0.329920947	

Pg dp 9

Mass to charge	Intensity	Type	Accuracy PPM	Structure
136.9915	495727	$^{3,5}A_{\alpha f}$	-0.7085	
138.9707	5021850	$^{2,4}A_{\alpha f}$+Na-SO_3	-0.2340	
151.9785	839998	Z_1^{2-}	-0.0492	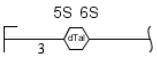
151.9785	839998	$B_{\beta 1}^{2-}$	-0.0492	
160.9526	3804316	$^{2,4}A_{\alpha f}$-SO_3	0.0754	
160.9838	1738705	Y_1^{2-}	-0.1561	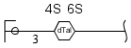
160.9838	1738705	$C_{\beta 1}^{2-}$	-0.1561	
163.0613	485912	Y_1-$2SO_3$	-0.6313	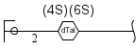
163.0613	485912	$C_{\beta 1}$-$2SO_3$	-0.6313	
182.997	1.04E+07	$^{0,2}A_{\alpha f}$-SO_3	-0.6435	

190.963	1121968	$^{1,4}A_{\alpha f}$-SO_3	0.9259	
204.9791	779451	$^{2,4}A_{\alpha f}$+Na-SO_3	-1.3324	
210.9917	467603	$^{2,5}A_1^{2-}$	0.4591	
225.0075	8.52E+07	Z_1-SO_3	-0.2358	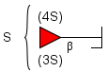
225.0075	8.52E+07	$B_{1\beta}$-SO_3	-0.2358	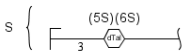
232.9733	508637	$[^{2,5}A_1+2Na]^{2-}$	1.8951	
239.9945	1670489	B_1^{2-}	0.1522	
241.0025	3237873	$[Y_2$-$SO_3]^{3-}$	-0.5745	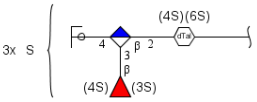
243.0181	1.42E+08	Y_1-SO_3	-0.3637	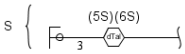
243.0181	1.42E+08	$C_{\beta 1}$-SO_3	-0.3637	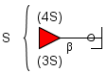
246.9895	1459961	Z_1+Na-SO_3	-0.4390	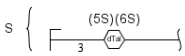

246.9895	1459961	$B_{1\beta}$+Na-SO_3	-0.4390	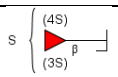
248.938	473664	$^{1,4}A_{\alpha f}$	0.1877	
250.9856	666913	$[B_1+Na]^{2-}$	-0.3632	
259.9906	691947	$[C_1+Na]^{2-}$	0.7353	
261.3327	887388	$[B_2+4H+Na]^{3-}$	2.3321	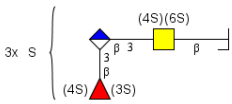
265	1.66E+07	Y1+Na-SO_3	-0.1651	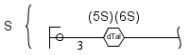
265	1.66E+07	$C_{1\beta}$+Na-SO_3	-0.1651	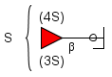
282.3098	497349	$[Y_2+5H+2Na]^{3-}$	-1.9028	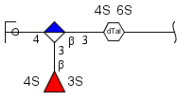
285.0285	3998186	$^{0,2}X_1$-SO_3	0.2677	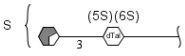
285.0285	3998186	$^{2,4}A_1$-SO_3	0.2677	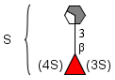
301.3163	1015104	$[C_2$-5H+2Na$]^{3-}$	0.3896	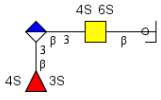

301.5563	868605	$[B_1\text{-}3SO_3]^{2-}$	-1.6066	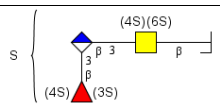
304.9644	2329106	Z_1	-0.4542	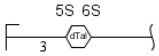
304.9644	2329106	$B_{\beta 1}$	-0.4542	
307.0111	958334	$^{0,2}X_1\text{+Na-}SO_3$	-1.8861	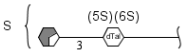
307.0111	958334	$^{2,4}A_1\text{+Na-}SO_3$	-1.8861	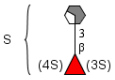
307.7239	801187	$[Y_3\text{-}7H\text{+}3Na]^{3-}$	-0.1151	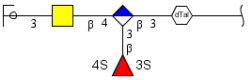
313.024	1533424	$[Z_2\text{-}2SO_3]^{2-}$	-1.6263	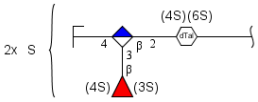
315.0392	2927359	$^{1,4}A\text{-}SO_3$	-0.1873	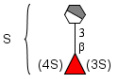
316.0228	511966	$[Y_3\text{-}4H\text{+}Na\text{-}3SO_3]^{3-}$	0.0019	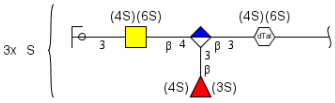
324.0145	2642940	$[Z_2\text{-}3H\text{+}Na]^{2-}$	-0.11343628 2	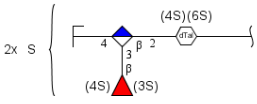

326.9462	4.97E+07	Z_1+Na	0.018737027	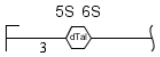
326.9462	4.97E+07	$B_{1\beta}$+Na	0.018737027	
333.0195	822986	$[Y_2\text{-}3H+Na\text{-}2SO_3]^{2-}$	0.737458317	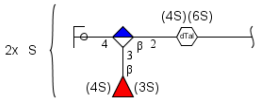
334.7172	641435	$[B_3\text{-}4SO_3]^{3-}$	-0.432266403	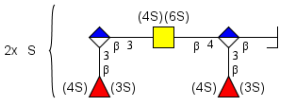
337.0215	1316859	$^{1,4}A_1$+Na-SO_3	-1.229512064	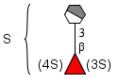
341.5343	1.94E+07	$[B_2\text{-}2SO_3]^{2-}$	-0.22608	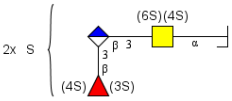
344.9568	1.60E+08	$C_{1\beta}$+Na	-0.0846	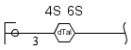
344.9568	1.60E+08	$Y_{1\beta}$+Na	-0.0846	
348.0304	686442	$[C_3\text{-}8H+4Na\text{-}5SO_3]^{4-}$	-2.2844	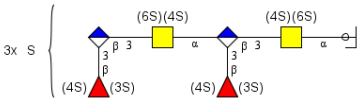
350.0023	1459148	$[Y_3+2Na\text{-}2SO_3]^{3-}$	0.2486	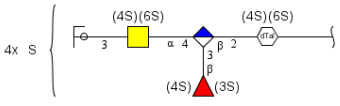

352.5252	1.06E+07	$[B_2+2Na-2SO_3]^{3-}$	-0.0139	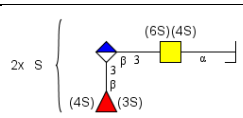
353.7242	827259	$[C_3-10H+7Na-SO_3]^{3-}$	1.2088	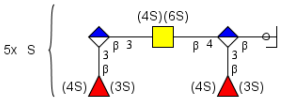
355.6599	798565	$[Y_{\beta 3}-11H+5Na-SO_3]^{6-}$	0.2255	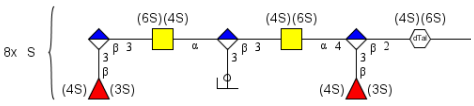
361.5305	2.13E+07	$[C_1+Na-2SO_3]^{2-}$	-0.0624	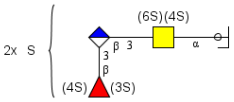
366.9388	2135444	Y_1+2Na	-0.2304	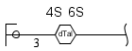
366.9388	2135444	$C_{1\beta}+Na$	-0.2304	
368.6966	8505279	$[B_3+4H+Na-3SO_3]^{3-}$	0.1131	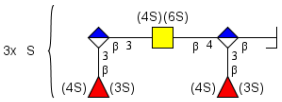
372.9516	3070221	$^{1,5}X_1+Na$	0.2291	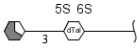
374.9835	2896425	$[Z_2-4H+2Na-SO_3]^{2-}$	0.9143	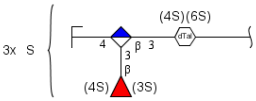
376.0241	3242167	$[B_3-5H+2Na-SO_3]^{3-}$	-0.3814	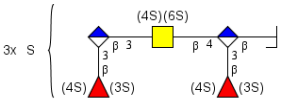

382.6159	9685830	[$Z_{6\beta}$-4H+2Na-SO_3]^{2}	-0.2224	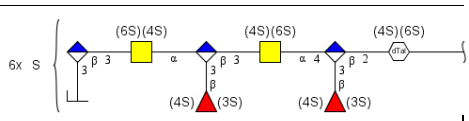
382.6159	9685830	[B_5-8H+3Na-SO_3]$^{5-}$	-0.2224	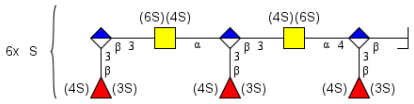
386.9673	1.32E+07	$^{0,2}X_1$+Na	0.0917	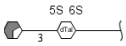
386.9673	1.32E+07	$^{2,4}A_1$+Na	0.0917	
389.639	1244389	[$Y_{6\beta}$-13H+7Na]$^{6-}$	1.4541	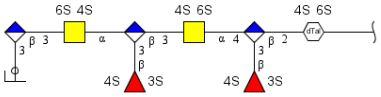
389.639	1244389	[C_5-13H+7Na]$^{6-}$	1.4541	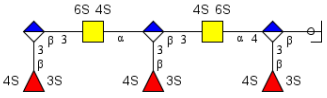
392.5035	4848655	[B_2-3H+Na-SO_3]$^{2-}$	0.2608	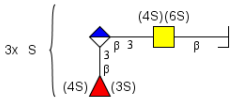
401.0395	1.43E+07	B_1-SO_3	0.0871	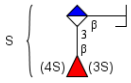
402.6762	5168919	[B_3-5H+2Na-SO_3]$^{3-}$	0.0698	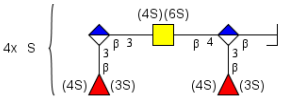
403.4941	5540141	[B_2-5H+2Na-SO_3]$^{3-}$	1.1765	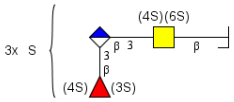
407.9979	598389	[C_4-8H+4Na-SO_3]$^{4-}$	-1.6768	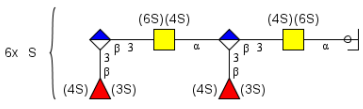

408.9489	676753	$^{0,2}X_1$+2Na	0.9295	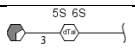
408.9489	676753	$^{2,4}A_1$+2Na	0.9295	
410.0025	880770	[B_3-6H+3Na]$^{3-}$	2.5439	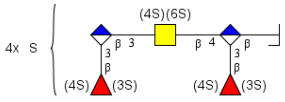
416.9763	1296344	$^{1,4}A_1$+Na	3.8376	
417.9613	773644	[Y_3-7H+3Na]$^{3-}$	0.6216	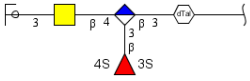
423.0211	3677266	B_1+Na-SO_3	0.8973	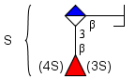
425.9532	635303	[Z_2-5H+3Na]$^{2-}$	0.0527	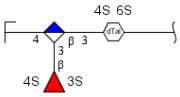
434.9564	686018	[Y_2-5H+3Na]$^{2-}$	4.8391	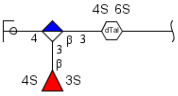
436.6561	799282	[B_3-6H+3Na-SO_3]$^{3-}$	-0.6538	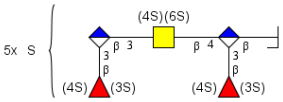
438.9597	2780531	$^{1,4}A_1$+2Na	0.3299	
441.0319	1.04E+07	C_1+2Na-SO_3	0.3271	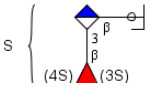

443.471	814061	$[B_2+2Na]^{2-}$	4.4692	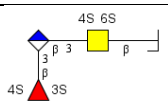
454.4639	978804	$[B_2+3Na]^{2-}$	0.1195	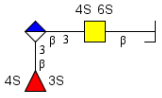
463.4688	1007466	$[C_2+3Na]^{2-}$	0.9421	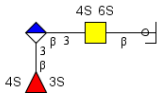
502.9779	2229281	B_1+Na	0.7836	
542.9712	1522588	C_1+2Na	-0.7304	

Ib dp 9

Mass to charge	Intensity	Type	Accuracy PPM	Structure
136.9914	4558944	$^{3,5}A_{\alpha f}$	0.021446602	
137.9811	1353582	$^{1,5}A_{\alpha f}{}^{2-}$	-0.4695	
138.9707	1.18E+08	$^{2,4}A_{\alpha f}$	-0.2339	
145.0506	826638	$B_{1\beta}$-2SO_3	0.2232	
145.0506	826638	Z_1-2SO_3	0.2232	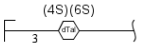
151.9785	7060891	$B_{1\beta}{}^{2-}$	-0.0492	

151.9785	7060891	Z_1^{2-}	-0.0492	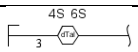
152.9863	4860738	$^{0,3}A_{\alpha f}$	0.1148	
160.9526	2.25E+07	$^{2,4}A_{\alpha f}$ + Na	0.07540	
160.9838	2.37E+08	$C_{1\beta}^{2}$	-0.1561	
160.9838	2.37E+08	Y_1^{2-}	-0.1561	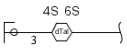
163.0611	828639	$C_{1\beta}$-2SO_3	0.5952	
163.0611	828639	Y_1-2SO_3	0.5952	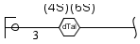
167.0018	1013608	$^{2,5}A_{\alpha f}$	1.0037	
168.9811	2437624	$^{1,4}A_1$+Na-SO_3	0.7822	
171.9747	1108003	$[C_{1\beta}+Na]^{2-}$	0.2744	
171.9747	1108003	$[Y_1+Na]^{2-}$	0.2744	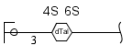
174.9683	1256489	$^{0,3}A_{\alpha f}$ + Na	-0.2161	
174.9811	1188143	$^{1,5}X_1^{2-}$	0.7554	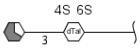
181.989	5831402	$^{2,4}A_1^{2-}$	0.3144	
181.989	5831402	$^{0,2}X_1^{2-}$	0.3144	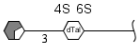
182.9969	1.05E+08	$^{0,2}A_{\alpha f}$	-0.0970	

190.9631	3839037	$^{1,4}A_{\alpha f}$ + Na-SO_3	0.4023	
197.0124	1016744	$^{1,5}A_{\alpha f}$ + Na-SO_3	0.6716	
200.016	1.28E+07	$[B_1\text{-}2SO_3]^{2-}$	0.6462	
205.9847	1241882	$[Y_1+Na]^{4-}$	- 0.282273392	
206.977	1322245	$[Z_1+2Na]^{4-}$	2.352164733	
207.9852	2725412	$[^{1,4}A_1 + Na]^{2-}$	0.537903659	
208.0001	2520442	$[^{1,5}A_1$ + Na-$SO_3]^{2-}$	2.4835	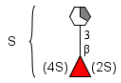
209.021	3072422	$[C_1\text{-}SO_3]^{2-}$	1.9691	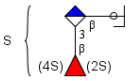
210.9917	1285711	$^{2,5}A_1$	0.4591	
225.0074	7.83E+08	$B_{1\beta}\text{-}SO_3$	0.2086	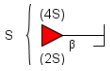
225.0074	7.83E+08	$Z_1\text{-}SO_3$	0.2086	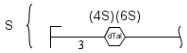
227.3535	889932	$[B_2\text{-}2SO_3]^{3-}$	0.9811	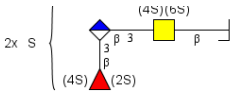
232.974	770333	$[^{2,5}A_1+2Na]^{2-}$	-1.1095	
233.3567	943712	$[C_2\text{-}2SO_3]^{3-}$	2.3338	
239.9945	3.20E+07	B_1^{2-}	0.1522	

241.0023	9547128	$[Y_3\text{-}SO_3]^{3-}$	0.2554	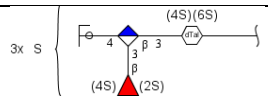
242.3261	1.02E+07	$[Y_3\text{+}Na\text{-}SO_3]^{3-}$	0.2264	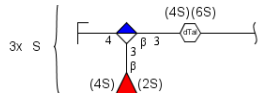
243.0179	1.57E+08	$C_{1\beta}\text{-}SO_3$	0.4593	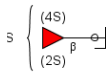
243.0179	1.57E+08	$Y_1\text{-}SO_3$	0.4593	
246.9894	5936870	$B_1\text{+}Na$	-0.0341	
246.9894	5936870	$Z_1\text{+}Na\text{-}SO_3$	-0.0341	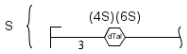
246.9894	5936870	$B_1\text{+}Na\text{-}SO_3$	-0.0341	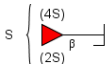
248.3297	2903034	$[Y_2\text{+}Na\text{-}SO_3]^{3-}$	-0.0949	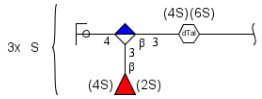
250.9853	3192646	$B_1\text{+}Na$	0.8321	
254.0059	2463466	$[B_3\text{-}SO_3]^{3-}$	0.3723	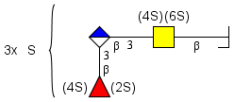
256.7544	1242949	$[Y_3\text{+}Na\text{-}2SO_3]^{2-}$	0.3310	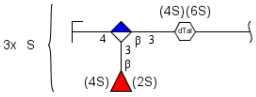
259.9907	4235170	$[C_1\text{+}Na]^{2-}$	0.3507	
261.3333	1.36E+07	$[B_3\text{-}Na\text{-}SO_3]^{3-}$	0.0361	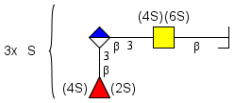

265	1.89E+07	$C_{1\beta}$+Na-SO_3	-0.1651	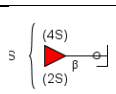
265	1.89E+07	Y_1+Na-SO_3	-0.1651	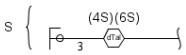
268.9775	856746	$[Z_3+Na]^{3-}$	3.4441	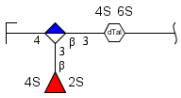
270.7751	3565821	$[B_3-3SO_3]^{4-}$	0.2807	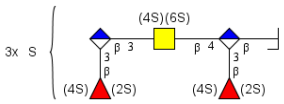
273.1859	1726052	$[B_3+2Na]^{5-}$	-1.2734	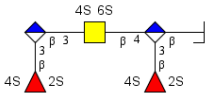
276.3057	9745737	$[Z_2+2Na]^{3-}$	0.1494	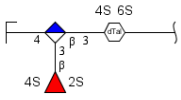
282.2391	8155136	$[Y_3+2Na-SO_3]^{3-}$	0.2650	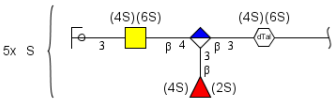
282.3092	8089999	$[Y_2+2Na]^{3-}$	0.2226	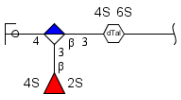
285.0286	2173108	$^{2,4}A_1$-SO_3	-0.0831	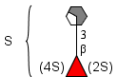
285.0286	2173108	$^{0,2}X_1$-SO_3	-0.0831	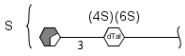
287.9857	5487893	$[B_2+Na]^{3-}$	-0.4133	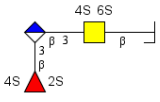
295.3129	9157774	$[B_2+2Na]^{2-}$	-0.0141	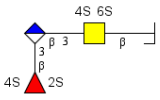

296.2599	2542698	$[B_3+Na-2SO_3]^{4-}$	-0.1154	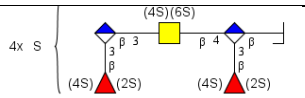
298.9511	1079593	$^{1,5}A_{\alpha f}+Na$	0.6406	
301.3166	4243260	$[C_2+Na]^{3-}$	-0.6060	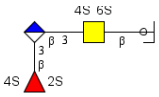
301.5559	776690	$[B_3+2Na-2SO_3]^{4-}$	-0.2802	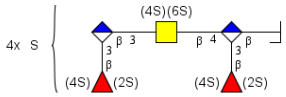
304.9643	1.99E+07	$B_{1\beta}$	-0.1263	
304.9643	1.99E+07	Z_1	-0.1263	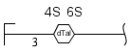
307.7238	1.81E+07	$[Y_3+3Na]^{4-}$	0.2099	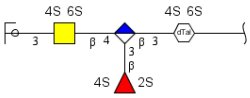
313.0232	1787891	$[Z_2-2SO_3]^{2-}$	0.9294	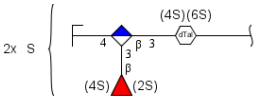
315.0395	1737906	$^{1,4}A_1-SO_3$	-1.1396	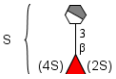
321.7446	3808759	$[B_3+2Na-SO_3]^{4-}$	-0.1380	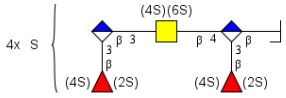
324.0145	1068437	$[Z_2+Na-2SO_3]^{2-}$	-0.11343	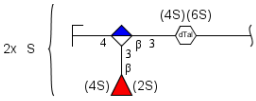
326.9462	2.60E+07	$B_{1\beta}+Na$	0.01874	
326.9462	2.60E+07	Z_1+Na	0.01874	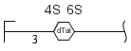

327.2401	1.01E+07	$[B_3+3Na-2SO_3]^4$	-0.1780	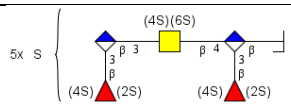
341.5341	2623305	$[B_2-2SO_3]^{2-}$	0.3595	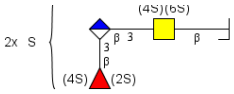
344.9568	1.86E+08	$C_{1\beta}+Na$	-0.0846	
344.9568	1.86E+08	Y_1+Na	-0.0846	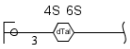
347.2294	4408868	$[B_3+3Na]^{4-}$	-0.4452	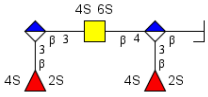
350.9691	763914	$^{1,5}X_1$	1.8258	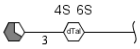
352.5251	1446460	$[B_2+Na-SO_3]^{2-}$	0.2698	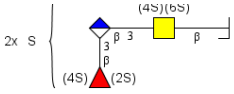
356.6377	800271	$[Y_5+6Na]^{6-}$	-1.3240	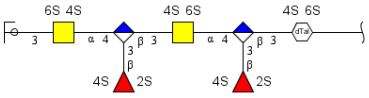
366.9394	801452	$C_{1\beta}+2Na$	-1.8656	
366.9394	801452	Y_1+2Na	-1.8656	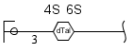
372.9531	1225865	$^{1,5}X_1+Na$	-3.7929	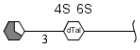
386.9674	2928568	$^{2,4}A_1+Na$	-0.1667	
386.9674	2928568	$^{0,2}X_1+Na$	-0.166685876	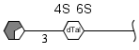

Pg dp 12

Mass to charge	Intensity	Type	Accuracy PPM	Structure
151.9785	441839	B_1^{2-}	-0.0492	
151.9785	441839	Z_1^{2-}	-0.0492	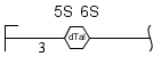
160.9837	998755	Y_1^{2-}	0.4651	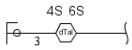
160.9837	998755	C_1^{2-}	0.4651	
225.0074	1.29E+07	Z_1-SO_3	0.2086	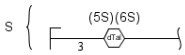
225.0074	1.29E+07	$B_{1\beta}$-SO_3	0.2086	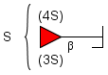
239.9946	1037838	B_2^{2-}	-0.2645	
243.0179	5717438	$C_{1\beta}$-SO_3	0.4593	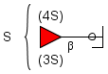
243.0179	5717438	Y_1-SO_3	0.4593	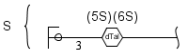
265	369793	$C_{1\beta}$+Na-SO_3	-0.1651	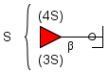
265	369793	Z_1+Na-SO_3	-0.16501	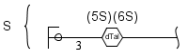
282.3086	357191	Y	2.3479	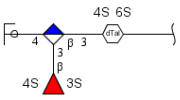
285.0283	376230	$^{0,2}X_1$-SO_3	0.9694	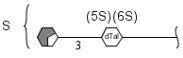

285.0283	376230	$^{2,4}A_1$-SO_3	0.9694	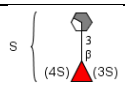
287.9855	483241	B	0.2811	
304.9643	1199450	Z	-0.1263	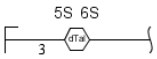
304.9643	1199450	B_1	-0.1263	
307.7235	537596	$[Y_3$-7H+3Na$]^{4-}$	1.1849	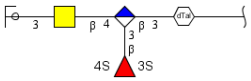
326.9461	7334029	B_1+Na	0.3246	
326.9461	7334029	Z_1+Na	0.3246	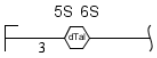
344.9568	2.46E+07	Y	-0.0846	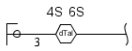
344.9568	2.46E+07	C	-0.0846	
372.952	569573	$^{1,5}X_1$+Na	-0.8434	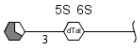
386.9672	861799	$^{0,2}X_1$+Na	0.3502	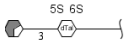
386.9672	861799	$^{2,4}A_1$+Na	0.3502	
401.0395	2734324	B_1-SO_3	0.0871	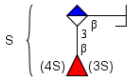
408.974	498443	$^{1,4}X_1$	2.9833	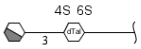
417.9614	2164516	$[Y_3$+4Na$]^{3-}$	0.3823	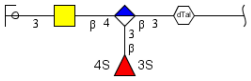

419.9776	475527	$[Y_7+4Na]^{7-}$	1.9147	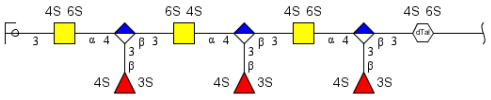
423.6849	667049	$[Z_7+6Na]^{7-}$	2.6480	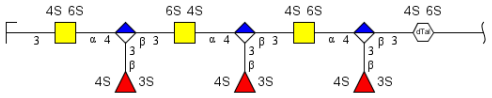
423.9684	842002	$[Y_2+2Na]^{2-}$	-2.0462	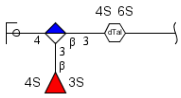
425.5545	1318302	$[Z_2+Na-4SO_3]^{2-}$	-0.8236	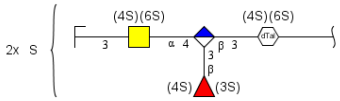
425.9524	738108	$[Z_2+2Na]^{3-}$	1.9308	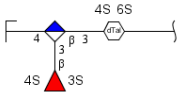
432.5628	3234763	$[Y_5+7Na]^{5-}$	-0.6528	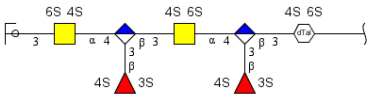
443.473	6940022	$[B_2+2Na]^{2-}$	-0.0406	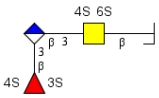
444.9723	554866	$^{2,5}A_1+Na$	1.1569	
446.8318	7394394	$[Z_{\beta 8}-18H+9Na-SO_3]^{7-*}$	0.2112	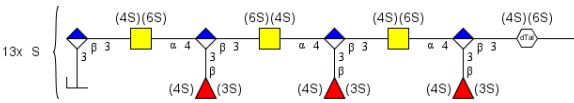
446.8318	7394394	$[B_7+9Na-SO_3]^{7-}$	0.2112	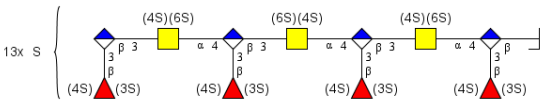
448.9682	2546239	$[B_4+5Na]^{4-}$	0.5972	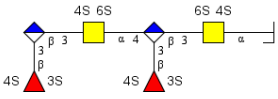

454.4638	1951775	$[B_2+3Na]^{2-}$	0.3395	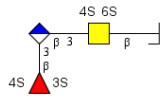
457.1757	781473	$[M\text{-}f]_z\text{-}5SO_3$	1.1830	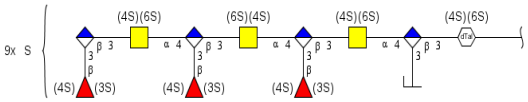
457.4659	953058	$[C_6+3Na]^{2-}$	-0.4042	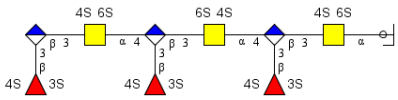
463.4692	1425772	$[C_3+5H+3Na]^{2-}$	0.0791	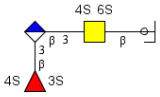
464.1667	2167794	$[B_5+7Na]^{5-}$	0.2634	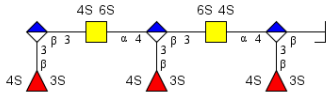
466.8121	1061252	$[^{2,4}X_6+4Na]^{6-}$	1.9856	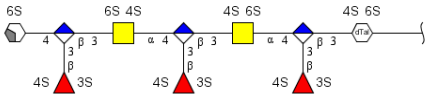
470.4773	1280834	$[^{2,4}X_6+5Na]^{6-}$	-1.3086	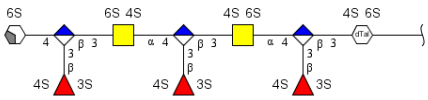
470.6346	1315248	$[B_3+4Na]^{3-}$	1.7018	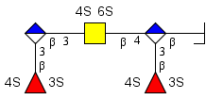
472.9874	1890423	$[^{2,4}X_4+Na]^{4-}$	0.3450	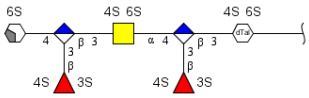
474.1662	622151	Z	-0.3500	
498.4725	1031471	$[^{3,5}A_3+3Na]^{2-}$	-1.0506	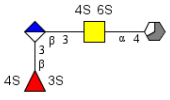
502.9792	2135604	B_1+Na	-1.8010	

504.7825	501710	$[B_3+3Na-3SO_3]^{3}$	0.3898	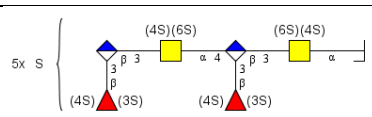
509.5016	1700947	$[B_5+5Na-3SO_3]^{4-}$	0.3213	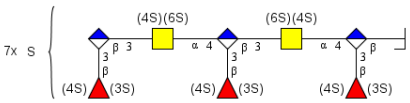
520.9638	692810	$[Z_6+6Na]^{5-}$	1.806	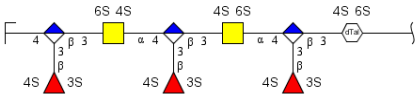
524.9607	1045045	B_1+2Na	-0.8786	
542.4804	1407005	^{2,4}X_{GlcA}	-0.2305	
542.9709	1346267	C_1+2Na	-0.1778	
564.7743	1036278	$[^{2,4}X_6+5Na]^{5-}$	-1.458	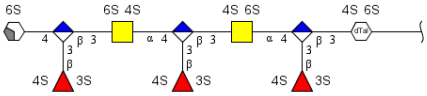
606.2893	649518	$[B_4+6Na]^{3-}$	-2.6425	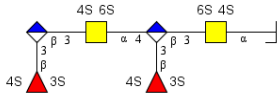
619.6183	1960455	$[C_4+7Na]^{3-}$	0.3782	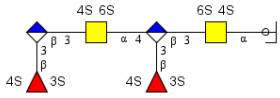

Ib dp 12

Mass to charge	Intensity	Type	Accuracy PPM	Structure
136.9915	1667749	$^{3,5}A_{\alpha f}$	-0.708525712	
138.9707	4.58E+07	$^{2,4}A_{\alpha f}$	-0.233891029	
145.0506	679177	Z_1-2SO_3	0.223204868	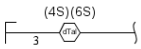
145.0506	679177	$B_{1\beta}$-2SO_3	0.223204868	
151.9785	5399159	Z_1^{2-}	-0.049164849	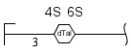
151.9785	5399159	$B_{1\beta}^{2-}$	-0.049164849	
152.9864	1750729	$^{0,3}A_{\alpha f}$	-0.538871429	
157.0161	500442	$^{1,4}A_1$-SO_3	-1.068177085	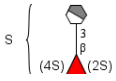
160.9526	9653767	$^{2,4}A_{\alpha f}$ + Na	0.075388655	
160.9838	2.05E+08	Y_1^{2-}	-0.156096452	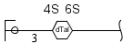
160.9838	2.05E+08	$C_{1\beta}^{2}$	-0.156096452	

167.0021	529803	$^{2,5}A_{\alpha f}$	- 0.792660691	
168.9812	1309836	$^{1,4}A_1$+Na-SO_3	0.190447221	
174.9811	976533	$^{1,5}X_1^{2-}$	0.755407298	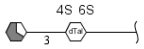
181.9892	986992	$^{0,2}X_1^{2-}$	-0.78458502	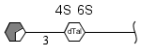
181.9892	986992	$^{2,4}A_1^{2-}$	-0.78458502	
182.9969	4.43E+07	$^{0,2}A_{\alpha f}$	- 0.097018037	
190.963	920898	$^{1,4}A_{\alpha f}$ + Na-SO_3	0.925938533	
197.0126	603208	$^{1,5}A_{\alpha f}$ + Na-SO_3	- 0.343582086	
207.9853	1212472	$[^{1,4}A_1$ + Na$]^{2-}$	0.057100189	
208.0002	1518769	$[^{1,5}A_1$ + Na-$SO_3]^{2-}$	2.0027	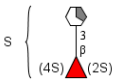
210.9918	1591495	$[^{2,5}A_1$ + Na$]^{2-}$	- 0.014844179	
225.0074	6.88E+08	Z_1-SO_3	0.208579807	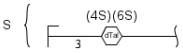
225.0074	6.88E+08	$B_{1\beta}$-SO_3	0.208579807	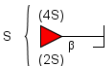

225.9972	1127460	$[^{1,5}A_1+Na]^{2-}$	-0.534471224	
234.9994	525148	$[Z_2-SO_3]^{3-}$	-2.38301885	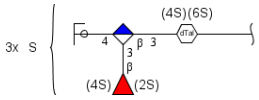
239.9946	5.25E+07	B_1^{2-}	-0.264497618	
242.3262	2937174	$[Z_2+Na-SO_3]^{3-}$	-0.186231067	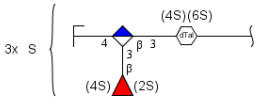
243.018	8.40E+07	Y_1-SO_3	0.047807158	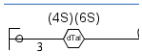
243.018	8.40E+07	$C_{1\beta}-SO_3$	0.047807158	
246.9894	1498694	$Z_1+Na-SO_3$	-0.034131019	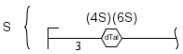
246.9894	1498694	$B_{1\beta}+Na-SO_3$	-0.034131019	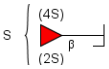
248.3296	2042947	$[Y_2+Na-SO_3]^{3-}$	0.307789862	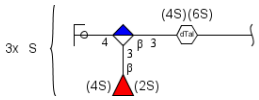
250.9855	2739414	B_1+Na	0.035225142	
254.006	4858152	$[B_3-SO_3]^{3-}$	-0.021391883	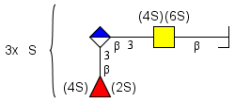
259.9908	3369616	$[C_1+Na]^{2-}$	-0.033908892	

261.3334	3.36E+07	$[B_3\text{-Na-SO}_3]^{3-}$	-0.34650884	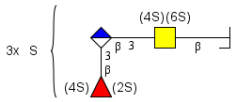
262.9841	713309	$[Y_2\text{+3Na-SO}_3]^{3-}$	0.784047401	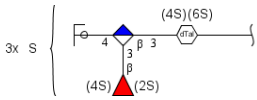
265	5896394	$Y_1\text{+Na-SO}_3$	-0.165071698	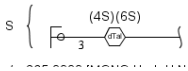
265	5896394	$C_{1\beta}\text{+Na-SO}_3$	-0.165071698	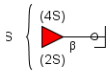
267.3369	4828098	$[C_2\text{+Na-SO}_3]^{3-}$	-0.258072617	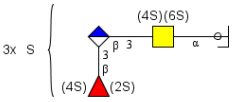
268.9777	678949	$[Z_2\text{-4H+Na}]^{3-}$	2.700558448	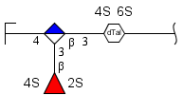
273.1856	4259384	$[B_3\text{+2Na}]^{5-}$	-0.175283763	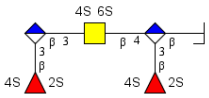
274.9814	789460	$[Y_2\text{+Na}]^{3-}$	1.992687505	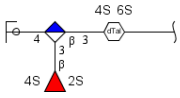
276.3058	8012552	$[Z_2\text{-5H+2Na}]^{3-}$	-0.212556764	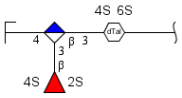
282.2392	1.11E+07	$[Y_3\text{-6H+2Na-SO}_3]^{4-}$	-0.089331142	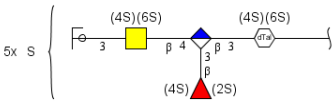
282.3093	8083657	$[Y_2\text{-4H+Na}]^{3-}$	-0.131659377	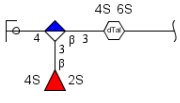
285.0279	1148320	$^{0,2}X_1\text{-SO}_3$	2.37276421	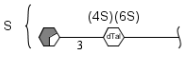

285.0279	1148320	$^{2,4}A_1$-SO_3	2.37276421	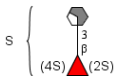
287.9857	1.61E+07	$[B_2+Na]^{3-}$	- 0.413338811	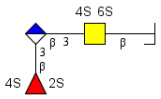
295.313	9896349	$[B_2+2Na]^{2-}$	- 0.352698098	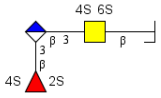
296.26	2703115	$[B_3+Na-2SO_3]^{4-}$	- 0.452932391	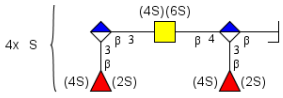
301.3165	5963090	$[C_2+Na]^{3-}$	- 0.274111552	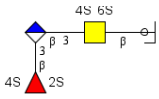
301.7554	5970271	$[B_3+2Na-2SO_3]^{4-}$	- 0.159156224	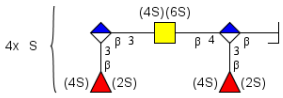
304.9643	2.07E+07	$B_{1\beta}$	- 0.126283634	
304.9643	2.07E+07	Z_1	- 0.126283634	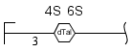
307.7239	2.36E+07	$[Y_3+3Na]^{4-}$	- 0.115084496	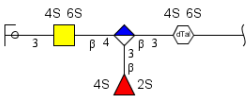
322.9755	621523	Y_1	- 2.086306856	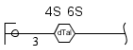
322.9755	621523	$C_{1\beta}$	- 2.086306856	

324.0149	577557	$[Z_2\text{-}4H+2Na\text{-}2SO_3]^{2-}$	- 1.347947271	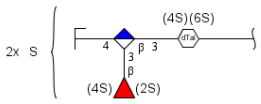
326.9463	1.22E+07	Z_1+Na	- 0.287123604	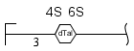
326.9463	1.22E+07	$B_{1\beta}+Na$	- 0.287123604	
327.2401	8770840	$[B_3+3Na\text{-}2SO_3]^{4-}$	- 0.177935864	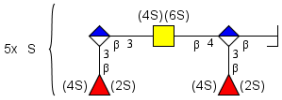
337.0218	822962	$^{1,4}A_1+Na\text{-}SO_3$	- 2.119661102	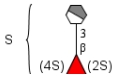
341.5342	3425637	$[B_2\text{-}2SO_3]^{2-}$	0.06672099	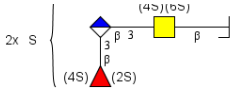
344.9568	1.02E+08	Y_1+Na	- 0.084613494	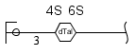
344.9568	1.02E+08	$C_{1\beta}+Na$	- 0.084613494	
347.2293	8228684	$[B_3\text{-}7H+3Na]^{4-}$	- 0.157212395	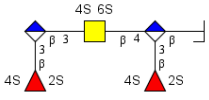
348.994	1576631	$[B_5\text{-}10H+4Na\text{-}2SO_3]^{6-}$	1.610275057	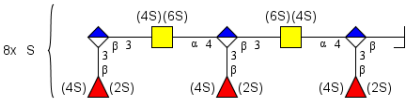
351.1705	1589926	$[Y_4\text{-}10H+5Na]^{5-}$	1.820822079	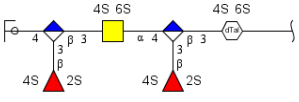

354.5776	998512	$[B_2\text{-}3H+Na\text{-}2SO_3]^{2-}$	- 1.888729575	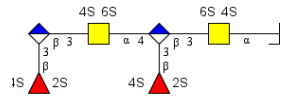
356.6369	2331367	$[Y_5\text{-}12H+6Na]^{6-}$	0.919209426	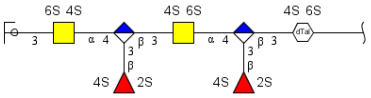
361.5311	572930	$[C_2\text{-}3H+Na\text{-}2SO_3]^{2-}$	- 1.721983254	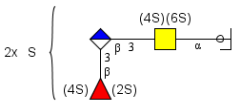
365.9844	2806308	$[B_5\text{-}13H+5Na\text{-}SO_3]^{6-}$	- 0.122476987	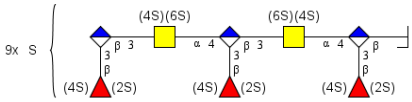
369.6473	1187585	$[B_5+6Na\text{-}2SO_3]^{6-}$	1.927824172	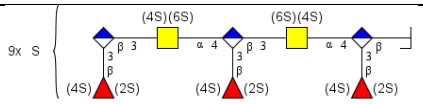
372.952	1096932	$^{1,5}X_1+Na$	- 0.843449023	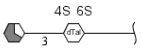
374.9836	2095751	$[Z_3+2Na\text{-}SO_3]^{2-}$	0.647606988	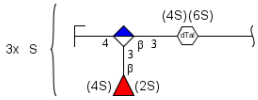
381.0937	3437337	$[Y_7+9Na]^{8-}$	0.549584328	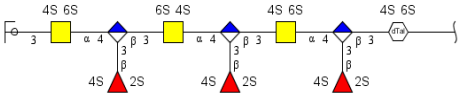
386.967	2573623	$^{0,2}X_1+Na$	0.866993826	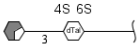
386.967	2573623	$^{2,4}A_1+Na$	0.866993826	
387.3518	685486	$[^{2,4}X_7+9Na]^{8-}$	0.645487835	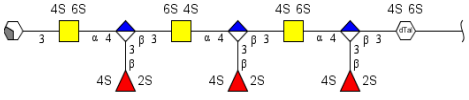

388.1042	3105935	$[B_7+8Na-SO_3]^{8-}$	0.1416	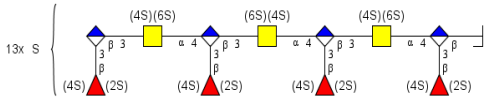
392.5037	3890175	$[B_2+Na-SO_3]^{2-}$	-0.2487	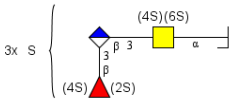
400.846	1571151	$[Z_{8\beta}+9Na]^{8-}$	1.4965	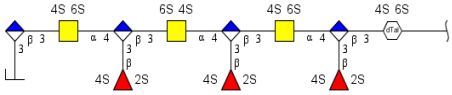
400.846	1571151	$[B_7+9Na]^{8-}$	1.4965	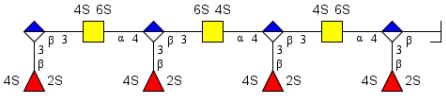
401.04	1382424	B_1-SO_3	-1.1597	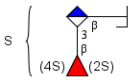
403.4943	2251645	$[B_2+2Na-SO_3]^{2-}$	0.6808	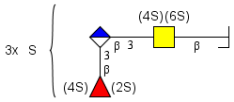
416.9787	1099891	$^{1,4}A_1+Na$	-1.9181	
417.9608	788238	$[Y_3+4Na]^{3-}$	1.8179	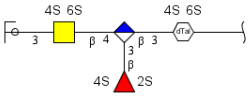

Pg dp 15

Mass to charge	Intensity	Type	Accuracy PPM	Structure
225.0074	5.52E+07	Z_1-SO_3	0.2086	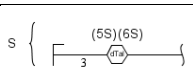
225.0074	5.52E+07	$B_{1\beta}$-SO_3	0.2086	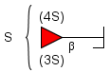
239.9945	2931234	B_1^{2-}	0.15212	
243.018	1.38E+07	Y_1-SO_3	0.0478	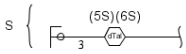
243.018	1.38E+07	$C_{\beta 1}$-SO_3	0.0478	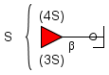
304.9643	1.10E+07	Z_1	-0.1263	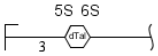
304.9643	1.10E+07	$B_{1\beta}$	-0.1263	
324.0143	1527523	$[Z_2$+Na-$SO_3]^{2-}$	0.5038	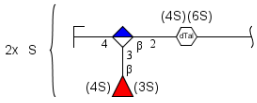
326.9463	1.87E+07	Z_1+Na	-0.2871	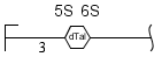
326.9463	1.87E+07	$B_{1\beta}$+Na	-0.2871	

333.0198	2292461	$[Y_2+Na-2SO_3]^{2-}$	-0.1634	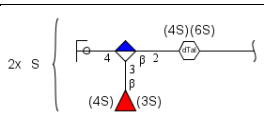
341.5343	1.67E+07	$[B_2-2SO_3]^{2-}$	-0.2261	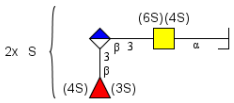
344.9568	1.15E+08	Y_1+Na	-0.0846	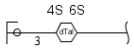
344.9568	1.15E+08	$C_{1\beta}+Na$	-0.0846	
350.0024	4414686	$[Y_3+2Na-2SO_3]^{3-}$	-0.0371	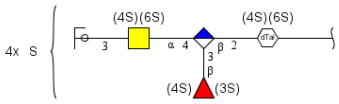
352.5252	8315825	$[B_2+2Na-2SO_3]^{3-}$	-0.0139	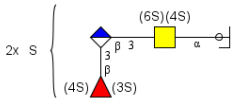
361.5304	3166804	$[C_1+Na-2SO_3]^{2-}$	0.2142	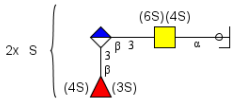
368.6966	1.42E+07	$[B_3+Na-3SO_3]^{3-}$	0.1131	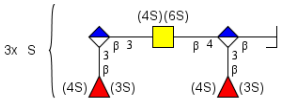
372.998	2722614	$[Y_2+Na-SO_3]^{2-}$	0.4098	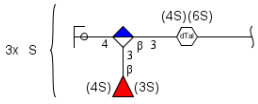
374.984	3045238	$[Z_2+2Na-SO_3]^{2-}$	-0.4191	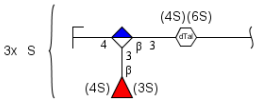
376.0241	2128108	$[B_3+2Na-SO_3]^{3-}$	-0.3814	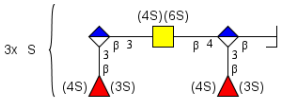

376.6547	2237787	$[Y_3+2Na-SO_3]^{3-}$	-0.1101	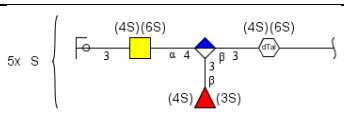
383.9827	2.47E+07	$[Y_3+3Na-SO_3]^{3-}$	-0.0693	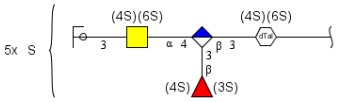
383.9884	5557651	$[Y_2+2Na-SO_3]^{2-}$	1.8886	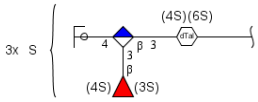
386.9677	1113550	$^{2,4}A_1+Na$	-0.9419	
386.9677	1113550	$^{0,2}X_1+Na$	-0.9419	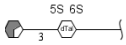
392.5036	5.40E+07	$[B_2+Na-SO_3]^{2-}$	0.0061	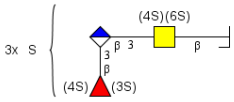
395.3493	5536513	$[B_3+2Na-2SO_3]^{3-}$	-0.9783	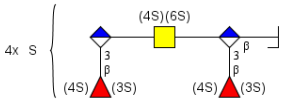
401.0396	2.34E+07	B_1-SO_3	-0.1623	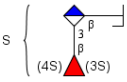
402.6763	5.02E+07	$[B_3+2Na-2SO_3]^{3-}$	-0.1785	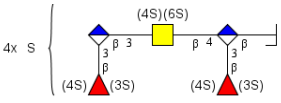
403.4944	1.25E+07	$[B_2+2Na-SO_3]^{3-}$	0.4330	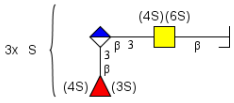
410.0037	6190583	$[B_3+3Na-2SO_3]^{3-}$	-0.3830	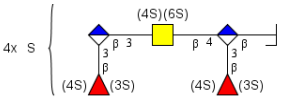

410.6343	1577449	$[Y_3+3Na]^{3-}$	-0.1341	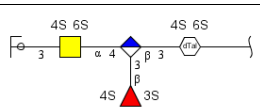
412.4999	6658169	$[C_2+2Na-SO3]^{2-}$	-0.1041	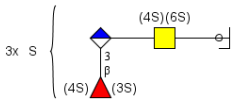
414.9621	1765513	$[Z_2+2Na]^{2-}$	0.3618	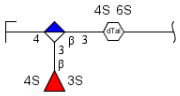
417.9616	3.01E+07	$[Y_3+4Na]^{3-}$	-0.0962	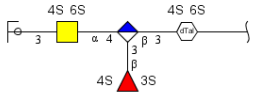
423.0218	2465405	$B_1+Na-SO_3$	-0.7575	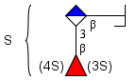
425.9533	5978956	$[Z_2+3Na]^{2-}$	-0.1821	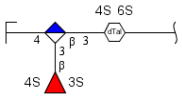
429.3284	6130707	$[B_3+2Na-SO_3]^{3-}$	0.2321	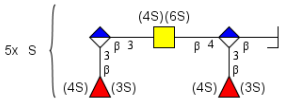
434.9587	4289627	$[Y_2-5H+3Na]^{2-}$	-0.4488	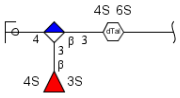
436.6558	9.09E+07	$[B_3+3Na-SO_3]^{3-}$	0.0332	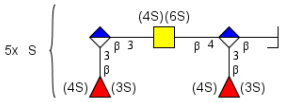
441.0321	2554702	$C_1+2Na-SO_3$	-0.1264	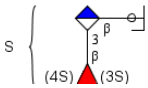
443.473	5.08E+07	$[B_2+2Na]^{2-}$	-0.0406	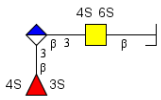

444.9726	1878850	$^{2,5}A_1$	0.4827	
454.4639	6129351	$[B_2+3Na]^{2-}$	0.1195	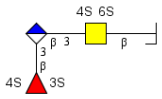
463.3088	3649142	$[B_3+3Na]^{3-}$	-1.5410	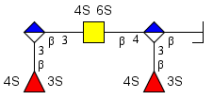
463.4694	7950300	$[C_2+3Na]^{2-}$	-0.3525	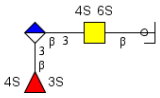
469.9962	3093990	$[Y_5+5Na-3SO_3]^{4-}$	0.3891	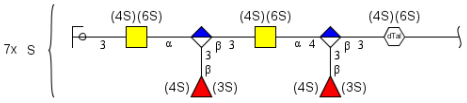
470.6353	1.94E+07	$[B_4+3Na]^{3-}$	0.2144	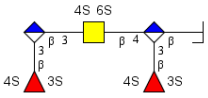
472.9877	7026925	$[^{2,4}X_4+Na]^{4-}$	-0.2893	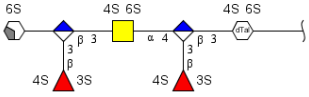
484.0172	6332564	$[B_5+4Na-4SO_3]^{4-}$	-0.2605	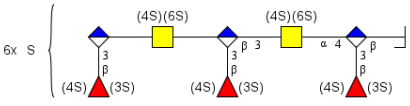
485.5287	5048852	$[Y_3+2Na-3SO_3]^{2-}$	0.2295	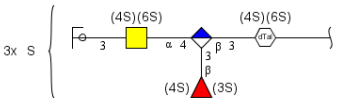
495.4815	9252679	$[Y_5+6Na-2SO_3]^{4-}$	0.1467	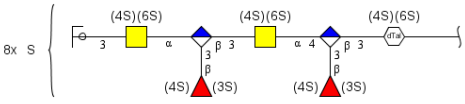
502.9783	1.83E+07	B_1+Na	-0.0117	

504.0058	3863552	$[B_5+4Na-3SO_3]^{4-}$	0.9475	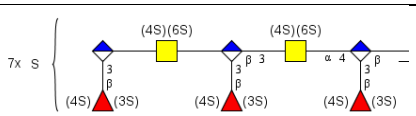
504.3494	8601264	$[B_4+3Na-3SO_3]^{3-}$	-0.1216	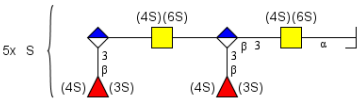
508.1457	8263113	$[B_7+9Na-2SO_3]^{6-}$	-0.1565	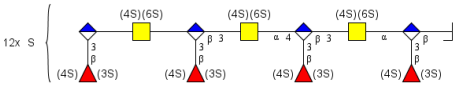
509.5019	1.89E+07	$[B_5+5Na-3SO_3]^{6-}$	-0.2675	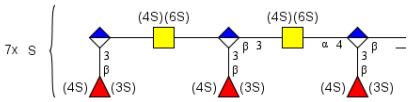
515.4691	2709084	$[Y_5+6Na-SO_3]^{4-}$	2.2820	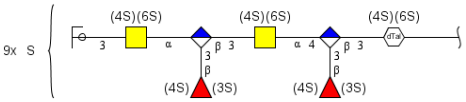
517.9811	7744118	$[M+13Na-4SO_3]^{8-}$	0.7841	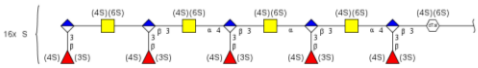
520.9657	2.72E+07	$[Y_5+7Na-SO_3]^{4-}$	0.1199	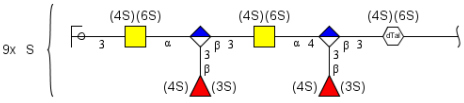
524.9588	4654470	B_1+2Na	2.7407	
534.9864	4.04E+07	$[B_5+6Na-2SO_3]^{4-}$	0.1000	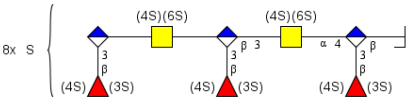
535.9855	6465278	$[C_5+9Na-3SO_3]^{4-}$	1.5850	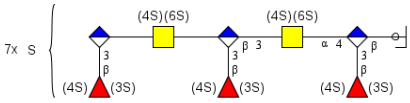
536.4183	4137789	$[Z_{10\beta}+10Na-4SO_3]^{7-}$	0.8760	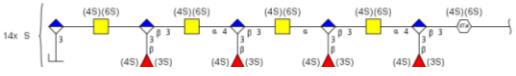

536.4183	4137789	$[B_9+10Na-4SO_3]^{7-}$	0.8760	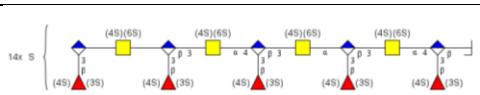
540.4671	2.63E+07	$[^{0,2}X_5+5Na]^{4-}$	-0.8604	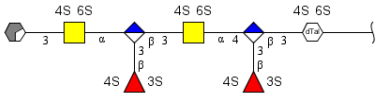
540.7189	4.42E+07	$[M+14Na-2SO_3]^{8-}$	-0.8290	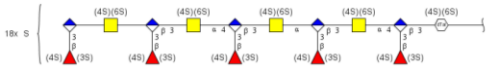
546.4505	2.23E+07	$[Y_5+8Na]^{4-}$	-0.0873	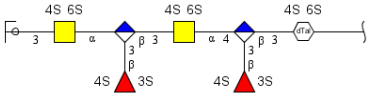
551.6605	2887288	$[C_4+5Na-2SO_3]^{3-}$	-2.0637	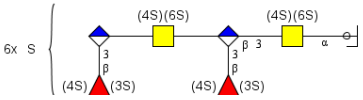
553.5484	9208020	$[B_3+Na-3SO_3]^{2-}$	0.3627	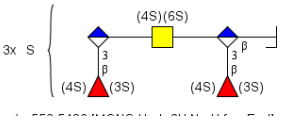
560.4711	529E+07	$[B_5+7Na-SO_3]^{4-}$	0.0773	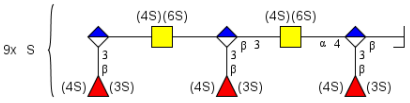
564.5392	1.56E+07	$[B_3+2Na-3SO_3]^{2-}$	0.6609	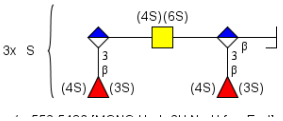
564.7736	7179912	$[^{2,4}X_6+5Na]^{5-}$	-0.2187	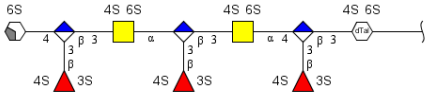
564.9736	9172915	$[C_5+7Na-SO_3]^{4-}$	0.3265	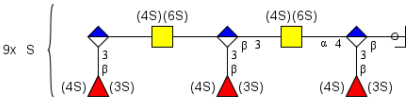
565.5444	1.02E+07	$[Z_{10\beta}+12Na-4SO_3]^{7-}$	-0.4780	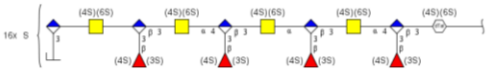

565.5444	1.02E+07	[B_9+12Na-4SO_3]$^{7-}$	-0.4780	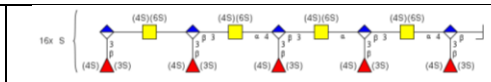
568.684	2.33E+07	[$Z_{10\beta}$+13Na-4SO_3]$^{7-}$	0.7165	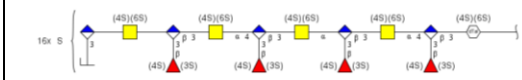
568.684	2.33E+07	[B_9+13Na-4SO_3]$^{7-}$	0.7165	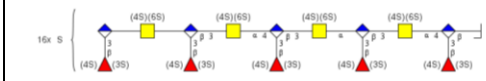
569.8279	3383750	[$^{2,4}X_6$+8Na]$^{7-}$	-2.7844	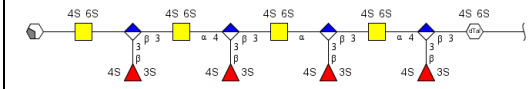
570.6864	3696288	[$Z_{10\beta}$+10Na-3SO_3]$^{7-}$	-0.7427	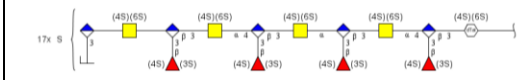
570.6864	3696288	[B_9+10Na-3SO_3]$^{7-}$	-0.7427	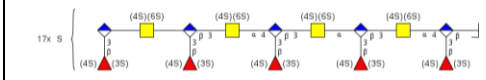
571.2581	8830123	[$Y_{10\beta}$+13Na-4SO_3]$^{7-}$	-1.3212	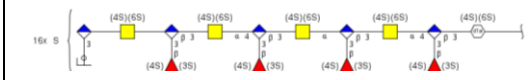
571.2581	8830123	[C_9+13Na-4SO_3]$^{7-}$	-1.3212	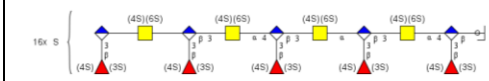
572.3081	3.37E+07	[B_4+5Na-SO_3]$^{3-}$	0.0200	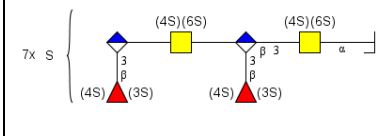
573.5972	7921618	[B_7+8Na-6SO_3]$^{3-}$	-0.2004	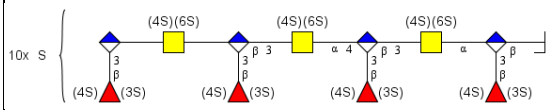
574.3975	1.58E+07	[$Y_{10\beta}$+14Na-2SO_3]$^{7-}$	0.2143	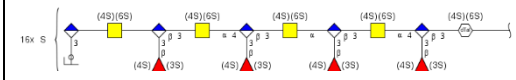

574.3975	1.58E+07	$[C_9+14Na-2SO_3]^{7-}$	0.2143	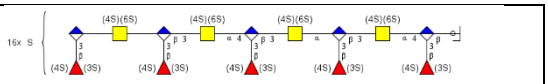
576.4773	2919527	$[Y_3+3Na-SO_3]^{2-}$	-1.2172	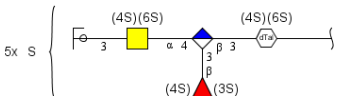
576.9649	3121387	$[Z_{10\beta}+12Na-SO_3]^{7-}$	2.8281	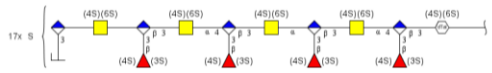
576.9649	3121387	$[B_9+12Na-SO_3]^{7-}$	2.8281	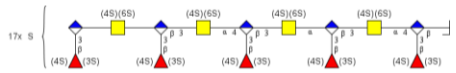
579.6352	3650283	$[B_4+6Na-SO_3]^{7-}$	0.3905	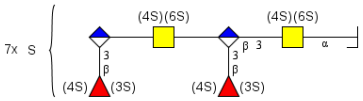
580.1074	6989630	$[Z_{10\beta}+13Na-SO_3]^{7-}$	-0.3283	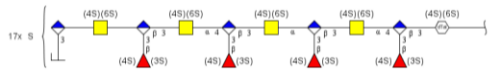
580.1074	6989630	$[B_9+13Na-SO_3]^{7-}$	-0.3283	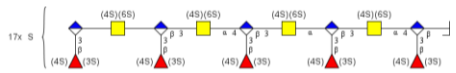
582.3877	3600267	$[^{2,4}X_9+12Na]^{7-}$	0.7290	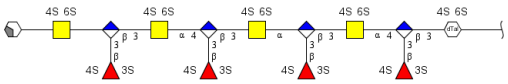
583.2454	6537338	$[Z_{10\beta}+14Na-SO_3]^{7-}$	2.8930	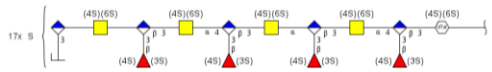
583.2454	6537338	$[B_9+14Na-SO_3]^{7-}$	2.8930	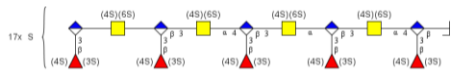
585.2473	1.22E+07	$[Z_{10\beta}+11Na]^{7-}$	2.3170	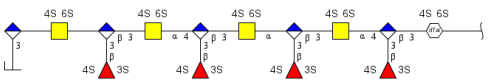

585.247 3	1.22E+ 07	$[B_9+11Na]^{7-}$	2.3170	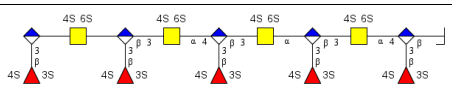
585.820 5	970360 4	$[Y_{10\beta}+14Na-SO_3]^{7-}$	-0.8105	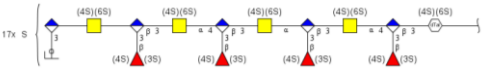
585.820 5	970360 4	$[C_9+14Na-SO_3]^{7-}$	-0.8105	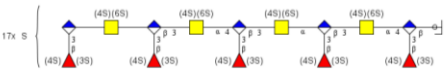
587.467 6	4.00E+ 07	$[Y_3+4Na-SO_3]^{2-}$	-0.050	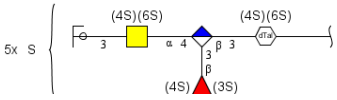
588.387 8	639363 3	$[Z_{10\beta}+7Na]^{6-}$	1.9270	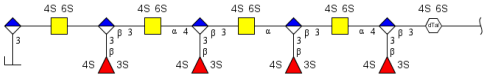
588.387 8	639363 3	$[B_9+7Na]^{6-}$	1.9270	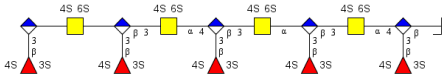
589.587 6	422675 8	$[B_7+8Na-3SO_3]^{6-}$	1.4382	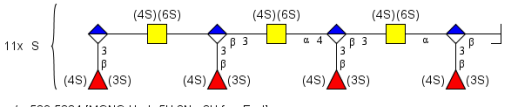
593.985	1.54E+ 07	$[B_7+9Na-3SO_3]^{6-}$	-0.2746	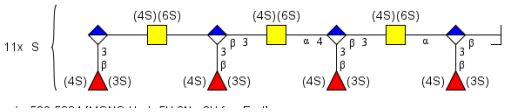
600.345 8	274582 3	$[Y_5+5Na-4SO_3]^{3-}$	-0.7810	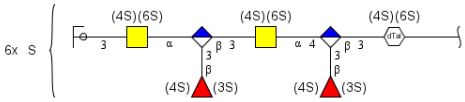
603.155 8	2.82E+ 07	$[Y_7+11Na-3SO_3]^{5-}$	0.3911	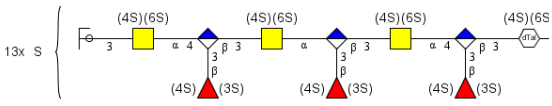
604.119 2	520030 3	B_2-3SO_3	-0.4843	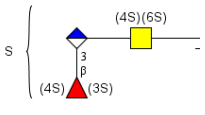

604.5182	4066310	B_3+2Na-2SO_3	-0.3633	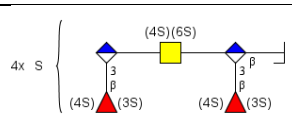
606.2877	2.26E+07	$[B_4+6Na]^{3-}$	-0.0035	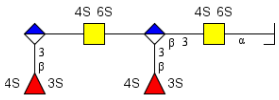
606.7514	4915464	$[Z_7+9Na]^{5-}$	2.4854	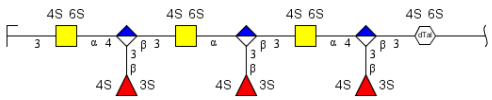
609.9755	5225885	$[B_7+9Na-2SO_3]^{5-}$	2.8395	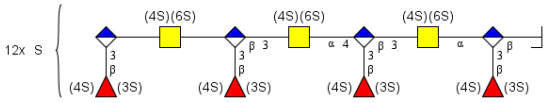
610.7774	2829865	$[C_7+12Na-3SO_3]^{5-}$	-2.1012	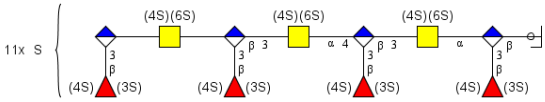
611.2403	6606656	$[B_6+7Na-3SO_3]^{4-}$	1.1230	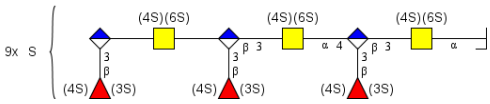
614.3724	2.57E+07	$[B_7+10Na-2SO_3]^{5-}$	0.3072	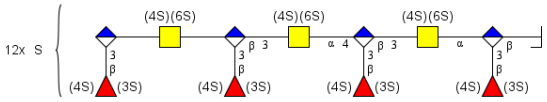
615.1727	1.49E+07	$[C_7+13Na-3SO_3]^{5-}$	-0.3161	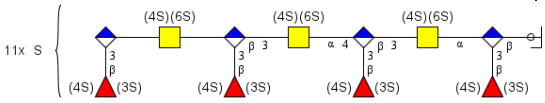
615.5087	1.96E+07	$[B_3+3Na-2SO_3]^{2-}$	0.4105	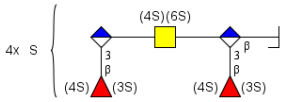
619.6186	337964	$[C_4+7Na]^{3-}$	-0.1060	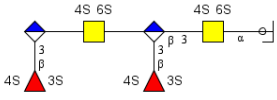
622.4697	3228719	$[Z_6+8Na-2SO_3]^{4-}$	0.9804	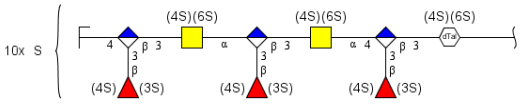

623.5437	1.22E+07	$[Y_7+12Na]^{5-}$	0.1407	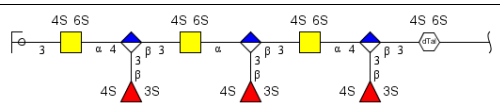
627.4447	251418 4	$[Y_3+4Na]^{5-}$	2.0367	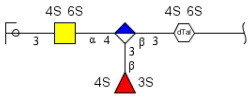
634.3248	366887 1	$[Z_{10\beta}+11Na-SO_3]^{6-}$	-1.6365	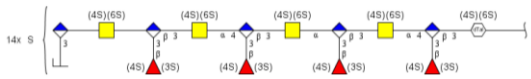
634.3248	366887 1	$[B_9+11Na-SO_3]^{6-}$	-1.6365	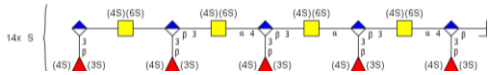
634.7599	1.45E+07	$[B_7+11Na-SO_3]^{6-}$	0.6941	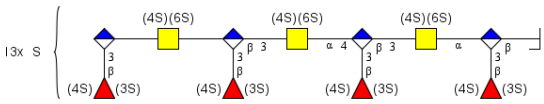
636.7259	880067 2	$[B_6+8Na-2SO_3]^{4-}$	-0.3514	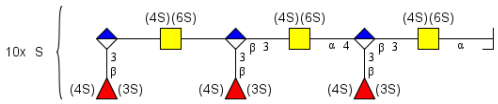
638.3126	707107 2	$[^{2,4}X_4+2Na]^{3-}$	0.8741	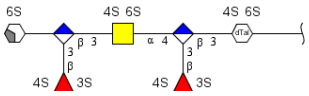
638.4368	4.38E+07	$[Y_3+5Na]^{5-}$	0.2353	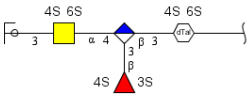
650.3053	427518 1	$[Z_{10\beta}+13Na-3SO_3]^{6-}$	2.4384	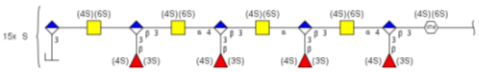
650.3053	427518 1	$[B_9+13Na-3SO_3]^{6-}$	2.4384	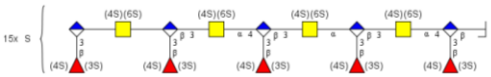
655.1486	217649 8	$[B_{10}+12Na]^{5-}$	-0.7748	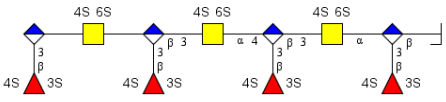

655.4871	4540733	$[B_3+3Na-SO_3]^{2-}$	0.3966	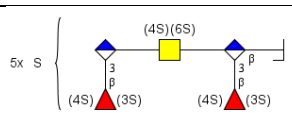
662.21	1.08E+07	$[B_6+9Na-SO_3]^{4-}$	0.5527	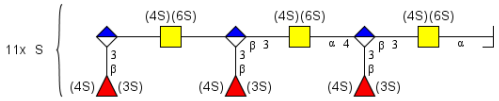
666.4783	1.68E+07	$[B_3+4Na-SO_3]^{2-}$	0.0485	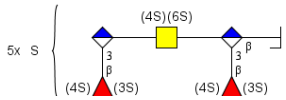
667.2955	3590286	$[Z_{10\beta}+14Na-3SO_3]^{6-}$	1.7667	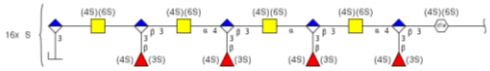
667.2955	3590286	$[B_9+14Na-3SO_3]^{6-}$	1.7667	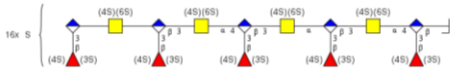
668.3041	6360360	$[Y_4+7Na-2SO_3]^{3-}$	0.6044	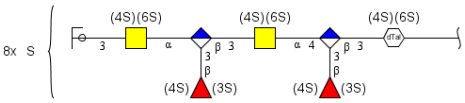
686.9982	4695553	$[B_4+6Na-3SO_3]^{3-}$	0.8131	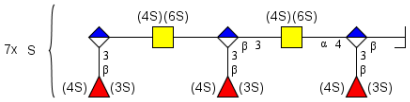
687.6946	5507192	$[B_6+10Na]^{4-}$	0.6628	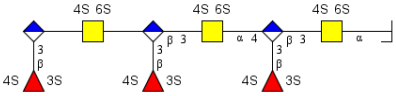
688.6936	2195755	$[C_6+13Na-SO_3]^{4-}$	1.9629	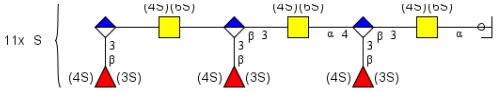
702.2841	1.09E+07	$[Y_4+8Na-2SO_3]^{3-}$	-0.0138	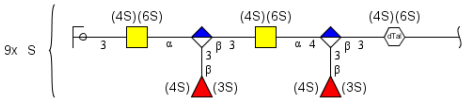
706.0576	8575835	$B_2+Na-2SO_3$	0.0943	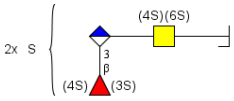

717.4469	621285 7	$[B_3+5Na]^{2-}$	1.1316	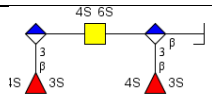
720.9777	552680 6	$[B_5+7Na-2SO_3]^{3-}$	0.8946	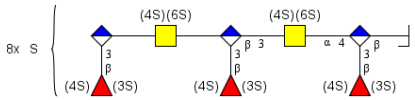
736.2639	704418 0	$[Y_5+9Na]^{3-}$	-0.3032	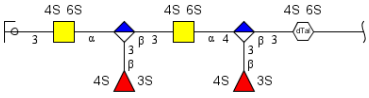
754.9571	346570 6	$[B_5+7Na-2SO_3]^{3-}$	1.1013	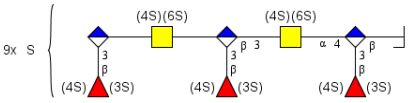
772.9585	167633 4	$[B_5+6Na]^{3-}$	-2.0613	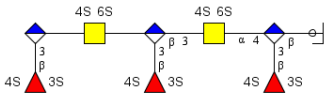
829.9779	373431 0	$B_2+3Na-SO_3$	0.5669	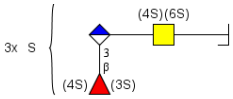
870.9226	190402 5	Y_2+3Na	1.9359	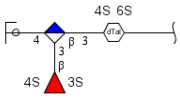

Ib dp 15

Mass to charge	Intensity	Type	Accuracy PPM	Structure
138.9707	820466	$^{2,4}A_{\alpha f}$	-0.2339	
160.9838	994779	Y_1^{2-}	-0.1561	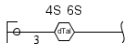
160.9838	994779	$C_{1\beta}^{2}$	-0.1561	
182.9969	3124804	$^{0,2}A_{\alpha f}$	-0.0970	
225.0074	2.58E+07	Z_1-SO_3	0.2086	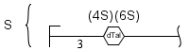
225.0074	2.58E+07	B	0.2086	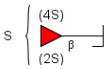
239.9946	1727538	B_1^{2-}	-0.2645	
243.018	6907123	Y_1-SO_3	0.0478	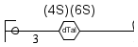
243.018	6907123	$C_{1\beta}$-SO_3	0.0478	
264.9999	1320826	Y_1+Na-SO_3	0.2123	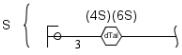
264.9999	1320826	$C_{1\beta}$+Na-SO_3	0.2123	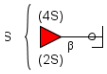

285.0286	1629043	$^{0,2}X_1$-SO_3	-0.0831	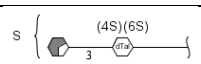
285.0286	1629043	$^{2,4}A_1$-SO_3	-0.0831	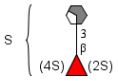
304.9642	4784334	Z_1	0.2016	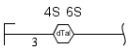
304.9642	4784334	$B_{1\beta}$	0.2016	
326.9463	1.07E+07	Z_1+Na	-0.2871	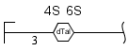
326.9463	1.07E+07	$B_{1\beta}$+Na	-0.2871	
344.9567	1.14E+08	Y_1+Na	0.2053	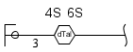
344.9567	1.14E+08	$C_{1\beta}$+Na	0.2053	
352.525	1483412	$[B_2$+Na-$SO_3]^{2-}$	0.5534	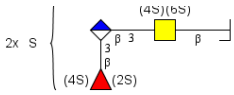
366.9378	1067462	Y_1+2Na	2.4948	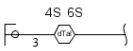
366.9378	1067462	$C_{1\beta}$+2Na	2.4948	

372.9519	2523290	$^{1,5}X_1$+Na	-0.5753	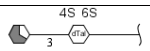
374.9838	9796040	$[Z_3$+2Na-$SO_3]^{2-}$	0.1143	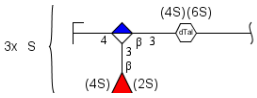
386.9674	7691205	$^{0,2}X_1$+Na	-0.1667	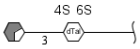
386.9674	7691205	$^{2,4}A_1$+Na	-0.1667	
412.4994	1859614	$[C_2$+2Na-$SO_3]^{2-}$	1.1080	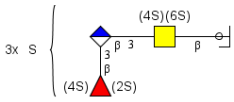
414.9617	2307508	$[Z_2$+Na$]^{2-}$	1.3257	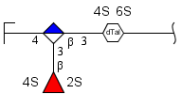
416.9776	1444748	$^{1,4}A_1$+Na	0.7199	
417.9616	4090871	$[Y_3$+4Na$]^{3-}$	-0.0962	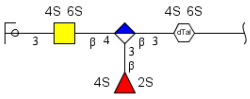
419.05	1197977	C_1-SO_3	0.2377	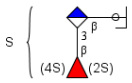
423.0213	2519960	B_1+Na-SO_3	0.4245	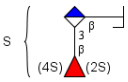
425.9536	1373665	$[Z_2$+3Na$]^{2-}$	-0.8864	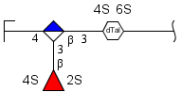

432.562	1350549	$[Y_5+7Na]^{5-}$	1.1966	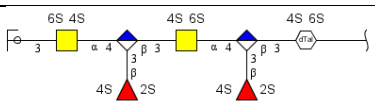
434.9588	1959562	$[Y_2+3Na]^{2-}$	-0.6787	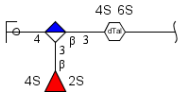
436.6559	3412277	$[B_3+3Na-SO_3]^{3-}$	-0.1958	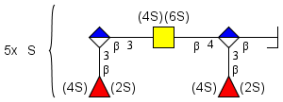
438.9598	3262115	$^{1,4}A_1+2Na$	0.1021	
441.0333	1342399	$C_1+Na-SO_3$	-2.8473	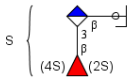
443.4731	6318659	$[B_2+2Na]^{2-}$	-0.2661	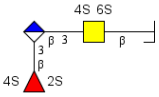
454.4639	4354065	$[B_2+2Na]^{2-}$	0.1195	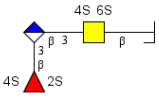
463.4695	2530866	$[C_2+3Na]^{2-}$	-0.5682	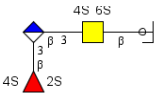
464.1676	2795000	$[B_5+7Na]^{5-}$	-1.6755	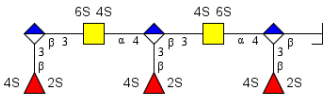
470.6357	3128673	$[B_3+4Na]^{3-}$	-0.6355	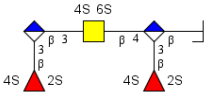
502.9784	1.28E+07	B_1+Na	-0.2105	

515.7897	1292709	$[Y_7+11Na]^{6-}$	-2.7409	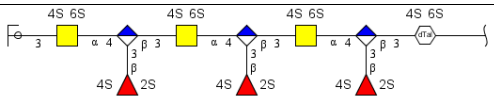
520.9651	1292808	$[Z_6+6Na]^{5-}$	-0.6893	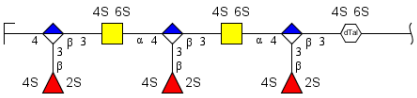
524.9604	2882361	B_1+2Na	-0.3072	
525.2094	1715944	$[Y_{10\beta}+15Na]^{8-}$	-0.8427	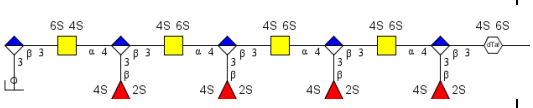
525.2094	1715944	$[C_9+15Na]^{8-}$	-0.8428	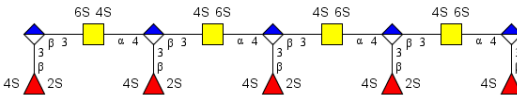
542.1256	1297969	$[B_7+11Na]^{6-}$	-0.7252	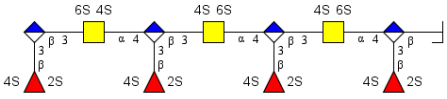
542.9715	1167270	C_1+2Na	-1.2829	
546.4504	2784747	$[Y_5+8Na]^{4-}$	0.0957	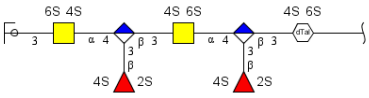
585.9555	1563586	$[Y_4+5Na]^{3-}$	2.1332	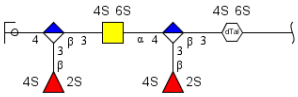
585.9555	1563586	$[B_5+8Na]^{4-}$	0.5685	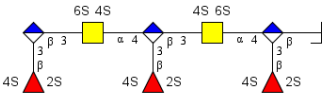
619.6187	1357506	$[C_3+7Na]^{3-}$	-0.2674	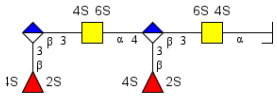

666.4792	1382565	$[B_3+4Na-SO_3]^{2-}$	-1.3019